Green Synthesised Zinc Oxide Nanoparticles and their Antifungal Effect on *Candida albicans* Biofilms

Mini thesis submitted in partial fulfilment of the requirements for the Masters' degree in Restorative Dentistry

MSc (Clinical) Restorative Dentistry

Dr Germana Vincent Lyimo, Student Number: 3714367

Supervisor: Dr RZ Adam, Department of Restorative Dentistry, Faculty of Dentistry

Co-Supervisor: Prof. RF Ajayi, Department of Chemistry, Faculty of Natural Sciences

Green Synthesised Zinc Oxide Nanoparticles and their Antifungal Effect on *Candida albicans* Biofilms

MSc Mini thesis, Department of Restorative Dentistry, Faculty of Dentistry, University of the Western Cape

ABSTRACT

Introduction: *Candida albicans* is a clinical fungal isolate that is most frequently isolated from different host niches, and is implicated in the pathogenesis of several fungal infections, including oral candidiasis. The pathogenesis and antifungal resistance mechanisms of Candida species are complex and involve several pathways and genes. Oral candidiasis incidence rates are rapidly increasing, and the increase in resistance to conventional antifungals has led to the need to develop innocuous and more efficacious treatment modalities. The purpose of this study was to explore a single pot process for phytosynthesis of zinc oxide nanoparticles (GZnO NPs) and to assess their antifungal potential.

Aim: To evaluate the antifungal effect of GZnO NPs on *Candida albicans* (ATCC 90028) biofilms.

Methods: Zinc nitrate hexahydrate [$Zn(NO_3)_2 \cdot 6H_2O$] was used as the inorganic metal oxide precursor. Extracts of banana (*Musa paradisiaca*) peel and tea leaves of Rooibos (*Aspalathus linearis)* infused with Buchu (*Agathosma betulina*) were the organic constituents used as reducing and capping agents during GZnO NPs synthesis. Validation of the formed GZnO NPs was done using; Ultraviolet-visible spectroscopy (UV-Vis), X-ray spectroscopy (XRD), Fourier-transform Infrared Spectroscopy (FTIR), High-resolution Transmission Electron Microscopy (HRTEM) with Energy-Dispersive X-ray spectroscopy (EDX) and **S**elected Area

Electron Diffraction (SAED), and High-Resolution Scanning Electron Microscopy with Energy-Dispersive Spectroscopy (HRSEM-EDS). The antifungal potential of the GZnO NPs against *C. albicans* was assessed using the modified Kirby-Bauer (disc diffusion) and Crystal Violet (CV) staining assays.

Results: The UV-Vis results revealed that GZnO NPs with have a peak at 290 nm, while HRTEM revealed cubic to spherical-hexagonal shaped GZnO NPs of diameter size 6.64 - 18.65 nm with moderate agglomerates. The average crystallite size calculated from the XRD is 13.22 nm. The average Candida growth inhibitory zones in response to the GZnO NPs exposure ranged between 12.94 and 30.44 mm. The CV assay revealed comparable antifungal potential between the GZnO NPs and the commercial antifungal agents, i.e. chlorhexidine and nystatin.

Conclusion: The GZnO NPs exhibited promising antifungal activity that was size- and concentration-dependent. Further, this report confirms the potential of banana peel and Buchu-infused Rooibos tea leaves for the synthesis of GZnO NPs in a straightforward, viable, and eco-friendly approach.

KEYWORDS

Agathosma betulina

Aspalathus linearis

Biofilm

Candida albicans

Denture stomatitis

Green synthesis (phytosynthesis)

Green Zinc Oxide Nanoparticles (GZnO NPs)

Musa paradisiaca

Nanoparticles (NPs)

Oral candidiasis

Single pot synthesis (one-pot synthesis)

Zinc oxide nanoparticles (ZnO NPs)

DECLARATION

I do hereby affirm that the Research Report **"Green Synthesised Zinc Oxide Nanoparticles and their Antifungal Effect on *Candida albicans* Biofilms"** is submitted to the Department of Restorative Dentistry, Faculty of Dentistry, University of the Western Cape (UWC). The report is an authentic document of an original and bona fide research project investigated by me under the supervision of Doctor Razia Adam (Department of Restorative Dentistry, UWC) and Professor Fanelwa Rachel Ajayi (SensorLab, Department of Chemistry, UWC).

Date: 06th August 2020

Place: University of the Western Cape, SA

Signature: 

DEDICATION

To my beloved parents, Vincent and Philomena Lyimo, your love and inspiration motivate and invigorate my spirit each day. You are the anchor I needed to face each day on this journey! My heart pours out love and immense gratitude for having the most thoughtful and loving parents!

To those who shall gather some new insights from it!

ACKNOWLEDGEMENTS

With deep respect expressed to Dr Razia Adam and Professor Fanelwa Ajayi, I am sincerely thankful for the guidance and mentorship. Your thoughtful criticism is well appreciated.

Appreciation is also extended to Professor Jose Frantz, the esteemed office of DVC, Research and Innovation, UWC, for laboratory material support. I sincerely appreciate the support and collaboration of the SensorLab members, Department of Chemistry, UWC, that ensured a pleasant and fruitful working experience.

I convey my deep sense of appreciation to Mr Ernest Maboza, Head of the Oral and Dental Research Institute (ORDI), UWC, for his tireless support. Sincere thankfulness goes to Professor Herman Kruijsse, ODRI, for data analysis consultancy services. Nokwanda Ngema (PhD incumbent, SensorLab), and Bih Chendi (PhD incumbent, Immunology Research Lab., SU), thank you for sharing Origin and GraphPad software whenever needed. To Mr Adrian Du Plooy, Division for Postgraduate Studies (DPGS), UWC, I acknowledge the writing fellowship grant that afforded the editorial services of Anneke Brand (PhD).

I sincerely appreciate the kind assistance that Miss Yolanda Mphentshu and Ms Reneda Basson granted whenever at ODRI.

Irene Nyamu, Nokwanda Ngema, Andisa Jamile (Dr), Joy Mwaniki, Ndiboho Thenjekwayo, Phoene Mesa Oware, Munyaradzi Mapfumo, Ida Nyangilisa Anyango Okeyo, and Carola Jacobs, thank you for sharing fond memories, treasured for a lifetime!

Last but not least, my heartfelt appreciation goes to my family, whose unwavering encouragement, support, and loving motivation keep me going. Thank you for all the sacrifices made, forever indebted!

Above all, I am utterly grateful to The Almighty God for His venerable grace, good health, opportunities, and the enormous blessings from His bounty, experienced on this journey!

Submitted by: Dr Germana Vincent Lyimo, Student Number: 3714367

CONTENTS

LIST OF FIGURES

LIST OF TABLES

ABBREVIATIONS

Ag	Silver
AIDS	Acquired Immunodeficiency Syndrome (AIDS)
Au	Gold
BHI	Brain Heart Infusion (BHI)
BPE	Banana Peel Extract
C	Carbon
CFU	Colony-Forming Units
CHX	Chlorhexidine
Cu	Copper
CuO	Copper Oxide
CV	Crystal Violet
DS	Denture Stomatitis
EDS	Energy-Dispersive Spectroscopy
EDX	Energy-Dispersive X-ray Spectroscopy
FE-SEM	Field Emission Scanning Electron Microscopy
FTIR	Fourier-transform Infrared Spectroscopy
HRSEM	High-Resolution Scanning Electron Microscopy
HRSEM-EDS	High-resolution Scanning Electron Microscopy with Energy-Dispersive Spectroscopy
HRTEM	High-Resolution Transmission Electron Microscopy
HRTEM-EDX	High-Resolution Transmission Electron Microscopy with Energy-Dispersive X-Ray
JCPDS	Joint Committee of Powder Diffraction Standards
K	Potassium

KBr	Potassium Bromide
MHA	Mueller-Hinton Agar
MIC	Minimum Inhibitory Concentration
MO NPs	Metal Oxide Nanoparticles
NPs	Nanoparticles
OD	Optical Density
ODRI	Oral and Dental Research Institute
PBS	Phosphate-Buffered Saline
PDT	Photodynamic Therapy
PLWH	People Living with HIV/AIDS
PMMA	Polymethyl Methacrylate
ROS	Reactive Oxygen Species
SAED	Selected Area Electron Diffraction
SEM	Scanning Electron Microscopy
STDEV	Standard Deviation
TEM	Transmission Electron Microscopy
TiO_2	Titanium Oxide
UV-Vis	Ultraviolet-visible Spectroscopy
XRD	X-ray Diffraction
Zn	Zinc
ZnO	Zinc Oxide
$Zn(NO_3)_2$	Zinc Nitrate
$Zn(NO_3)_2 \cdot 6H_2O$	Zinc Nitrate Hexahydrate

SYMBOLS AND SIGNS

β	Beta
cosθ	Cosine theta
°C	Degrees Celsius
g	Gram
g/mol	Grams per mole (molar mass)
keV	Kilo electron-volt
meV	Millielectron-volt
ml	Millilitre
µL	Microlitre
mm	Millimetre
MM	Molar mass
nm	Nanometre
%	Percent
®	Registered
λ	Wavelength

CONFERENCE PARTICIPATION

1. Poster presentation titled: "*Aspalathus linearis* and *Musa paradisiaca* mediated zinc oxide nanoparticles against fungal pathogens" at the First African Chapter of the established **"International Conference on Surfaces, Coatings and Nanostructured Materials (NANOSMAT-Africa)"** held in Cape Town, South Africa, 19-23 November 2018.

2. Oral presentation titled: "Antifungal effects of zinc oxide nanoparticles (ZnO NPs) on *Candida albicans* biofilm" at the **Dentistry Faculty Research Day**, UWC, 15th May 2019.

3. Poster presentation titled: "Electroanalysis of *Aspalathus linearis* and *Musa paradisiaca* mediated zinc oxide nanoparticles against fungal pathogens" at the **70th Annual International Society of Electrochemistry (ISE) Meeting, "Electrochemistry: Linking Resources to Sustainable Development",** held in Durban, South Africa, 4-9 August 2019.

4. Poster and oral presentations titled: "Novel Green Bioinspired Zinc Oxide Nanoparticles (ZnO NPs) against *Candida albicans*" at the **International Association for Dental Research (IADR) South African Division Annual Meeting**, held in Pretoria, South Africa, 12-13 September 2019.

5. Oral presentation titled: "The electrochemical and antifungal effects of *Musa paradisiaca* and *Aspalathus linearis* zinc oxide nanoparticles" at the **5th International Symposium on Electrochemistry,** "**Electrochemistry at Nanostructured interfaces"**, organised by ElectroChemSA, in Cape Town, South Africa, 11-14 August 2019.

INTRODUCTION

Currently, fungal infections afflict more than a billion individuals globally (Bongomin *et al.*, 2017; Marquez & Quave, 2020). Every year, fungal infections cause 1.6 million deaths (Tiew *et al.*, 2020), with opportunistic infections being reported the most reported (Tiew *et al.*, 2020). In the oral cavity, Candida species act as commensal yeasts, which, under predisposing systemic and/or local circumstances, can be responsible for a wide variety of clinical manifestations, collectively termed as oral candidiasis. The annual global incidences of mucosal (oral and oesophageal) Candida infections are about 2 000 000 and 1 300 000, respectively (Bongomin *et al.*, 2017). Mucosal candidiasis is among the most prevalent fungal infections and mostly occurs as a consequence of multiple chronic systemic diseases and conditions. For instance in individuals with weakened immune systems (cancer, stem cell and organ transplant recipients), the immunosuppressed, and people living with HIV/AIDS (PLWH) (Coogan *et al.*, 2005; Fourie *et al.*, 2016; Hellstein & Marek, 2019; Klein *et al.*, 1984; Lalla *et al.*, 2013; Lewis & Williams, 2017; Patton, 2013). Notably, *Candida albicans* has also been reported to cause dysbiosis of the resident mucosal bacterial microbiota, thereby increasing the risk for invasive fungal infections (Bertolini *et al.*, 2019; Bertolini & Dongari-Bagtzoglou, 2019; Janus *et al.*, 2017; Kilian *et al.*, 2016; Pellon *et al.*, 2020).

The serious current burden of fungal infections in Africa has been documented in multiple reports (Badiane *et al.*, 2015; Dunaiski & Denning, 2019). In Malawi, oral candidiasis was reported to be the most common opportunistic infection in PLWH (Kalua *et al.*, 2018). Ghana, Mozambique, and Congo reported 27100, 260025, and 12320 collective mucosal candidiasis cases, respectively (Amona *et al.*, 2020; Ocansey *et al.*, 2019; Sacarlal & Denning, 2018). In Senegal, oral candidiasis was prevalent in about 53% of individuals with opportunistic fungal infections in 2015 (Badiane *et al.*, 2015). Collectively, in other parts of Africa, estimates of

oral Candida infections affect a significant number of individuals. For instance: Ethiopia, 76 300 (Tufa & Denning, 2019); Nigeria, 253 000 (Oladele & Denning, 2014); South Africa, 828 666 (Schwartz *et al.*, 2019); Tanzania, 81051 (Faini *et al.*, 2015); and in Kenya the estimated prevalence of oral thrush was 768 in 100 000 in PLWH (Guto *et al.*, 2016).

Oral candidiasis is a biofilm-associated infection and remains one of the biggest challenges in health care afflicting most communities of all age groups worldwide (Cavalheiro & Teixeira, 2018; Nett & Andes, 2020). Biofilms are communities of microbes that attach to surfaces where they aggregate and produce an extracellular polymeric substance that ensures their survival (Holt *et al.*, 2017; Nett & Andes, 2020; Sheppard & Howell, 2016). Biofilm-related infections such as oral candidiasis could lead to severe problems in both industrial and clinical settings (Kernien *et al.*, 2018; Nobile & Johnson, 2015). Additionally, global climatic and environmental changes can lead to terrestrial fungal species causing diseases in humans (Fisher *et al.*, 2012; Garcia-Solache & Casadevall, 2010).

Candida albicans is the most prevalent fungal pathogen and is responsible for a significant proportion of oral candidiasis cases (Guinea, 2014; Vila *et al.*, 2020). The association of Candida with other microbes, the existence of complex multispecies biofilms (Nett & Andes, 2020), and the development and shifts in health care practices can contribute to the development of new drug-resistant strains of fungi (Vanden Bossche *et al.*, 1998; Cavalheiro & Teixeira, 2018; Jensen, 2016). The earlier make the treatment of candidiasis reasonably complicated. *C. albicans* has been implicated in the initiation of proinflammatory cytokine production that is an important etiological factor responsible for oral cancer development (Bakri *et al.*, 2010). New evidence has suggested an association between oral cancer and periodontal disease, and inflammatory cascades as a result of a chronic disease process that

could be the main causing factor in both pathologies (Gholizadeh *et al.*, 2016; Verma *et al.* 2018). Understanding the relationship between oral microbiome epidemiology and Candida virulence (Seneviratne *et al.*, 2008) as well as their susceptibility is essential in order to carry out practical diagnostic actions. Henceforth, govern the crucial measures for improvement in disease management and treatment outcomes for candidiasis (Chattopadhyay *et al.*, 2019).

To date, in developing nations, communities suffer from numerous non-communicable diseases, including oral candidiasis. Elderly patients with diabetes mellitus have a 4.4-fold risk to develop oral candidiasis as compared with diabetes mellitus-free individuals (Bianchi *et al.*, 2016). Furthermore, a positive association has been reported between oral candidiasis in elderly users and non-users of dental prosthesis and its predisposing factors. Importantly, the use of oral prosthetics and poor oral hygiene in elderly individuals predispose them to the development of oral candidiasis (Altarawneh *et al.*, 2013; Bianchi *et al.*, 2016; Contaldo *et al.*, 2019; Javed *et al.*, 2017). Appropriate oral hygiene measures are paramount for the treatment and prevention of possible reinfection. In case of severe clinical symptoms or as prevention for complications in immunocompromised individuals, topical and/or systemic therapeutic options for oral candidiasis can be administered (Millsop & Fazel, 2016; Lalla *et al.*, 2013; Schiefersteiner *et al.*, 2019). The burden of chronic systemic conditions combined with the introduction of drug-resistant strains and changes in hosts' local oral factors contribute to increasing oral candidiasis incidences. Thus warrants a need for exploration of alternative fungal therapeutics (Cavalheiro & Teixeira, 2018; Girardot & Imbert, 2016b; de Oliveira Santos *et al.*, 2018). For instance, the utilisation of phytochemicals (flavonoids) in the inhibition of dental plaque associated with microbial organisms causing dental caries (Gutiérrez-Venegas *et al.*, 2019).

Nanotechnology offers unique applications as the most rapidly emerging field in technology, allowing various consumer and biomedical solutions. The minute size of the nanoparticles (NPs), coupled with the large surface area per unit volume convey features that can be beneficial in antimicrobial applications (Agarwal *et al.*, 2018; Benelli, 2019; da Silva *et al.*, 2019a). For instance, a nano-based conventional disinfectant has been proposed to combat oral Candida biofilm infections (Rodrigues *et al.*, 2016). Apart from the application of nanotechnology to modify dental materials. Other dental and clinically related applications of nanoparticles include in anti-inflammatory agents, treatment of periodontitis, antimicrobial infections, hypersensitivity, prevention of remineralising agents in dental caries, and dentifrices (Carrouel *et al.*, 2020; Castillo *et al.*, 2019; Monteiro *et al.*, 2015). Of relevance to this study, green synthesis of zinc oxide (ZnO) NPs and exploration of their potential antifungal activity was considered a practical and cost-effective approach.

The above evidence supports the need to promote eco-friendly methods for synthesising ZnO NPs devoid of contaminants and hazardous by-products. In this study, the "green synthesised zinc oxide nanoparticles", hereon referred to as "GZnO NPs", were synthesised for the first time using banana peel and Buchu-infused Rooibos extracts. Other "green ZnO NPs" formulated using other natural ingredients in referenced studies are referred to as "green-mediated ZnO NPs". Finally, the antifungal properties of the formulated GZnO NPs in this study were studied against *C. albicans* ATCC 90028.

CHAPTER ONE – Literature review

1.1 Nanotechnology

Nanotechnology is defined as the study and use of structures between 1 nanometer (nm) and 100 nm in size. The word "nano" is derived from the Greek word "nannos", meaning "dwarf", and literally means one-billionth of physical size (Elhissi & Subbiah, 2019; Hong, 2018; Hornyak *et al.*, 2018; Makhlouf & Barhoum, 2018; Ozak & Ozkan, 2013; Sanders, 2018).

Nanoparticles are broadly classified into two classes, namely organic and inorganic NPs. The organic NPs comprise carbon-based NPs, while the inorganic NPs comprise inert metal nanoparticles [e.g. gold (Au) and silver (Ag)], magnetic, and semiconductor [e.g., ZnO and titanium oxide (TiO_2)] NPs. Nanoparticles are further morphologically categorised as spherical, cubic, and needle-like, within the acceptable nanoscale range (Jeevanandam *et al.*, 2018). All these NPs have unique characteristics and are currently employed and vigorously explored in numerous disciplines of science and technology (Bhavikatti *et al.*, 2014).

1.2 Morphological and structural features of nanoparticles

The exact morphology of a NP is dependent on the methods of its synthesis. NPs can be acquired in different crystalline morphologies by specified deposition techniques, which presently remains a quite intriguing avenue of scientific research. For instance, ZnO NPs has a hexagonal crystal-like wurtzite structure upon microscopic assessment. Customarily, ZnO can exist in any of the following three distinctive crystalline forms: cubic rocksalt, cubic, and hexagonal wurtzite forms, and examples supporting the same are summarised in Table 1. The earlier occurs infrequently, and the latter (wurtzite) configuration is the most common and steady at ambient surroundings.

Table 1: Green-mediated methods for ZnO NPs using plants and their respective morphological descriptions

Plant common name and part extracted	**Plant (scientific name)**	**Size (nm)**	**Structure and/or shape(s)**	**Author(s)**
Dark opal basil (leaf extract)	*Ocimum basilicum L. var. purpurascens*	50 (XRD)	Hexagonal crystalline	Salam *et al.*, 2014
Rambutan (fruit peel extract)	*Nephelium lappaceum L.* (*Sapindaceae*)	50.95 (XRD)	Needle-like with agglomerates	Yuvakkumar *et al.*, 2014a
Brown marine macroalgae (aqueous extract)	*Sargassum muticum* (*S.muticum*)	30-57 (FESEM)	Hexagonal wurtzite	Azizi *et al.*, 2014
Rambutan (fruit peel extract)	*Nephelium lappaceum L.* (*Sapindaceae*)	50.95 (XRD)	Needle-like with agglomerates	Yuvakkumar *et al.*, 2014a
Neem (leaves)	*Azadirachta indica* (*Meliaceae*)	9.6-25.5 (TEM)	Spherical	Bhuyan *et al.*, 2015
Neem (fresh leaves)	*Azadirachta indica* (*Meliaceae*)	18 (XRD)	Spherical	Elumalai & Velmurugan, 2015
Aloe vera (leaf peel)	Aloe vera (*Liliaceae*)	25-65 (SEM and TEM)	Hexagonal, spherical	Qian *et al.*, 2015
Buchu (dry leaves)	*Agathosma betulina* (Rutaceae)	15.8 (TEM) 12-26 (HRTEM)	Quasi-spherical with agglomerates	Thema *et al.*, 2015b
Ginger (dry rhizome extract)	*Zingiber officinale (Zingeiberaceae)*	24.5 (XRD) 23-26 (SEM)	Spherical with agglomerates	Janaki *et al.*, 2015
Mexican mint (leaf extract)	*Plectranthus amboinicus* (*Lamiaceae*)	88 (SEM)	Rod with agglomerates	Fu & Fu, 2015
Kapurli (leaf extract)	*Anisochilus carnosus* (*Lamiaceae*)	56.14 (30 ml), 49.55 (40 ml), 38.59 (50 ml) (XRD) 30-40 (TEM) 20-40 (FESEM)	Quasi-spherical, hexagonal wurtzite	Anbuvannan *et al.*, 2015a
Bhuiamla, stone breaker (leaf extract)	*Phyllanthus niruri* (*Phyllanthaceae*)	25.61 (FESEM, XRD)	Hexagonal wurtzite, quasi-spherical	Anbuvannan *et al.*, 2015b

Plant common name and part extracted	**Plant (scientific name)**	**Size (nm)**	**Structure and/or shape(s)**	**Author(s)**
Rooibos (leaf extract)	*Aspalathus linearis*	1-8.5	Quasi-spherical	Diallo *et al.*, 2015
Indian Beech (fresh leaf extract)	*Pongamia pinnata* (*Fabaceae*)	26 (XRD) 100 (TEM)	Spherical, hexagonal, rod with agglomerates	Sundrarajan *et al.*, 2015
Rambutan (fruit peel extract)	*Nephelium lappaceum L.* (*Sapindaceae*)	25.67 (XRD) 25-40 (SEM)	Spherical with agglomerates	Karnan & Selvakumar, 2016
Aloe vera (leaf extract)	*Aloe Vera* (*Liliaceae*)	8-0 (XRD) 15 (XRD)	Spherical, oval, hexagonal	Ali *et al.*, 2016
Neem (fresh leaves)	*Azadirachta indica* (*Meliaceae*)	9-40 (XRD) 10-30 (TEM)	Hexagonal, nanobuds	Madan *et al.*, 2016
Jacaranda (flower extract)	*Jacaranda mimosifolia*	2-4 (XRD, TEM)	Spherical with agglomerates	Sharma *et al.*, 2016
Tomato Orange Grapefruit Lemon (peel)	*Citrus sinensis* *Citrus paradise* *Lycopersicon esculentum* *Citrus aurantifolia*	9.7±3 (TEM) 19.66, 12.55, 11.39, and 9.01 (XRD)	Hexagonal (wurtzite), crystalline, and polyhedral	Nava *et al.*, 2017a
Cumin Jeera	*Cuminum cyminum*	7 (TEM)	Spherical or oval	Zare *et al.*, 2017
Passifloraceae (fresh leaves)	*Passiflora caerulea*	37.67 (XRD) 30-50 (SEM)	Spherical	Santhoshkumar *et al.*, 2017
Moringa (dried leaves)	*Moringa oleifera* (*Moringaceae*)	12.27-30.51 (TEM)	Spherical, small rods	Matinise *et al.*, 2017a
Tea plant (dried leaves)	*Camellia sinensis*	17.47, 13.51, 10.34, and 9.04 (XRD) 8 ±.5 (TEM)	Spherical, hexagonal wurtzite crystal	Nava *et al.*, 2017b
Canadian Horseweed (leaves extract)	*Conyza canadensis* (*Asteraceae*)	___	Spherical	Ali *et al.*, 2018
Madagascar periwinkle (leaves extract)	*Catharanthus roseus*	50–92 (TEM)		Gupta *et al.*, 2018
Stevia (extract)	*Stevia rebaudiana (Asteraceae)*	10-90	Rectangular	Khatami *et al.*, 2018
Cape/swamp Lily (leaf extract)	*Crinum latifolium* (*Amaryllidaceae*)	10-30 (TEM)	Pleomorphic i.e. hexagonal, rod-like, rectangular, and spherical	Jalal *et al.*, 2018

Plant common name and part extracted	**Plant (scientific name)**	**Size (nm)**	**Structure and/or shape(s)**	**Author(s)**
Pinwheel flower (leaf extract)	*Tabernaemontana divaricata (Apocynaceae)*	20-50 (TEM)	Spherical, hexagonal wurtzite	Raja *et al.*, 2018
Oak trees (jaft extract)	*Quercus spp*. (*Proteaceae*)	34 (FESEM)	Spherical	Sorbiun *et al.*, 2018
Hill Glory Bower Wild Jasmine Country Mallow (aqueous extracts)	*Clerodendrum infortunatum Clerodendrum inerme Abutilon indicum*	16.72, 17.49, 20.73 (XRD)	Crystalline, spheroid-to-rod-like	Khan *et al.*, 2018
Gin berry (leaf extract)	*Glycosmis pentaphylla*	30 (XRD) 32-36 (SEM, TEM)	Hexagonal wurtzite	Vijayakumar *et al.*, 2018a
Wild Lime tree (leaf extract)	*Atalantia monophylla*	33.01 (XRD) 30 (TEM)	Spherical, hexagonal wurtzite	Vijayakumar *et al.*, 2018
Chavir (plant extract)	*Ferulago angulata* (*Apiaceae*)	32-36 (FESEM)	Spherical	Shayegan Mehr *et al.*, 2018
Painted Spiral Ginger (leaves)	*Costus pictus* (*Costaceae*)	20-80 (TEM)	Hexagonal, spherical, or rod-shaped	Suresh *et al.*, 2018
Pennyroyal (aqueous leaf extracts)	*Mentha pulegium L*	44.94 (XRD) 38-49 (FESEM) 40 (TEM)	Crystalline, Semi-spherical	Rad *et al.*, 2019
Cane Buckthorn (aqueous solution)	*Rhamnus virgata*	20 (XRD) 20-30 (TEM)	Triangular, hexagonal	Iqbal *et al.*, 2019
Alpine Almond (extract)	*Hydnocarpus alpina*	38.84 (XRD) 20-45 (FESEM) 45 (TEM)	Spherical, hexagonal (wurtzite) with agglomerates	Ganesh *et al.*, 2019
Ringworm bush (fresh leaf extract)	*Cassia alata*	60-80 (SEM)	Spherical with agglomerates	Happy *et al.*, 2019
Baikal skullcap (root extract)	*Scutellaria baicalensis* (*Lamiaceae*)	50 (FETEM)	Spherical	Chen *et al.*, 2019
Lebbek tree (stem bark extract)	*Albizia lebbeck (Fabaceae)*	66.25 (Zetasizer)	Irregular spherical with the presence of Zn, C, O, Na, P, and K	Umar *et al.*, 2019
Jackfruit banana (peel extract)	*Musa* species	14.93-25.78 (XRD)	Crystalline, hexagonal (wurtzite)	Abdol Aziz *et al.*, 2019

Plant common name and part extracted	**Plant (scientific name)**	**Size (nm)**	**Structure and/or shape(s)**	**Author(s)**
Yellow trumpetbush or Ginger thomas (leaf extract)	*Tecoma castanifolia (Bignoniaceae)*	70-75 (XRD)	Hexagonal phase of wurtzite, spherical	Sharmila *et al.*, 2019
Tasmanian blue gum (dried leaves)	*Eucalyptus globulus (Myrtaceae)*	52-70 (TEM)	Spherical, and some particles elongated	Ahmad *et al.*, 2020
Moringa (flower, seed, and leaf extracts)	*Moringa Oleifera (Moringaceae)*	Crystallite size 13.2, 13.9 and 10.8 respectively (XRD)	Pure Wurtzite (Hexagonal structure)	Ngom *et al.*, 2020
D. tortuosa (aerial parts extract)	*Deverra tortuosa (Apiaceae)*	9.26 - 31.18 (TEM)	Hexagonal phase, (wurtzite structure)	Selim *et al.*, 2020
Beetroot or garden beet, wild cabbage, ceylon cinnamon tree and Indian bay leaf respectively	*Beta vulgaris (Amaranthaceae), Brassica oleracea var. Italica, Cinnamomum verum (Lauraceae) and Cinnamomum tamala (Lauraceae)*	(20 – 47) ±2 (TEM)	Hexagonal phase	Pillai *et al.*, 2020
American basil (leaf extract)	*Ocium americanum* (*Lamiaceae*)	45-50 (TEM)	Hexagonal phase, (wurtzite structure)	Vidhya *et al.*, 2020
Sweet wormwood (stem bark extract)	*Artemisia annua* (*Angiospermae)*	20 (TEM)	Spherical with agglomerates	Wang *et al.*, 2020

Abbreviations: transmission electron microscopy (TEM), field emission TEM (FETEM) high-resolution TEM (HRTEM), scanning electron microscopy (SEM), field emission SEM (FESEM), X-ray diffraction (XRD)

1.2.1 Size and surface area of nanoparticles

One of the most critical advantages of NPs is their minute size (Albanese *et al.*, 2012; Nasrollahzadeh *et al.*, 2019; Sanders, 2018). The size influences the colour emission of nanocrystals upon light absorption. As NPs get smaller and smaller, they alter their crystalline behaviour such as their morphology and crystallinity. Due to their minute size, NPs have multidisciplinary applications in the fields of aerospace, biotechnology, computer science, defence, electronics, environmental science, energy, food science, materials science, medical

science, pharmaceutical science, and transportation (Flores *et al.*, 2020; Singh *et al.*, 2019; Sun *et al.*, 2018; Villanueva-; Zare *et al.*, 2017). The smaller the size, the larger the surface area, which contributes to cellular interactions, improved binding to its surfaces, and toxic manifestation (Agarwal *et al.*, 2018; Holgate, 2010; Husen, 2019; Pasquet *et al.*, 2014). Significantly, the increased surface area influences the antimicrobial effectiveness and contributes to enhanced surface reactivity (da Silva *et al.*, 2019a; Mohanan *et al.*, 2017). As the features of a NP are almost entirely size-dependent, as opposed to their micro or macro-sized counterparts (Khan & Javed, 2018). The NP size also influences spectroscopic, electromagnetic, as well as chemical interaction behaviours (Hoshyar, *et al.*, 2016; Nasrollahzadeh *et al.*, 2019; Sanders, 2018). Also, as the particles approach nano-size, the saturation of atomic molecules on the material's surface begin to influence the characteristics of the material profoundly (Villanueva-Flores *et al.*, 2020).

The characteristic properties and behaviour of most conventional materials are altered once reduced and converted to NPs (Bandeira *et al.*, 2020). In contrast to micro- or macroparticles, the architectural morphology of NPs influences their large surface area per weight ratio. As a result, they are more reactive than other molecules. The size-related features of nanomaterials enhance their efficiency and new functionalities are achievable for a broad spectrum of nano-products including NPs (Husen & Siddiqi, 2014; Nasrollahzadeh *et al.*, 2019; Siddiqi & Husen, 2016). For instance, the size of ZnO NPs have been shown to influence the antimicrobial activity, and smaller NPs were found to be more toxic to microorganisms (da Silva *et al.*, 2019a). Therefore, size contributes significantly to the unique features of NPs as opposed to their larger counterparts (Khan & Javed, 2018). The existing evidence indicates that there is no single optimum (universal) size for nanoparticle uptake because an ideal size of nanoparticulate is cell-dependent (Villanueva-Flores *et al.*, 2020). Nonetheless, the majority of studies have

recommended a diameter of 50 nm to be an acceptable dimension for significant uptake of NPs (Katas *et al.*, 2019).

1.2.2 Shape of nanoparticles

During NP(s) synthesis, the concentration and type of the stabilising and reducing agent, as well as the reaction temperature of the reacting solution influenced the final product in terms of, for example, size and shape (Bandeira *et al.*, 2020). The shape of NPs has been described as an essential determinant of the physical, chemical, and structural properties. Shape tremendously influenced cellular uptake, bioavailability, and bio-distribution, which subsequently affects its *in vivo* performance (da Silva *et al.*, 2019a; Flores *et al.*, 2020; Hoshyar *et al.*, 2016; Jindal, 2017; Villanueva-; Khatami *et al.*, 2018;). Moreover, the shape of NPs influences their interaction with cells in different ways. For instance, spherical NPs have been studied to assess the effect and performance in relation to the size of the nanomaterials synthesised. Any alteration pertaining to reducing or stabilising agents will govern the formulation of NPs (Bandeira *et al.*, 2020; Husen & Iqbal, 2019).

For instance, for the synthesis of spherical NPs, a stabilising agent must cover the entire surface of the nanoparticulate. Also, an increase in temperature increases the mean adsorption of capping atomic molecules on the NPs' surface. The shape acquired upon synthesis dictates the interaction, function, and other essential features such as the optical properties of the NPs (Albanese *et al.*, 2012; Nasrollahzadeh *et al.*, 2019). Spherical, ovoid, crystalline, rod-like, and hexagonal ZnO NPs have been documented by Ahmed *et al.* (2017). Plant extracts, enzymes, or proteins are the biological constituents responsible for reducing and stabilising NPs, including ZnO NPs, in biogenic synthesis methods (Ahmed *et al.*, 2017; Bandeira *et al.*, 2020;

Basnet *et al.*, 2018). As a focus of this study, a summary of numerous plant products utilised in formulating green-mediated ZnO NPs and their subsequent shapes are tabulated in Table 1.

1.2.3 Optical features of nanoparticles

Optical features of NPs such as reflection, transmission, optical absorption, wide band gap, transparency, and photoluminescence in the visible and near ultraviolet range of the light spectrum are influenced by the size, aggregation state, shape, and local environment. Size-dependent optical features can be detailed for metal with strong ultraviolet-visible spectroscopy (UV-vis) high exciton band gap of (3.37 eV) and a high exciton binding energy (60 meV) at room temperature something not common in bulk metal (Khan & Javed, 2018; Nasrollahzadeh *et al.*, 2019). Nanoparticles possess interesting optical properties, due to their minute structure that enables them to restrict and contain electrons and subsequently propagate quantum properties. Nanoparticles are also suitable for a variety of biomedical applications because of their size and surface characteristics, site-specific targeting ability, regulated release, and particle degradation properties that are readily modulated. Thus NPs can have drug-loading abilities which allow their incorporation into biological or biomedical systems without propagating chemical reactions (Bhavikatti *et al.*, 2014; Vijayalakshmi & Kumar, 2006; Villanueva-Flores *et al.*, 2020).

1.2.4 Agglomeration of nanoparticles

The loose assembling of NPs in a suspension is referred to as agglomeration. A simple mechanical force can disassemble agglomerates. On the other hand, aggregation signifies a definite clubbing phenomenon of molecules or atoms. Forces that hold agglomerates together are usually van der Waals (weak) forces, while those that hold molecules or atoms together in aggregates are stronger chemical bonding forces. Agglomeration presents a mechanism that

destabilises the colloidal systems. In an aggregated state, dispersed particles in aqueous state clump onto each other, spontaneously formulating irregular clusters (Nasrollahzadeh *et al.*, 2019). Therefore, agglomeration and aggregation are dependent on the strength of binding forces as well as a high surface area in an aqueous state. For instance, the studies listed in Table 1 have shown that the formation of agglomerates is not uncommon during the phytosynthesis of ZnO NPs.

The shape influences the mechanism of particle uptake by cells. Other influencing features are size, surface energy, composition, as well as the agglomeration behaviour of the particle of interest (Ashraf *et al.*, 2018; Halamoda-Kenzaoui *et al.*, 2017; Nasrollahzadeh *et al.*, 2019). Although it is yet to be detailed in the literature, agglomeration is nonetheless among the crucial factors governing the performance of NPs in the aqueous state. Interestingly, it was highlighted that increased agglomeration enhanced cellular uptake, with a definite influence on biological reaction (Halamoda-Kenzaoui *et al.*, 2017; Hoshyar *et al.*, 2016). Other factors that can influence agglomeration include temperature, pH, ionic strength, and mixing rate. At a higher pH, negatively charged NPs form agglomerates because of a high salt composition in the solution.

1.2.5 Additional features of nanoparticles

The basic structure of a NP is illustrated in Figure 1 below. Additional features that influence NP's cellular uptake include hydrophobicity, concentration, surface status (e.g. roughness, presence of defects, photo-excited holes, oxygen vacancies), catalytic ability, and charge (Camarda *et al.*, 2016; Fierascu *et al.*, 2019; Janotti & Van De Walle, 2009; Nasrollahzadeh *et al.*, 2019).

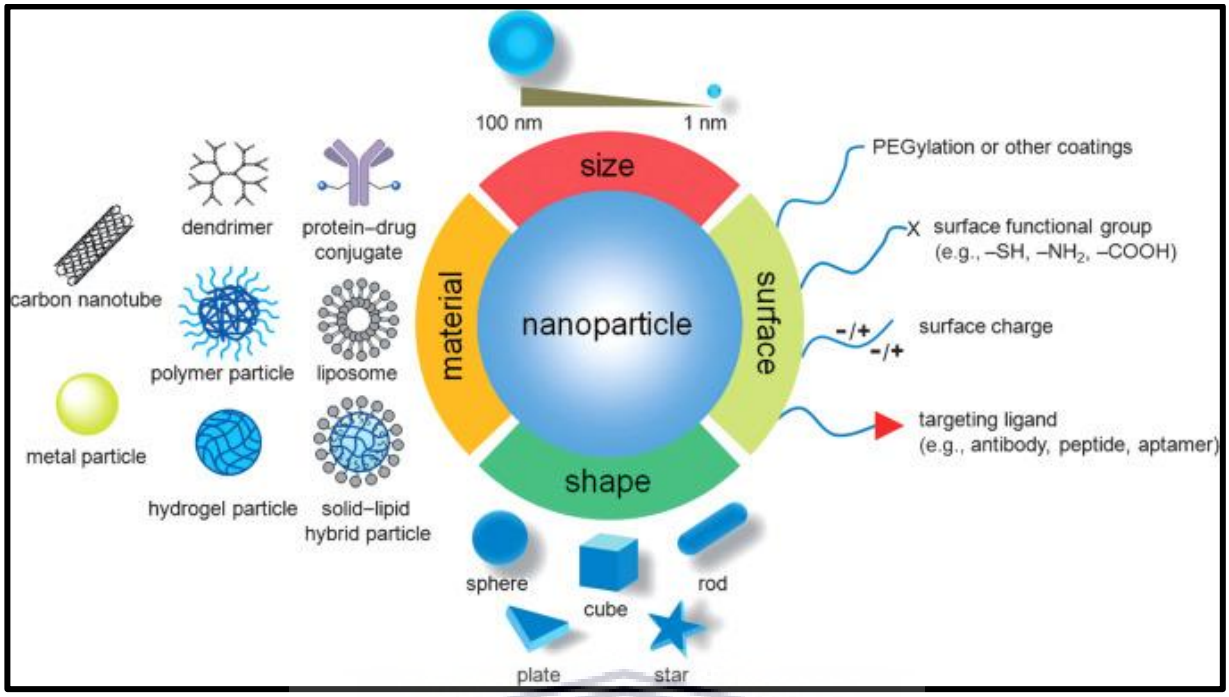

Figure 1: Basic illustration of the structure of a nanoparticle (from Heinz *et al.*, 2017)

1.3 Biomedical applications of nanoparticles

Metal oxide nanoparticles (MO NPs) efficiently control and inhibit the growth of a broad spectrum of Gram-negative and -positive microorganisms (Hoseinzadeh *et al.*, 2016; Kadiyala *et al.*, 2018; Kanwar *et al.*, 2019; Sánchez-López *et al.*, 2020). The development of these MO NPs offer promising biomedical, as well as antimicrobial agents. The subsequent agents can be employed in combating prevailing microbial drug resistance and increased biofilm-associated infections (Allaker & Yuan, 2019; Baptista *et al.*, 2018; Dizaj *et al.*, 2014; Kadiyala *et al.*, 2018; Khan & Javed, 2018; Mahamuni-Badiger *et al.*, 2019; Raghunath & Perumal, 2017; Sánchez-López *et al.*, 2020; Vallet-Regí *et al.*, 2019). Biofilm-related oral infections can also be fought (Vargas-Reus *et al.*, 2012).

Metal oxide NPs that are well-documented for their potential antibacterial include, but are not limited to, Ag, TiO_2, copper oxide (CuO), iron oxide (Fe_3O_4), and ZnO, among others (Agarwal *et al.*, 2018; Vallet-Regí *et al.*, 2019; Sánchez-López *et al.*, 2020;). The biological effectiveness

of metallic and MO NPs is hypothesised to be related to their large surface area rendered by their minute size, thus ensuring their close interaction with contact surfaces, including microbial membranes. These close interactions can enhance the antimicrobial effect. Apart from their antimicrobial activity, another interesting aspect of NPs in terms of biomedical potential is their anticancer ability, particularly for the green-mediated NPs (Kalpana & Rajeswari, 2018; Kanwar *et al.*, 2019; Karmous, Pandey *et al.*, 2019).

The distinct structure and characteristics of ZnO NPs make it suitable for the numerous applications in the biomedical sciences, as illustrated in Figure 2. Some of the highlighted applications include, but are not limited to, antibacterial, antifungal, antiviral and anticancer (Agarwal *et al.*, 2018, 2019; Jiang *et al.*, 2018; Kamonkhantikul *et al.*, 2017; Khezerlou *et al.*, 2018; Mishra *et al.*, 2017; Sánchez-López *et al.*, 2020). Recently, ZnO-based nanostructures, including composites, have been successfully applied to medical devices and were assessed for its antibacterial and anti-biofilm properties (Akbar *et al.*, 2020; Mahamuni-Badiger *et al.*, 2019).

Various antimicrobial effects and mechanisms of metal and MO NPs, including ZnO NPs, have been summarised in recent reviews of literature (Azizi-lalabadi *et al.*, 2019; da Silva *et al.*, 2019a; Król *et al.*, 2017; Mohanan *et al.*, 2017; Sánchez-López *et al.*, 2020). Azizi-lalabadi *et al.* (2019) elaborated that the particle size, type, and shape of the NPs are crucial factors towards ensuring antimicrobial effectiveness. Furthermore, the application of NPs as antimicrobial agents in biomedical sciences is a potential strategy to overcome pathogenic and resistant microorganisms. Besides, ZnO NPs is relatively affordable, safe, and biocompatible as compared to other MO NPs compounds (Agarwal *et al.*, 2017; Cierech *et al.*, 2019; Jiang *et al.*, 2018; Kalpana & Rajeswari, 2018; Madhumitha *et al.*, 2016; Padovani *et al.*, 2018;

Raghunath & Perumal, 2017; Zare *et al.*, 2017), which further supported its application in this study.

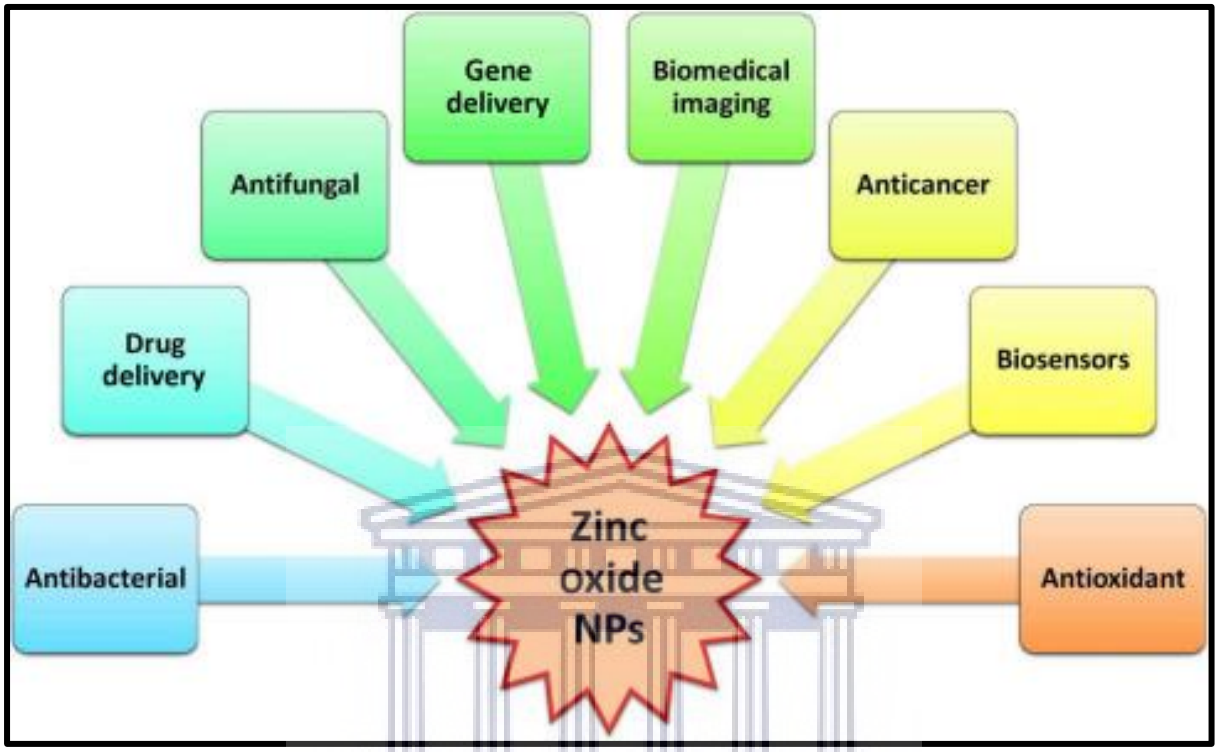

Figure 2: Biomedical applications of zinc oxide nanoparticles (ZnO NPs) (from Rajeshkumar, *et al.*, 2019)

1.4 Dental application of nanoparticles

In the oral cavity, live bacteria, viruses, and yeast aggregate in common matrices (biofilms). The oral biofilm form as a result of the aggregation of microorganisms (microbial cell adherence to each other and onto different substrates and surfaces). Up to 1000 different species of mixed microbes exist in about 10^8 to 10^9 cells per ml of saliva or per mg plaque, and 50% of it can be cultured (Deo & Deshmukh, 2019; Huttenhower *et al.*, 2012). The prevention and treatment of oral infections that are biofilm-related is still a challenge. In the oral cavity, locally applied (topical) regimens can be rapidly cleansed by salivary. They are thus leading to reduced desired efficacy, adequate substantivity (retention on tooth surfaces) and penetration into the

polysaccharide matrix to combat progressive biofilm initiation and maturation. Further, oral biofilm lowers oral pH, rendering a more acidic environment which impedes the efficacy of many antimicrobials (Benoit *et al.*, 2019). The altered microenvironment in the biofilm hinders drug substantivity and subsequently triggers antibiotic tolerance. Thus, for most antimicrobial agents to be effective, repeated use over an extended period with minimum toxicity is necessary.

Recent regimens for the management of oral biofilm-related diseases are restricted to wide-spectrum and long-term antimicrobial regimens. For example, the long-term use of chlorhexidine (CHX) mouthwash has been associated with side effects. These include staining of teeth, restorations, dorsum of the tongue and mucosa epithelium, an increase of calculus formation (Addy *et al.*, 1982; Slot *et al.*, 2014; Supranoto *et al.*, 2015; Zanatta *et al.*, 2010), and more rarely oral mucosa desquamation and parotid swelling (Zanatta *et al.*, 2010). Therefore, this regimen may not be prescribed for long-term daily use. Alternative antimicrobial and anti-biofilm agents consist of organic regimens such as essential oils and flavonoids that disturb accumulation of cariogenic biofilms and/or lower the production of extracellular polysaccharides. These alternative regimens influence the production of oral acid, the viability of certain organisms, such as *Streptococcus mutans* and its acid tolerance, and the acidic pH synthesis of the polysaccharide matrix (Benoit *et al.*, 2019). Therefore, these alternatives might have a positive effect on efficacy by improving; substantivity, solubility, bioavailability, and infiltration of the polysaccharide matrix.

For the past few decades, dissemination and propagation of resistant pathogenic microbes (bacteria, fungi, and viruses) have led to significant health and food safety challenges. At present, nanotechnology, with emphasis on NPs, is acknowledged as a feasible alternative

method to counteract this challenge as NPs have innate antimicrobial potential when combined with or synthesized from the correct antimicrobial agent (Baptista *et al.*, 2018; Hoseinzadeh *et al.*, 2016; Khezerlou *et al.*, 2018; Król *et al.*, 2017; Mohanan *et al.*, 2017; Raghunath & Perumal, 2017; Vallet-Regí *et al.*, 2019). The use of nanotechnology extends the prospect to inhibit biofilm formation and development through the application of NPs with biocidal, anti-adhesive, and drug delivery capabilities. Physicochemical and material features such as shape, charge, and size can also be manipulated to guarantee suitable NPs synthesis and increase anti-biofilm effectiveness (Allaker, 2010; Benoit *et al.*, 2019; Hu *et al.*, 2019; Mahamuni-Badiger *et al.*, 2019).

The application of nanotechnology in the biomedical and dental sciences is intensely studied with the objectives of disease diagnosis and prevention (AlKahtani, 2018; Allaker & Memarzadeh, 2014; Ficai *et al.*, 2016; Melo *et al.*, 2013; Ozak & Ozkan, 2013). Of interest to dentistry, nanotechnology is currently explored and applied, as described by Khurshid *et al.* (2015) and tabulated in Table 2 below. Other additional nanotechnological innovation applications being the manufacture of dentifrices and related oral personal care product.

Table 2: Nanotechnology applications in dental sciences (from Khurshid *et al.*, 2015)

Nanotechnology	**Applications in Dentistry**
Nanocomposites and nanoclusters	Local anaesthesia
Nano-glass ionomer (light curable)	Hypersensitivity cure
Impression materials (nano-based)	Tooth regeneration
Bone replacement types of cement (nano-based)	Orthodontic treatment nanorobotics
Nanoencapsulation	Nano diagnosis
Nanoneedles	Oral tissues biomimetic
Nanoparticle coating in implants	Endodontic regeneration
	Impression materials

Extensive application of nanoparticles in dentistry has been on their incorporation in dental restorative materials to improve the physicochemical properties of these materials (Ferrando-Magraner *et al.*, 2020). Most of the studies reported on the varied NPs in dentistry utilised the conventional NPs, including ZnO NPs but not green-mediated ZnO NPs (refer to Table 3, below). Recently, NPs have been incorporated into the denture acrylic and resilient denture liners used in prosthodontics to prevent Candida infections (AlKahtani, 2018; Cierech *et al.*, 2016b; Gad *et al.*, 2016). In another study, Cierech *et al.*, (2019) incorporated conventional ZnO NPs into PMMA, and a (PMMA)-ZnO nanocomposite was developed. Then the release of ions from the PMMA and the generation of a ZnO NPs layer on the pure PMMA was studied. Further, Cierech *et al.*, (2019) also assessed the impact of their final conventional ZnO NPs concentration on cytotoxicity and the prospective application as an alternative material to conventional acrylic denture bases.

Today, nanotechnology is an interdisciplinary and emerging field in medical and dental sciences (Shashirekha *et al.*, 2017; Ferrando-Magraner *et al.*, 2020). By designing nano-based materials, researchers are capable of mimicking some of the structural and mechanical features of biological tissue and thus promoting bio integration. Examples of studies that utilised metals and MO NPs, including ZnO for modification of dental materials, are tabulated in Table 3. Most of these studies were conducted *in vitro*, except for the research by (Gutiérrez *et al.*, 2019), in which both *in vivo* and *in situ* approaches were employed when applying the ZnO NPs. In most studies, the physicochemical properties of materials were assessed after modification using conventional ZnO NPs. Other applications were explored for oral anticancer (tongue cancer) potential with promising prospects (Wang *et al.*, 2018). However, few studies have reported on the use of green-mediated ZnO NPs for the modification of dental materials.

Table 3: Dental material modification and other dental-related applications using conventional or green-mediated ZnO NPs

Synthesis methods	**Targeted application (dental material modification)**	**Important findings**	**Characteristics of nanoparticles**	***In vitro* or *in vivo***	**Author(s)**
Conventional ZnO NPs	Modification of composites using ZnO NPs and determination of physicochemical characteristics and antibacterial potential against *Streptococcus mutans*	Improved antibacterial potential and physicochemical characteristics (flexural strength and compressive modulus) against *Streptococcus mutans*	Hexagonal crystal structure, average 20 nm, purity 99.8%	*in vitro*	Tavassoli-Hojati *et al.*, 2013
Conventional ZnO NPs	Determination of a system of coating with ZnO NPs to prevent adherent bacterial activity and promote osteoblastic activity	Optimal nano-ZnO coating (biocompatible with antimicrobial potential) can be applied to improve future bone implants		*in vitro*	Memarzadeh *et al.*, 2015
Conventional Ag, ZnO, and TiO NPs	Effect of Ag, ZnO, and TiO NPs on SBS		21±5 nm (average)	*in vitro*	Reddy *et al.*, 2016
Conventional ZnO NPs	Effect of adding ZnO NPs to dental adhesives on their antimicrobial and bond strength properties	Modification of dental adhesives did affect bond strength properties	Crystalline, 20 nm	*in vitro*	Saffarpour *et al.*, 2016
Conventional ZnO NPs	Incorporation of ZnO NPs to modify root canal filling and sealing materials to improve physicochemical characteristics and optimal functioning	ZnO NPs improved: setting time, solubility, flowability, dimensional stability, and radiopacity of Grossman sealer	20 nm	*in vitro*	Versiani *et al.*, 2016
Conventional ZnO NPs	ZnO NPs incorporated into acrylic resin used to produce denture bases.	SEM-EDS analysis: successful introduction of ZnO NPs into acrylic resin Biomaterial roughness: not statistically	30 nm	*in vitro*	Cierech *et al.*, 2016

Synthesis methods	**Targeted application (dental material modification)**	**Important findings**	**Characteristics of nanoparticles**	***In vitro* or *in vivo***	**Author(s)**
		significantly different before and after incorporation of the NPs			
Conventional ZnO NPs and CHX	Comparison of 0.12% CHX and ZnO NPs on the μSBS of dentin with a 5th generation dental adhesive system upon acid etching	Pre-treatment with nZnO or CHX separately and simultaneously did not affect the MSBS of the 5th generation dental adhesive		*in vitro*	Alaghehmad *et al.*, 2018
Conventional ZnO NPs	Determination of anticancer potential of ZnO NPs on human tongue cells	The ZnO NPs: - Increased intracellular ROS levels - Decreased mitochondrial membrane potential in a time-dependent manner - MIC_{50} = 25 μg/ml Decreased the tongue cancer cell viability	50 nm (average)	*in vitro*	Wang *et al.*, 2018
Conventional ZnO NPs	Investigation of properties of zinc oxide polymethyl methacrylate (ZnO-PMMA) nanocomposites that can influence the microorganism deposition on their surface.	After modification of the material with zinc oxide nanoparticles: - Roughness: did not change. - Properties of acrylic resin: no significant deterioration - Increased hydrophilicity and hardness with absorbability within the normal range (reducing microorganism growth)	22-25 nm	*in vitro*	Cierech *et al.*, 2018
Conventional ZnO NPs	Effect of ZnO-nanoparticles (ZnO-NPs) against *S. mutans* biofilm on resin composites	- The incorporation of 2/5 weight by % of ZnO NPs: improved antibacterial of resin composites,	7-10 nm,	*in vitro*	Brandão *et al.*, 2018

Synthesis methods	Targeted application (dental material modification)	Important findings	Characteristics of nanoparticles	*In vitro* or *in vivo*	Author(s)
	Effect on physicochemical properties of modified composites	without alteration of their physicochemical properties			
Conventional ZnO and Cu NPs	Effect on MMP inhibition of ZnO and Cu NPs modified dental adhesives on antimicrobial activity, ultimate tensile strength, nano-leakage in *vitro* degree of conversion and resin-dentin bond strength and *in situ*-dental caries on caries-affected dentin	The addition of up to 5/0.2 weight % of ZnO or Cu NPs incorporation: awarded favourable anti-MMP properties and improved the integrity of hybrid layer on caries-affected dentin	10-30 nm	*in vitro/ in situ*	Gutiérrez *et al.*, 2019
Conventional Ag-doped ZnO NPs	Modification of composite resin using Ag-doped ZnO NPs and evaluation of physicochemical and antibacterial characteristics	Nanospheres of ZnO/Ag had better biofilm inhibition than nanoplates. Modified composite with ZnO/Ag nanoplates had no compressive strength that was statistically significantly different from the conventional composites	Spherical, average diameter 10-23 nm	*in vitro*	Dias *et al.*, 2019
Conventional (Ag, ZnO and TiO) NPs	Investigation of the effect of intraradicular dentin pre-treatment with three different NPs on the PBS of fibre posts to root dentin	Intraradicular dentin pre-treatment with three other NPs did not interfere with the PBS of the fibre posts	20-50 nm	*in vitro*	Jowkar *et al.*, 2020

Abbreviations: Chlorhexidine (CHX), copper (Cu), matrix metalloproteinase (MMP), nanoparticle (NPS), polymethyl methacrylate (PMMA), push-out bond strength (PBS), reactive oxygen species (ROS), scanning electron microscopy with energy-dispersive X-ray spectroscopy (SEM-EDS), shear bond strength (SBS), silver (Ag) titanium oxide (TiO), zinc oxide (ZnO)

1.5 Physical and electrochemical features of zinc oxide nanoparticles

Zinc is an essential trace element in human physiological systems (Auld, 2001). It is involved in the orchestration of all aspects of most metabolic processes as well as the regulation of many physiological activities in human cells (Husen, 2019; Jansen *et al.*, 2009). From time immemorial, ZnO has been a renowned antibacterial agent (Frederickson *et al.*, 2005). It has been employed in several ointments for the treatment of boils (skin infections) and injuries (Halioua & Ziskind, 2005). ZnO is an inorganic compound also known as zincite, in a solid-state usually appears as a crystalline powder, white in colour and insoluble in water. However, manganese commonly renders it impure, giving it an orange or red colour.

Most ZnO is synthetically manufactured and commercially used, and belongs to the II-VI semiconductor group with a wide band gap (3.3 eV at 300 K, for bulk ZnO). ZnO also has features such as high electron mobility, good transparency, semi-conductivity, and high room temperature luminescence. These features enable the incorporation of ZnO into NPs for various functions and applications. It is currently often utilised in solar cells, memory devices, light-emitting diode (LED) lights, photoconductive materials, sunscreen lotion, and cosmetics (Husen, 2019; Klingshirn, 2007; Özgür *et al.*, 2005). Limited quantities of macro and micro ZnO are utilised in medicine, because even in trace amounts, compounds of Zn are conceivably toxic to plants and mammals (Husen, 2019; Patnaik, 2003). On the other hand, conventional ZnO NPs and Zn NPs have been employed in the treatment of ulcers, wounds, the eradication of microbial infections, as well as in drug delivery including cancer therapeutics (Husen, 2019; Siddiqi *et al.*, 2018). In overall, ZnO NPs also have unique electrical, optical and antimicrobial characteristics that support their versatility for multidisciplinary applications in science, technology and biomedical applications. Further, green-mediated ZnO NPs have been commended for their impressive anti-inflammatory potential (Agarwal *et al.*, 2019; Akbar *et*

al., 2020). As previously mentioned, there is a clear relationship between various physical, chemical, and structural features of NPs, including surface modifications and antimicrobial activity (da Silva *et al.*, 2019a).

1.6 Antimicrobial mechanism of zinc oxide nanoparticles

The primary mechanisms of ZnO NPs include cell wall interaction, ion liberation and reactive oxygen species (ROS, or oxidative stress) formation (Agarwal *et al.*, 2018, 2019; da Silva *et al.*, 2019a; Castillo *et al.*, 2019; Król *et al.*, 2017). Cell wall interaction and ion liberation initiate oxidative stress, and as a result, the cell expires and loses its viability (Castillo *et al.*, 2019; Shoeb *et al.*, 2013). The application of green-mediated ZnO NPs as a potential antimicrobial agent to combat microbial pathogens is currently explored (Gharpure 2019; Pillai *et al.*, 2020). As indicated in previous reports, the versatility of ZnO NPs is linked to its high surface area due to its small particle size, which allows increased surface interaction and ultimately improves antimicrobial action.

The antimicrobial mechanism of ZnO NPs has been studied in pathogenic yeast and bacteria affecting plants (Arciniegas-Grijalba *et al.*, 2019; He *et al.*, 2011; Rajwade *et al.*, 2020; Singh *et al.*, 2019), as well as humans (da Silva *et al.*, 2019a; Kamonkhantikul *et al.*, 2017; Król *et al.*, 2017; Lipovsky *et al.*, 2011; Madhumitha *et al.*, 2016). In plants, ZnO NPs can inhibit fungal growth by interfering with the functioning of the cell and subsequent deformation of fungal hyphae. ZnO NPs have demonstrated to prevent the development of conidia and conidiophores, which eventually lead to the death of the fungal hyphae (Busi & Paramanantham, 2018).

In humans, *C. albicans* is responsible for genital, cutaneous, and oral infections in more than 90% of fungi-infected individuals (Castillo *et al.*, 2019; Dadar, Tiwari, Karthik, *et al.*, 2018). Of particular interest to dentistry is the virulence characteristics of *C. albicans* in the host oral cavity, including its biofilm formation ability, ability to adhere to surfaces, to secrete enzymes responsible for hydrolysis, and fast yeast hyphae morphogenesis (Castillo *et al.*, 2019). Therefore, more specific antifungal treatments containing ZnO NPs with low and selective toxicity towards normal cells is the focus of this study. The unique structure and properties of ZnO NPs enable them to have a broad spectrum of applications, including biomedical and dental applications, as described in sections 1.3 and 1.4.

da Silva *et al.* (2019a) highlighted findings on the mechanisms of ZnO NPs (mostly conventional) with enhanced ability to fight against resistant microbial strains. ZnO NPs is getting more interest due to the non-specific action of this inorganic antimicrobial. Authors explained, similarly as above that, the minute particulate size contributing to the increased surface area to volume of ZnO NPs enhances its antimicrobial action, leading to an improved surface interaction. Additionally, surface modifiers used to cover ZnO nanoparticles play a fundamental role in facilitating the antimicrobial activity. The surface characteristics of nanomaterials modify the way they interact with cells, which may, in turn, affect the antimicrobial effectiveness of ZnO NPs. Perhaps, the utilisation of surface modifiers with compounds with possible toxicity to microbes may enhance the antimicrobial mechanism of ZnO NPs. Authors emphasised the significance of in-depth knowledge of the precise mechanisms of toxicity to explain the antimicrobial action of ZnO NPs in bacteria and fungi (da Silva *et al.*, 2019a).

Plant leaves and other components have been investigated extensively for the synthesis of green-mediated ZnO NPs, as summarised in Table 1 (Agarwal *et al.*, 2018, 2019; Ahmed *et al.*, 2017; Akbar *et al.*, 2020; Dhanemozhi *et al.*, 2017; Janaki *et al.*, 2015; Siriyong *et al.*, 2017; Yuvakkumar *et al.*, 2014b). The green synthesis method is declared to be eco-friendly (Agarwal 2017; Ahmed *et al.*, 2017; Akbar *et al.*, 2020; Mirzaei & Darroudi, 2017; Prabu, 2018) and has been utilised for its antibacterial (Agarwal *et al.*, 2018; Mirzaei & Darroudi, 2017) and antifungal properties (Agarwal *et al.*, 2017; Jamdagni *et al.*, 2018; Kamonkhantikul *et al.*, 2017; Madhumitha *et al.*, 2016). A recent study evaluated the potential of ZnO NPs against fluconazole-resistant *Candida tropicalis*. The biologically formulated ZnO NPs were considered as a potential new agent for the prevention of the formation of *C. tropicalis* biofilms, particularly those growing on medical devices and leading to nosocomial infections (Jothiprakasam *et al.*, 2017). Nonetheless, limited reports are available on green synthesis of ZnO NPs and their effects against *C. albicans* (Janaki *et al.*, 2015; Matinise *et al.*, 2017).

1.7 Synthesis of zinc oxide nanoparticles

There are numerous approaches for the preparation of stable ZnO NPs, including chemical precipitation, sol-gel, solid-state pyrolysis, solution-free mechano-chemical methods, microwave-assisted combustion, chemical or direct precipitation, and sonochemical methods, as illustrated in Figure 3 below (Agarwal *et al.*, 2017; Jiang *et al.*, 2018; Kalpana & Rajeswari, 2018; Mirzaei & Darroudi, 2017; Mishra *et al.*, 2017; Naveed Ul Haq *et al.*, 2017; Prabu, 2018; Zare *et al.*, 2017).

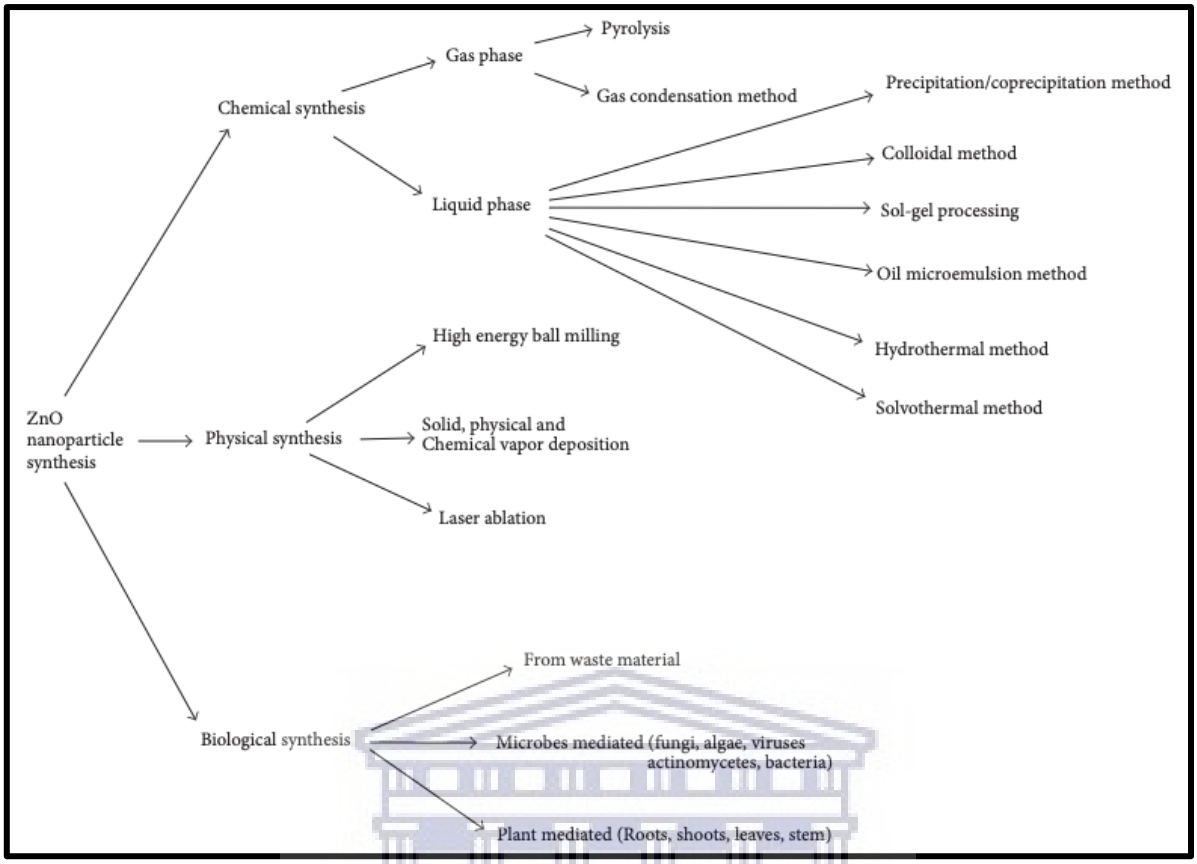

Figure 3: Different approaches to the synthesis of nanoparticles (from Naveed Ul Haq *et al.*, 2017)

The physical synthesis of NPs requires the utilisation of costly equipment, operation at high temperatures and pressure, as well as spacious areas for the equipment. The chemical method uses toxic chemicals that are hazardous for the environment and humans (Bandeira *et al.*, 2020). Thus, it was necessary to derive a more cost-effective, bio-safe, and biocompatible method for NPs synthesis, particularly for the use in biomedical applications such as drug carriers, fillers in medical and dental biomaterial, and for cosmetics (Agarwal *et al.*, 2017).

On the other hand, the biological synthesis (biosynthesis) of NPs uses either microorganisms (Ahmed *et al.*, 2017; Moghaddam *et al.*, 2015; Yusof *et al.*, 2019) or plants (Akbar *et al.*, 2020; Bandeira *et al.*, 2020; Basnet *et al.*, 2018). This approach is cost-efficient, environmentally friendly, less toxic, and more biocompatible. Besides, it is less time-consuming, does not require the utilisation of intermediate substances, ensures high-purity

products, and the physical process is uncomplicated (Bandeira *et al.*, 2020; Mishra *et al.*, 2017). In addition, these biological methods, mainly when using plants (phytosynthesis), have better biomedical adaptability compared to conventional methods (Agarwal *et al.*, 2018).

1.7.1 Biological synthesis of zinc oxide nanoparticles

Several studies have described that the use of diatoms and other algae, fungi, bacteria, human cells, and different plant components including leaves, fruits, seeds, roots, and stems in the formulation of NPs (Agarwal *et al.*, 2017; Bandeira *et al.*, 2020; Jiang *et al.*, 2018; Mirzaei & Darroudi, 2017; Mishra *et al.*, 2017; Ruddaraju *et al.*, 2020). Examples of biosynthesis sources for NPs are itemised in Table 4 below.

Table 4: Examples of biosynthesis of ZnO NPs (from Mirzaei & Darroudi, 2017)

Polymers	**Plants**	**Algae**	**Bacteria**	**Fungi**
Gelatin Starch	*Calotropis gigantean* *Medicago sativa* *Camellia sinensis* *Abrus precatorius* *Aloe barbadensis* *Cassia auriculate* *Acalypha indica* *Parthenium hysterophorus* *Calotropis procera* *Musa balbisiana* *Citrus paradise*	*Marine macroalgae* *Caulerpa peltata* *Hypnea Valencia* *Sargassum myriocystum* *Sargassum muticum*	*Enterococcus faecalis* *Lactobacillus sporogen* *Aeromonas hydrophila* *Bacillus cereus*	*Aspergillus aeneus* *Fusarium species* *Aspergillus fumigates*

The use of plants for the production of the green-mediated type of NPs is a fast, cost-effective, environmentally friendly process and the products are safe for human use (Husen & Iqbal, 2019; Madhumitha *et al.*, 2016; Ruddaraju *et al.*, 2020). A basic summary of the process is

illustrated in Figure 4. The exact mechanism of how ZnO NPs is biologically synthesised is still under investigation (Bandeira *et al.*, 2020). One of the most acceptable and efficient methods for NPs biosynthesis is the "bottom-up" approach. This approach incorporates stabilising and reducing agents such as phytochemicals in extracts, enzymes, and proteins (Ahmed *et al.*, 2017; Husen & Iqbal, 2019). The main philosophy behind the plant-based synthesis of ZnO NPs depends on the harnessing of beneficial properties from natural material products. The beneficial compounds include phytochemicals (polyphenols, saponins, and terpenoids) that can reduce or stabilise the precursor during NPs synthesis (Ahmed *et al.*, 2017; Bandeira *et al.*, 2020; Baranwal *et al.*, 2016; Basnet *et al.*, 2018). The metal (Zn) is reduced to the 0-valence state, and then through calcinations, the oxide may be added to the metal (Basnet *et al.*, 2018). Of relevance to our study, we considered numerous plants or plant-related products that have been applied for the formulation of ZnO NPs for many different applications, as summarised in Table 1.

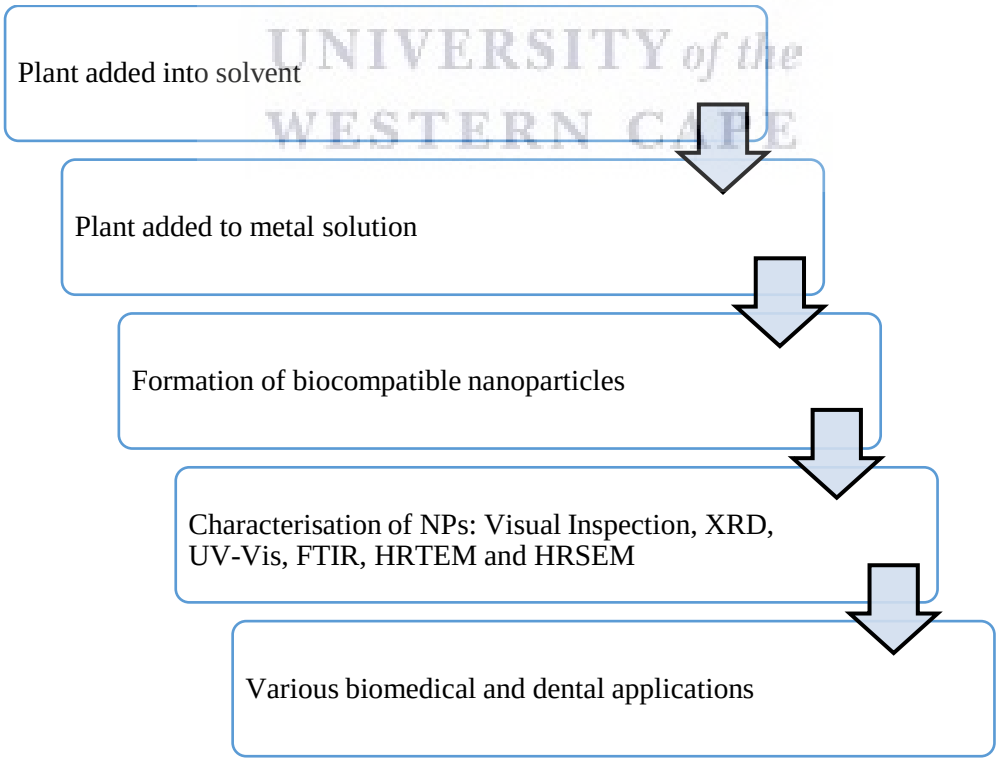

Figure 4: Basic steps involved in the plant-mediated (green) synthesis of nanoparticles

Most of the biological methods for the synthesis of ZnO NPs are similar to each other, with little or no modifications (Agarwal *et al.*, 2017; Bandeira *et al.*, 2020; Basnet *et al.*, 2018; Kalpana & Rajeswari, 2018; Thema *et al.*, 2015a). Typically, in the green approach of ZnO NPs production, plant parts (e.g. leaves) are prepared by washing it thoroughly with deionised or distilled water. The leaves are then neatly cut into fine pieces and left to dry (at room temperature or by the sun). Commonly, preparation of extracts involves measuring a specified weight of the dried sample, followed by soaking and boiling (simmering) in a calibrated volume of distilled or deionised water (for a required concentration).

An alternative approach involves weighing a quantity of the dried sample, grind it in a mortar, obtaining a powder, and then boiling the powder to the required concentration under continuous stirring. The resultant solution is filtered using Whatman paper, and the filtrate (the liquid part) is used in the experiments. In a typical experimental setup for the formulation of green-mediated ZnO NPs, 2 g of a Zn metal precursor (Zn nitrate or Zn acetate) is mixed into 40 ml of plant extract. The dissolved mixture is then stirred for 15 min, and placed in a water bath shaker for another 3-6 h at about 60-80 °C. The solution is then heated and finally calcined at 200-400 °C. In an alternative experimental setup, the same amount of the Zn precursor is added to the extract, and then boiled at the desired temperature and time to ensure sufficient homogenous mixing. Colour changes are observed in the mixture during the incubation period (Agarwal *et al.*, 2017; Basnet *et al.*, 2018).

The choice of matrix materials is usually dependent on various characteristics: inherent properties such as aqueous stability and solubility, size of the NPs, surface features, e.g. permeability, surface charge, etc., and the desired drug-release profile. The green-mediated NPs can be formulated using one or more stabilising natural products (Basnet *et al.*, 2018;

Husen & Iqbal, 2019). In chemical sciences, a "single-pot" or "one-pot" synthesis is an approach to improve chemical reaction efficiency by subjecting a reactant to a single reactor in consecutive chemical reactions. When a protocol utilises two or more extracts for the formulation of the NPs in the same flask using a single precursor salt, it is referred to as a "single pot green synthesis" (Sydnes, 2014). Several "one-pot" green protocols have previously been explored and successfully used to formulate nanomaterials including graphene, Au, Ag, and Zn (Ansari & Alzohairy, 2018; Hussein *et al.*, 2018; Kumar *et al.*, 2019; Rathour & Bhattacharya, 2018; Somu & Paul, 2019). This protocol was also adopted in this study to formulate the desired GZnO NPs.

Thus, to validate the formation of ZnO NPs, several characterisation techniques are conducted. Some of the characterisations include UV-Vis, Fourier-transform infrared spectroscopy (FTIR), X-ray diffraction (XRD) spectroscopy, transmission electron microscopy (TEM), and scanning electron microscopy (SEM), as illustrated in Figure 4.

1.7.1.1 The use of *Aspalathus linearis* (Rooibos) for the synthesis of zinc oxide nanoparticles

Aspalathus linearis, commonly known as Rooibos, is a popular herbal plant in South Africa. Rooibos is indigenous to the South African Cape Floristic Region, and widely used to produce Rooibos tea. This tea is a famous herbal tea, and is naturally free of caffeine, and low in tannin content as compared to its green tea (*Camellia sinensis*) counterpart. *A. linearis* is a potential source of beneficial and unique compounds, perceived to contribute towards health benefits. Rooibos is also among the most commercially relevant and commonly consumed herbal teas in South Africa. Antimicrobials have always been the most prescribed traditional medication. Considerable concurrent utilisation of antibiotics and Rooibos is prone to occur in South Africa, due to the high consumption of the popular herbal beverage. Hübsch *et al.* (2014a)

investigated such concurrent use with conventional antimicrobial agents including penicillin G, ciprofloxacin, gentamicin, erythromycin, tetracycline, amphotericin B, and nystatin using a human embryonic kidney (HEK)-293 cell line. Results presented that when combined with nystatin, an antifungal agent, but not the rest of the antimicrobials, Rooibos was possibly not safe, hence warranting further investigations prior such a combination (Hübsch, *et al.*, 2014a). However, the *Fabaceae* family (which *A. linearis* belongs to) are among the most common plant families employed in the plant-based synthesis of ZnO NPs (Basnet *et al.*, 2018).

Certain phenols occur naturally in healthy plant tissues (Crozier *et al.*, 2009). For example, plants in the *Fabaceae* family (including Rooibos) are rich in alkaloids, flavonoids, polyphenols, and saponins. Plant phenols can mainly be categorised into flavonoids and non-flavonoids (Crozier *et al.*, 2009). Studies report that the flavonoids hold numerous benefits for health, including osteogenic regulation, enzyme regulation, and anti-inflammatory, antimicrobial (antibacterial and antifungal), as well as anticancer activity (Pereira *et al.*, 2009; Yao *et al.*, 2004). Additionally, various green metal and MO NPs have been synthesised using natural sources containing phenols, and their anti-inflammatory potential have been elucidated (Agarwal *et al.*, 2019). They were thus corroborating that, the resultant green-mediated NPs as an alternative regimen for management or treatment of inflammation.

Among the most explored health benefits, antioxidant properties are studied extensively. The antioxidant potential is attributed to, amongst other things, the presence of flavonoids, which contributes to the prevention of oxidative stress (Ajuwon *et al.*, 2015). These phytochemicals are also essential for the synthesis of complexes of Zn metal salts (Basnet *et al.*, 2018) and are responsible for reducing metal salt precursors during ZnO NPs formation.

Rooibos is rich and saturated with unique phytochemicals. The phytochemical composition in this herbal beverage is distinct because of the monomeric flavonoids, comprising two unique components, namely aspalathin and aspalalinin, both of which are unique to Rooibos (Figure 5). These Rooibos-based phytochemicals are rich in antioxidant compounds such as dihydrochalcones. In addition, the Rooibos herb is one of only three sources of nothofagin. Other important flavonoids in Rooibos include iso-orientin, flavanones orientin, and vitex and isovitexin, the latter two being analogues of nothofagin (Figure 5).

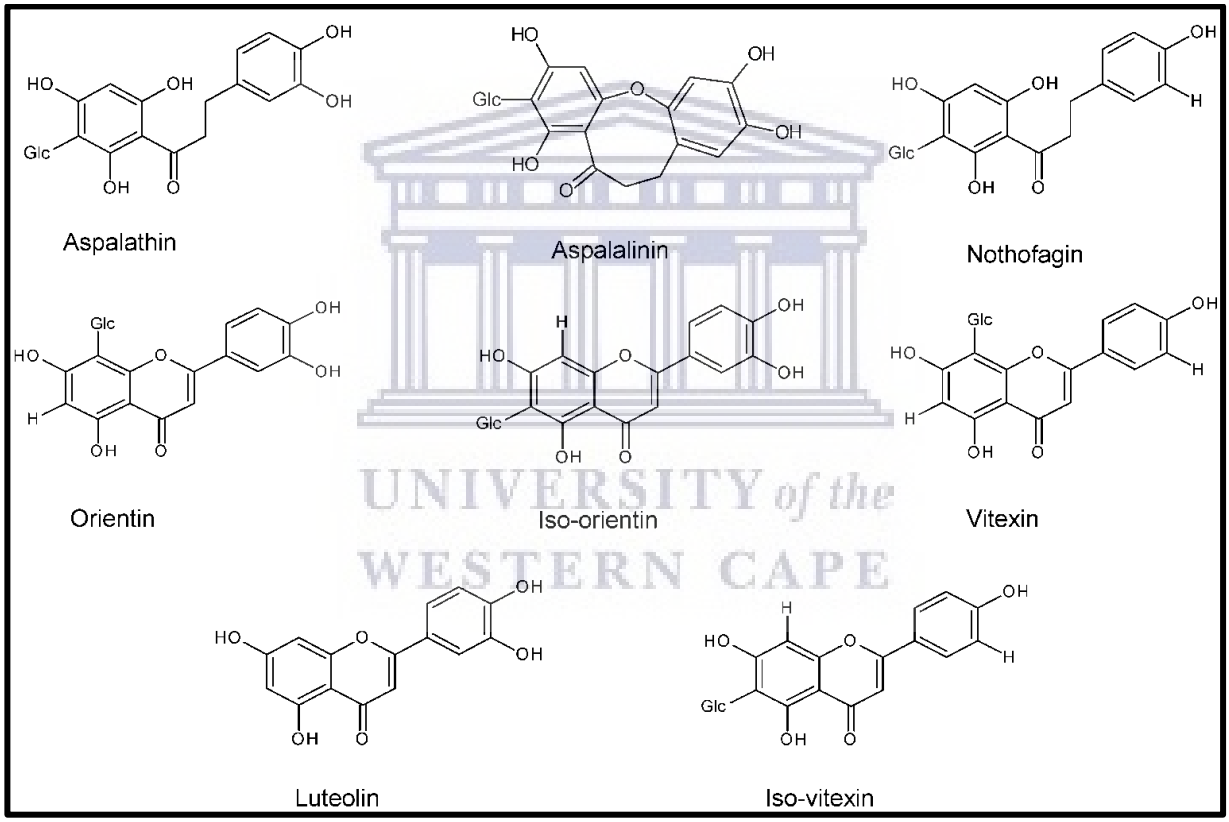

Figure 5: Major flavonoids identified from Rooibos (from Ajuwon *et al.*, 2015)

Additionally, the Rooibos herb has been documented to contain lignans, phenolic acids, xanthones mangiferin, catechin, as well as the flavanones hesperetin and isokuranetin, and polyphenols (Ajuwon *et al.*, 2015; Diallo *et al.*, 2015; McKay & Blumberg, 2007). All these elements aid in the health benefits of Rooibos. Rooibos is also a naturally rich source of

different unique glycosylated plant polyphenols with the potential for several health-promoting benefits. For instance, the glycosylated Rooibos polyphenols can be useful in regulating and managing diabetes mellitus (Sasaki *et al.*, 2018).

In order to yield the unique phytochemicals from Rooibos, specific extraction times and temperatures have been documented. The effect of temperature and time has been studied and measured for the main phenolic constituents (flavonoids, tannins, flavanols, total phenolic content, and ortho-diphenols), reducing agents and antioxidants, and antimicrobial components. In general, the extraction of Rooibos constituents at 85 °C for 10 min resulted in the highest antioxidant activity and valuable interaction when measured by all assays. On the other hand, when extracted at 65 °C, the Rooibos extract presented with a reversed performance. When extracted at 75 °C, the Rooibos extract showed with average moderate performance. Therefore, the evidence revealed that extracting Rooibos at 85 °C has a significant influence contributing to the high acquisition of potent bioactive molecules (Santos *et al.*, 2016). This offered us direction to prepare the Buchu-infused Rooibos extracts in order to harness the essential and functional constituents of the Rooibos, which consequently contributed to the nature of NPs formulated after that.

Rooibos tea is commonly used to treat hyperactive gastrointestinal, cardiovascular, and respiratory disorders. Rooibos extracts have been investigated as a possible antihypertensive and bronchodilator and for its antispasmodic activities, with efforts to explain the various therapeutic applications. Khan and Gilani (2006) successfully provided a plausible mechanism for the foundation for the extensive biomedical and therapeutic utilisation of Rooibos tea for several diseases and conditions (Khan & Gilani, 2006). Additionally, the use of Rooibos has been supported for its antioxidant, anti-inflammatory and anti-diabetic properties (Johnson *et*

al., 2018), as well as its regulation activities in the immune system, lipid metabolism, and adrenal steroidogenesis (Smith & Swart, 2018).

Herbal teas such as Rooibos have quite several health advantages, which are frequently grounded on subjective validation and with very few findings covering the antimicrobial actions. Dube *et al.* (2017) used agar disk diffusion assays to study the antimicrobial potential of the several Honeybush extracts, and the MIC values were obtained for *Staphylococcus aureus*, *Streptococcus pyogenes*, and *C. albicans.* The report documented that the majority of the Honeybush extracts displayed antimicrobial potential. The green and fermented extracts had been most efficacious against *S. aureus* and *C. albicans*. In addition, the green extracts mostly presented the most significant antioxidant capability in comparison to the fermented counterpart. It was also observed that the total polyphenol levels were the highest in green extracts when water was used as the primary solvent as opposed to methanol (Dube *et al.*, 2017). Although the various solvent extracts could have been weak antimicrobial agents, the plant extracts were a reliable source of the distinctive combination of naturally occurring antioxidant phytochemicals as well as antimicrobial compounds (Ahmed *et al.*, 2017; Dube *et al.*, 2017). The extracts showed definite action and thus granted fundamental insight to explore the utilisation of similar extracts to stabilize the GZnO NPs in this study, and further elucidate the antimicrobial effect against *C. albicans*.

In 2015, Diallo *et al.* shared one of the first reports on the green synthesizing of ZnO NPs using an extract of *A. linearis* leaves. The extract was used as the primary natural reducing and stabilising agent. Dark deposits were formed, and high-resolution transmission electron microscopy (HRTEM) and SEM confirmed the presence of non-agglomerated quasi-spherical shaped NPs with an average diameter ranging between 1 and 8.5 nm. The structural and

crystallographic analysis revealed a hexagonal wurtzite structure of their ZnO NPs (Diallo *et al.*, 2015).

1.7.1.2 The use of *Agathosma betulina* (Buchu) for the synthesis of zinc oxide nanoparticles

Agathosma betulina, commonly known as Buchu, is an indigenous plant to South Africa and a common herb for treating several ailments (Iwu, 2016; Simpson, 1998). Scientists have explored this plant for various medicinal benefits, including as a diuretic, for the treatment of urinary tract infections (UTI), as an analgesic, and for its antimicrobial properties. Buchu has been used traditionally for the treatment of UTI and stomach upset. Buchu is also widely available as a dietary supplement or herbal tea (Masondo & Makunga, 2019; Moolla & Viljoen, 2008; Van Wyk, 2008). Further, Hübsch *et al.*, (2014b) investigated the interaction of several conventional antimicrobials when utilised in combination with medicinal plants such as Buchu. The authors reported negligible synergistic, antagonistic, additive, and indifferent interactions. The report further highlighted that Buchu presented minor synergistic interaction with ciprofloxacin against *Escherichia coli* (Hübsch *et al.*, 2014b). It is imperative to comprehend that plants can be sources of new antimicrobials with resistance-modifying agents (Ayaz *et al.*, 2019; Cheesman *et al.*, 2017; Shin *et al.*, 2018; Zacchino *et al.*, 2017a). The potential of such combinations can be explored to tackle the heightened incidence of multidrug-resistant microbial strains, due to the reduced efficacy of several conventional antimicrobials.

In recent years, Buchu has also been utilised in the formulation of NPs. The *Rutaceae* family (which includes *A. betulina*) is among the most famous families of plants used for the synthesis of ZnO (Basnet *et al.*, 2018). Recently, Thema *et al.*, (2015b) reported for the first time a successful green synthesis of ZnO NPs using a Buchu leaf extract, and their NPs had a quasi-spherical structure, and a diameter of 15.8 nm. Furthermore, the authors successfully confirmed

the phytosynthesis of the pure ZnO NPs with standard characterisation techniques (Thema *et al.*, 2015b). Other NPs formulated using green Buchu include nickel oxide (NiO) and cadmium oxide (CdO) NPs, both of which were for the first time synthesised by employing Buchu as the stabilising agent for their successful synthesis (Thema *et al.*, 2015b; 2016). The thriving green syntheses of NPs mentioned earlier are yet to be explored for their biomedical application, including antimicrobial potential (Basnet *et al.*, 2018; Thema *et al.*, 2015b; 2016).

Chiguvare (2015) studied Buchu oil constituents and established essential elements, including flavonoids, tannins, saponins, glycosides, carbohydrates, alkaloids, terpenes, proteins, and steroids. Subsequently, the authors successfully formulated Ag NPs with Buchu (Chiguvare *et al.*, 2016). The attained NPs formulation had better analgesic and anti-inflammatory activities than aspirin (Chiguvare, 2015; Chiguvare *et al.*, 2016).

Buchu has been highlighted to have several pharmacological properties, including antimicrobial, antioxidant, and anticancer potential (Witbooi *et al.*, 2017). These properties can be associated with the innate phytochemical contents in this plant (Witbooi *et al.*, 2017). The antimicrobial and antioxidant activity and biocompatibility of extracts of 17 species of Buchu have been investigated in order to confirm the historical and continual utilisation of Buchu (Moolla *et al.*, 2007). The antimicrobial activity, or minimum inhibitory concentrations (MICs), was analysed against four microbes, namely *Bacillus cereus*, *S. aureus*, *Klebsiella pneumoniae*, and *C. albicans*. The studied Buchu species were observed to have considerable antioxidant constituents that may contribute to the health benefits of Buchu (Moolla *et al.*, 2007).

1.7.1.3 The use of *Musa paradisiaca* (banana) peel extract for the synthesis of zinc oxide nanoparticles

Current applications of *Musa paradisiaca*, or banana peel extracts (BPE) include the production of fungal biomass and the adsorption of heavy metals from water (Bankar *et al.*, 2010a). Banana peel contains enormous quantities of phenols that promote the formulation of metallic or metallic oxide NPs (Abdullah *et al.*, 2020; Bankar *et al.*, 2010b; 2010c; Orsuwan *et al.*, 2017). The application of BPE s is also a simple, non-toxic, eco-friendly, and affordable means for the synthesis of NPs and can in the future possibly supersede costly conventional protocols for synthesising NPs (Bankar *et al.*, 2010c; Ibrahim, 2015; Rigopoulos *et al.*, 2018).

Banana peel is also a good source of natural antioxidants, phytochemicals, and pro-vitamin A because they are rich in biogenic amine molecules, carotenoids, and phenolic compounds (Singh *et al.*, 2016). It has also been employed in the production of allopathic medicine and phytomedicines (Pereira & Maraschin, 2015). Additionally, the abundant compounds from the banana peel are popular for facilitation and propagation of wound healing (Naganathan & Thirunavukkarasu, 2017). Studies have also applied green methods using the banana peel for the synthesis of Ag and Au NPs (Naganathan & Thirunavukkarasu, 2017; Narayanamma, 2016).

Furthermore, a biological route for the synthesis of palladium NPs using BPE has been documented (Bankar *et al.*, 2010a). The investigators postulated that the BPE comprised of polymers like lignin, hemicelluloses, and pectin that aided the phytosynthesis of the NPs. *Azadirachta Indica* (Neem), *Medicago sativa* (Alfalfa), *Aloe vera*, and microorganisms have also previously been applied for the formation of Ag and Au nanoparticles (Duran *et al.*, 2005; Narayanan & Sakthivel. 2010; De Souza, 2007). The authors reported that the BPE interceded

the organising of the NPs into a microwire matrix, and the formulated Au NPs showed antibacterial and antifungal potency against pathogenic bacterial and fungal cultures.

Additionally, it has been documented that BPE has very potent free radical scavenging characteristics *in vitro* (Mokbel & Hashinaga, 2005). Banana peel is also rich in dopamine, serotonin, tyramine, and histamine (Borges *et al.*, 2019). The neurotransmitters and amino acids have numerous vital functions, such as signal transmission (dopamine and serotonin), mood stabilisation and wound healing (serotonin), blood pressure regulation (tyramine and histamine), and promoting alertness (histamine). Furthermore, regardless of the banana species, temperatures during processing influence the content of amines constituents in extracts (Borges *et al.*, 2019). Of relevance to dentistry, it was recently reported that BPE has potential antimicrobial properties against pathogens responsible for causing periodontitis, including *Porphyromonas gingivalis* and *Aggregatibacter actinomycetemcomitans*, previously called *Actinobacillus actinomycetemcomitans* (Kapadia *et al.*, 2015). Studies that utilised green and conventional ZnO NPs for antimicrobial purposes relevant to dentistry, are summarised in Table 5.

Table 5: Antimicrobial applications of conventional and green-mediated ZnO NPs relevant to dentistry

Synthesis methods	**Targeted application (microbial organisms)**	**Important findings**	**Size and characteristics of NPs**	***In vitro* or *in vivo***	**Author(s)**
Conventional ZnO NPs	Antibacterial effectiveness of ZnO-NPs against *Streptococcus sobrinus* ATCC 27352 planktonic and biofilms on composites	MIC_{50} in *Streptococcus sobrinus* planktonic culture: l g/ml. ZnO NPs-modified composites (10%) qualitatively: less biofilm after 24h, however, did not significantly reduce after 3 days	40-100 nm Hexagonal crystals Rod-like	*in vitro*	Sevinç & Hanley, 2010
Conventional ZnO NPs	Investigation of the effect of ZnO NPs on the viability of the pathogenic yeast, *Candida albicans*	Reduction of *Candida albicans* at 0.1 mg/ml (97.5%) and 1 mg/ml (99.5%)	40-25 nm	*in vitro*	Lipovsky *et al.*, 2011
Conventional (Ag, Cu_2O, CuO, ZnO, TiO_2, WO3) NPs, (Ag + CuO and Ag + ZnO) composites	Antimicrobial effect of six metal and MO NPs and two of their composites against peri-implantitis pathogens: *Porphyromonas gingivalis, Fusobacterium nucleatum, Prevotella intermedia,* and *Aggregatibacter actinomycetemcomitans* under anaerobic conditions	NPs antimicrobial activity in descending order: Ag > Ag + CuO > Cu_2O > CuO > Ag + ZnO > ZnO > TiO_2 > WO3. 250MIC/MBC against *Porphyromonas gingivalis*: l g/ml 1000 MIC/MBC against *Prevotella intermedia:* l g/ml 250 MIC/MBC against *Aggregatibacter* Actinomycetemcomitans: l g/ml	10-50 nm	*in vitro*	Vargas-Reus *et al.*, 2012
Conventional ZnO NPs	*Streptococcus mutans*	Biofilm inhibition; 500 MIC/MBC (l g/ml)	120-180 nm;	*in vitro*	Eshed *et al.*, 2012
Conventional (ZnO and CuO) NPs	Effect of ZnO- and CuO-NPs on biofilms of *Streptococcus mutans* and *Actinomyces viscosus*	Significant reduction of oral bacterial load Inhibit the growth of oral biofilm colonizers	Average 35 nm (ZnO NPs) 40 nm (CuO NPs)	*in vitro*	Khan *et al.*, 2013

Synthesis methods	**Targeted application (microbial organisms)**	**Important findings**	**Size and characteristics of NPs**	***In vitro* or *in vivo***	**Author(s)**
Conventional ZnO NPs	Modification of composites using ZnO NPs and determination of physicochemical characteristics and antibacterial potential against *Streptococcus mutans*	Improved physicochemical characteristics (flexural strength and compressive modulus) and improved antibacterial activity against *Streptococcus mutans*	Average 20 nm, Purity 99.8% Hexagonal crystal structure	*in vitro*	Tavassoli-Hojati *et al.*, 2013
Conventional ZnO NPs	Effect of ZnO NPs on two bacterial isolates from the oral cavity: *Rothia dentocariosa* and *Rothia mucilaginosa*	Potential antimicrobial and anti-biofilm activity: 76 µg/ml = (IC_{50}) for *Rothia dentocariosa* 53 µg/ml = (IC_{50}) for *Rothia mucilaginosa*	Average 35 nm	*in vitro*	Khan *et al.*, 2014
Conventional ZnO NPs	Antimicrobial assay of Chitosan-based ZnO NPs against *Micrococcus luteus*, *Candida albicans*, and *Staphylococcus aureus*	Antimicrobial efficiency was more on *Micrococcus luteus* and *Staphylococcus aureus* than on *Candida albicans*	93.2-403 nm	*in vitro*	Dhillon *et al.*, 2014
Conventional ZnO NPs	Antibacterial properties of dental composite resins modified with (Ag and ZnO) NPs on *Streptococcus mutans* and *Lactobacillus acidophilus*	Antibacterial activity against *Streptococcus mutans* and *Lactobacillus acidophilus*: higher in composites containing ZnO NPs or Ag NPs compared to the control group ($p < 0.05$) ZnO NPs: more effective on *Streptococcus mutans* than Ag NPs ($p < 0.05$). Antibacterial activity against	Average 50 nm	*in vitro*	Kasraei *et al.*, 2014

Synthesis methods	**Targeted application (microbial organisms)**	**Important findings**	**Size and characteristics of NPs**	***In vitro* or *in vivo***	**Author(s)**
		Lactobacillus: no significant differences in composites containing ZnO NPs or Ag NPs			
Conventional ZnO NPs	A novel system of coating with ZnO NPs to prevent biofilm attachment and promote osteoblastic activity	Optimal ZnO NPs coating can be applied on future bone implants that with acceptable biocompatibility and improved antimicrobial properties		*in vitro*	Memarzadeh *et al.*, 2015
Green-mediated ZnO NPs	Antimicrobial activity of ZnO NPs against *Klebsiella pneumonia, Staphylococcus aureus, Candida albicans,* and *Penicillium notatum*	ZnO NPs showed significant antimicrobial properties	23-26 nm	*in vitro*	Janaki *et al.*, 2015
Conventional ZnO NPs	Effect of adding ZnO NPs to dental adhesives on their antimicrobial and bond strength properties	Modification of dental adhesives increased antimicrobial properties without affecting their bond strength	20 nm Crystalline	*in vitro*	Saffarpour *et al.*, 2016
Conventional ZnO NPs	Composite material with antifungal properties for denture bases to be used as an alternative protocol in denture stomatitis treatment and prevention	Positive antifungal activity of both nanocomposites PMMA ZnO NPs and the efficacy of sputtering of ZnO NPs on the PMMA *Candida albicans* biofilm inhibition: antifungal properties directly proportional to the concentration of ZnO NPs	Type 2 layer: regular ZnO NPs (size ≈30 nm) Type 1 layer: composed of small (<50 nm) and large (<180 nm) NPs	*in vitro*	Cierech *et al.*, 2016a
Conventional ZnO NPs	ZnONPs incorporated into acrylic resin used	MIC: 0.75 mg/mL	Average 30 nm	*in vitro*	Cierech *et al.*, 2016b

Synthesis methods	**Targeted application (microbial organisms)**	**Important findings**	**Size and characteristics of NPs**	***In vitro* or *in vivo***	**Author(s)**
	to produce denture bases				
Conventional ZnO NPs	Bactericidal and fungicidal activity against *Bacillus subtilis*, *Escherichia coli*, and *Candida albicans*	A significant reduction in the growth of all tested organisms was recorded at 0.50 mg/ml MIC: 8 μg/ml	~25nm, ~20nm, ~7nm and~3nm, respectively, at 500, 1000, 1500 and 2000 rpm	*in vitro*	Khan *et al.*, 2016
Conventional ZnO NPs	Antibacterial activity of ZnO NPs0%, 1%, and 2% by weight incorporated into self-cured GIC and light-cured resin-modified GIC on *Streptococcus mutans* biofilm at one and seven days	GIC modified with ZnO NPs had no improved antimicrobial activity against *Streptococcus mutans*	Average20 nm	*in vitro*	Garcia *et al.*, 2017
Conventional ZnO NPs	*Streptococcus mutans* in interim restorations	MICs against *Streptococcus mutans* were 61.94 mg/g and 0.25% v/ respectively	60-80 nm, Average 71 nm	*in vitro*	Andrade *et al.*, 2018
Conventional (ZnO and Ag) NPs	Antibacterial effects of two gels containing ZnO and ZnO/Ag NPs and a mixture of calcium hydroxide and 0.12% chlorhexidine as intracanal medicaments in root canals contaminated with *Enterococcus faecalis* at different time intervals	The mixture of calcium hydroxide/chlorhexidine as an intracanal medicament was more effective ZnO and ZnO/Ag NPs gels		*in vitro*	Samiei *et al.*, 2018
Conventional ZnO NPs	Investigation of properties of ZnO PMMA nanocomposites on the influence of microorganism deposition	After modification of PMMA with ZnO NPs: Roughness: No changes Properties of acrylic resin: no significant deterioration Increased hydrophilicity and hardness with	22-25 nm	*in vitro*	Cierech *et al.*, 2018

Synthesis methods	**Targeted application (microbial organisms)**	**Important findings**	**Size and characteristics of NPs**	***In vitro* or *in vivo***	**Author(s)**
		absorbability within the normal range (reducing microorganism growth)			
Conventional ZnO NPs	Effect of ZnO NPs) against *Streptococcus mutans* biofilm on resin composites Effect on physicochemical properties of modified composites	The incorporation of 2/5 wt.% of ZnO NPs improved antibacterial activity of resin composites, without alteration of their physicochemical properties	7-10 nm, Average 12±19 nm	*in vitro*	Brandão *et al.*, 2018
Green-mediated ZnO NPs	Effect of green-mediated ZnO NPs on the virulence of clinical isolates of *Candida albicans* and non-albicans strains	Remarkable reduction of germ tube formation of *C. albicans* at 0.062 mg/ml. Significant lowering of proteinase secretion at 0.25 mg/ml. CSLM revealed that green-mediated ZnO NPs suppressed biofilm formation up to 85% at 0.25 mg/ml.	10-30 nm (TEM) Hexagonal, rod-like, rectangular, and spherical NPs	*ex vivo*	Jalal *et al.*, 2018
Green-mediated ZnO NPs	The antibacterial activity of green-mediated ZnO NPs with varied concentrations against *Bacillus cereus, Staphylococcus aureus, Shigella dysenteriae, Salmonella paratyphi, Candida albicans,* and *Aspergillus niger*	The maximum zone of inhibition in ZnO NPs (100 µg/ml) was against *Shigella dysenteriae* (42 ± 2.24 mm) followed by *Bacillus cereus* (41 ± 2.18 mm), *Salmonella paratyphi* (40 ± 3.66 mm) and *Candida albicans* (34 ± 1.28 mm)	30 (XRD) 32-36 (SEM and TEM) Hexagonal wurtzite	*in vitro*	Vijayakumar *et al.*, 2018
Conventional ZnO NPs	Safe alternative PMMA ZnO nanocomposites for denture bases, which release ZnO	*Candida albicans* biofilm development prevention		*in vitro*	Cierech *et al.*, 2019

Synthesis methods	**Targeted application (microbial organisms)**	**Important findings**	**Size and characteristics of NPs**	***In vitro* or *in vivo***	**Author(s)**
Conventional ZnO NPs	Coating of TiO_2 NTs grown on medical-grade Ti-6Al-4V alloy with a layer of ZnO NPs To determine the stability of antimicrobial properties with a final layer of HA on the composite	Coating with ZnO NPs: 70% biocidal activity of ZnO NPs on TiO_2 NTs: stable antimicrobial coating most of the biocidal properties remained in the presence of nano-HA on the coating. Antimicrobial Zn release: eradicated 60% of *Staphylococcus aureus* attached to the coating		*in vitro*	GuNPsuth *et al.*, 2019
Conventional ZnO NPs	Effect on MMP inhibition of (ZnO and Cu) NPs modified dental adhesives on antimicrobial activity, ultimate tensile strength, nano-leakage in *vitro* degree of conversion and resin-dentin bond strength and *in situ*-DC on caries-affected dentin	The addition of up to 5/0.2 wt% of (ZnO or Cu) NPs in dental adhesives exhibited antimicrobial potential	10-30 nm	*in vitro /in situ*	Gutiérrez *et al.*, 2019
Conventional ZnO NPs 60 °C for 12 h	Antibacterial activity on *Porphyromonas gingivalis, Actinomyces naeslundii*	MIC against *Porphyromonas gingivalis* and *Actinomyces naeslundii*: 10 µg/mL and 40 µg/mL, respectively	Diameter: 10 nm	*in vitro*	Wang *et al.*, 2019
Conventional ZnO NPs	Antimicrobial effect of various sizes and concentrations of ZnO NPs on *Enterococcus faecalis, Lactobacillus fermentum, Streptococcus mutans,* and *Candida albicans*	ZnO NPs20 nm and 40 nm exhibited most excellent inhibitory zones against *Streptococcus mutans,* while 140 nm ZnO NPs formed the most significant inhibition zones against *Streptococcus*	Solutions at the concentration of 10 µg/ml were prepared using 20 nm,40 nm, and 140 nm nano ZnO powder	*in vitro*	Mirhosseini *et al.*, 2019

Synthesis methods	Targeted application (microbial organisms)	Important findings	Size and characteristics of NPs	*In vitro* or *in vivo*	Author(s)
		mutans and *Enterococcus faecalis* Smallest inhibition zones were observed against *Candida albicans* with the three ZnO NP sizes MICs for *Candida albicans* with 40 nm and 140 nm NPs and *Lactobacillus fermentum* with 140 nm NPs were higher than 10 µg/ml A significant correlation: particle size and the antibacterial activity against *Streptococcus mutans* (P = 0.00), *Lactobacillus fermentum*, and *Enterococcus faecalis* (P < 0.02) Antimicrobial activity of ZnO NPs increases with decreased particle size. Most significant antimicrobial effect was observed against *Streptococcus mutans* and *Enterococcus faecalis* *Streptococcus mutans* is more sensitive to changes in particle size compared to other bacteria			
Conventional Ag-doped ZnO	Modification of composite resin using Ag-doped ZnO NPs	Nanospheres of ZnO/Ag: better	Average diameter 10-23 nm	*in vitro*	Dias *et al.*, 2019

Synthesis methods	Targeted application (microbial organisms)	Important findings	Size and characteristics of NPs	*In vitro* or *in vivo*	Author(s)
	Evaluation of antibacterial of modified composite resin	biofilm inhibition than nanoplates	Spherical		
Green-mediated *Ci*-ZnO NPs	Novel ZnO NPs using the *Costus igneus (Ci)* leaf extract	Promising antibacterial and biofilm inhibition activity against *Streptococcus mutans, Lysinibacillus fusiformis, Proteus vulgaris, and Vibrio parahaemolyticus*	Average 26.55 nm Hexagonal	*in vitro*	Vinotha *et al.*, 2019

Abbreviations: confocal scanning laser microscopy (CSLM), copper (Cu), dental caries (DC), glass ionomer cement (GIC), hydroxyapatite (HA), matrix metalloproteinase (MMP), nanoparticles (NPs), nanotubes (NTs), polymethyl methacrylate (PMMA), silver (Ag), transmission electron microscopy (TEM), scanning electron microscopy (SEM), X-ray diffraction (XRD), zinc oxide (ZnO)

1.8 Oral candidiasis

Since the time of Hippocrates, candidiasis has been described as "a disease of the diseased" (Lewis & Williams, 2017). Oral candidiasis is a common opportunistic fungal infection that is associated with the elderly, children, the medically compromised, and immunosuppressed individuals (Blignaut, 2017; Lohse, Gulati, Johnson, *et al.*, 2018; Vila *et al.*, 2020). In recent years, there has been an escalation in both the common and uncommon forms of candidiasis. This can be attributed to the haphazard use of broad-spectrum antibiotics and the increase in diabetic and acquired immunodeficiency syndrome (AIDS) patients. Oral candidiasis may cause significant pain and discomfort to sufferers. Candida species naturally occur in the mouths of all healthy individuals (Lewis & Williams, 2017). *C. albicans* is the most common and most crucial etiological organism for oral candidiasis (de Barros *et al.*, 2020; Fourie *et al.*, 2016; Lewis & Williams, 2017; Lohse *et al.*, 2018; Sharma, 2019).

1.9 Predisposing factors for oral candidiasis

1.9.1 Local factors

Saliva: The incidence of dry mouth (xerostomia) and its associated side effects are increasing as a result of some systemic diseases and conditions, ageing, and medication (Vila *et al.*, 2020). Once saliva production and function are reduced, patients are prone to experience dental caries, discomfort on wearing dentures, as well as opportunistic infections and diseases such as oral candidiasis. Salivary gland dysfunction, which affects the quality and quantity of saliva, can also contribute to an increased risk for oral candidiasis (Anil *et al.*, 2016; Turner *et al.*, 2008; Vila *et al.*, 2020).

Dental prostheses: Denture-related stomatitis is the most common type of oral candidiasis associated with mucosal changes in complete or partial denture wearers. This inflammatory condition could be attributed to fungal cells adherence to the denture acrylic, ill-fitting dentures, hyposalivation, and poor oral and denture hygiene (Neppelenbroek, 2016; Patil *et al.*, 2015; Vila *et al.*, 2020).

Topical medication: The use of topical and inhalational corticosteroids suppresses local immunity and may cause an imbalance in the oral flora resulting in oral candidiasis (Patil *et al.*, 2015; Vila *et al.*, 2020).

Smoking: The exact mechanisms of how smoking contributes to oral candidiasis, has not yet been determined. However, it has been suggested that the suppression of local immunity may indirectly affect the levels of blood glucose predisposing individuals to oral candidiasis (Munshi *et al.*, 2015; Patil *et al.*, 2015; Vila *et al.*, 2020).

1.9.2 Systemic factors

Age: Elderly patients are more likely to have compromised immunity, which predisposes them to the development of oral candidiasis (Fourie *et al.*, 2016; Quindós *et al.*, 2019).

Nutritional status: Iron deficiency is the most common cause of oral candidiasis (Patil *et al.*, 2015).

Systemic drugs: The use of antibiotics, immunosuppressants, and medications resulting in a dry mouth over an extended time, favours the development of oral candidiasis (Martins *et al.* 2014).

Endocrine disorders: Patients with diabetes and Cushing's disease frequently suffer from oral candidiasis (Patil *et al.*, 2015; Quindós *et al.*, 2019).

Immune disorders: AIDS patients are predisposed to Candida infections (Martins *et al.*, 2014; Quindós *et al.*, 2019).

Malignancies: Patients receiving chemotherapy and radiotherapy have compromised host defence mechanisms (Martins *et al.*, 2014; Patil *et al.*, 2015; Vila *et al.*, 2020).

1.10 Characteristics of *Candida albicans*

Candida albicans is described as a dimorphic or pleomorphic yeast. It exists in three different morphological forms: the yeast cell, the septate filamentous form called the pseudohypha, and the hypha. Systemic and local predisposing factors promote the transition of Candida as a normal innocuous commensal organism to a problematic pathogen. Virulence factors facilitate the adhesion of the fungus to the epithelium, colonization, proliferation, and finally invasion (Fourie *et al.*, 2016; Lewis & Williams, 2017). In oral candidiasis, Candida's ability to adhere in the mouth prevents removal of the fungus by the effects of salivary flow and swallowing (Castillo *et al.*, 2019; Lewis & Williams, 2017). Adherence to dentures or other oral devices

also hinders removal from the cavity. Candidal filamentous elements can invade the epithelium resulting in an inflammatory reaction that presents as a clinical infection (Fourie *et al.*, 2016).

1.11 Classification of oral candidiasis

In 1997 a classification system was introduced by Axéll *et al.* (1997), which was modified by Singh *et al.*, (2014) as listed in Table 6.

Table 6: Classification of oral candidiasis (from Singh *et al.*, 2014)

Primary candidiasis	**Secondary candidiasis**
Acute Pseudomembranous Erythematous	Oral manifestations of systemic mucocutaneous Candidiasis due to diseases (thymic aplasia) or endocrinopathy syndrome
Chronic Pseudomembranous Hyperplastic Erythematous Nodular Plaque-like	
Candida associated lesions Angular cheilitis Denture stomatitis Median Rhomboid glossitis	
Keratinized primary lesions with Candidal superinfection Leukoplakia Lichen planus Lupus erythematosus	

1.12 Pathogenesis of *Candida albicans*

As previously mentioned, *C. albicans* asymptomatically colonises mucosal epithelial tissue surfaces as a normal commensal organism (Pellon *et al.,* 2020). A disturbance in the mucosal epithelial tissues of the host due to underlying diseases or conditions as a result of immunosuppressed, immunocompromised, or immunological dysfunctional states, accelerates *C. albicans*'s ability to multiply and colonise at practically at any other site (Castillo *et al.*, 2019; Mothibe & Patel, 2017).

The pathogenesis of denture stomatitis (DS) is mostly associated with hypersensitivity reaction propagated (modulated) by cascades of inflammation against Candida (Fidel, Yano, Esher, *et al.*, 2020). In humans, *C. albicans* is the most common fungal pathogen, which can cause mycoses on oral mucous epithelial tissues as well as systemic infections (Fidel *et al.*, 2020). The prevalence of *C. albicans* species has the highest infection rates among the Candida strains and is isolated and confirmed in about 50-98% of cases. Unlike C. *albicans*, other species such as *Candida glabrata* and *C. tropicalis* are commonly isolated from the palatal mucosa of healthy individuals wearing dentures, denture acrylic surfaces, and individuals with DS (Bueno *et al.*, 2015).

Importantly, Candida species have various virulence factors that enable their adaptable alteration from a normal commensal organism to a pathogen. More specific factors are conferred by their capability to change their morphology and characteristics as well as the ability to form biofilms (de Barros *et al.*, 2020; Calderone & Fonzi, 2001; Cutler, 1991; Fidel *et al.*, 2020; Lohse *et al.*, 2018). The pathogenesis of C. *albicans* is also principally favoured by these two virulence factors. This is evident as a substantial amount of oral *C. albicans* candidiasis cases are linked to biofilm formation on the host's mucosal epithelial tissues or

prostheses (Cavalheiro & Teixeira, 2018; Fidel *et al.*, 2020; Lohse *et al.*, 2018; Tsui *et al.*, 2016). Over time, the polymorphic fungus C. *albicans* has evolved and is resilient in several niches of the human body, favouring its adaptation to vulnerable mucosal epithelial surface leading to propagation of opportunistic infections and systemic invasion (Nikou *et al.*, 2019; Pellon *et al.*, 2020).

Hyphae formation (De Barros *et al.*, 2020; Lohse *et al.*, 2018; Naglik *et al.*, 2017; Susewind *et al.*, 2015) is another virulence factor that convenes biofilm formation and is supported by several conditions such as serum, temperature, proteins (amino acids), and carbon dioxide and pH levels (Castillo *et al.*, 2019). The morphogenesis of *C. albicans* hyphae is crucial and instrumental for successful evasion and lysis prevention by the phagocytes of the host's immune system. Phagocytosis propagates an alteration in morphological features of the pathogen cell from yeast to hyphae. In hyphae state, the fungi cell can elongate and subsequently perforate the macrophage membrane, resulting in the death of the macrophage and permitting phagocytosed *C. albicans* to be evaded (Berman & Sudbery, 2002; Jacobsen *et al.*, 2012; Kong & Jabra-Rizk, 2015).

1.13 Management and treatment of oral candidiasis

Several studies have previously been conducted to assess the probable causal elements of denture-related stomatitis (Altarawneh *et al.*, 2013; Budtz-Jørgensen, 1981; Emami *et al.*, 2014; 2017; Gendreau & Loewy, 2011; Reeve & Van Roekel, 1987; Sharma, 2018; Webb *et al.*, 1998). However, no consensus has been reached in terms of a sole cause, and currently, the disease is considered to have multifactorial influences.

The most common fungal infection encountered in dermatology is oral candidiasis as a result of an overgrowth of *C. albicans* on mucosal areas of the oral cavity (Pellon *et al.*, 2020). Comprehensive management to control DS must include thorough oral and denture hygiene practices coupled with antifungal or antibacterial therapy (Hellstein & Marek, 2019; Millsop & Fazel, 2016; Fidel *et al.*, 2020; Vila *et al.*, 2020).

Several different therapeutic regimens are recommended for the treatment and management of DS. Some of them include the application of topical and/or systemic antifungal therapy, oral hygiene measures, and acrylic denture prosthesis hygiene and disinfection. Other pursuits for the management of DS include; correction of anatomic irregularities on dentures, replacement or repair of broken or old dentures, correction of traumatic occlusion, removal of dentures when sleeping (at night), nutritional restitution (Neppelenbroek, 2016), mouthwash antiseptics, natural antimicrobial remedies, photodynamic therapy (PDT) and microwave disinfection (Bandara *et al.*, 2017; Černáková *et al.*, 2019; Emami *et al.*, 2014; Iqbal & Zafar, 2016; Matsubara *et al.*, 2016; Rodrigues *et al.*, 2019).

Clinicians routinely use antifungal medication for the treatment and management of oral candidiasis, based on the evidence that Candida is the primary etiological factor for DS onset (Neppelenbroek, 2016). Re-colonisation of Candida and high recurrence rates related to DS upon cessation of antifungal regimens also often occurs (Emami *et al.*, 2014). Prevention solely relies on the elimination of contact between the infected tissues and acrylic denture bases by inserting denture-relining material. Resilient denture liners are commonly prescribed to allow the recovery of inflamed mucosal tissue and to provide comfort to the patient. Therefore, modification of these temporary tissue conditioners (liners) to include an antifungal agent allow less frequent application of topical antifungals, improved patient compliance, and simultaneous

treatment of the inflamed denture-bearing mucosal tissues and Candida infection. Depending on the clinical situation, the intervention and management of oral candidiasis may involve one of the following regimes (Hellstein & Marek, 2019; Millsop & Fazel, 2016):

a. Topical antifungal agents
b. Systemic antifungal agents
c. Alternative antifungal agents

1.13.1 Conventional topical antifungal agents

The most utilised topical antifungal agents are nystatin and miconazole. These two agents are sufficiently efficacious; however, both require prolonged use to eliminate the candidiasis. Miconazole has a better pharmacological performance and more patients prefer it, but it is likely to have interactions with other medications, warranting careful assessment before prescribing it (Lygre *et al.*, 2015; Quindós *et al.*, 2019; Skupien *et al.*, 2013). Other topical agents for oral candidiasis, include itraconazole capsules and oral solution, miconazole oral gel and buccal tablets, fluconazole, ketoconazole, amphotericin B, or clotrimazole (Fang *et al.*, 2020). However, the availability of most of these antifungal medications in most countries is limited. Nystatin and chlorhexidine have extensively been used in dentistry to locally control oral infections, as adjuncts to manual oral debridement procedures, especially in patients with immune or endocrine dysfunctions as they become vulnerable to opportunistic infections (Bescos *et al.*, 2020; Scheibler *et al.*, 2018)

1.13.1.1 Nystatin as a conventional topical antifungal agent

For a long time, nystatin has demonstrated good antifungal properties. However, it has been associated with lingering possibility for chronic recurrence and persistence of oral *C. albicans* infections. The substantial differences in nystatin-induced post-antifungal effects amongst non-*albicans* species can also have inevitable clinical consequences, pertaining to the nystatin

regimen applied during treatment and management of these fungal infections (Ellepola & Samaranayake, 2007). For infants, children, and immunosuppressed individuals (e.g. HIV/AIDS patients), nystatin has been documented as inferior to fluconazole for the treatment of oral candidiasis (Lyu *et al.*, 2016).

Furthermore, Fang *et al.*, (2020) conducted a probabilistic graphical model (Bayesian networks) using available randomised controlled studies. The authors predicted the comparative efficacy of conventional antifungal treatments on oral candidiasis (Fang *et al.*, 2020). Using both the meta-analysis and the Bayesian network model, the authors established that, all the conventional antifungals [amphotericin B, clotrimazole, fluconazole, itraconazole (capsule and oral solution), ketoconazole, miconazole oral gel, miconazole buccal tablets and nystatin] had better performance than the placebos. Fluconazole, miconazole and ketoconazole had better efficacy than nystatin. Overall, fluconazole efficacy in reducing mucosal fungal infection was better than all the treatments (Fang *et al.*, 2020).

1.13.1.2 Chlorhexidine as a conventional topical antifungal agent

Since 1970, chlorhexidine (CHX) has regularly been used in dental practice as an antimicrobial agent, due to its long-term antibacterial potential and a broad spectrum of activity (Löe & Rindom Schiøtt, 1970). Since then, several clinical trials have demonstrated the successful effects of CHX in managing and controlling gingival inflammation, bleeding, and dental plaque (Afennich *et al.*, 2011; Gunsolley, 2010; James *et al.*, 2017; Van Strydonck *et al.*, 2012). There exists a high level of evidence that CHX is a versatile antimicrobial agent (James *et al.*, 2017; Paulone *et al.*, 2017), in a mouth rinse or in topical gel form (Fiorillo, 2019). However, it has a few notable unwanted effects during prolonged use (over 4 weeks) (Ardizzoni *et al.*, 2018). These include extrinsic staining effects (De Baat *et al.*, 2017; James *et al.*, 2017; Van Strydonck

et al., 2012; Supranoto *et al.*, 2015) associated with a rapid build-up of calculus and transiently altered taste (James *et al.*, 2017). There is also a concern when using CHX alongside nystatin, as they are prone to interact with each other, and negatively influence their metabolisation (Scheibler *et al.*, 2018).

Recently, Mishra *et al.* (2016) conducted a clinical trial and proposed an equivalent probiotic-containing mouth rinse as an alternative to CHX for children. Their rationale for the use of probiotics was that natural agents are better, and suggested it as an alternative therapeutic agent for managing oral conditions more naturally (Mishra *et al.*, 2016). More recently, a systematic review highlighted the possible reduced efficacy of CHX in the alleviation of oral mucositis in patients on chemo-radiotherapy (Cardona *et al.*, 2017). Very recently, (Bescos *et al.*, 2020) conducted a multicentre study to evaluate the use of CHX as a widely accessible over-the-counter mouthwash in healthy patients. The authors concluded that only limited evidence is available to support that CHX promotes a healthy oral microbiome, or that it causes an alteration in the oral microbiome associated with the disease. They further demonstrated that mouthwash containing CHX might lead to a significant alteration in the microbiome composition in saliva, contributing to a considerable acidic environment and reduced nitrite present in healthy individuals, and subsequently affecting their blood pressure (Bescos *et al.*, 2020). Thus, a thorough clinical and medical history must be conducted to acquire information on any underlying systemic diseases and conditions before prescribing CHX. Any conditions causing immunosuppression or immunocompromised states should also be managed accordingly.

1.13.2 Systemic antifungal agents

Orally-administered fluconazole is an effective antifungal regimen for managing oral candidiasis that does not respond to topical agents. Alternative systemic antifungal agents including intravenous and other orally-administered agents such as voriconazole, itraconazole or posaconazole are less commonly administered. Other accessible newer agents include isavuconazole and echinocandins (Caspofungin and Anidulafungin). Echinocandins can only be administered intravenously, while isavuconazole is available for both intravenous and oral administration (Quindós *et al.*, 2019). Several other possible alternatives include the utilisation of antibodies, cytokines, and antimicrobial peptides (lipids like amphotericin B).

1.13.3 Alternative antifungal agents

There are several alternative approaches for the treatment and management of DS, most of which are ineffective in the long term. These include the use of a combination of anticandidal medicines, disinfectants, oral antiseptics, natural antimicrobial remedies, PDT, and microwave prosthetic disinfection (Bandara *et al.*, 2017; Černáková *et al.*, 2019; Emami *et al.*, 2014; Fidel *et al.*, 2020; Rodrigues *et al.*, 2019).

In addition, the use of essential oils, extracts, honey, and isolated molecules, alone or as adjuncts to conventional antifungal medication, have shown promising prospects (Černáková *et al.*, 2019; Felipe *et al.*, 2018; Girardot & Imbert, 2016b; Kokoska *et al.*, 2018; Rodrigues *et al.*, 2019; Zacchino *et al.*, 2017a, 2017b). For instance, the proposed mechanism of action of essential oils involves disintegration of the mitochondria membrane resulting in interference with the fungal electron system. Besides, essential oils have been reported to have the potential to cross fungal cell walls and subsequently disrupt ATP assembly and cell wall integrity (Tariq *et al.*, 2019).

Further, to the above methods, modification of denture base material, resilient liners and tissue conditioners have been reported as alternative approaches for the management and treatment of DS as concerns for microbial tolerance, toxicity and efficacy of antimicrobial increases (Ahmad *et al.*, 2020; Bueno *et al.*, *et al.*, 2017; Cierech *et al.*, 2018; Cierech *et al.*, 2016b; Garaicoa *et al.*, 2018; Kamonkhantikul *et al.*, 2017; Lygre *et al.*, 2015; Nam & Lee, 2019). Advancement and development related to materials for dentures have focused on ways to inhibit and control the formulation, adherence, and maturation of biofilms. The significance of this is targetting the reduction in fungal and bacterial colonisation on denture acrylic or tissue conditioner materials. Coupled with meticulous prosthesis hygiene practices, the earlier can subsequently contribute to a decrease in incidences and prevalences of oral candidiasis, and denture-related stomatitis (Lygre *et al.*, 2015).

Furthermore, the utilisation of probiotics (Bandara *et al.*, 2017; Matsubara *et al.*, 2016; Mishra *et al.*, 2016; Morse *et al.*, 2019; Ohshima *et al.*, 2016; Rodrigues *et al.*, 2019), drug delivery systems (Liang *et al.*, 2020) as well as various NPs(de Alteriis *et al.*, 2018; de Barros *et al.*, 2020; Bujdáková, 2016; Castillo *et al.*, 2019; Cierech *et al.*, 2018, 2019; Halbandge *et al.*, 2019; Monteiro, Arias, Araujo, *et al.*, 2020; Monteiro, Silva, Negri, *et al.*, 2013; Monteiro *et al.*, 2015; Mousavi *et al.*, 2018, 2019; Rozman *et al.*, 2019; Seong & Lee, 2018), and genomic exploration through transcriptional regulation and translational control (Kadosh, 2019), have been explored as promising alternative antifungal therapies. As shown in Figure 6, the application of NPs with antimicrobial properties has been studied and discussed in this report as an alternate and viable option for the management of oral Candida infections, particularly persistent oral candidiasis associated with biofilm accumulation.

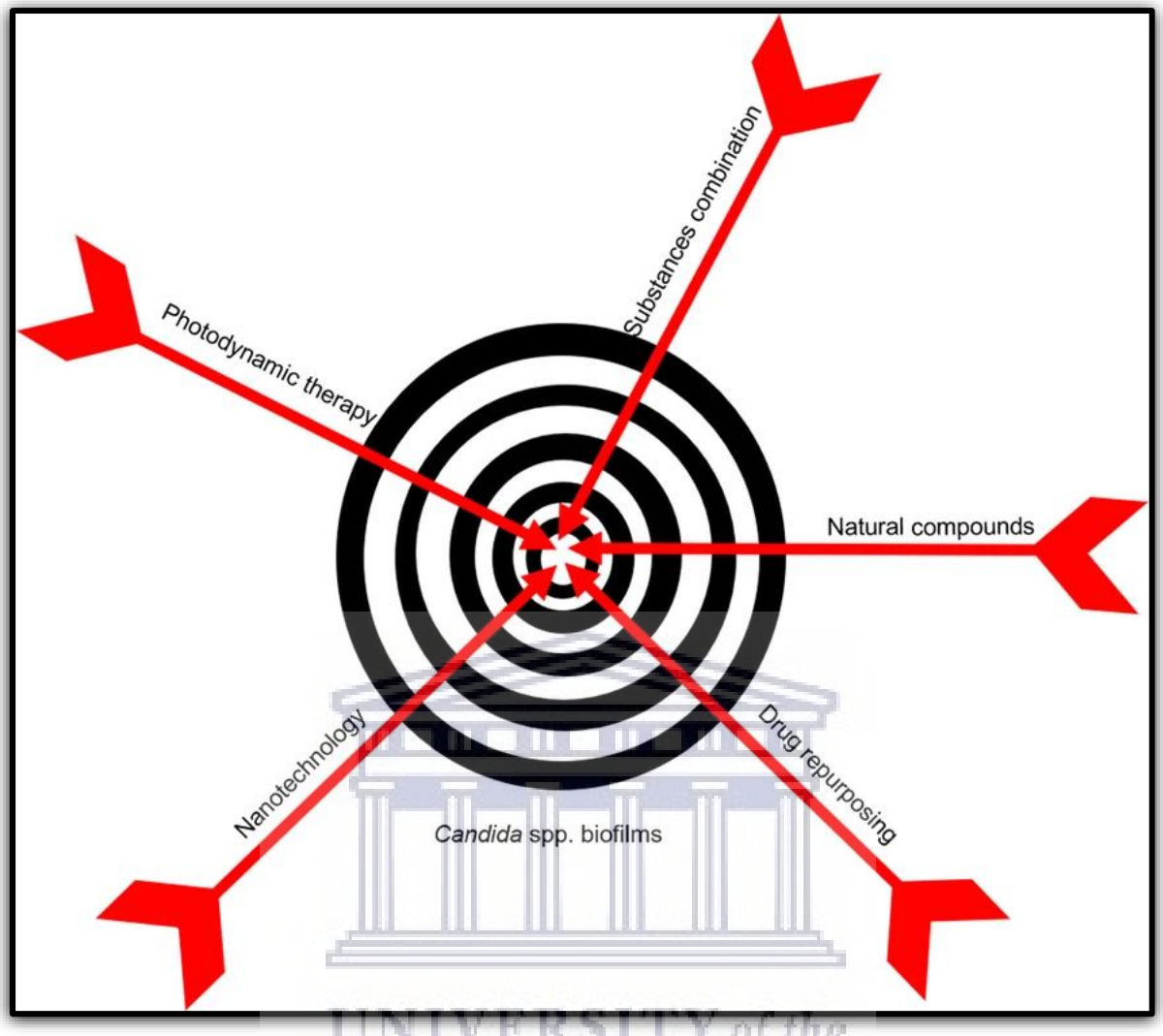

Figure 6: Representation of alternative antifungal methods for controlling biofilms of Candida species (from de Barros *et al.*, 2020)

1.14 Problem statement

To date, in most developing nations, communities suffer from numerous communicable diseases and opportunistic infections. Oral candidiasis (opportunistic infection) is a biofilm-associated infection and remains one of the biggest challenges in health care and communities at large across all age groups. Furthermore, development and shifts in health care practices can contribute to new drug-resistant strains of fungi. Moreover, global climatic and environmental changes can lead to terrestrial fungal species causing diseases in humans.

Oral candidiasis is a public health concern due to the increased burden of multiple chronic systemic diseases and conditions including increased numbers of individuals with weakened immune systems leading to opportunistic infections (cancer patients, organ transplant recipients, individuals with HIV/AIDS, and stem cell transplant patients). Recently, Nobile and Johnson (2015) reported on 150 different species that were isolated from oral cavity lesions in seroconverted patients. The isolated *C. albicans* showed 35% resistance to fluconazole (Nobile & Johnson, 2015). The burden of chronic systemic conditions combined with the introduction of drug-resistant strains and changes in hosts' local oral factors, contribute to increasing oral candidiasis incidences that warrant a need for exploration of alternative fungal therapeutics.

1.15 Significance of the study

Nanotechnology offers unique solutions as one of the most rapidly emerging technologies, availing numerous consumer and biomedical products. The minute size of NPs, coupled with large surface area per unit volume, convey features that are beneficial in microbiology as antimicrobial agents (Agarwal *et al*., 2018; da Silva *et al*., 2019a). The application of ZnO NPs is precisely encouraging, practical, and cost-efficient modality for combatting drug resistance while ensuring biofilm control and inhibition. There is also an apparent demand for eco-friendly methods for synthesising ZnO NPs devoid of contaminants and hazardous by-products. Therefore, a combination of banana peel and Buchu-infused Rooibos tea leaves extracts are explored in the production of GZnO NPs.

CHAPTER TWO - Aims and objectives

2.1 Aim

To synthesise GZnO NPs and determine their antifungal effect on *C. albicans* biofilms.

2.2 Objectives

- To synthesise GZnO NPs from extracts of *A. linearis* (Rooibos), *A. betulina* (Buchu) and *M. paradisiaca* (banana).
- To characterise the formulated GZnO NPs from extracts of *A. linearis* (Rooibos), *A. betulina* (Buchu) and *M. paradisiaca* (banana).
- To investigate the antifungal effect of the GZnO NPs on *C. albicans*.
- To compare the antifungal effects of the GZnO NPs on *C. albicans* with that of nystatin and 0.2% CHX gluconate.

Null Hypothesis

GZnO NPs formulated from extracts of *A. linearis* (Rooibos), *A. betulina* (Buchu) and *M. paradisiaca* (banana) do not have any effect on *C. albicans*.

CHAPTER THREE - Methodology

3.1 Study design

This was an exploratory experimental (*in vitro*) study. Experiments were conducted in two laboratories: The Chemical Sciences (SensorLab), main campus, and The Oral and Dental Research Institute (ODRI), at the Tygerberg Campus, UWC. The study did not involve the use of any biological tissues or patients. The study was carried out as outlined in Figures 7 and 8 below.

1. Synthesis of GZnO NPs
2. Characterisation of GZnO NPS

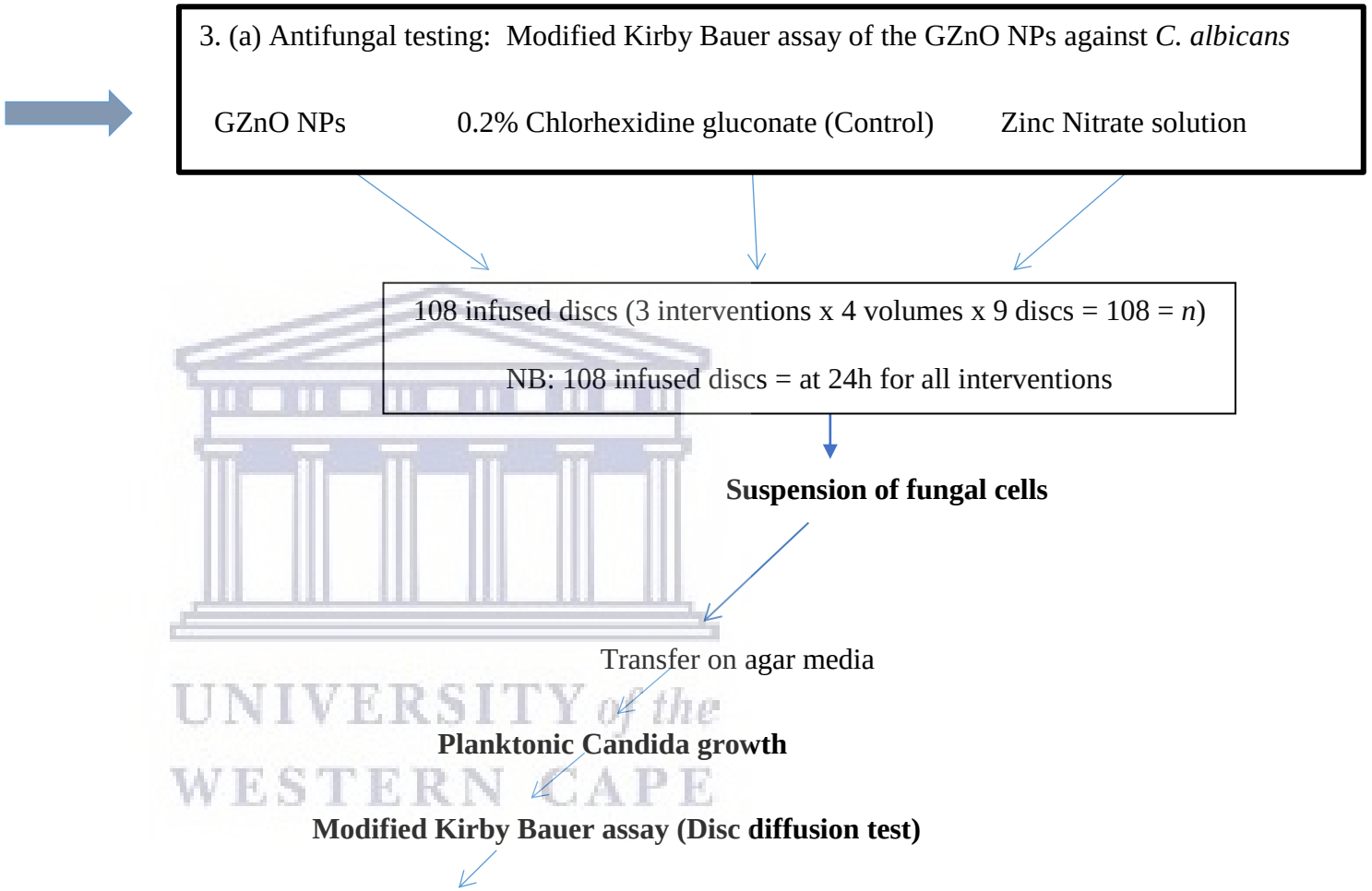

Figure 7: Study Summary (Section 3.4.1)

1. Synthesis of GZnO NPs
2. Characterisation of GZnO NPs

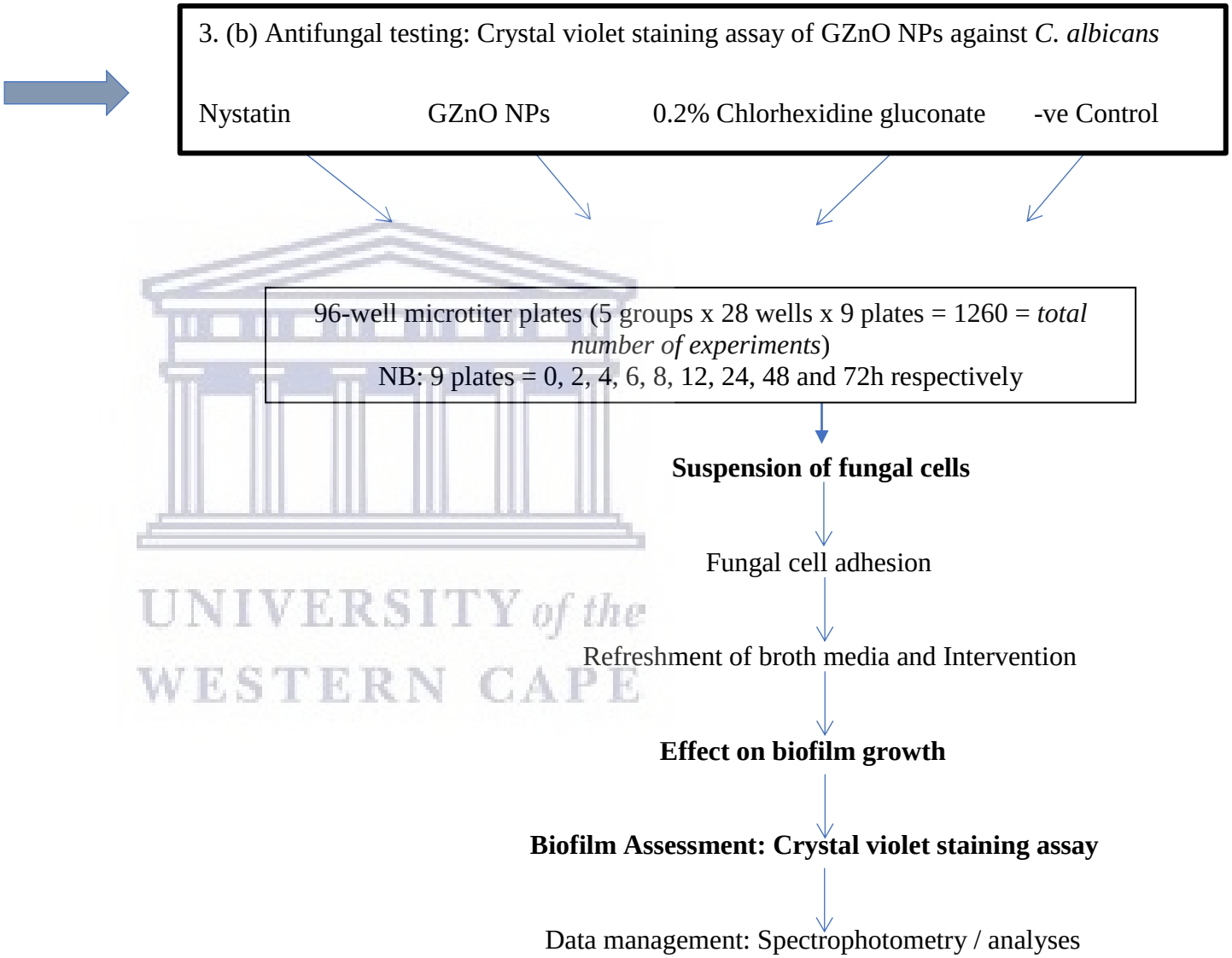

Figure 8: Study Summary (Section 3.4.2)

3.2 Synthesis of green zinc oxide nanoparticles

3.2.1 Armamentarium, reagents, and materials

The materials and reagents for the green synthesis of ZnO NPs were distilled water, Rooibos and Buchu tea leaves (commercially available, manufactured by Biedouw Valley Rooibos, Western Cape, SA) (Figure 9 below). Banana peel (collected as remains of organic banana fruit), and zinc nitrate hexahydrate ($Zn(NO_3)_2 \cdot 6H_2O$ purchased from Sigma Aldrich, Merck (Pty) Ltd, South Africa. Essential lab equipment included a magnetic stirrer, a hot plate with a thermometer, glass beakers, aluminium foil sheets, and conical glass flasks.

The Zn was sourced from $Zn(NO_3)_2 \cdot 6H_2O$, which was dissolved in distilled water. The GZnO NPs were manufactured using a mixture of *M. paradisiaca* (BPE), as well as two tea leave extracts from *A. linearis* (Rooibos) and *A. betulina* (Buchu). Three protocols were adopted and slightly altered to achieve a green single pot synthesis method. The first two adopted protocols were for the Rooibos and Buchu green tea mixture (Diallo *et al.*, 2015; Thema *et al.*, 2015b) and were combined with a third protocol (Maruthai *et al.*, 2018). Equal volumes (10 ml) of the green teas of Rooibos and Buchu were used as reducing and stabilizing agents for the synthesis of ZnO NPs.

3.2.2 Preparation of the banana peel extract

The BPE was prepared according to the protocol by Maruthai *et al.* (2018), with slight modifications. The peels were washed and rinsed with distilled water, allowed to dry, and cut into thin slices, after which 100 g of peels were boiled in 300 ml distilled water for 30 min at 70 ^{O}C under magnetic stirring. The banana extract was cooled naturally to room temperature (25 °C) and poured out gently and centrifuged at 1000 rpm for 15 min. The acquired supernatant (clear extract) was poured out, leaving insoluble fractions of precipitate and

macromolecules. The extract was stored in a well-labelled clean glass bottle as a stock extract solution (4 °C) until further use.

3.2.3 Preparation of Buchu-infused Rooibos extracts

These extracts were prepared with minor modifications of protocols by Diallo *et al.* (2015) and Thema *et al.* (2015b). In a clean container, 5 g (4:1) of a mixture of Rooibos and Buchu ground tea leaves (Figure 9) was dissolved in 100 ml distilled water. The solution was then boiled at 80 ºC for 2 h under mechanical stirring (1000 rpm) after which it was allowed to cool naturally to room temperature (25 °C) and poured out gradually. The solution was then centrifuged at 1000 rpm for 15 minutes, and the supernatant (clear extract) was poured out, leaving insoluble fractions of precipitate and macromolecules. The resultant extract was stored (at 4 ^{O}C) in a clean storage bottle as a stock extract solution until further use.

Figure 9: Buchu and Rooibos tea leaves for the preparation of extracts

3.2.4 Phytosynthesis of zinc oxide nanoparticles

In order to synthesize the ZnO NPs, a solution of $Zn(NO_3)_2.6H_2O$ (0.1 M) was prepared in 50 ml distilled water in an ultrasonic vibrator to ensure complete dissolution of the salt. Following the completion of the procedures described in sections, 3.2.2 and 3.2.3 stock solutions were obtained, which were used in the final step of ZnO NPs formulation, as illustrated in Figure 10 below. For this single pot synthesis, the $Zn(NO_3)_2 \cdot 6H_2O$ solution together with two equal portions (10 ml) of the stock solutions of BPE and Buchu-infused Rooibos extract were added to a sterile conical flask under continuous stirring. At a regular speed, the mixture was magnetically stirred while wrapped with an aluminium foil sheet to prevent photoactivation of the zinc nitrate during the synthesis procedure. Temperatures were monitored to remain between 65 and 70 °C for 5 h, as illustrated in Figure 10. The resultant mixture was naturally left to gradually cool to 25 °C (room temperature). Upon completion of the green synthesis of the ZnO NPs, the colour changes in the mixture were recorded, and the mixture stored in a sterile brown bottle at room temperature for further characterisation and antimicrobial testing.

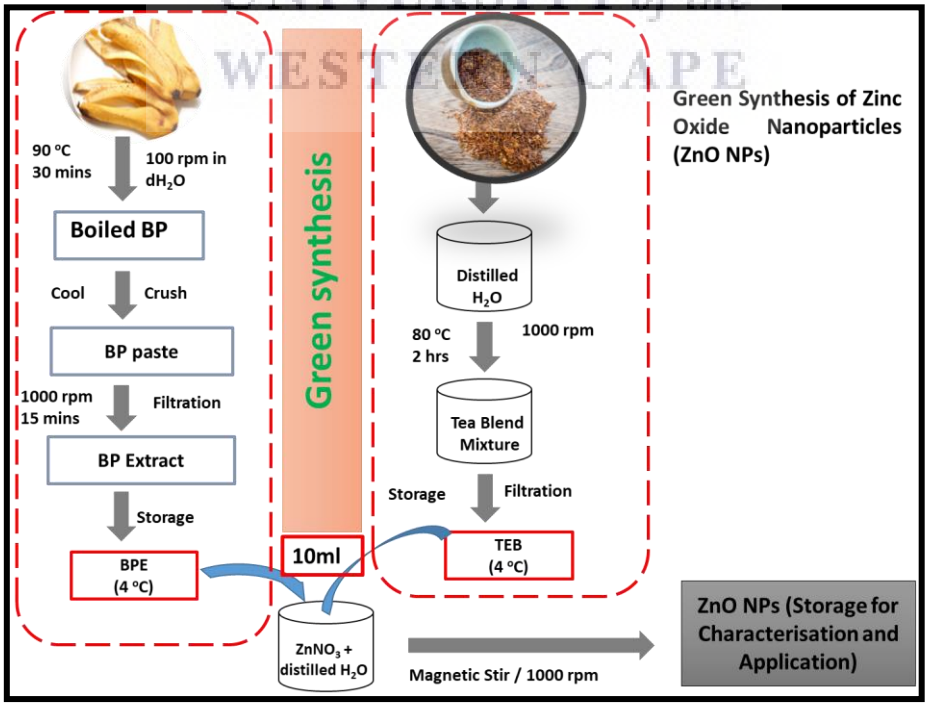

Figure 10: Procedures, materials, and conditions for the phytosynthesis of GZnO NPs

3.3 Characterisation of the banana and Buchu-infused Rooibos phytosynthesised zinc oxide nanoparticles

In this research study, characterisation was performed using various techniques, mainly drawn from the field of materials science. The sample(s) were individually customised before characterisation, to successfully validate the GZnO NPs using the methods listed below in the following forms, either dry the aqueous NPs, dilute the aqueous NPs, formulate pellets, or to use the aqueous NPs *de novo*. A series of standardized analysis methods, such as UV-vis, XRD, FTIR and electron microscopy (HRTEM or HRSEM), were used to study the structural properties (morphology, optical properties) of the green ZnO NPs.

The grouping of characterised samples was as follows:

A total of fifteen samples (n = 15) were prepared, and the tests performed in triplicate for each group to validate the successful synthesis of the GZnO NPs. The sample specimens were divided into five groups, as elaborated below:

Group I: Aqueous GZnO NPs sample for UV-Vis analyses;

Group II: Solid (freeze-dried) GZnO NPs for XRD analyses;

Group III: Solid (oven-dried) GZnO NPs mixed with potassium bromide (KBr) salt for FTIR analyses;

Group IV: Solid (freeze-dried) GZnO NPs for HRTEM and HRSEM analyses; and

Group V: Aqueous sample solution of GZnO NPs for antimicrobial tests (described in section 3.4)

3.3.1 Ultraviolet-visible spectroscopy analysis

An aqueous sample of GZnO NPs and plant extracts were studied using UV-Vis equipment, as seen in Figure 11 to determine their absorbances. The selection of wavelength was set

between 200 and 600 nm (Kumar, 2013), and a calibration curve was captured and measured at a set wavelength as per standard protocols.

Figure 11: Ultraviolet-visible (UV-Vis) spectrophotometer (from AZoOptics "The Different Types of Spectroscopy for Chemical Analysis")

3.3.2 X-ray diffraction analysis

A dry sample of synthesised GZnO NPs was obtained by freeze-drying the aqueous solution of NPs obtained upon completion of the procedure in section 3.2.4 above. The amorphous sample obtained after freeze-drying was further dried in an oven overnight at 70 ºC before assessing the sample under the microscope. In this study, the structure and morphology of the GZnO NPs were interrogated using XRD analysis. It is a primary technique for probing the structure of nanomaterial. XRD analyses the structural design from a scattering pattern produced when the radiation beam interacts with the material. It is a non-destructive method

that is primarily employed for the identification of the phase of materials, for example, crystallinity. The size of a crystal and the orientation pattern details and the imperfections of natural and synthetic compounds can also be determined with this technique (Mourdikoudis *et al.*, 2018).

Furthermore, the technique is not only powerful, but also allows for rapid, qualitative and quantitative analysis of nanomaterials, and ensures that data interpretation is relatively straightforward. The data captured is reflected as peaks. Each peak generated represents a unique feature of a crystalline structure and provides a powerful tool for identification of the phase composition of powder and crystallin which can be verified using archived fingerprint data in the X-ray diffractometer (Treacy & Higgins, 2007).

3.3.3 Fourier-transform infrared spectroscopy analysis

Fourier-transform infrared spectroscopy (FTIR) is another essential technique done to validate the GZnO NPs. FTIR is also among the non-destructive characterisation methods, and the instrument that was used can be seen in Figure 12. The vibrational spectroscopic approach of the FTIR technique awards quantitative as well as qualitative analysis for virtually any state of a material sample (organic or inorganic). It is also an efficient technique to analyse and determine functional groups of the material while displaying the various chemical bonds in the material (Griffiths & De Haseth, 2006; Mourdikoudis *et al.*, 2018). In this study, solid samples were prepared by mixing 1 µl of the aqueous ZnO NPs obtained as described in section 3.2.4, with small amount of KBr salt and dried in an oven at 70 ºC overnight. Before loading it into the machine, the sample was ground in a mortar and pestle until a homogenous powder consistency obtained. The powder was then pressed using a quick press KBr pellet kit to form a thin disc (pellet) that was spectroscopically analysed.

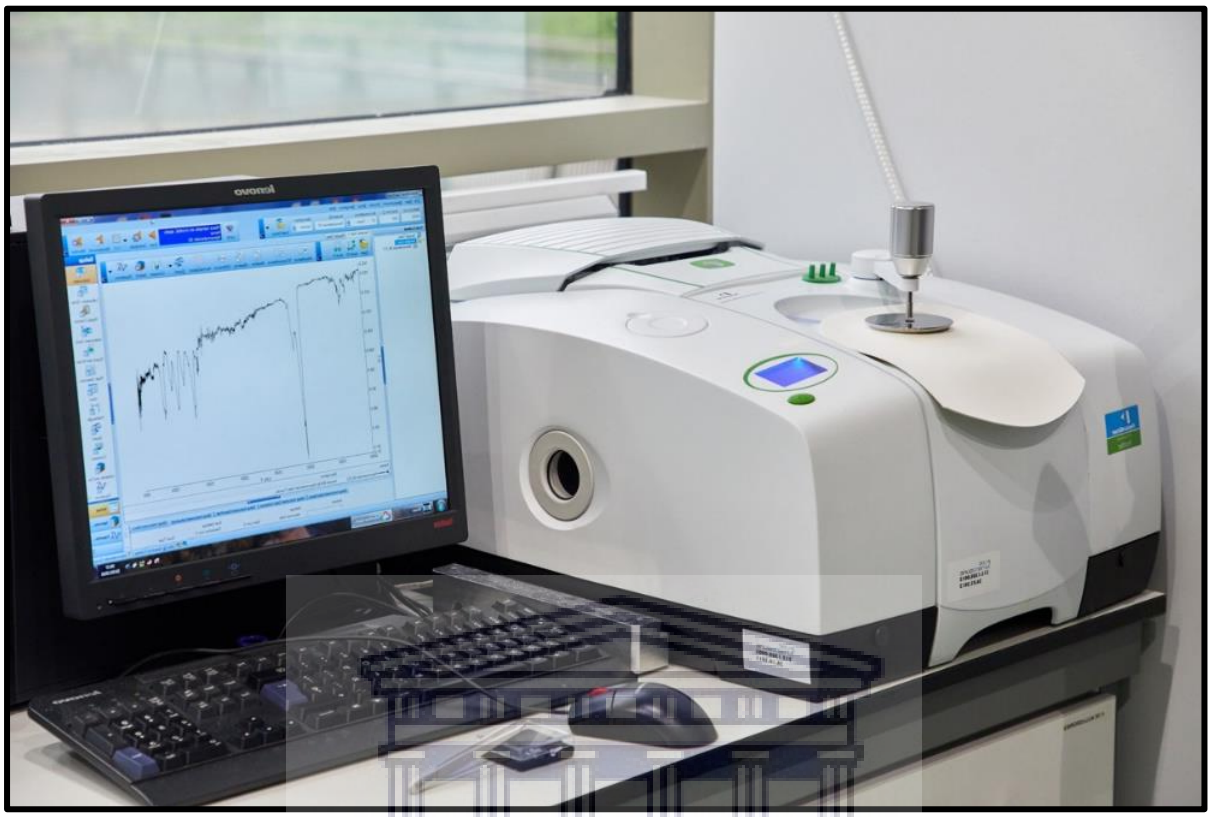

Figure 12: Fourier-transform Infrared Spectroscopy (FTIR) instrument (from 'FTIR Spectrometer PerkinElmer Frontier | External Services | CIC nanoGUNE')

3.3.4 High-resolution transmission electron microscopy, energy-dispersive X-ray spectroscopy, and selected area electron diffraction analyses

A dry sample of synthesised GZnO NPs was obtained by freeze-drying the aqueous solution of NPs obtained upon completion of the procedure in section 3.2.4 above. The amorphous sample obtained following freeze-drying was further dried in an oven overnight at 70 ºC before analysing the sample under the microscope. The HRTEM technique is versatile in gathering details on the internal structure of a particulate, crystal structure, size, sample density, sample appearance, as well as the orientation and stress state of the material sample. This imaging technique uses high magnification to capture and record the internal morphological structure of nanomaterials upon transmission of electrons through the sample. The HRTEM imaging

also allows crystallographic and structural analyses of material samples at the atomic scale level (Mourdikoudis *et al.*, 2018; Williams & Carter, 2009). The TEM functions by the transmission of an electron beam through a transparent particulate surface, resulting in a shadow (dark and light regions) of the transparent particle surface and subsequently allowing capturing of an image. Additionally, this technique is also useful in extrapolating the crystallinity and size of the material, thus complementing the XRD analysis. In this study, Selected Area Diffraction Electron Diffraction (SAED), a crystallographic investigation procedure was steered in the TEM to validate the crystallinity of the GZnO NPs. Usually, if spots are captured in the SAED pattern, it means that the material is crystalline. If the interrogated sample is amorphous, diffuse rings are observed. If crystalline, bright spots are observed. If sample material is polynanocrystalline, minute spots making up rings, are observed. Each spot is arising from Bragg reflection from an individual crystallite. Also, for the same sample, the information acquired from SAED analysis usually corresponds to the data from XRD analysis. In addition, along with the internal structure assessment of the material, energy-dispersive X-ray spectroscopy (EDX) analysis was performed in HRTEM. EDX and EDS are semi-quantitative assessments for material samples (presented as percentage atomic compositions). These analyses are conducted in HRTEM or HRSEM equipment.

3.3.5 High-resolution scanning electron microscopy and energy-dispersive spectroscopy analyses

The microscopy technique, HRSEM, functions by firing a primary electron beam on a conductive particle surface. As a result, inelastic scattering of a secondary electron from the nanoparticulate surface is produced and captured (Figure 13). As a cutting-edge imaging system, this technique can provide detail on crystallinity, electrical characteristics, grain size, and topographical features. The magnification in the SEM technique can be over six orders – approximately 10 to 500000 times. In this study, a dry sample of synthesised GZnO NPs was

obtained following freeze-drying of the aqueous solution of NPs. The sample was then dried further in an oven overnight at 70 °C before microscopic analysis. The EDS analysis method for SEM (SEM-EDS) allows the inspection of material compositional constituents, to avail information on the presence of contaminants, as well as the identification of their origin in the sample material. Therefore, HRSEM was applied as an adjunct technique to validate nanomaterials (Mourdikoudis *et al.*, 2018; Zhou & Wang, 2007).

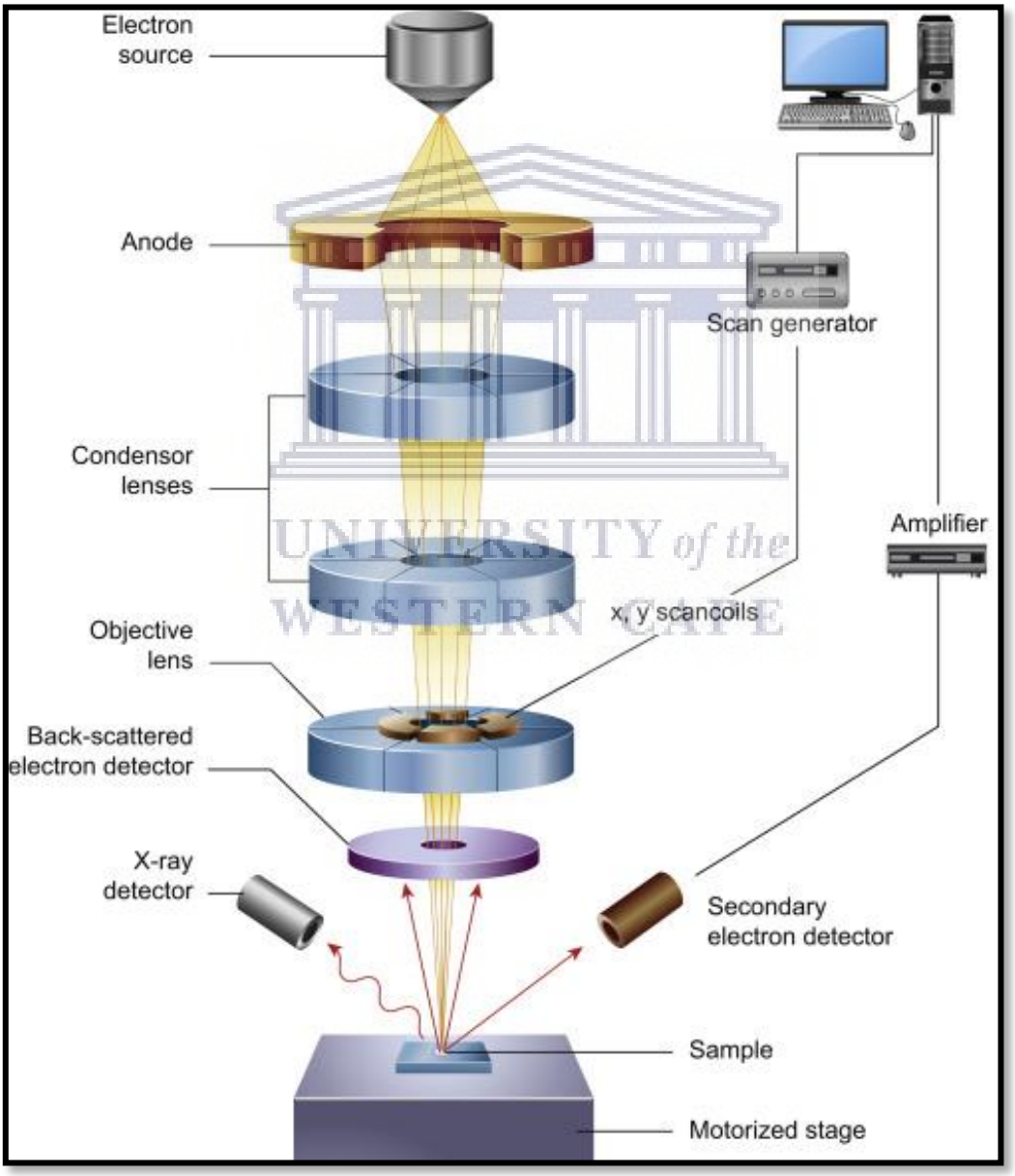

Figure 13: An illustration of a Scanning Electron Microscope's main components (from Inkson, 2016)

3.4 Available *in vitro* antifungal activity options

Several assays have been used for *in vitro* quantification of antimicrobial and antibiofilm regimens on *Candida albicans* (Balouiri *et al.*, 2016; Gulati *et al.*, 2018). The conventional fungal culture plating approach and the counting of CFUs is a primary quantification method (Saubolle & Hoeprich, 1978). However, this method is laborious. Another method documented is the microtiter plate assay using 96-well microtiter plates for biofilm quantification. The CV assay was described for the first time by Christensen *et al.* (1985). Since then, several modifications have been made to improve the accuracy and reliability of this assay (Haney *et al.*, 2018; Shukla & Rao, 2017; Stepanović *et al.*, 2000). The improved approaches strive to improve the "edge effect" and reduce assay errors. Several other colourimetric, fluorescein di-acetate, 3-(4, 5-Dimethyl-2-thiazolyl)-2, 5-diphenyl-2H-tetrazolium bromide (MTT), or 2,3-bis-(2-methoxy-4-nitro-5-sulfophenyl)-2H-tetrazolium-5-carboxanilide (XTT) metabolic staining approaches have been reported for the quantification of biofilm formation using the microtiter plate assay (Haney *et al.*, 2018). In addition, for Candida biofilm quantification, the XTT assay has been commended for its reproducibility, accuracy, and efficiency (Taff *et al.*, 2012), while the CV assay remains an easy, affordable, and adaptable version of the microtiter plate assays and therefore still a useful tool for studying biofilms. In this study, CV assay was used to assess the effects of the interventions on Candida biofilms, and all spectrophotometric readings were captured at 560 nm.

Usually, optical densities can be captured from a spectrophotometer. Optical density (OD) is a factor of turbidity or attached materials and cells from samples. The Beer-Lambert rule governs optical density, i.e. absorbance, is directly proportional to the concentration of the chromophore and wavelength traversing through it. The fungal proliferation in the liquid broth involves four stages (lag, log, stationary, and death). During the lag phase, fungi cultures adapt to growth

conditions, and the log phase is when the cell division or proliferation phase commences. In the stationary phase, the culture is stable, and death and growth of cells are almost equal (Uppuluri & Chaffin, 2007). During the last (death or decay) phase, a decline of ODs can be observed. The decay is due to the exhaustion of the nutritional elements in broth media, or formation of growth initiating elements in the medium. Besides, it is essential to consider other coloured elements of dissolved materials in the suspension that might contribute to a shift of chromophores and consequently, turbidity.

3.4.1 *In vitro* antifungal activity assessment of the green zinc oxide nanoparticles against *Candida albicans*

At the beginning of this phase of experiments, it was hypothesised that the GZnO NPs, precursor salt, CHX, and nystatin have no effect on *C. albicans* (ATCC 90028). The effects of interest were (1) inhibition of growth of planktonic yeast cells and (2) influence on 24-hour biofilm. These effects were tested using two different assays. For the first effect, the antifungal activity was assayed using the Kirby-Bauer susceptibility diffusion test (an agar disc-diffusion method). While for the latter effect, CV staining assay was then employed as detailed by Shukla & Rao (2017).

3.4.2 Modified Kirby-Bauer assay on *Candida albicans* planktonic cells

This is an accepted and approved method published in M 61 of the Clinical and Laboratory Standards Institute (CLSI) for antifungal susceptibility assessment (Alexander *et al.*, 2017). In this study, this assay was conducted to test a hypothesis (H_0) that, there is no effect due to CHX, salt precursor or ZnO NPs. The experimental procedures for the same are detailed below.

3.4.2.1 Materials and equipment used for the Modified Kirby-Bauer assay

The following materials were acquired from Sigma-Aldrich (Merck) for the Kirby- Bauer assay: Mueller-Hinton agar (MHA), phosphate-buffered saline (PBS, P4417-100TAB), Sabouraud 4% dextrose agar (SDA, 89579-500G-F). Petri dishes, 9 mm filter paper discs (FLAS3526009), sterile swabs, and Bio-pointe filter barrier pipette tips (200 µl) were acquired from Lasec (SA). Incubators (static and shaking), autoclave machine, DensiChek™ spectrophotometer, vortex mixer (Eins-Sci E-VM-A Analogue Vortex Mixer Touch Operation, SA), class II safety cabinet, sterile water, and an electronic digital calliper were accessible at ODRI.

3.4.2.2 Muller Hinton agar media preparation

MHA agar (HG000C37.500) media was weighed then dissolved (38 g of powder into 1 litre of sterile distilled water) as according to the manufacturer's instructions. The media was then sterilised by autoclaving (121 °C for 15 min). The sterile media was left to cool gradually to 45-50 °C after which it was poured onto sterile Petri dishes, and then left to further cool and solidify at room temperature (25 °C). The set plates were stored at 4 °C until use.

3.4.2.3 Inoculum strain acquisition and growth conditions

The yeast, *C. albicans*, was obtained from a standard culture stock archived at the Oral and Dental Research Institute, UWC. This *C. albicans* is a reference strain from the American Type Culture Collection, an ATCC 90028. The obtained strain was sub-cultured on BHI agar for a day (24 h) at 37 °C and after that stored at 4 °C until use. These cultures were refreshed for every subsequent experiment. The reactivation of strains and preparation of the inoculum was performed in a biological class II safety cabinet.

3.4.2.4 Ascertaining the authenticity of the *Candida albicans*

Gram staining was performed on the 24 h culture to confirm that the culture sample was Gram-positive oval yeast.

3.4.2.5 Preparation of intervention (infused discs)

A total of 108 sterile test disc (9 mm in diameter) were grouped into three groups and aseptically infused with the interventions in a class II safety cabinet. There were 36 discs per group equally divided for 50 µl, 100 µl, 150 µl and 200 µl of each of the interventions. These intervention groups included aqueous GZnO NPs (test), $Zn(NO_3)_2 \cdot 6H_2O$ solution (test comparison), and 0.2% CHX (positive control). The infused antibiotic test discs were left to dry in an oven at 25 °C for 48 h. The grouping for the modified Kirby-Bauer assay was as follows:

Group I: (50, 100, 150, and 200) µL of 0.2% CHX gluconate (positive control group)

Group II: (50, 100, 150, and 200) µL of aqueous ZnO NPs (test group)

Group III: (50, 100, 150 and 200) µL of $Zn(NO_3)_2 \cdot 6H_2O$ solution (test comparison group)

Then once the infused discs were dry, they were aseptically placed on inoculated MHA plates as elaborated in the following step. The test comparison was used to elucidate whether the potential effect could be due to it (as a precursor salt) or the resultant GZnO NPs.

3.4.2.6 McFarland adjustment of the test organisms

For each experiment, the amount of test organism was calibrated as follows: A single colony of the test organism was transferred from 24 hour-old agar plate aseptically into PBS and then homogenised using a vortexer (Eins-Sci E-VM-A Analogue Vortex Mixer). The vortexing was performed to ensure that the yeast cells are randomly suspended in the solution. The resultant

homogeneous suspension was then calibrated to a concentration of 0.5 McFarland, which corresponds to 1.5 x 10^6 colony-forming units (CFU)/ml, using DensChek™ spectrophotometer as depicted below (Figure 14).

Figure 14: DensChek™ spectrophotometer used for McFarland's adjustment

3.4.2.7 Spread plating and placement of interventions on agar plates

A single colony of the test organism was transferred aseptically directly into PBS and then suspended using a vortexer. Vortexing was performed to ensure that the yeast cells were suspended homogeneously in the solution. The resultant homogeneous suspension was then calibrated to provide a standardised concentration of 0.5 McFarland, which corresponds to 1.5 x 10^6 colony-forming units (CFU)/ml. Random allocation of the sterile MHA plates to intervention groups was performed. Then a hundred microlitres (100 µL) of fungal suspension containing a concentration of 1.5 x 10^6 CFU/ml was aseptically spread plated onto the MHA plates. A glass hockey stick was used while ensuring no creeping of inoculum while spreading. Then the pre-infused and dried sterile discs were aseptically and gently placed on to the sterile MHA agar plates. The inoculated fungal plates were incubated at 37 °C for a day (24 h). Then the zones of inhibition were gauged using an electronic digital calliper.

3.4.3 Crystal violet staining assay on sessile *Candida albicans*

This assay was done to test the hypothesis that, there is no difference in effect due to nystatin, CHX, salt precursor or ZnO NPs. For this assay, an accepted and approved methodology published in M 61 of the Clinical and Laboratory Standards Institute (CLSI) for antifungal susceptibility assessment was adopted (Alexander *et al.*, 2017). Due to material availability, the adopted protocol was slightly customised to allow using of BHI instead of MHA broth. The effect due to the interventions on adhered biofilms onto the well walls and the flat bottom surfaces of the TPP® plates were then assessed. The experiments were performed in triplicates, under the same optimal conditions (i.e. temperature, incubation time, growth medium). All experiments included positive and negative controls in each of the 96-well plates.

3.4.3.1 Materials and equipment for the Crystal violet staining assay

The following materials were procured from Sigma-Aldrich (Merck) for the antifungal testing of sessile microorganisms: brain heart infusion (BHI) broth and agar, Techno Plastic Products (TPP®) clear polystyrene 96-well (8x12) sterile microtiter plates, volume approximate 300 µl with a flat bottom (Figure 15), alphanumerically coded, PBS, Sabouraud 4% dextrose agar (SDA), nystatin bioreagent (suitable for cell culture), crystal violet (CV) solution and 30% acetic acid. Some of the equipment used were similar to those described in 3.4.2.1 (Figures 14 above and 16 below).

3.4.3.2 Microtiter tissue culture plate description

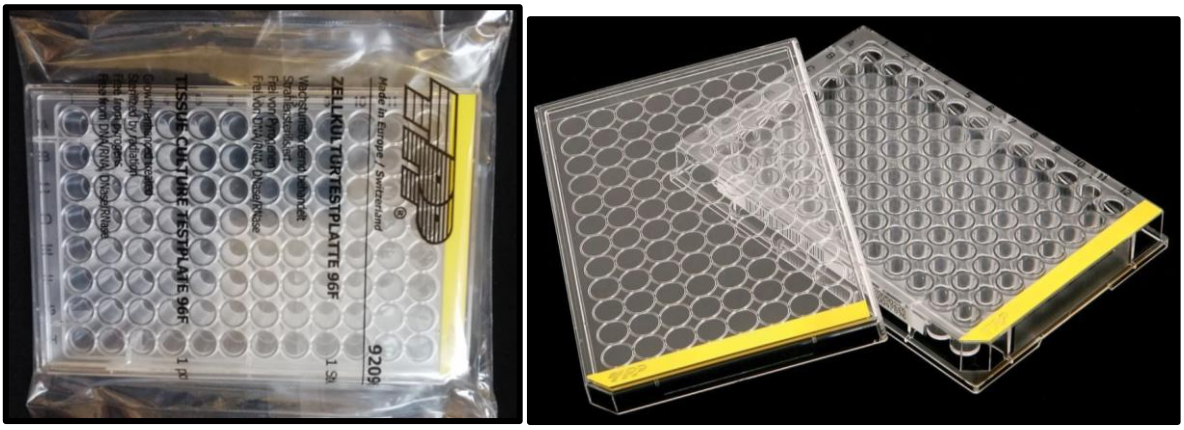

Figure 15: TPP® 96-well microplate (tissue culture plate) with flat bottom wells

TPP® flat bottom tissue culture plates (Sterile polystyrene, 0.34 cm^2, 108/cs) (Figure 15) were selected to study Candida biofilms. The justification for choosing these F-base (flat bottom) TPP® tissue culture plates included:

1. The plates have a lid that guarantees adequate ventilation, with the ability to control gas exchange adequately and with a low evaporation rate;
2. The TPP® plates have sloped edges allowing for only a single path insertion of the lid;
3. The yellow strip marking on the plate and lid allows precise lid orientation, i.e. match yellow on yellow;
4. The ridged grip area guarantees that the investigator has a secure grasp, preventing the accidental lifting of the lid;
5. The TPP® plates are clearly labelled alpha-numerically between the wells for easy orientation during spectrophotometric analysis and have clearly labelled black numbering on the side.

Other advantageous features include that TPP® plates limit growth only on the spherical area zone on the flat growth surface. Generally, plates stack up securely together, ensuring the safe handling of multiple plates. Also, these plates are entirely transparent. The F-base allows

excellent optical features, suitable for precision measurements of optical characteristics. Usually, for a TPP® plate, the measuring light ray is neither hindered by the microscopy applications nor the geometrical orientation.

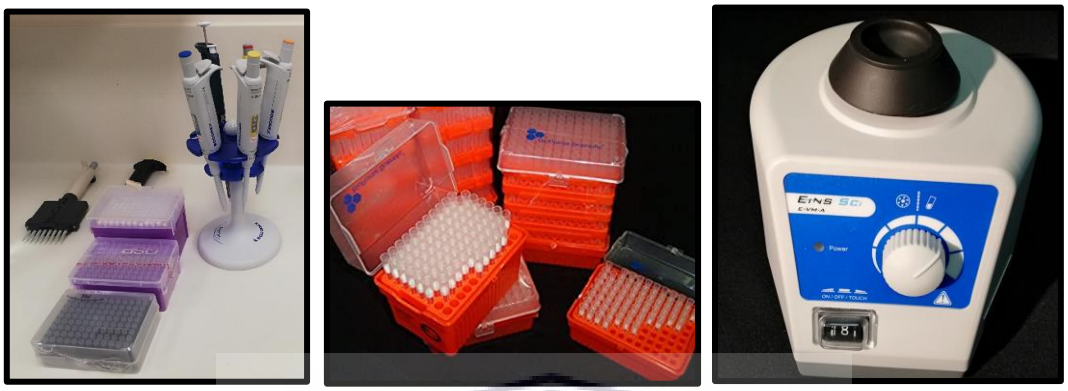

Figure 16: Pipettes, filter barrier pipette tips, and a vortex mixer

3.4.3.3 Crystal violet staining assay procedure

The CV staining assay was performed as previously described by Gulati *et al.*, (2018) and illustrated in Figure 17 and detailed as follows:

Steps 1-2: 24-hour yeast cell culture was adjusted to 0.5 McFarland's and dispensed into a TPP® 96-well microplate (200 µL/per well; at 1:1, culture to media, respectively).

Step 3: The *C. albicans* culture was incubated in a non-shaking incubator (at *37 °C for 24 h*) to initiate biofilm growth and yeast *cell attachment on the surfaces of the wells.*

Step 4: The C. *albicans* culture and media poured out, and the wells washed thrice to remove planktonic cells before the intervention solutions were dispensed into the microplate.

Step 5: After incubation of the biofilm with the intervention solutions, the wells were washed, allowed to dry, and then stained with 0.1% CV solution.

Step 6: Stained *C. albicans* biofilms were washed to remove excess dye, and 250 *µl* of a 30% acetic acid solution was added into the wells to re-solubilise the CV trapped in the bound biomass.

Step 7: 200 µl per well of the re-solubilised CV solution was transferred into fresh plates, and plates were read using a spectrophotometer.

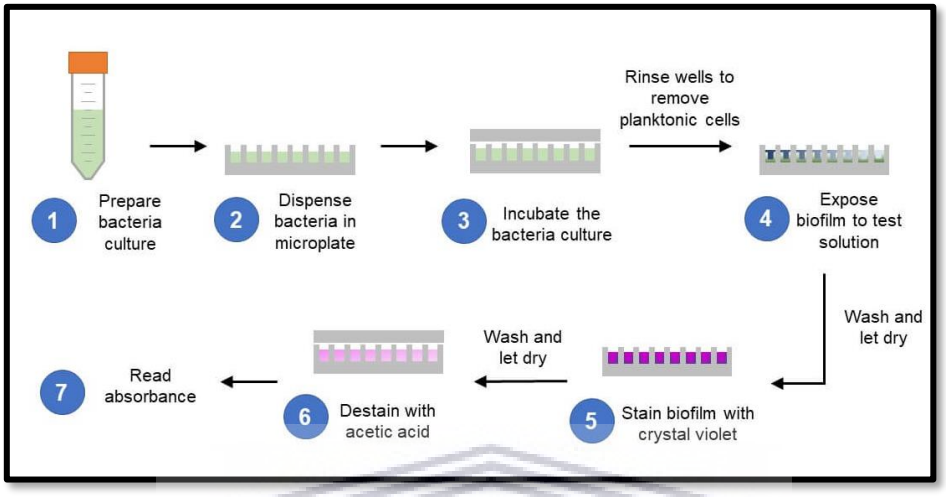

Figure 17: Description of the steps for crystal violet staining assay for biofilm assessment (from Biofilm Eradication Testing for Antimicrobial Efficacy, 2019)

Steps 1 -7 were performed in nine plates which representing different time points, as detailed below. For step 4, plates containing samples with adherent yeast cells were incubated (at 37 ºC, 150 rpm) for 0, 2, 4, 6, 8, 12, 24, 48, and 72h, representing effects at different intervention time points for mature biofilm.

The groups for the antifungal biofilm testing were as follows:

Group I: BHI (Culture media)

Group II: Untreated *C. albicans* (negative control group)

Group III: *C. albicans* and 100 µl Zn $(NO_3)_2 \cdot 6H_2O$ solution (test comparison group)

Group IV: *C. albicans* and 100 µl aqueous GZnO NPs (test intervention group)

Group V: *C. albicans* and 100 µl 0.2% CHX gluconate (positive control, intervention group)

Group VI: *C. albicans* and 100 µl nystatin (positive control, intervention group)

Group VII: Blank wells (background)

Five groups consisting of test and control groups each with 28 specimens, and sixth and seventh groups, with 28 culture media and 24 blank control specimens, respectively, were studied. The five groups of samples were pipetted into nine microplates for determination of antifungal properties and these groups were studied at nine different intervals (0, 2, 4, 6, 8, 12, 24, 48, and 72 h). The experiments were performed in triplicates for each time point. Therefore, a total of n =1260 experiments were studied across the nine different time points as summarised in Figure 18 below, using nine microtiter plates conferring to the arrangement in Figure 19 below.

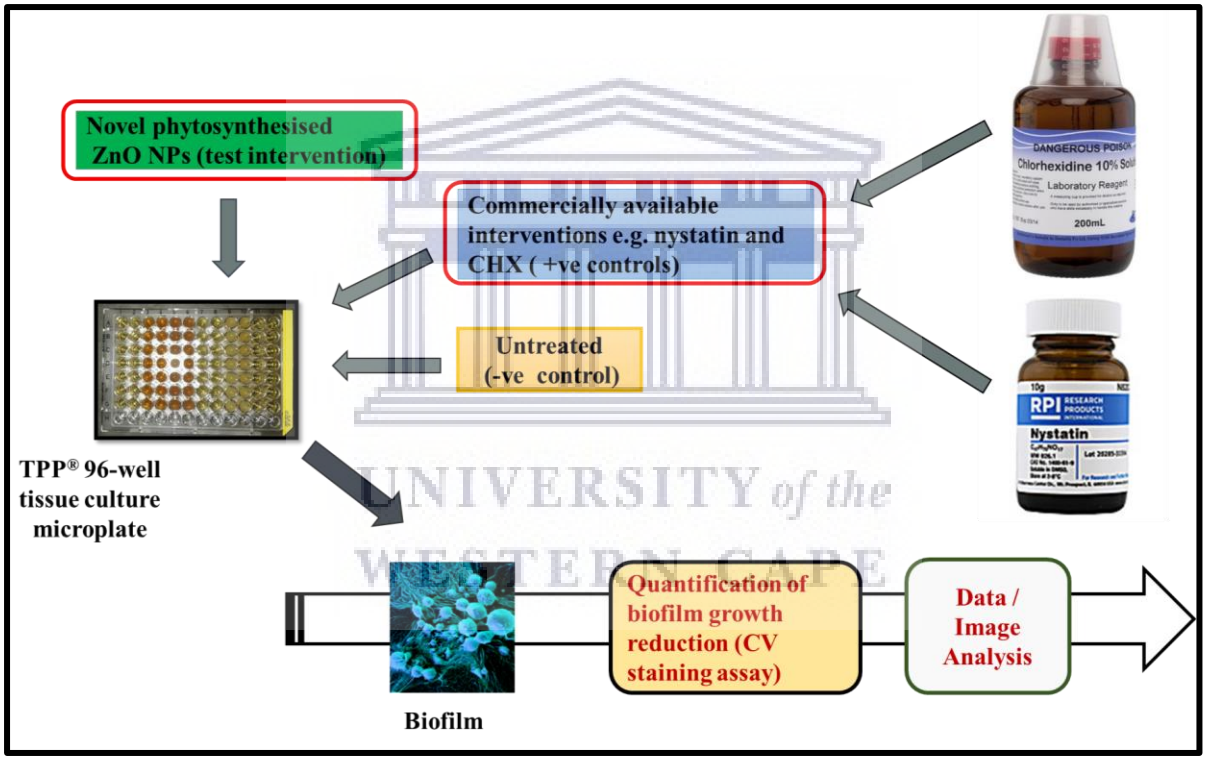

Figure 18: Summary of steps and products used for the crystal violet colourimetric assay for the antifungal assessment

	1	2	3	4	5	6	7	8	9	10	11	12
A												
B												
C												
D												
E												
F												
G												
H		B	A	C	K	G	R	O	U	N	D	

Figure 19: Schematic depiction of sample allocation in each 96-well microtiter plate

Colour legend and rows: 1-2: media (BHI), 3-4: Candida 5-6: Candida and nanoparticles 7-8: Candida and zinc nitrate hexahydrate solution 9-10: Candida and 0.2% chlorhexidine 11-12: Candida and nystatin

3.4.3.4 Brain heart infusion broth preparation

BHI broth (53286-500G) media was prepared by weighing and then dissolving (37 g of powder into 1 litre of sterile distilled water) as according to the manufacturer's instructions. Sterilisation of both BHI mixture was achieved upon autoclaving (for 15 min at 121 °C). The sterile BHI broth media was left to cool gradually to room temperature (25 °C), and stored until use.

3.4.3.5 Yeast cells suspension: reactivation and preparation of the inoculum

The fresh culture samples were prepared from the cultures stored in the fridge after step 3.4.2.3. An inoculum of Candida, one loopful of (3-5) single colonies, was dispensed into 10 ml of BHI medium, to permit reactivation of the yeast cell stain. This suspension was then incubated in a static incubator (at 37 °C for 24 h) to allow the growth of yeast cells to log phase. At the log

phase, the culture was inoculated into plates for biofilm formation (step 1-7, in section 3.4.3.3).

3.4.3.6 Yeast cell adhesion and biofilm development (growth phase, 2-3days)

For this step of the CV assay, each 96-well plate was sectioned to contain media broth, suspended Candida, and treatments of interest, i.e. $Zn(NO_3)_2 \cdot 6H_2O$ solution, 0.2% CHX, nystatin, and ZnO NPs. Biofilm formation was done by adding 100 µL of Candida cell suspension in PBS (0.5 McFarland's) into all wells with 150 µL MHA except for groups I and VII (Blank control samples). For the adhesion phase, nine plates were carefully placed in a 37 ºC static incubator for 24 h. Then, after the 24 h incubation, the broth and unbound candida were discarded, and further growth was terminated. The 96-well plates were rinsed thrice with 250 µL of sterile water to remove non-adherent *C. albicans* cells. After that, the interventions and fresh media were added on the formed biofilms were further incubated in shaking incubator (at 150 rpm, 24 h, at 37 °C). The reaction was terminated by discarding the media with interventions from the microtiter plates whenever the different time points elapsed, i.e., (0, 2, 4, 6, 8, 12, 24, 48, and 72 h). The plates were then allowed to dry.

3.4.3.7 Biofilm assessment (crystal violet staining assay on sessile *C. albicans*)

The evaluation of the effect of the interventions on 24h biofilm was done as detailed hereunder. Upon complete drying (detailed in the last part of 3.4.3.6), 250 µL of CV reagent (0.1% concentration) was added in all the 96 wells of each plate. The plates were then allowed to stand for 30 minutes at room temperature (25 °C) for the biofilm to absorb the CV. Then the CV was discarded, and the microtiter plates were rinsed by submerging in a water tub. The plates were then vigorously tapped on a stack of paper towels to rid the plate of all excess cells and remnants of dripping dye. After that, the microtiter plates were turned upside down and allowed to dry completely (at 25°C). Upon drying, re-solubilisation was performed by adding

250 µL of 30% acetic acid into each well of the TPP® microtiter plate which was then incubated at room temperature for 10-15min. Then 200 µL of the solubilised CV was transferred into each well of a new sterile TPP® microtiter plate, with 30% acetic acid in water as the blank, and optical density (OD) measured by a spectrophotometer [Smart ELISA Microplate Reader (SMR 19.14, USCN Life Science Kit Inc., China)] at 560 nm, (Figure 20). The resultant biomass was measured using CV colourimetric staining assay on 24 h *C. albicans* biofilm. The data converted into an excel spreadsheet and saved using an inbuilt programme in the spectrophotometer until further analysis. The effects of the three antifungal interventions; GZnO NPs, nystatin and 0.2% CHX were then tested on the biofilm. Reporting and discussion of the results were done according to guidelines for minimum information of spectrophotometric approach for assessment of *C. albicans* biofilm formation in 96-well microplates (Allkja *et al.*, 2020).

Figure 20: Spectrophotometer: Smart Microplate Absorbance Reader

3.5 Tools and software programmes for data presentation and statistical analysis

Assessment of data for statistical inferencing was conducted using either Microsoft Excel, OriginLab (version 17, © OriginLab Corporation, USA), ImageJ software [Fiji version, © National Institutes of Health (NIH) and the Laboratory for Optical and Computational

Instrumentation (LOCI, University of Wisconsin), USA], Statistical Package for the Social Sciences (SPSS version 20, SPSS Inc., USA), or GraphPad Prism (version 8, GraphPad Software Inc., USA). Data processing and analysis were performed according to available guiding standards.

3.5.1 Data presentation and statistical analysis for the characterisation of ZnO nanoparticles

The qualitative (e.g. micrographs, SAED, graph plots) and quantitative (e.g. EDX, EDS, raw data) data collected during the characterisation of the GZnO NPs were processed accordingly upon completion of specified interrogation techniques. Plotting of the obtained data at each interrogation step was performed using OriginLab software, and the resultant plots were assessed whether if matched to the characteristic standard plot curves for ZnO NPs. Additional structural and morphological data were presented using micrographs obtained at various magnifications confirming the size, shape and surface topography of the GZnO NPs.

3.5.2 Data processing, presentation, and statistical analysis for antifungal tests

Processing of raw data (antifungal testing) involved the calculation of the means, as well as standard deviations (STDEV) with 95% confidence intervals and tables with raw data, are included in the Results section. The data sets were assessed for the presence of outliers. The need for normalisation of the data was established (using either log transformation, standard curves, or square roots), as well as appropriate reporting of transformed data for normality testing. Description of statistical as well as any post hoc tests performed and the rationale for selection of tests is described in the results section (i.e. small sample, paired, parametric or non-parametric, etc.). Information regarding test parameters are also provided, descriptive statistics including statistically significant differences, standard deviation, standard errors,

variances, and confidence intervals were also calculated and availed. Additionally, the descriptive statistics for the controls used in the experiment were included.

The presentation of data from the antifungal susceptibility testing was conducted using suitable types of graphs (box, whisker plots, or scatter plots, and rarely histograms or line graphs) for displaying antifungal results. The figures were prepared to provide all relevant and essential details to support the understanding of the findings. Plotting of data in tandem using means and STDEVs was performed to allow transparent data evaluation. Descriptive data analysis was conducted using SPSS and Microsoft Excel. Using GraphPad Prism software, in-depth comparative analysis of zones of inhibition from all three triplicate sets of data were evaluated. One-way analysis of variance (ANOVA) tests, followed by a Bonferroni comparison (Bonferroni correction) post hoc analysis was performed. No open-source systems such as R software packages were used. For data with several time points, Tukey's HSD test was conducted to determine which specific pairs (when compared with each other) were genuinely different. The means of all the absorbances of the different samples were adjusted by deducting the negative matching control (group I, BHI only) values.

CHAPTER FOUR - Results

4.1 Visual colour change observations of the GZnO NPs

The ZnO NPs formation was monitored visually by recording colour changes during the entire course of the reaction. Figure 21 below represents colour changes observed in mixture solutions of banana peel and Buchu-infused Rooibos tea leaves extracts used in the phytosynthesis of the ZnO NPs. The colour of the mixture gradually changed from red-orange to orange and finally to yellow-white after 5 h at 70 ° C, validating the synthesis of ZnO NPs (Figure 21). The changes are attributed to the conversion of Zinc nitrate precursor to ZnO. Zinc nitrate is an inorganic chemical compound with the formula $Zn(NO_3)_2$, it is a white, crystalline solid, highly deliquescent, and typically found as hexahydrate, $Zn(NO_3)_2 \cdot 6H_2O$. It is soluble both in water and in alcohol. The reaction was thus accomplished with evident colour changes captured.

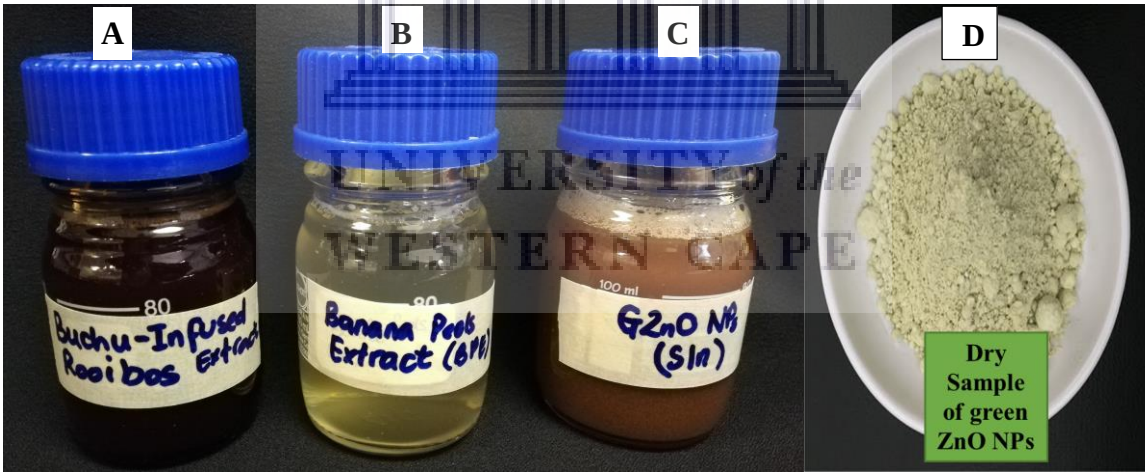

Figure 21: Colour changes observed during the formation of GZnO NPs; Buchu-infused Rooibos extract (A), banana peel extract (B), aqueous GZnO NPs (C), and dry GZnO NPs (D)

4.2 Ultraviolet-visible spectroscopy analysis of the GZnO NPs

An aqueous sample (Group I) prepared, as described in section 3.2, was used for this interrogation technique. Dilution of a small aliquot of the sample was done using distilled water

to ensure capturing of the peak within the range of 200-800 nm. A strong absorption peak was recorded at 290 nm (Figure 22).

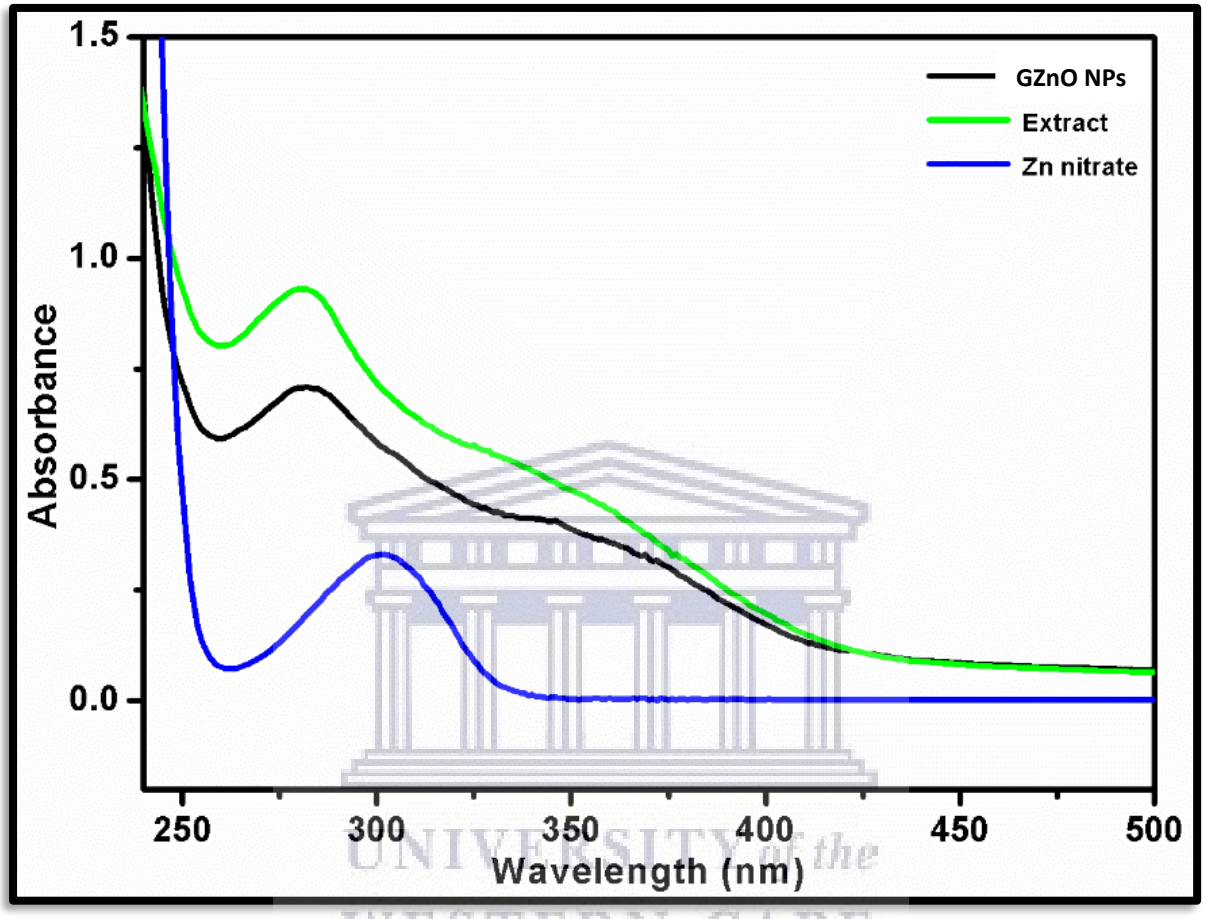

Figure 22: Ultraviolet-visible (UV-Vis) spectrum of the GZnO NPs

4.3 X-ray diffraction analysis of the GZnO NPs

A solid dry yellowish-white sample of the green ZnO (Group II), as described in section 3.3, was characterised using XRD. The XRD evaluation shown in Figure 23 confirms that the synthesised ZnO NPs were of high quality (pure) rock salt cubic and spherical crystals, with a hexagonal lattice, with prominent characteristic peaks of ZnO NPs validating the crystalline nature of the GZnO NPs.

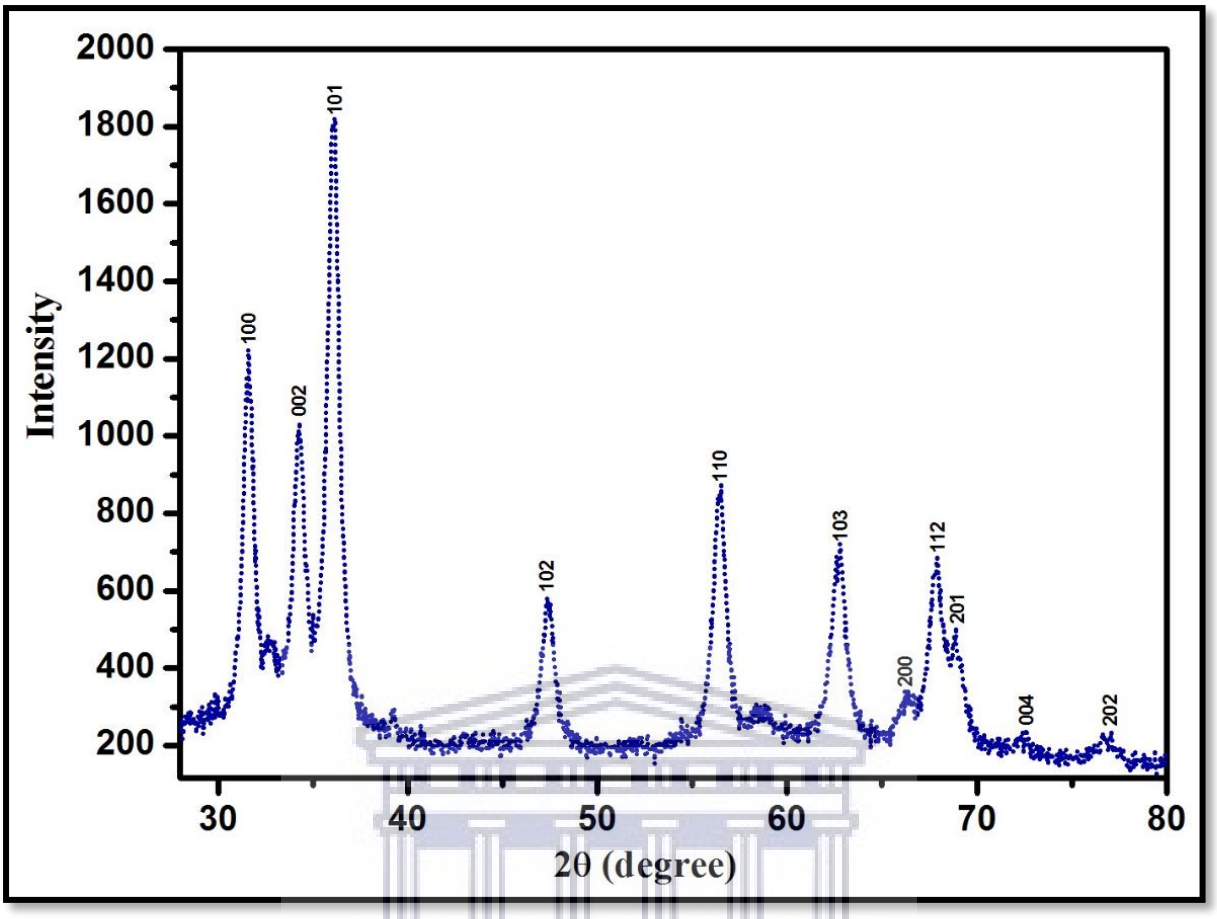

Figure 23: X-ray diffraction (XRD) patterns of the GZnO NPs

The above XRD patterns (Figure 23) shows Debye-Scherer diffraction rings of the synthesised GZnO NPs at 2θ values indexed as (100), (002), (101), (102), (110), (103), (200), (112), (201), (004), and (202) reflection planes of face-centred cubic (rock salt), as well as spherical crystalline hexagonal structures of GZnO NPs. These findings confirm that the synthesised ZnO NPs possess high-quality crystallinity and that the peaks correspond with Joint Committee of Powder Diffraction Standards (JCPDS) card number 00-036-1451, from a sample source of the New Jersey Zinc Co., Bethlehem, PA, USA. The structure was determined by Bragg and Darbyshire, (1932) and refined by Abrahams and Bernstein, (1969). The sample's polymorphism presented as a high-pressure cubic sodium chloride-type (rock salt) of ZnO as reported by Bates *et al.*, (1962) and a cubic, sphalerite (wurtzite) type as documented by

Radczewski, Schicht (Zagorac *et al.*, 2011). The Scherer's equation was employed to estimate the crystalline size of ZnO $\left(\frac{0.9\lambda}{\beta*\cos\theta}\right)$. According to Langford and Wilson (1978) and Gupta *et al.*, (2018), the determined average crystallite size determined by XRD is 13.22 nm. Finally, using the XRD, the GZnO NPs were found to be highly pure (94.32%).

4.4 Fourier-transform infrared spectroscopy analysis of the GZnO NPs

The FTIR technique was employed to assess the functional groups (capping biomolecules) responsible for the reduction, stabilisation, and production of the GZnO NPs. Therefore, a dry sample (Group III) prepared, as described in section 3.3, was utilised for this interrogation technique. Further, in order to determine an adequate time for the formulation of the GZnO NPs, initial optical testing was done on three GZnO NPs samples, synthesised at different times, to achieve an optimised method for this step. The longer the synthesis time, the more prominent and stable the peaks were of the sample observed. Therefore, a 5 h synthesis time was chosen and maintained in all subsequent experiments.

4.4.1 Fourier-transform infrared spectroscopy analysis of Buchu infused Rooibos and banana peel extracts

All the information gathered from the FTIR analysis prove that the extracts had inherent beneficial properties necessary for stabilisation and capping of the GZnO NPs that were formulated (Figure 24).

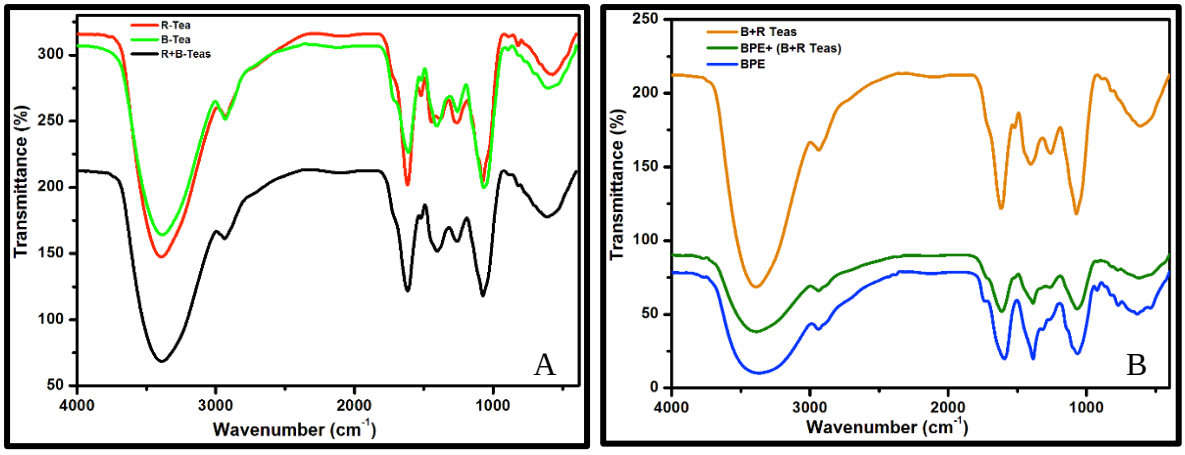

Figure 24: A) Fourier-transform infrared comparison of the green tea extracts; Rooibos tea (R-Tea), Buchu tea (B-Tea), and their combination, Buchu and Rooibos (B+R Teas). B) Fourier-transform infrared comparison of Buchu and Rooibos (B+R Teas), banana peel extract (BPE) and the combined extract of banana peel (BPE) and Buchu and Rooibos (B+R Teas)

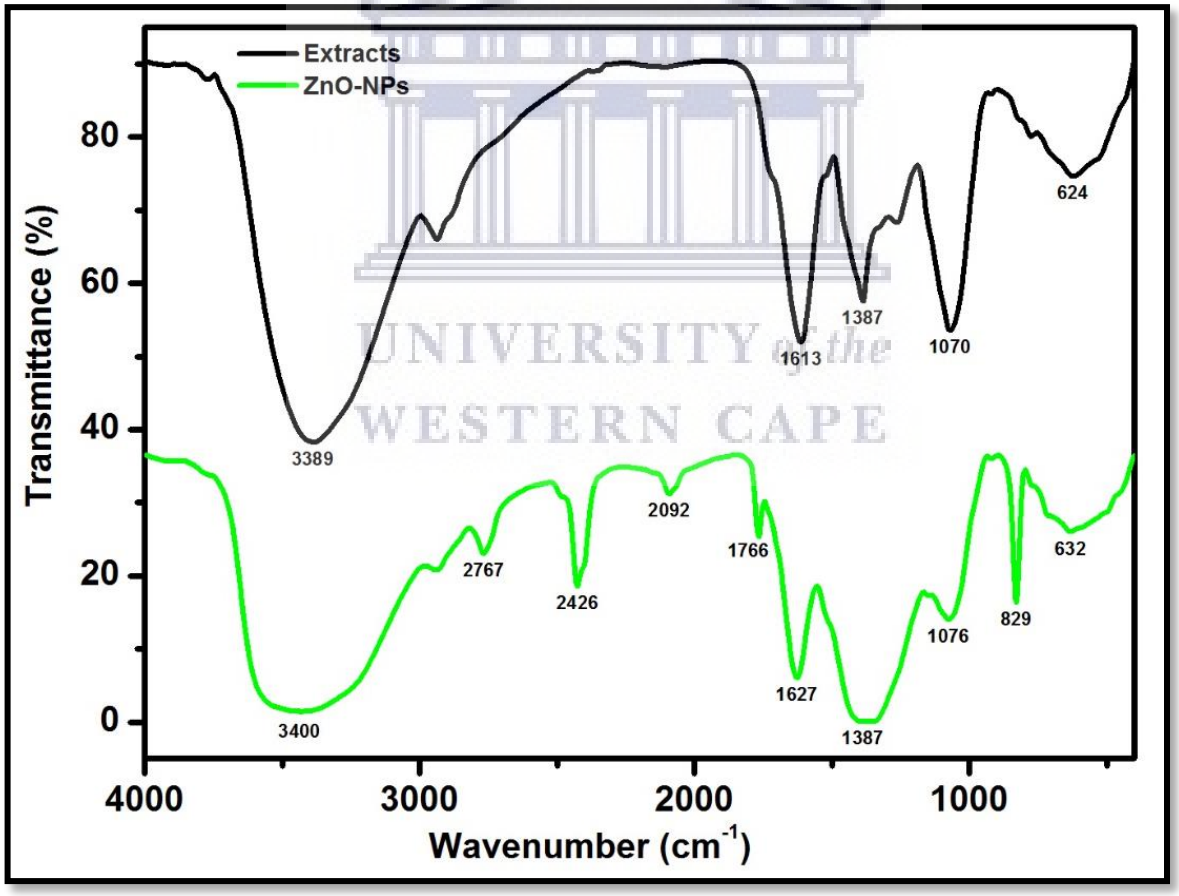

Figure 25: Fourier-transform infrared (FTIR) analysis of the GZnO NPs in comparison to all extracts combined

Furthermore, in this study, several absorption peaks were recorded between 400-4000 cm^{-1} related to the vibrational mode of compounds such as carboxylate, alkane, and hydroxyl groups. The FTIR findings shown in Figure 25 support important and distinctive stretches of 829, 775 and 632 cm-1 corresponding to functional groups of the ZnO NPs. Approximately between 2800-1070 cm^{-1}, the functional groups attributable to the extracts (polyphenols, antioxidants and phenolic acids) were identified.

4.5 High-resolution transmission electron microscopy and energy-dispersive X-ray

The HRTEM analysis technique was used to examine the dried solid sample of GZnO NPs (Group IV) as described in section 3.3. HRTEM analysis was conducted to establish the morphology and size of the acquired nanomaterial according to Korgel *et al.*, (2006) and Williams *et al.*, (1996). Detailed microstructural morphology was confirmed with HRTEM micrographs (Figure 26), HRTEM-EDX analysis, as well as SAED. HRTEM-EDX detected the quantities of constituents of the GZnO NPs. The amounts of zinc and oxygen elements detected among others were in accord with the HRSEM-EDS (Section 4.6).

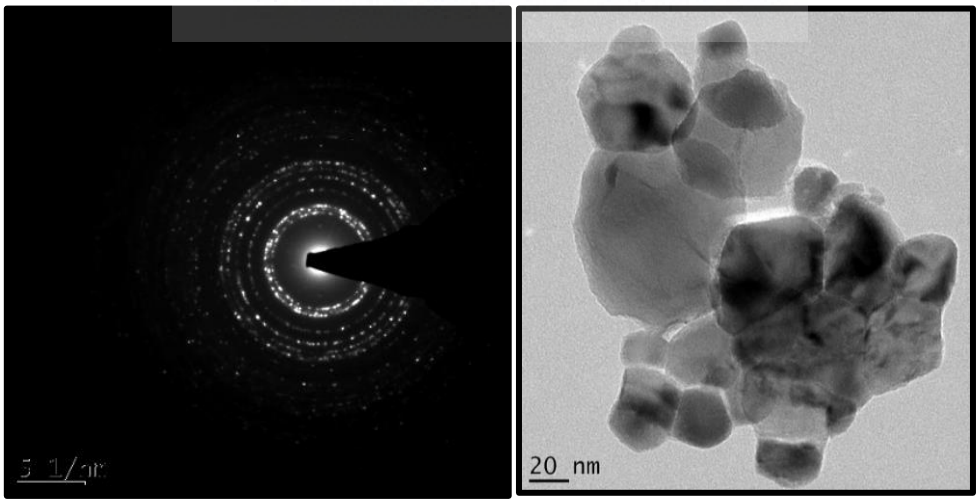

Figure 26: High-resolution transmission electron microscopy and selected area electron diffraction representations of the GZnO NPs

Figure 26 above represents HRTEM micrographs, where the morphologies were observed to be cubic and spherical crystalline structures with a hexagonal lattice, and wurtzite characteristics. The sample had minimal agglomerates and was adequately dispersed throughout the grid. The GZnO NPs were heterogeneous, and the particle sizes ranged between 6.64 and 18.65 nm at varied magnifications, and the mean measured dimensions were coherent to the XRD results. The SAED patterns depicted in HRTEM data (Figure 26) illustrated Debye-Scherer diffraction rings of the GZnO NPs corresponding to XRD patterns as (100), (002), (101), (102), (110), (103), (200), (112), (201), (004), and (202) representing matched reflection planes of face-centred polycrystalline hexagonal structures of GZnO NPs.

In the EDX graph below (Figure 27), concentrated peak signals of Zn were recorded at 82, 523, 1000, 1050, and 1120 keV. Other signals captured included those of copper (Cu), carbon (C), oxygen (O), and potassium (K). The appearance of C and O could be attributed to the C-containing molecules and polyphenol groups in the tea and BPE as well as $Zn(NO_3)_2$ (precursor metal). In contrast, Cu element was attributed to the sample holder material. The HRTEM-EDX test showed peaks and constituents in coherence with the HRSEM-EDS pattern shown in Figure 28. Overall, the elemental profile of synthesised NPs using banana peel and Buchu-infused Rooibos extracts indicated elevated counts at 0.98 keV due to Zn. Thus, this further supported the development of the desired GZnO NPs.

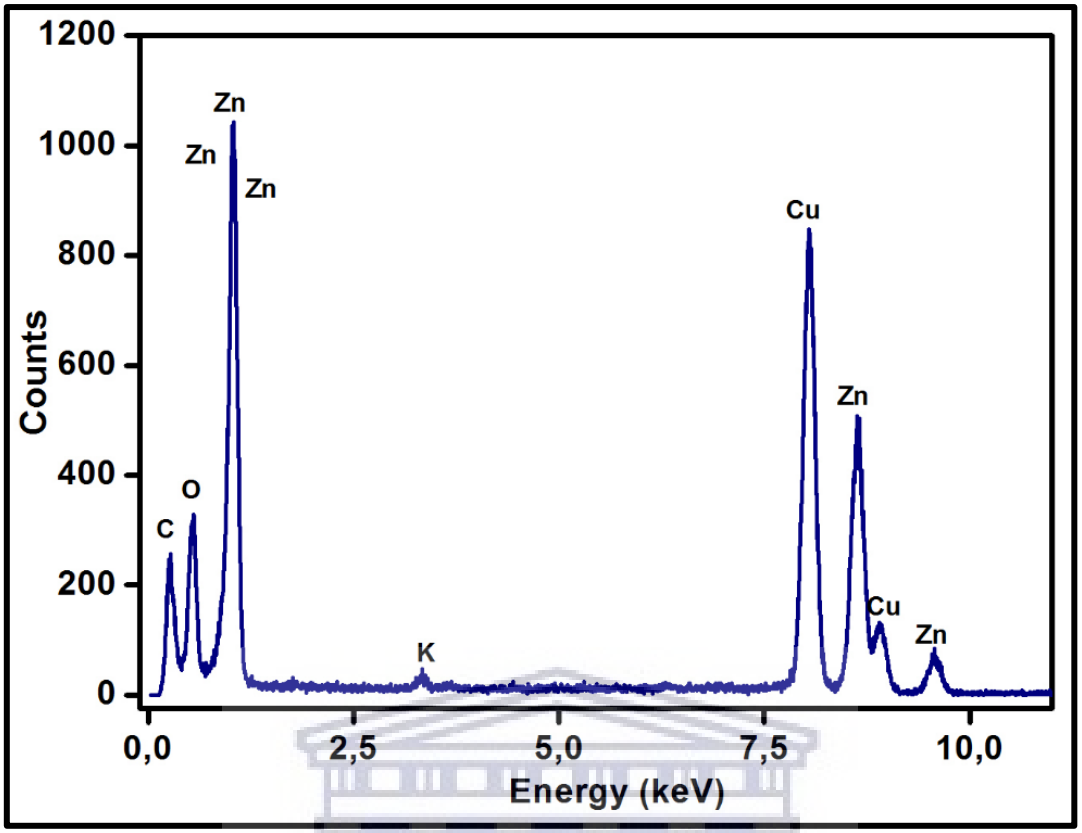

Figure 27: HRTEM Energy-dispersive X-Ray analysis spectrum of the GZnO NPs

4.6 High-resolution scanning electron microscopy and energy-dispersive spectroscopy

The qualitative and quantitative elemental analyses, with available information on the chemical composition of the formulated dry (solid) GZnO NPs, were also conducted to validate the obtained material. The electron interactions with the atoms of ZnO NPs in the sample yield various signals resulting in data on the surface structure and composition. The structural and morphological studies of green synthesized ZnO NPs were analysed at magnifications of 5.00 K X, 10.00 K X, and 25.00 K X as shown Figure 28 A, B, and C, respectively. The composition gradient was also determined and is graphically illustrated in Figure 29 below. The HRSEM micrographs show that the ZnO NPs were rod-like with minor aggregation.

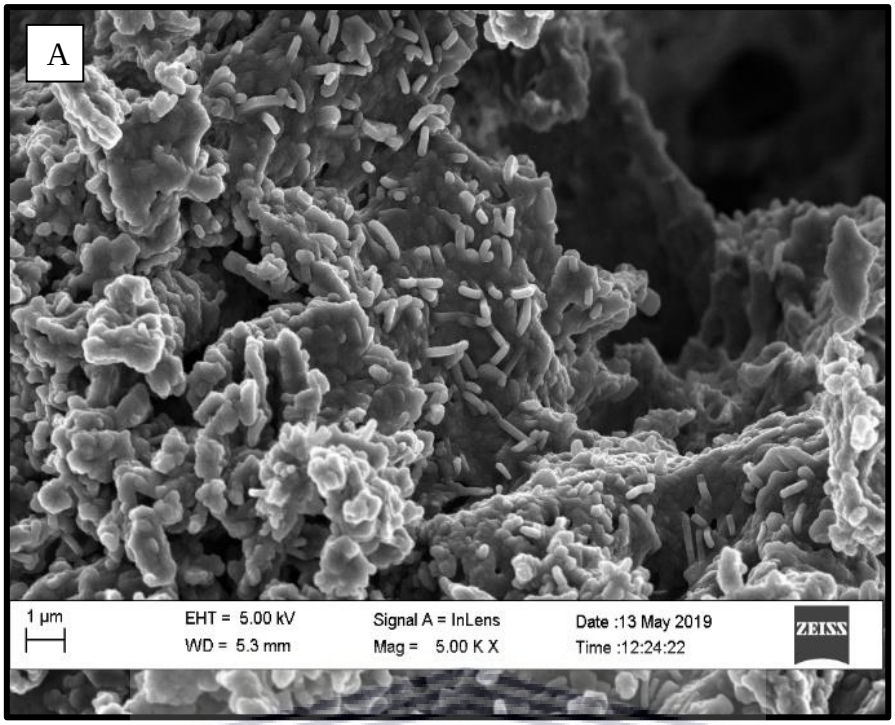

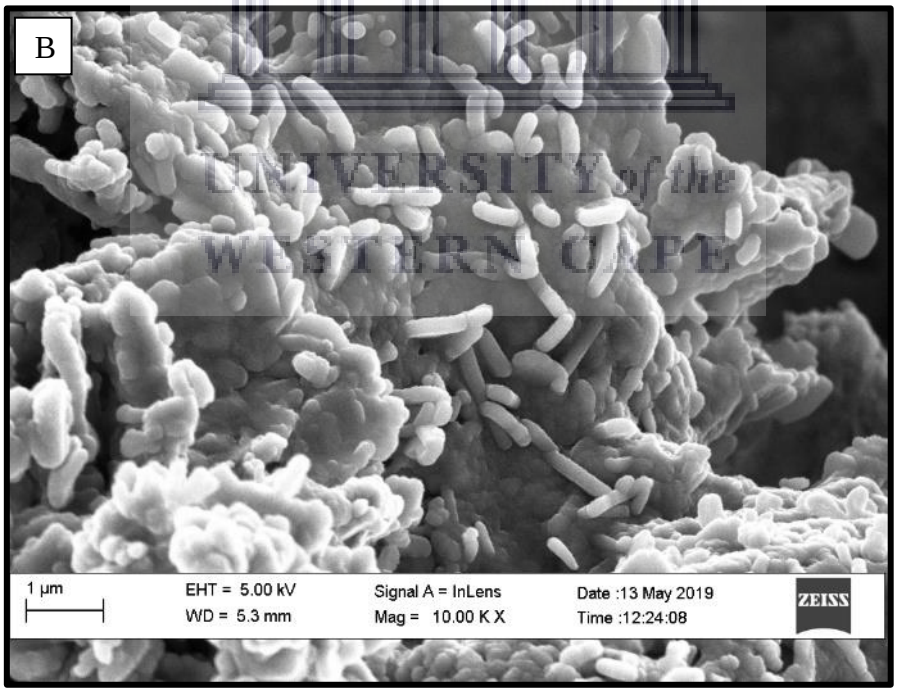

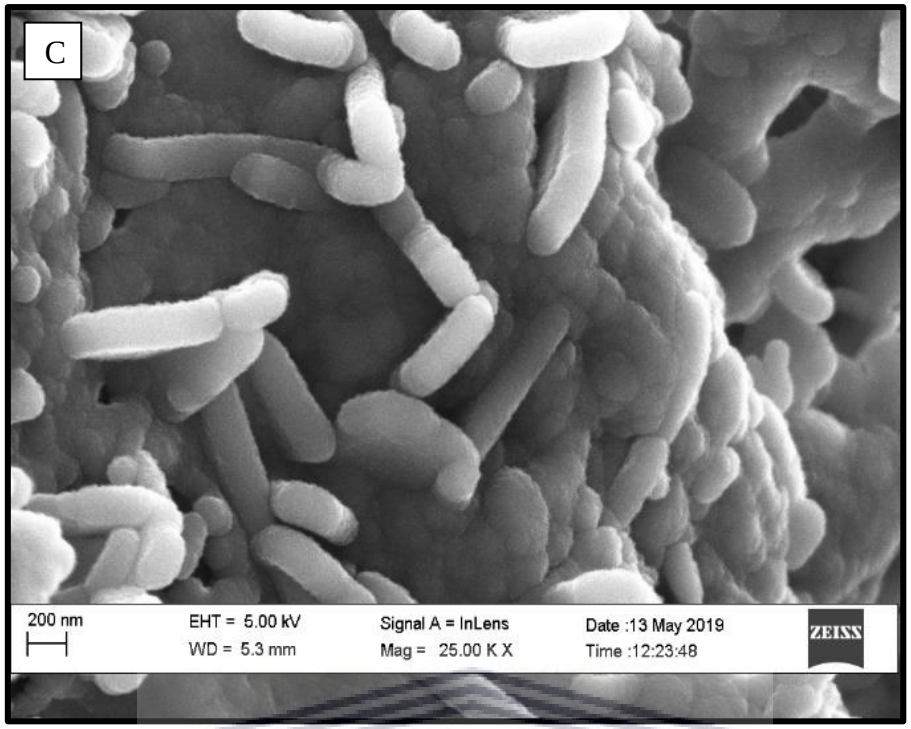

Figure 28: High-resolution scanning electron microscopy (HRSEM) micrographs of the GZnO NPs at magnifications 5.00 K X (A), 10.00 K X (B), and 25.00 K X (C)

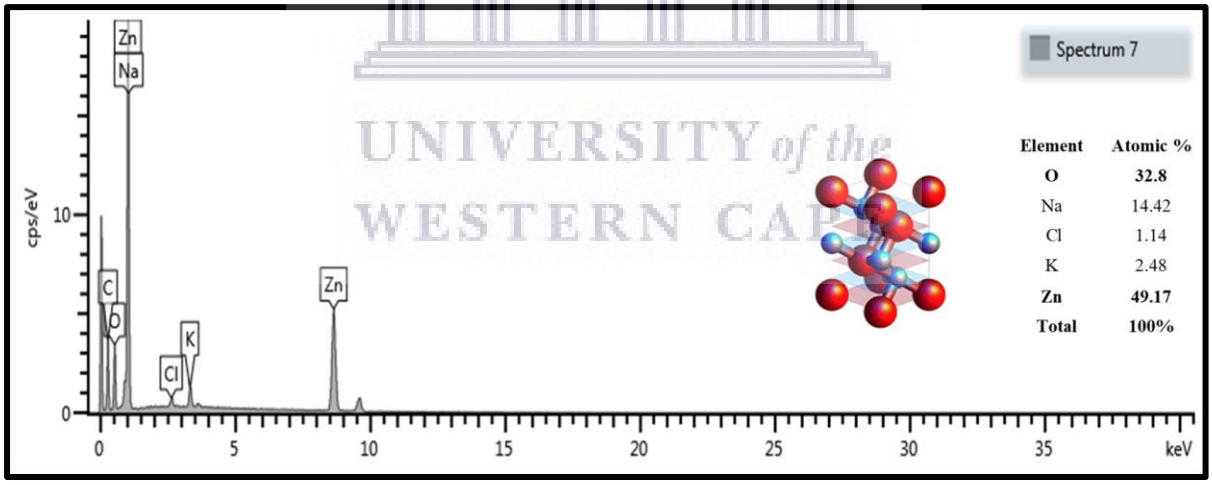

Figure 29: Scanning electron microscopy with energy-dispersive spectroscopy and elemental composition, as well as crystalline structure description of the GZnO NPs

The EDS assessment was done to disclose the fundamental elements attributable to the phytosynthesis of NPs, as depicted in Figure 29 above. Signals observed included oxygen (O), carbon (C), sodium (Na), chloride (Cl), and potassium (K). The presence of Na and Cl signifies

that the formulated NPs have a face-centred cubic rock salt crystalline structure with a hexagonal lattice. The O and C signals originate from the Zn $(NO_3)_2$ precursor, Buchu-infused Rooibos extract, and BPE obtained during the phytosynthesis in the single pot. The appearance of C, Na, and Cu could be an outcome of C coating and sample holder material, respectively. In summary, the EDS analysis revealed that the GZnO NPs are highly pure (81.97%), of crystalline nature, and with a hexagonal lattice. These results complement those found in XRD and HRTEM described above and illustrated in Figures 23 and 27, respectively.

4.7 Calculation of the concentration of the GZnO NPs

Mass, volume, and concentration of nanoparticles are fundamental characteristics of nanoparticles. In this study, the concentration of the nanoparticles was calculated and expressed as molarity. This referred to the number of moles of a substance per litre and presented per 100 µL. This allowed elucidating the working concentration for the GZnO NPs used in the antifungal assessment. Several other analytical techniques such as Malvern NanoSight, Nanotracking analysis (NTA), as well as Zetasizer, are reported to be applicable for calculation of NPs concentration in conjunction to size established from TEM or SEM. Alternative approaches involve the theoretical approaches using computational models to predict the optical properties of a particular geometry particle (spherical, cubical, rod-like). However, overall, it is remarkably challenging to calculate the NPs with precision. It was beyond the scope of this study to explore the intricate models; however, the applied standard method used is among the recommended in basic chemistry and biology (molarity). Therefore, in this study, the calculation was done as follows:

The molar mass of Zinc Hexahydrate (MM) = 297.4815g/mol

Molecular mass of Zinc (MM) = 65.38g/mol

$$\frac{M \times MM\ (\text{Zinc Hexahydrate}) \times V}{1000}$$

$$\frac{\frac{0.1\text{mol}}{\text{L}} \times 297.4815\frac{\text{g}}{\text{mol}}\ \text{X}\ 0.1\ \text{L}}{1000} = \mathbf{2.975 \times 10^{-3}\ g}$$

Zn = 65.38 g in 297.4815g in 100ml

$$\therefore \left[(\mathbf{2.975 \times 10 - 3\ g} \times 65.38\text{g/mol}) / 297.4815\text{g}\right] / \text{mol}$$

$$= \mathbf{6.538 \times 10^{-4}\ g\ in\ 100\ mL}$$

$$\mathbf{\therefore\ in\ 1ml\ 6.538 \times 10^{-6}\ g/ml}$$

$$6.538\mu\text{g/mL}$$

$$= \mathbf{0.006538\ \mu g/mL}$$

100µL= X

1 µL = 0.006538 µg

∴ 0.6538 µg/ 100µL

4.8 Antifungal testing on *Candida albicans*

The antifungal effects of the GZnO NPs on *C. albicans* was studied using the Kirby-Bauer susceptibility diffusion test and the CV staining assay.

4.8.1 Modified Kirby-Bauer assay on *Candida albicans*

The susceptibility of *C. albicans* was tested against 0.2 % CHX gluconate (control group), GZnO NPs (test group) and a $Zn(NO_3)_2 \cdot 6H_2O$ (negative control group). Each of the three groups was studied using nine samples (n = 9 per volume tested) for each of the four different volumes: 50, 100, 150, and 200 µL. The zones of inhibition were then measured using a Vernier calliper as shown in Supplemental tables 1 and 2 in the appendix, and Figure 30 (A-I) below.

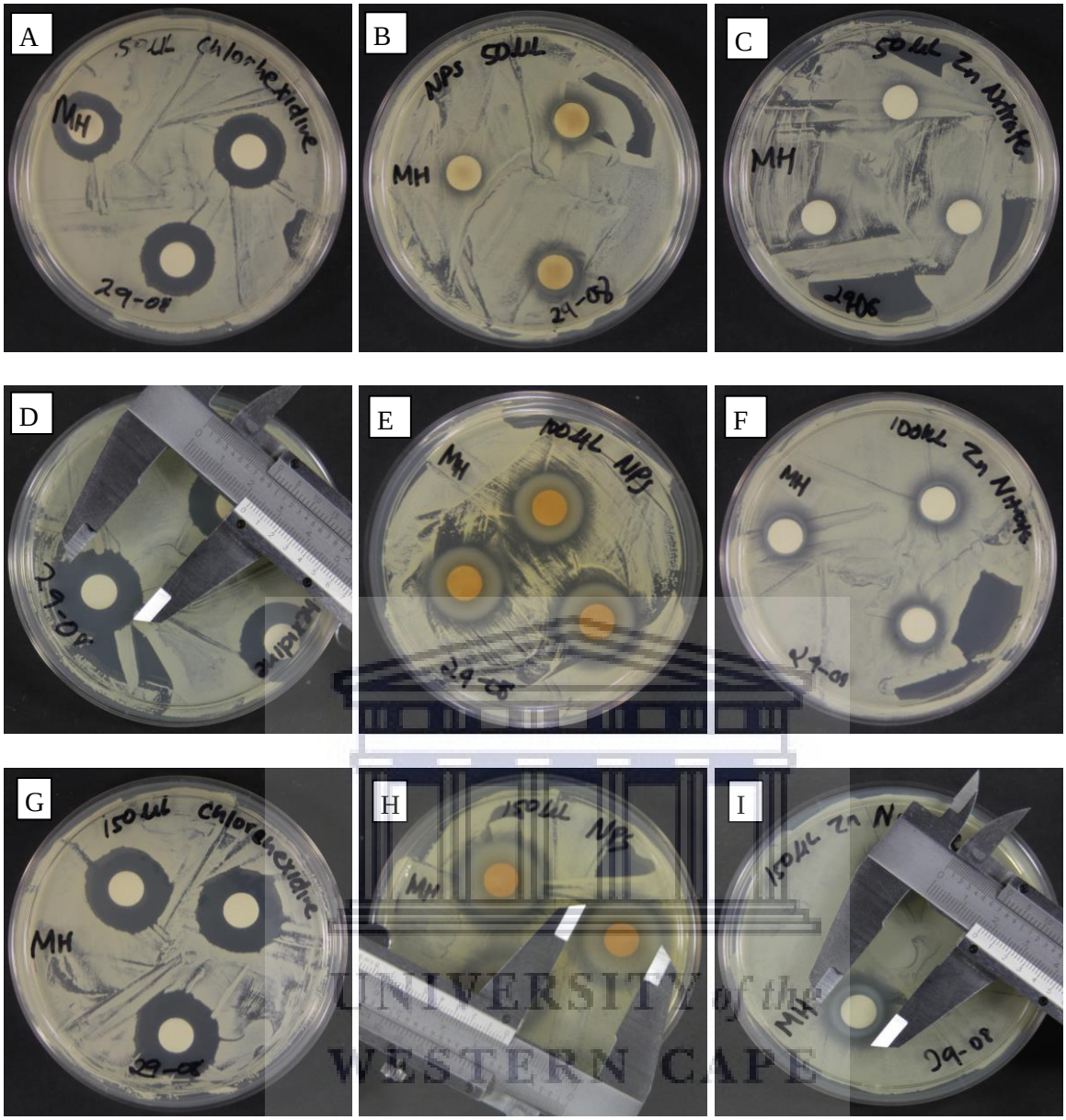

Figure 30: Zones of inhibition for CHX (A, D, G); GZnO NPs (B, E, H); and [Zn $(NO_3)_2 \cdot 6H_2O$] (C, F, I)

The means for each group and their respective standard STDEV values are graphically presented (Figure 31, below) and tabulated (Supplemental Table 2, see appendix). The information demonstrates the inhibition zone sizes corresponding to varied volumes for the three intervention groups. For instance, at 200ml, the mean zones of inhibition are 27.111±0.697, 30.444±1.0134, and 17.500±0.433, for CHX, GZnO NPs and Zinc nitrate hexahydrate solution, respectively, at 95% CI for n=9.

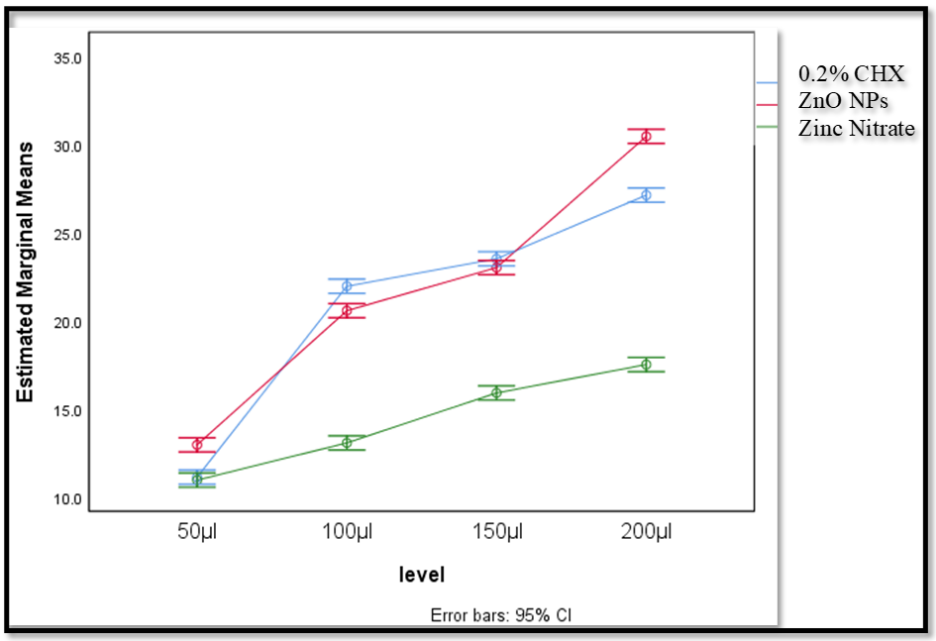

Figure 31: Estimated marginal means for inhibition zones representing the response of *Candida albicans* to the three interventions at different volumes using Kirby Bauer assay

Figure 32 below, presents a box and whisker plot for the ANOVA-F test results at 200µl. At this volume, the difference between the three treatment groups was $F_{(2,24)} = 716.88$, $p < 0.01$.

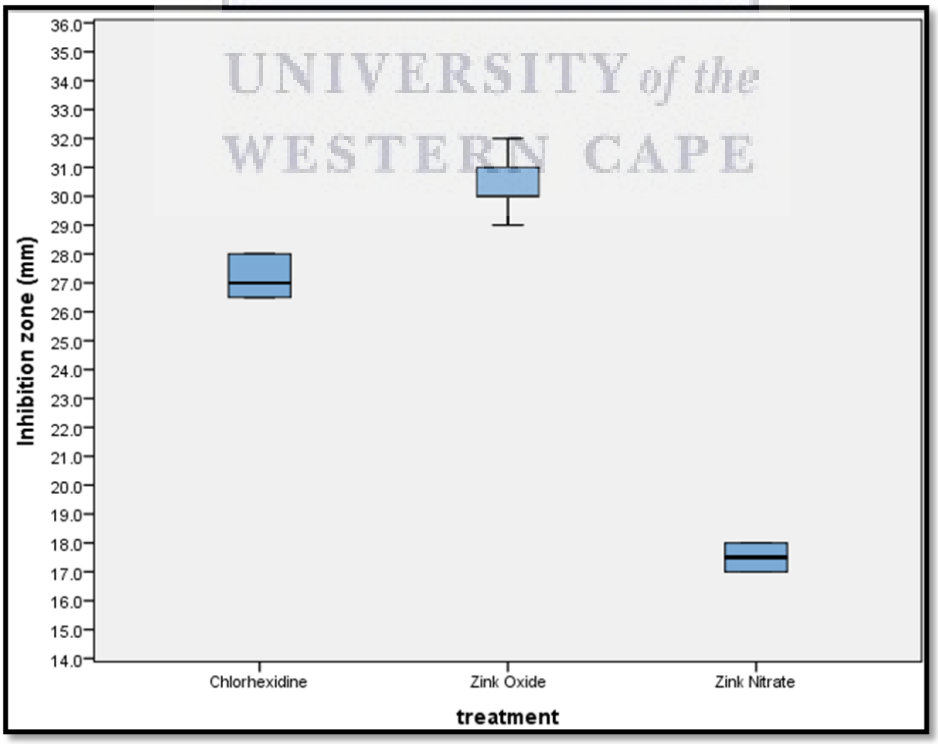

Figure 32: Box and whisker plots presenting the means of inhibition zones at 200 µL for the three treatments at 24 h incubation

A post hoc test was performed for multiple in-depth comparison of the means among the three treatment groups. The Bonferroni test (also known as the "Bonferroni correction" or "Bonferroni adjustment") was used to perform post hoc testing to ensure that no false-positive results (statistical errors) occurred among the three treatment groups at 200µl (Table 7).

Table 7: The confidence levels (multiple comparisons; Bonferroni) of the treatments at the highest volume level

(I) Intervention	(J) Intervention	Mean difference (I-J)	Standard error	Significance (P-value)	99% Confidence interval	
					Lower bound	Upper bound
0.2 % Chlorhexidine gluconate	**Zinc oxide**	-3.333*	0.3550	0.000	-4.490	-2.177
	Zinc nitrate	9.611*	0.3550	0.000	8.454	10.768
Zinc oxide nanoparticles (GZnO NPs)	**Chlorhexidine**	3.333*	0.3550	0.000	2.177	4.490
	Zinc nitrate	12.944*	0.3550	0.000	11.788	14.101
Zinc nitrate hexahydrate solution	**Chlorhexidine**	-9.611*	0.3550	0.000	-10.768	-8.454
	Zinc oxide	-12.944*	0.3550	0.000	-14.101	-11.788

4.8.2 Colourimetric analysis (Crystal violet staining assay on sessile *Candida albicans*)

150 µL of fresh BHI broth and the three interventions; 100 µL Zn NPs (0.6538 µg/100 µL), 100 µL nystatin, and 100 µL CHX (0.2%) were pipetted into their respective wells as described in Figure 19 in section 3.4.2.3. Subsequent procedures as described in were used to study all the 96 well plates as depicted in Figure 33 below (the interventions and controls pipetted in their respective wells). A descriptive analysis table of effects of the three interventions (Supplemental Table 3, see Appendix) presents the means, and STDEV read as optical densities (560 nm) at their respective different time points. The obtained OD values represent both CV staining bound to the biomass of *C. albicans* and that bound to the three individual interventions.

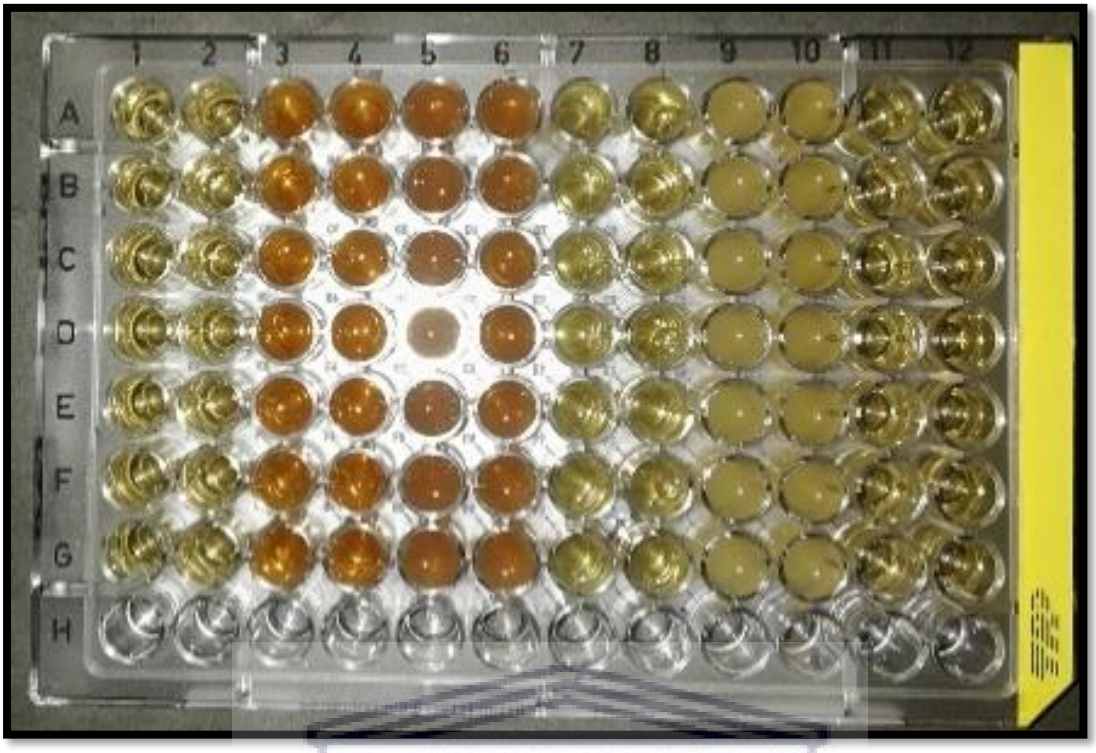

Figure 33: Exposure of 24 h biofilm to the three interventions and controls in a 96-well microtiter plate for further incubation

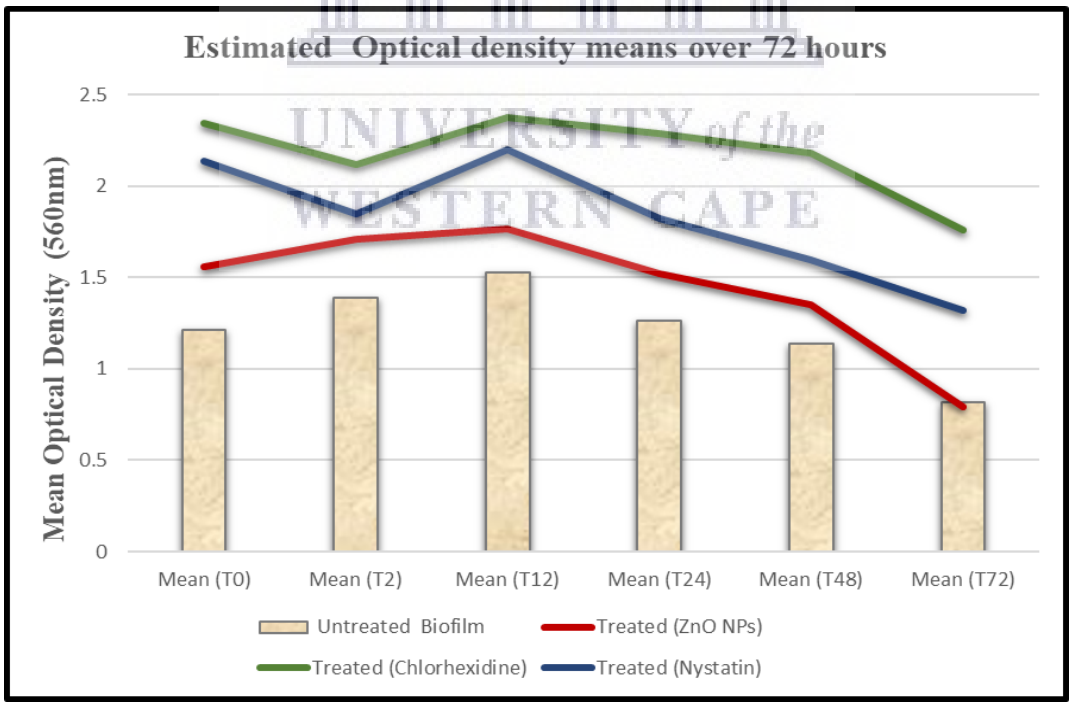

Figure 34: Means of optical density curves over 72 hours for *Candida albicans* (untreated biofilm) and treated with ZnO NPs, CHX and nystatin

In Figure 34 above, are linear plots of OD mean values at 560 nm for 200 µL nystatin, CHX and ZnO NPs (intervention groups) and histogram representing the ODs of Candida biofilm (untreated group) are presented. The ODs for nystatin and CHX decreased in the first 2 h, and then increased until after 12 h of incubation and consistently decreased thereafter. The OD for ZnO NPs gradually increased until after 12 h, later, presented similarly to the other interventions. Chlorhexidine showed the highest OD values among the three interventions, while the optical density values of the untreated group were low (histograms, Figure 34). All ODs (treated groups and untreated group) consistently decreased after 12 h onwards.

The scatter plots in Figure 35 below represents a one-way ANOVA (GraphPad Prism version 8) of the means of optical densities for the three interventions at different time points. This statistical analysis was done in order to test the null hypothesis (H_0) that, all means of optical densities at 0, 2, 4, 6, 8, 12, 24, 48 and 72h in the CV assay for the three intervention groups (0.2 % chlorhexidine gluconate, GZnO NPs and nystatin) are equal. The plots (Figure 35) demonstrate that the results from the three interventions are different at all times.

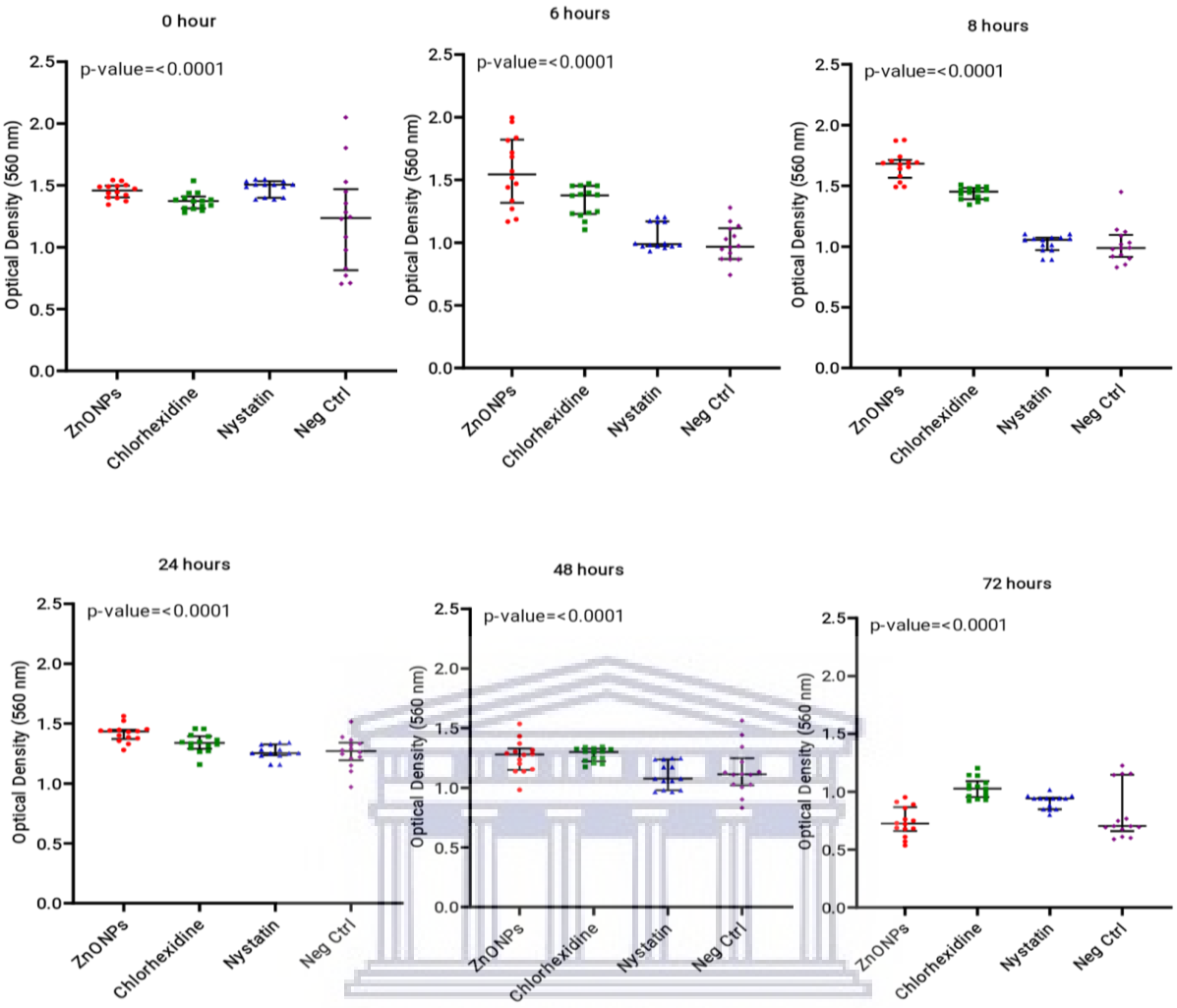

Figure 35: Scatter plots for the distribution showing the effect of the three interventions at 560 nm against *Candida albicans* using the crystal violet assay

In order to ascertain whether there are differences among specific groups, the Tukey's HSD test was performed as described in section 3.6.2 and presented in Supplemental Table 4 (see Appendix) and Figure 35. This is a post hoc test for an in-depth comparison of the means across the three interventions at 200 µL. Thus, actual significant differences were elucidated. Generally, significant differences ($p < 0.001$) were noted at different times (Supplemental Table 4, see Appendix). The effects due to the interventions on biofilm reduction were elucidated following the correction of ODs of the interventions using the ODs of the negative control (Figure 36 below; Supplemental Table 5).

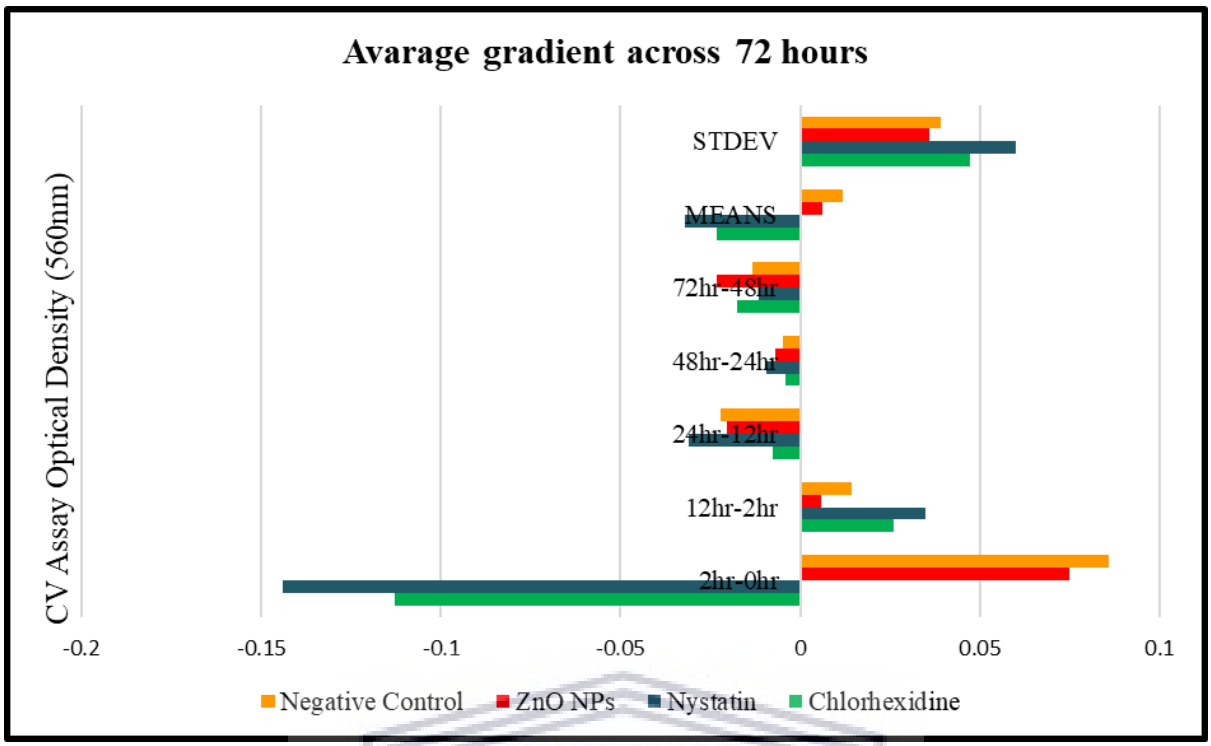

Figure 36: Forest plots of means for biofilm reduction of *Candida albicans* for the three inventions at different time points using CV staining assay

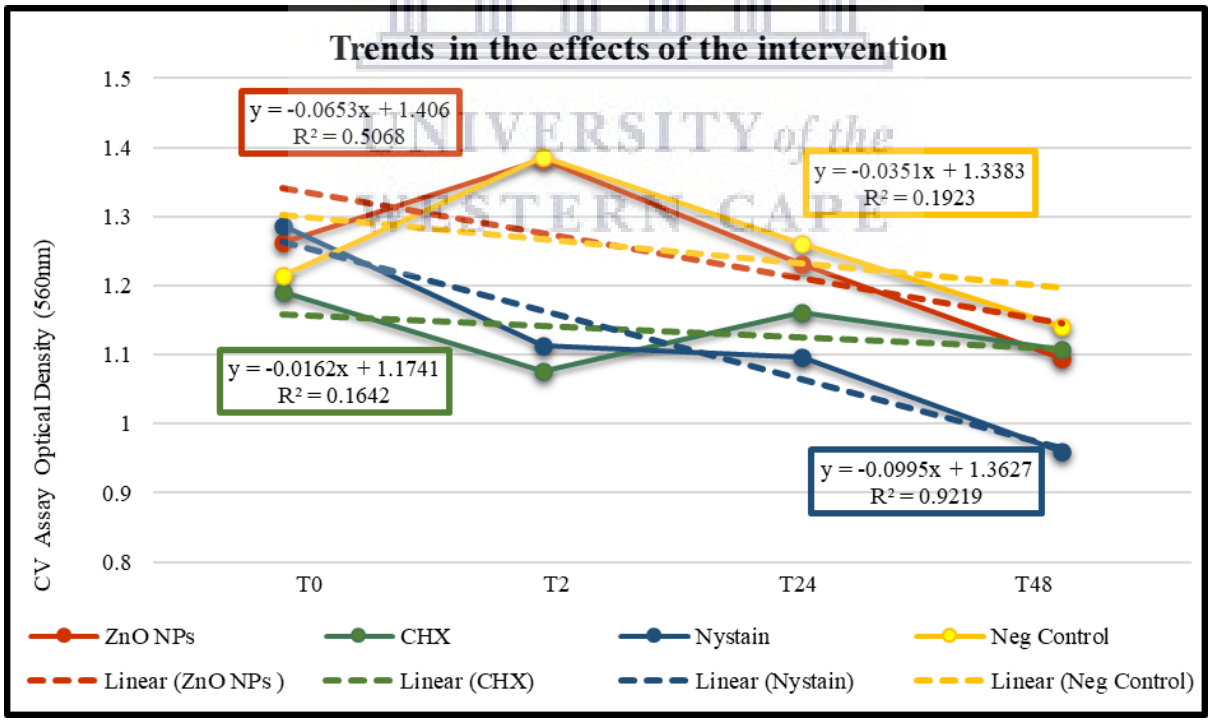

Figure 37: These are gradients illustrating the trends of the means across the 48 hours.

Overall, Figure 37 above, illustrates the trends of the ODs across the 72 h for the three interventions, compared to the untreated samples. The untreated biofilm showed the lowest gradient after 24 h, as compared to the three interventions.

4.9 Summary of results

For the first time, according to our knowledge, a green and straightforward single-pot approach has been successfully developed for the synthesis of GZnO NPs using Buchu-infused Rooibos and banana peel extracts as biological reducing and stabilising agents. An eco-friendly method is thus presented for the ZnO NPs synthesis; the method is also efficient and affordable. Initially, the oxidation of $Zn(NO_3)_2$ metal to ZnO NPs was monitored by evaluating and recording visual colour changes. Further in-depth interrogations to validate the development of the GZnO NPs were done using UV-Vis, XRD, FTIR, HRTEM (EDX and SAED) and HRSEM-EDS techniques.

A broad absorbance band at 290 nm was revealed by UV-Vis spectroscopy and confirmed the presence of the synthesised ZnO NPs. In comparison, HRTEM and HRSEM indicated hexagonal wurtzite rock salt (cuboidal) and spherical shaped particles with average sizes ranging between 6.64 - 18.65 nm. Their major functional groups were demonstrated in FTIR studies. X-ray diffraction revealed a highly pure crystalline zincite (GZnO NPs) (94.32%), cubic (a high-pressure cubic NaCl-type), with an average size of 13.22 nm. The GZnO NPs were applied to assess their effect on *C. albicans* using the modified Kirby-Bauer and CV staining assays. CV staining assay was used to evaluate the trends in biofilm reduction for CHX, nystatin, and GZnO NPs were assessed.

CHAPTER FIVE - Discussion

In the past few decades, nanotechnology has advanced as an important and interesting research field of contemporary biomaterial sciences. MO NPs, including ZnO NPs, have unique physicochemical properties and multi-functionality, attributed to their nanoscale size and high density of the surface sites, thus offering great potential for complex biomedical applications (Chavali & Nikolova, 2019; Nikolova & Chavali, 2020). Green synthesis methods using either enzymes, microorganisms (Jayaseelan *et al.*, 2012), plants, or plant extracts and fruit peel (Fierascu *et al.*, 2020) have gained extensive attention owing to their advantages in the potential for rapid, innocuous, affordable, eco-friendly production and thus alternative options to the physical and chemical approaches (Fierascu *et al.*, 2020; Jiang *et al.*, 2018; Kalpana & Rajeswari, 2018; Mirzaei & Darroudi, 2017; Prabu, 2018). Moreover, additional benefits for using plant-based extracts for NPs synthesis are: (1) they are less likely to be contaminated; (2) they do not require special storage conditions and (3) have high stability in harsh conditions (high temperature, pH). During plant-mediated NP synthesis, the extract is mixed with metallic salt at different temperatures for different times. The increase in the stability is attributed to the formation of bonds between the NPs and the phytochemicals in plant extracts. The phenols and alkaloids have been reported to passivate and stabilise the reduced NPs. The reduction of metal ions leads to the formation of nucleation centres which sequester additional metal ions and formulate nanoparticles. Therefore, the phytosynthesis methods harness the advantages of capping with phytochemicals, and as a result, this type of bio-inspired manufacturing can improve their biocompatibility.

For the first time in this study, we report a successful phytosynthesis of GZnO NPs from a combination of *A. betulina* (Buchu) infused *A. linearis* (Rooibos) tea leaves and *M. paradisiaca* (banana) peel extracts as biological reducing and stabilising agents. Validating tests were

performed on these GZnO NPs to confirm their successful synthesis. Further, the antifungal activity of the GZnO NPs was tested against *C. albicans* (ATCC 90028) biofilms, and ultimately the antifungal effects of these GZnO NPs were compared to two positive controls (0.2% CHX gluconate and nystatin).

Metal-based NPs, including ZnO NPs, have been reported to have wide-spectrum applicability in various fields, including food packaging, skincare products, agriculture, and biomedical and dental products. Currently, ZnO NPs are applied in multiple formulations, including those of paints, sunscreens, hair care products, and ceramic fabrication (Heng *et al.*, 2011). Besides, ZnO is at present identified as safe by the US Food and Drug Administration (FDA) as a food preservative because zinc is an essential trace element. The advent of nanotechnology has led to the development of materials with properties for use as antimicrobial agents (Ali *et al.*, 2018; Espitia *et al.*, 2016; Institute of Medicine (US) Food Forum, 2009; Jiang *et al.*, 2018; Raghunath & Perumal, 2017). Moreover, recent reviews have proposed the utilisation of ZnO NPs for various biomedical applications, particularly for antimicrobial purposes (Benoit *et al.*, 2019; Bertoglio *et al.*, 2018; Fang *et al.*, 2020; Hoseinzadeh *et al.*, 2017; Hu *et al.*, 2019; Kuang *et al.*, 2018; Liu *et al.*, 2019; Rai *et al.*, 2016; Sánchez-López *et al.*, 2020; Shaikh *et al.*, 2019; Sportelli *et al.*, 2020; Tobal *et al.*, 2020; Vallet-Regí *et al.*, 2019; Wang *et al.*, 2017).

In this study, the ZnO NPs formulation was monitored by visual inspection as reported in previous studies (Chaudhuri & Malodia, 2017; Santhoshkumar *et al.*, 2017). Observed colour changes were recorded during the entire course of the reaction. Changes are perceived to be attributable to the conversion of the precursor $Zn(NO_3)_2$ to ZnO. Zinc nitrate is a white, highly deliquescent crystalline solid and is typically found as hexahydrate $Zn(NO_3)_2 \cdot 6H_2O$. It is also soluble in alcohol and water. The typical chemical reaction is as follows:

$$Zn + 2\ HNO_3\ (diluted) \rightarrow Zn\ (NO_3)_2 + H_2$$

$$4\ Zn + 10\ HNO_3\ (concentrated) \rightarrow 4\ Zn\ (NO_3)_2 + NH_4NO_3 + 3\ H_2O$$

Upon heating, thermal decomposition occurs to form ZnO, nitrogen dioxide, and O_2:

$$2\ Zn\ (NO_3)_2 \rightarrow 2\ ZnO + 4\ NO_2 + O_2$$

The structural, optical, and morphological properties of the green synthesized ZnO NPs were characterised by visual inspection, UV–Vis, XRD, FTIR, [TEM; (EDX and SAED)] and (SEM-EDS) techniques. UV-vis analysis was employed as an initial technique to analyse the optical properties of the GZnO NPs. A shift to short-wavelength (also called hypsochromic), can be expressed in the UV-vis results. ZnO NPs are perceived as a group of chromophores with colours ranging from 200 - 400nm. Hence, in this study, peaks due to GZnO NPs were investigated between 200 – 800 nm, and the most prominent peak was noted at 290 nm (Figure 22). Our findings are similar and within the range of findings reported at peaks of 290 to 300 nm for other phytosynthesised ZnO NPs by Shekhawat and Manokari (2014). Several other studies have reported peaks of green-mediated ZnO NPs at 352 nm (Vijayakumar *et al.*, 2018b), 374 nm (Jayaseelan et al., 2012), and 370 nm (Zare *et al.*, 2017). Generally, a broad peak in UV-vis spectra is an indication that the size and shape distribution of the nanosize ZnO is somewhat broad, confirming that the sample tested (GZnO NPs) had a heterogeneous population of nanoparticles.

Fundamentally, the UV spectra of ZnO NPs have emission bands in the UV and visible (yellow, green, blue, and purple) regions. UV emission is the characteristic of ZnO, which is attributed to the excitonic combination or the transition of the edge. The excitonic effect in ZnO is a result of one of the following, singly ionized oxygen vacancies (interstitial oxygen dislocation),

surface defects, photo-excited holes, presence of –OH groups (mostly in chemical synthesis methods), defect complexes, and zinc vacancies (Leung et al., 2013). Both the defects and charges have a critical role to play in bioactivity. Such defects deliberately change the physical characteristics and properties of the particle boundary (Ali *et al.*, 2018).

Consequently, the excitonic effects impact the optical features of the ZnO NPs, and these features become more interesting as dimension (size and shape) is reduced to the nanoscale range. In turn, these size and shape-related characteristics dictate the physicochemical properties and multi-functionality of the NPs. As a result, this offers improved applications for multifaceted potentials (bioactivity), including biomedical and antimicrobial applicability (Ali *et al.*, 2018). For example, a blue shift is associated with a reduction in the size of NPs. Apart from to particle size, other factors that influence the characteristic behaviour of these materials include the method of fabrication (i.e. green or conventional); concentration and pH; doping, surface state; the interaction of NP with solvent; temperature; surrounding chromophores in an excited state; as well as corresponding band gap. Thus, the absorbance (intrinsic particle absorption) increases linearly with increase in particle size and concentration (Goh et al., 2014). Usually, the optical band gap of a semiconductor increases with the reduction of the NP's size (Debanath & Karmakar, 2013), and different shapes, e.g. rods, needles and shells at same excitation can display different colour shifts in the UV-vis region (Djurišić et al., 2006).

The size and shape of the green synthesized ZnO NPs were then corroborated by TEM and XRD techniques in this study. These morphological characteristics are perceived to be influenced by the nature of the plant extracts. The XRD studies showed that all samples of the GZnO NPs had a typical pattern of ZnO NPs. All the captured peaks in the XRD pattern were indexed to ZnO with the hexagonal wurtzite structure and were consistent with the standard

hexagonal-structured nano ZnO card (Figure 23). The XRD report of the signature spectra in this study is similar to previous reports of the green-mediated ZnO NPs by Rad *et al.*, (2019). Additional information from XRD revealed that the GZnO NPs have a cubic rock salt (Na-Cl) and spherical crystalline structure, with a hexagonal lattice in wurtzite phase with other minor additional diffraction peaks. Similar findings of stable hexagonal phases of GZnO NPs were reported in several other studies (Pillai *et al.*, 2020; Sundrarajan *et al.*, 2015; Vidhya *et al.*, 2020 & Wang *et al.*, 2020). In this study, from the XRD the crystallite size of the GZnO NPs was 13.22 nm on average, and this is in accord to the XRD findings reported by Ali *et al.* (2016), Nava *et al.*, (2017a; 2017b), and Ngom *et al.*, (2020), also charted in Table 1.

Fourier-transform infrared spectroscopy was also performed to re-validate the zincite nature and purity of the synthesized NPs. Figure 25 shows the characteristic FTIR band of the pressed powder in the spectral range of 400-4000 cm^{-1}. The IR transmission was mapped to identify the significant absorptions detected at the lower wavenumbers. Usually, a broad peak in the range of 3500 to 3000 cm^{-1} is assigned to the water of hydration present in the solution O-H group (O-H stretching mode of the hydroxyl group) (Thema *et al.*, 2015b). The hydroxyl probably results from the hygroscopic nature of ZnO, while carboxylate is derived from the reactive C of plasma groups when ZnO NPs are formulated. Due to the relative intensity of the Zn-O peaks (stretches) of the adsorbed OH compounds, the high crystallinity and purity of the synthesized ZnO NPs can be pre-concluded. Like most wurtzite crystal structure materials, ZnO belongs to the hexagonal system (Thema *et al.*, 2015b). Further, the FTIR spectroscopic study emphasises the role of phenolic compounds in reducing and stabilising the ZnO NPs (Ali *et al.*, 2016b) (Figure 24). Thus, the perceived principal biomolecules involved in the green synthesis process were confirmed by the FTIR spectroscopy.

It has also been documented that peaks between 2825-3000 cm^{-1} are due to the C-H vibration of the different alkane groups. Peaks at 1470 cm^{-1} are associated with C-O-H bonds, and those between 2500-1380 cm^{-1} are attributed to asymmetrical and symmetrical C=O bonds. Furthermore, the peaks observed at 1384 cm^{-1} are due to the symmetrical and asymmetrical extension of the zinc carboxylate groups. The peaks observed from 1333-415 cm^{-1} correspond to the vibration of the C-H group. The peaks at 1052 cm^{-1} were also vibration mode of the C-O groups. It has also been reported that the vibration of C-N bonds is observed at 1010 cm^{-1}. The peaks in the region between 800 and 400 cm^{-1} are allotted to Zn-O bonds. (Geetha *et al.*, 2016; Happy *et al.*, 2019).

In this research report, peaks between 828.61 and 631.54 cm^{-1} were recorded as presented in Figure 25. These are characteristic bands conforming to the Zn-O stretching mode, which is concurrent with other findings reported by (Fakhari *et al.*, 2019; Nava *et al.*, 2017a; Thema *et al.*, 2015a). Occasionally, the FTIR technique can present some challenges because of insufficient archived information in the FTIR repository. Thus lack of information on all the bonding information present in functionalised C nanomaterials. This limitation can lead to difficulties in the validation of the intended material. Nevertheless, such was not experienced in this study.

Another characterisation technique applied in this study was HRTEM analysis. According to TEM, the average size of the GZnO NPs in this study ranged between 6.64 - 18.65 nm, at varied magnifications. The size established in HRTEM was coherent to those found in XRD. Interestingly, a few more researchers have documented similar structural properties of ZnO NPs (Bhuyan *et al.*, 2015; Geetha *et al.*, 2016; Selim *et al.*, 2020; Stan *et al.*, 2015; 2016 & Suresh *et al.*, 2015). Ishwarya *et al.*, (2018) and Madan *et al.*, (2016) recorded their GZnO

NPs sizes at slightly wider ranges, i.e. 10-50 and 9-40 nanometres, respectively. Further, the HRTEM investigation of ZnO NPs revealed predominantly spherical to ovoid ZnO NPs, and this is also similar to several other reports (Jayaseelan *et al.*, 2012; Sangeetha *et al.*, 2011; Vanathi *et al.*, 2014). These findings are comparable with the results of other green-mediated ZnO NPs from diverse plant extracts. For instance, Thema *et al.*, (2015b) reported ZnO NPs with sizes ranging between 12-26 nm (HRTEM). However, a few other studies that synthesised GZnO NPs documented slightly different findings in terms of size (Rad *et al.*, 2019; Raja *et al.*, 2018) but all within the nanoscale range. The argument for the size and shape variations can be due to different reducing and capping agents employed in the latter. In another study, the presented biologically synthesized ZnO NPs had particle sizes in the range of 8.48-32.51 nm as determined by HRTEM analysis (Nagajyothi *et al.*, 2013), which is still comparable to the findings in this study. Furthermore, the SAED patterns of prepared ZnO NPs are presented in Figure 26. The configuration reveals distinctive bright rings which verify the preference for nanocrystalline orientation. These findings are similar to previous studies conducted on the interrogation of ZnO NPs (Khoshhesab *et al.*, 2011).

HRSEM was an additional characterisation technique applied to investigate the GZnO NPs. The HRSEM findings were coherent with previously described and documented results on other phytosynthesised ZnO NPs using aqueous green extracts as their primary reducing and stabilising agents. More, the micrographs acquired during SEM interrogation in this study revealed rod-like GZnO NPs at various magnifications (Figure 28). Several other reports have also described the similar presentation of their green-mediated ZnO NPs (Jalal *et al.*, 2018; Khan *et al.*, 2018; Matinise *et al.*, 2017; Suresh *et al.*, 2018). However, Suresh *et al.*, (2018) found rod-like ZnO NPs with a slightly larger size. Subsequently, HRSEM-EDS output assessment to verify the purity and elemental composition of the samples was done. The

HRSEM-EDS analysis is a qualitative and quantitative technique employed to study the formulated nanomaterials (GZnO NPs). It provided the fundamental elemental constituents by the EDX and EDS analyses. The crystalline structure of the GZnO NPs was further validated (Figure 29). Comparable to the HRSEM-EDS, the HRTEM-EDX findings also showed peak signals of elemental constituents of the GZnO NPs (Figures 29 and 27, respectively). The most concentrated peaks were those of Zn at 82, 523, 1000, 1050, and 1120 keV. Other signals observed included oxygen (O), carbon (C), copper (Cu), Sodium (Na), Chloride (Cl) and potassium (K) in traces. It has been conveyed in the literature that during the biological synthesis (here referring to single pot synthesis) of the GZnO NPs, the C signal is essentially attributed to the C-containing molecules and polyphenol groups in the Buchu-infused Rooibos and banana peel extracts. The oxygen signal is present due to the zinc precursor. The Na and Cl signals signify that the formulated NPs have a face-centred cubic Na-Cl base (rock salt) crystalline structure with a hexagonal lattice. This study found that the purity of the GZnO NPs from XRD, HRTEM-EDX and HRSEM-EDS was 94.32%, 91.34%, and 81.97%, respectively. It was therefore verified with consistency from these analyses that the green synthesis of the ZnO NPs was efficient and of high purity.

Concerning the antimicrobial effect of ZnO NPs, numerous researchers have investigated it on several Gram-negative and Gram-positive bacteria (Ali *et al.*, 2016b; Almoudi *et al.*, 2018; Alzahrani & Ahmed, 2016; Ann *et al.*, 2014; Applerot *et al.*, 2009; Gupta *et al.*, 2018; Jayabalan *et al.*, 2019; Khan *et al.*, 2014; Mohamad Sukri *et al.*, 2019; Perelshtein *et al.*, 2015; Raghupathi *et al.*, 2011; Sánchez-López *et al.*, 2020; Sirelkhatim *et al.*, 2015; Sundrarajan *et al.*, 2015; Vallet-Regí *et al.*, 2019; Wang *et al.*, 2017; Xie *et al.*, 2011). One such report showed that even when compared to other metal oxides, ZnO NPs demonstrated the highest antimicrobial potential (bactericidal action) against both Gram-positive and -negative bacteria

as compared to their counterparts, the micro-and macro-particles (Azam *et al.*, 2012). Relevant to dentistry, a substantial number of antibacterial investigations on activities against oral pathogenic bacteria including pathogens responsible for dental caries, endodontic infections, and periodontitis have been conducted (Andrade *et al.*, in press; Dias *et al.*, 2019; Garcia *et al.*, 2017; Kasraei *et al.*, 2014; Khan *et al.*, 2014; Mirhosseini *et al.*, 2019; Samiei *et al.*, 2018; Vargas-Reus *et al.*, 2012; Vinotha *et al.*, 2019; Wang *et al.*, 2019).

A few studies have investigated the effects of ZnO NPs on both bacteria and fungi, including *C. albicans* (Mousavi *et al.*, 2019; Gunalan *et al.*, 2012; Jayaseelan *et al.*, 2012; Vijayakumar *et al.*, 2018b). ZnO NPs possess natural antimicrobial properties when created through the green synthesis method, which may produce novel medicines for microbial therapy. Jalal *et al.* (2018) informed that GZnO NPs inhibited 85% of biofilm growth at 0.25 mg/ml. It is crucial to appreciate that the fungicidal effect observed due to ZnO NPs can never be identical. It is because biological ecologies never behave identically, even in similar *in vitro* conditions. Notably, the work by Lipovsky *et al.* (2011) offered an elucidation on the possible mechanism of action of ZnO NPs as an antifungal agent against *C. albicans,* man. The researchers identified a link between ZnO NPs and ROS that initiates cell injury and therefore, the fungicidal effect (Lipovsky *et al.*, 2011; Rosa-garcía *et al.*, 2018).

Noticeably, fewer studies have investigated the interactions of the ZnO NPs with fungal pathogens affecting humans (Cierech *et al.*, 2016a, 2019; Jalal *et al.*, 2018; Khan *et al.*, 2016; Lipovsky *et al.*, 2011; Mirhosseini *et al.*, 2019; Aguilar-Méndez *et al.*, 2011; Bramhanwade *et al.*, 2016; Malaikozhundan *et al.*, 2017; Wani & Shah, 2012). When in a human host, Candida species can form biofilms on practically any substrate including surfaces of appliances and prostheses inserted in or utilised by the host. The accumulation of biofilms leads to recurring

and persistent invasive candidemia, and this form of infection is challenging to eliminate. The reason being that the biofilm matrix presents great resistance to host defence mechanisms as well as antimicrobial medications and demonstrate an exceptional capability to adhere to various biomaterials. These biofilms are one of the main reason for the death of hospitalised patients and immunocompromised individuals (Cuéllar-Cruz *et al.*, 2012).

In this report, the antifungal action of the GZnO NPs (0.6538 µg/ 100µL) was tested on MHA using the disc diffusion test with different volumes. The initial *C. albicans* concentration was adjusted to 0.5 McFarland's. The diameters of the inhibition zones around the antimicrobial discs, as reflected in Figure 30 (B, E, and H), show that these NPs have antifungal activity against *C. albicans.* These zones of inhibition increased with increasing volumes pipetted onto the sterile discs. Wahab *et al.*, (2010) reported similar results with their working concentration of ZnO NPs. This could be due to the increase in NPs concentration with increased volume.

The sizes of zones of inhibition in this study ranged between 19-22, 22-24, and 29-32 mm for 100, 150, and 200 µL, respectively. The zones of inhibition were measured at 24 h incubation of the yeast cells with the three interventions (0.2 % CHX gluconate, GZnO NPs, and Zn $(NO_3)_2 \cdot 6H_2O$). For all the three intervention groups, the zones significantly increased with an increase in volume. Zinc nitrate had the least effect across all volumes (Figure 31). This effect is substantially different from that due to the ZnO NPs ($p < 0.001$) (Figure 31). Therefore, the apparent effect due to the NPs could not have been due to the precursor salt, i.e. zinc nitrate. Following this conclusion, further comparison in the Kirby-Bauer assay will involve the effect due to ZnO NPs and CHX. The results at 100 µl (Figure 31), showed that ZnO NPs had a slightly lower effect than CHX (Estimated marginal mean for the zones of inhibition = 20.56±0.88; 21.94±0.17, respectively). However, at 200 µL, the ZnO had a higher effect, than

CHX (Estimated marginal mean for the zones of inhibition = 30.44±1.01; 27.11±0.70, respectively). Figure 31 shows that the flexion occurs around 150 µL. The highest differences in the effect between ZnO NPs and CHX was observed at 200 µL. Overall, for all the three intervention groups (0.2 % CHX gluconate, GZnO NPs, and Zn $(NO_3)_2 \cdot 6H_2O$), similar trends were observed. The additional analysis here onwards will focus on the effects at 200 µL.

Statistical analysis was done to investigate the null hypothesis that all means of inhibition zones in the Kirby-Bauer assay for the three intervention groups (0.2 % CHX gluconate, GZnO NPs, and Zn $(NO_3)_2 \cdot 6H_2O$) are equal. One-way ANOVA-F test was performed to determine whether there was any statistical significance for the means of the zones of inhibition against *C. albicans.* The ANOVA-F test confirmed that there were significant differences ($p < 0.0001$) across the three groups (Figure 32 and Table 7). These differences are best demonstrated at the highest volume (200 µL), ($F_{(2,24)} = 716.88$ $p < 0.01$) (Figure 32). The ZnO NPs showed the highest effect. Zinc Nitrate hexahydrate solution had the least activity among the three intervention groups. The activity differences show that the effect in ZnO NPs is not due to residue of the salt precursor used in its synthesis. However, ANOVA-F did not specifically identify pairs of significance. It purely highlighted that the zones of inhibition of at least a pair within groups were significantly different when discs were infused with 200 µL of either of the three interventions.

The p-value from the ANOVA F- test for the means of the inhibition zones was less than 0.01 among the three groups; hence, the null hypothesis (H_0) is rejected. In order to ascertain which specific groups differed from each other, a Bonferroni adjustment post hoc test was carried out (Table 7) in the results section. The advantage of the Bonferroni test is that it attempts to prevent data from being erroneously qualified as significantly different by adjusting data

analysis for comparison. The application of the Bonferroni correction test (Table 7) emphasized the statistical significance for the means ($p < 0.000^*$) across the three intervention groups at 200 µL as demonstrated by the ANOVA F-test in Figure 32. Therefore, the null hypothesis (H_0) is further rejected. In overall, from the Kirby-Bauer assay, we can conclude that the ZnO NPs does have an effect against *Candida albicans.* ZnO NPs inhibited the growth of Candida comparable to the CHX.

The disc diffusion findings of this study resonate with the results by Wahab *et al.* (2010), i.e. the fungicidal effect of our GZnO NPs was also concentration-dependent. Similarly, Elumalai *et al.*, (2015) used a green method for the synthesis of ZnO NPs from leaves of *Vitex trifolia*, and their findings showed that the zones of inhibition were dependent on the concentration of the ZnO NPs. Vijayakumar *et al.* (2018) reported that the maximum zones of inhibition recorded for *C. albicans* upon exposure to 100 µg/ml Zn NPs was 34 ± 1.28 mm. This effect is higher than in our study. This observed difference could be attributed to a higher concentration of ZnO NPs and the green synthesis that they used. In the nanoscale range of NPs, the concentration of Zn plays a crucial role in several biological activities. Higher concentrations of the ZnO NPs, as well as other nanoscale range materials, offers a larger surface area, thus governing the outcomes upon their application. Consultation with current literature has shown that most common ZnO NPs utilised were of the conventional form, and only fewer studies utilised green methods as described by Dhillon et al (2014), Janaki *et al.* (2015), Jalal *et al.* (2018), Vijayakumar *et al.* (2018), and Vinotha *et al.*, (2019).

After observing the effects of the GZnO NPs on unbound yeast, their effect on bound yeast biomass (biofilm) was tested. In order to achieve this, 96-microtiter-plate CV assay, an indirect approach for biofilm quantification was done (Figure 33). The formed biofilms are presented

as biomasses, and the biomasses are a result of binding of yeast cells to the interventions (CHX, ZnO NPs, nystatin), the biofilm, and the combination of interventions and the biofilms on the microtiter plates, which were read as optical densities. Then the trends in biomass (optical densities) of the CV staining assay were analysed across 72 hours. CV staining assay was used to study the effect of the interventions on 24 h yeast sessile (biofilm) was studied after reading the samples in a spectrophotometer. For all the interventions, the ODs of biofilms were significantly different at all time points (Figure 35). High ODs in this study were associated with high antibiofilm potential (as described in section 4.8.2) (Figure 36 and Supplemental Table 4 in the Appendix).

Further, for the CV assay results, a one-way ANOVA was done to compare the three intervention groups, at different time points (refer to Figure 35 in results and Supplemental Table 4 in the Appendix). This analytical test revealed significances across groups as graphically presented in Figure 35. However, the ANOVA comparison has an inherent limitation of not showing the specific groups with significant differences. It basically showed that at least one of the four groups (the three interventions and negative control) was significantly different ($p < 0.001$, 95% CI). For in-depth comparison whether specific groups differed from each other, the Tukey's HSD (post hoc) test was performed as mentioned in section 3.5.2. Thus, the actual statistical significances were elucidated. Selected time point analyses are graphically presented in Figure 35, with a complete presentation in the appendix (Supplemental Table 4). Generally, the post hoc analysis revealed significant differences ($p < 0.001$, 95% CI) at most times (Supplemental Table 4, in the Appendix). Hence, at these points there, the H_0 was not supported. That is, there is a plausibility that the observed differences were due to the different interventions. Nonetheless, the Tukey's HSD test also revealed $p >$

0.05, at fewer time points, e.g. at 4 h for ZnO NPs against nystatin ($p = 0.8115$). Whenever the $p < 0.05$ from the post hoc tests, the null hypothesis (H_0) was rejected.

Analysis of trends was done to compare the rate of effects by the different interventions on the mature biofilm. Both the optical densities and trends will be discussed below to elucidate if the intervention of interest had effect. These trends observed due to the effects of the interventions were explained, as illustrated in Figures 37. The resultant ODs were also compared to control treatments (nystatin and CHX), and the trends for the same were elucidated analytically using a linear regression approach (Figure 37).

The variation noted between the two assays used (Kirby-Bauer and CV susceptibility staining) were attributed to the ecological and biological nature of the fungi, as well as the quantification technique (Gulati *et al.*, 2018). Further, in an actual clinical scenario, additional advantages include their existence in biofilms coupled with the polymicrobial ecological character of the biofilms with other bacterial species compared to planktonic growth (Lohse *et al.*, 2018). Therefore, in order to demonstrate the overall differences within this study, trends in biofilm reduction due to the interventions were assessed by linear regression analysis at selected time points (Figure 37). The resultant gradients were -0.10, -0.065, -0.016, and -0.035 for nystatin, ZnO, CHX, and negative controls, respectively. Finally, the hypotheses tested experimentally using the CV staining assays, i.e., H_0: Effect of NPs on *C. albicans* biofilm is equivalent to that of untreated biofilm, and H_0: Effect of NPs on *C. albicans* biofilm is comparable to that of conventional interventions on biofilm were both rejected.

When linking the available evidence on characteristic features of ZnO NPs and their antimicrobial potential, different arguments predominate. For instance, regarding the

significance of particle size, several findings have shown that miniature ZnO particles have superior interactions and effects on several microbial organisms (Yamamoto, 2001; da Silva *et al.*, 2019b). Notably, the antimicrobial efficacy of NPs is dependent on the nanoparticulate grain size (Dizaj *et al.*, 2014b; Khezerlou *et al.*, 2018). Similarly, the findings of this study also resonate to these reports, with NPs sizes ranging between 6.64 - 18.65 nm, and had comparable efficacy to CHX and nystatin. Further, the reduced size of the NPs in comparison to fungal spores is possibly advantageous since they can cross the cell membrane with ease (Zhang & Chen, 2009). It is also suggested that antifungal activity is likely to be attributed to the electrostatic attraction between the positively charged NPs and the negatively charged cell membranes of microbes (Allaker, 2013; Wang *et al.*, 2017). However, minute particle sizes have been associated with increased toxicity (Heng *et al.*, 2011) and special precautions have to be taken, mainly when used in food and medical applications. Nonetheless, it was beyond the scope of this study and will be investigated in further research. Therefore, understanding of the mechanisms of antifungal resistance in Candida biofilms, linked to the chemical constituents of the materials utilised to manufacture medical devices or prostheses, as well as the Candida proteins and genes necessary for antifungal resistance, is critical (Cuéllar-Cruz *et al.*, 2012).

Another essential and discussed feature is the shape of the NPs with respect to their performance. The biological activities of NPs are shape-dependent, and these have been linked to their faceted hexagonal structural design. The active peak (facet) concentration as determined by XRD of NPs, including that of ZnO NPs is crucial for these biological interactions. Further, the synthesis method and conditions influence the formation of these active facets. For instance, facets (100), (002), and (101) are indicative of pure wurtzite structural architecture of ZnO NPs (Khan *et al.*, 2016), additionally (002) is suggestive of good

crystallisation. Furthermore, rod-like NPs have predominantly (100) and (111) peaks, while the spherical NPs have mostly (100) facets (Ali *et al.,* 2018). High concentrations of (111) have also been liked to significant biological activity (Ali *et al.,* 2018; Cierech *et al.,* 2019). Nonetheless, the peak-dependent ZnO NPS activity has been scarcely investigated (Cierech *et al.,* 2019). Depending on the shape (e.g. nanospheres, nanoplates, nanorods, nanocubes etc.), ZnO NPs can have varied functional behaviour, mechanism of action and internalisation capability. The ability to penetrate a microscopic structure (organelle or cell) or environmental matrix (air, soil, water, etc.) is generally easier for a nanoscale particulate than its macroscopic counterparts (Ali *et al.,* 2018; Cierech *et al.,* 2019).

In addition, the relevance of the peaks to several biological activities relies on the presence of higher numbers of these peaks, allowing more oxygen vacancies and subsequently, improved internalization. The oxygen vacancies are essential for the generation of ROS, and therefore influences antimicrobial actions as well as other related biological activities. For example, the antimicrobial action of ZnO NPs is attributable to the facet (001), which has a positive charge and an unsaturated oxygen orientation. Coupled with its improved binding capacity to oxygen molecules and OH^- ions might result in increased production of $OH^•$ and H_2O_2 radicals and therefore improved antimicrobial potential (da Silva *et al.,* 2019a).

The developed *C. albicans* biofilms are typically tolerant to most conventional antifungal therapies, and hence the susceptibility of these biofilms to traditional therapeutic agents remains low (Cavalheiro & Teixeira, 2018; Jabra-Rizk *et al.,* 2004; Kernien *et al.,* 2018; Koo *et al.,* 2017; Nett, 2016; Tournu & Van Dijck, 2012; Tsui *et al.,* 2016; Vila *et al.,* 2020). Malaikozhundan *et al.* (2017) were one of the few groups that investigated the antifungal properties of ZnO NPs against *C. albican*s. In their report, they documented good antifungal

activity from ZnO NPs, that were synthesised using a *Pongamia pinnata* seed extract, against *C. albicans* at different concentrations. It is suggested that the ZnO NPs disrupts the fungal membranes with elevated rates of reactive oxygen species, thus causing yeast cell death (Malaikozhundan *et al.*, 2017). Comparably, in this study, we investigated the possible antifungal effects of GZnO NPs synthesised from a mixture of Buchu-infused Rooibos tea leaves and banana peel extracts.

Recently the spread and increased resistance of pathogenic microbial agents (bacteria, fungi, and viruses) to conventional antimicrobial agents has contributed to alarming and challenging food and health issues. Currently, nanoscience and nanotechnology, in particular the utilisation of NPs, have presented new methods to tackle this challenge due to their intrinsic superior antimicrobial potential of NPs. Similar results are demonstrated at 72 h (Figure 35) in this study, where the effect due to ZnO NPs superseded that of the conventional interventions. Metal and MO NPs are extensively studied as a cluster of biomaterials due to their antimicrobial qualities (Dizaj *et al.*, 2014; Khezerlou *et al.*, 2018). Therefore, the antifungal behaviour of the GZnO NPs using Buchu-infused Rooibos and banana peel extracts indicate that these green method NPs can be further explored for potential biomedical applicability, including the control unfavourable microbial growths. Among the challenges observed in literature was a lack of standardisation in relation to the microbial strains used. Different studies utilised diverse methodologies for microbiological testing, leading to inconsistent reports and findings (da Silva *et al.*, 2019a). Although this was an exploratory study, it strived to adopt and implement *in vitro* assessment using standardised microbiological tests to permit adequate reporting.

CHAPTER SIX – Conclusion, Limitations and Recommendations

6.1 Conclusion

For the first time, using a combination of $Zn(NO_3)_2$ (metal precursor), fruit peel (BPE) and green tea (Buchu-infused Rooibos) extracts, GZnO NPs were synthesised using a green single pot method. The GZnO NPs synthesis protocol established in this research study followed basic green protocols to formulate the intended ZnO NPs. Results revealed that a direct and highly pure green synthesis protocol for GZnO NPs was developed. Accordingly, this study proposes to present a new practical biosynthetic approach for GZnO NPs using natural, affordable, and environmentally friendly materials and conditions.

Validation (characterisation) of the NPs was done using visual inspection, UV-Vis, XRD, FTIR, HRTEM (EDX and SAED) and SEM-EDS. Colour changes in the visual assessment were observed and captured. FTIR analysis confirmed significant and distinctive stretches corresponding to functional groups of the ZnO NPs at 829, 775, and 632 cm^{-1}.

XRD analysis confirmed phase identity, crystallinity as well as the size of the GZnO NPs. The GZnO NPs crystals were heterogeneous with a hexagonal lattice, with a percentage purity of 94.32%. The shape of the GZnO NPs was cubic Na-Cl base (rock salt) and spherical, of average size 13.22 nm. Using XRD, Debye-Scherer diffraction rings of the synthesised ZnO NPs at 2θ values were indexed as (100), (002), (101), (102), (110), (103), (200), (112), (201), (004), and (202).

In this study, HRTEM (EDX and SAED) and HRSEM-EDS, were used to analyse the cross-sectional morphology and topographical microstructure of the GZnO NPs, respectively. The HRTEM confirmed NPs grain sizes ranging between 6.64 - 18.65 nm. Further, the SAED in

TEM revealed spots in rings coherent with the Debye-Scherer diffraction rings (in XRD) signifying that the material was highly polycrystalline and existed in wurtzite and rocksalt phases. The topographical analysis using HRSEM exhibited rod-like ZnO NPs at varied magnifications. Additionally, the EDX in TEM and EDS in SEM confirmed the elemental compositions of the GZnO NPs.

Furthermore, determination of the antifungal effects of the GZnO NPs (0.6538 µg/ 100µL) was performed on *C. albicans* (AT90028). The modified Kirby-Bauer assay (disc-diffusion method) and a colourimetric assay (CV staining assay) were employed to determine these antifungal effects. Nystatin and 0.2% CHX were used as positive controls. The ZnO NPs showed promising antifungal activity against *C. albicans*.

6.2 Limitations

The following were considered the limitations to this study:

a. The utilisation of green commercial products (i.e. Rooibos and Buchu tea leaves produced by Biedouw Valley Rooibos, Western Cape, SA) as the capping and stabilising agents may have additional influence on observed characteristics. Perhaps the use of natural green extracts would have the same or different effects on the quality of NPs.
b. The use of CV assay for the quantification avails only the biomass which does not distinguish between viable and dead cells *in vitro*. XTT is recommended as the more sensitive assay particularly to changes in cell metabolism (e.g. the antifungal effects of the NPs on yeast cells). It can be used to estimate and distinguish the number of viable cells *in vitro*, thus allowing more accurate quantitative information. Nonetheless, CV

assay was used in this study because of the encountered delays in the supply chain for the XTT assay.

c. The used organism was a laboratory isolate (i.e. isolated from their usual biological environment), which allowed a more detailed or more convenient analysis. However, results may be different when clinical isolates are used.
d. Therefore, as an *in vitro* study, the observed effects of the GZnO NPs on yeast cells may be of low ecological validity and difficult to generalise to actual clinical situations.

6.3 Recommendations

The effective control of oral biofilm-associated infections is still a great challenge globally. In the struggle to fight the emerging resistance against conventional antimicrobials, the recurrences of ailments, as well as the occurrences of hundreds of new infections, a need for new eco-friendly, economically feasible, and efficient alternatives is imperative. Hence the exploration of antimicrobial options using both metal and MO NPs, including ZnO NPs (Mahamuni-Badiger *et al.*, 2019). The microbiological organisms existing in biofilm matrices exhibit increased tolerance in comparison to the planktonic microorganisms, therefore prompting the exploration of innovative alternative strategies for controlling oral biofilm-related infections should be studied. There is also a significant need for detailed studies on the biochemical and molecular interactions, and mechanisms of these novel biomaterials to fully comprehend their antimicrobial activity.

So far, it is observed that there is an extensive repository of nanotechnology research. Nonetheless, the criteria pertaining to storage conditions, NPs concentration, incubation time, and sample manipulation present considerable variation among studies. Despite this heterogeneity of findings, it can be concluded that the incorporation of NPs, such as ZnO NPs,

into dental materials (denture PMMA, dental adhesives systems, dental implant surfaces, and basic restorative materials) can be considered for increasing antimicrobial activity. The antifungal or antibacterial properties of denture bases and dental adhesive systems modified with the conventional ZnO NPs showed significant improvement, as compared to original materials. The presentation of this heterogeneity across studies highlights the need for further studies to allow for better designing of standardised study protocols in terms of concentration, dental material modification, NPs type, as well as standardised reporting.

As mentioned earlier, generally, the incorporation of NPs (modification of dental materials) has shown favourable antimicrobial effects. However, most of these studies are performed *in vitro*. The actual environment and nature of the oral cavity is an appreciably complex ecosystem, and science has not yet fully established how the modifications of various dental materials may behave in or influence the *in vivo* environment. Therefore, it is imperative to consider issues like bioavailability, as well as the fact that the antimicrobial activity can be different in *in vivo* and *in vitro* conditions.

Apart from conventional ZnO NPs which were clinically tested for potential antimicrobial applications in denture tissue conditioners, green-mediated ZnO NPs have not been subjected to clinical testing. Thus, scientists need to take full advantage of this developing technology to formulate specific antimicrobial NPs against pathogens of human concern.

In addition, the focus of nanotechnology research should encourage the exploration of other phytosynthesised metallic and metallic oxide NPs, including their potential for biomedical and dental application regulated by their biocompatibility. With strong consideration and insight from literature, NPs have versatile potential, in particular the phytosynthesised NPs. Therefore,

green-mediated NPs are expected to go beyond *in vitro* (laboratory experimentation) to *in vivo* (clinical trials) conditions. For such prospects to be realised, more evidence on the mechanism of action and biocompatibility of these materials is imperative to inform the scientific community on the readiness to embark on *in vivo* studies with these biomaterials at biologically innocuous dosing that can be subjected to clinical testing and applications.

Among the common knowledge gathered, the postulated mechanism of action for ZnO NPs includes the production of ROS. However, it is also well understood that ROS is a double-edged sword; therefore, it can harm host cells. Green-mediated NPs are commended for better biocompatibility as opposed to their conventional counterparts. However, there is limited evidence on the balance between the biosafety (biocompatibility) and antimicrobial capability of these phytosynthesised nanomaterials.

It is evident that the utilisation of various metallic salt precursors, alongside plant or plant product extracts, can provide a large variety of phytosynthesised NPs with different shapes and sizes and hence other applications. Meanwhile, a thorough understanding of optimal production and control of these green synthesis procedures should be sought to contribute towards the production of homogenous NPs. In turn, this can be beneficial not only to the green nanotechnology and nanoscience fields, but also the biomedical and dental science fields at large. There is a need for further exploration, optimisation, and scaled-up production of green-mediated NPs, including ZnO NPs. This is so to meet the growing demands of a wide range of industries (agricultural, pharmacological, health and medical, biotechnological, biomedical and life sciences, environmental, engineering and aeronautics), as these materials have the potential for better functionalisation, biocompatibility and performance.

REFERENCES

Abdol Aziz, R.A., Abd Karim, S.F., Ibrahim, U.K. & Sanuddin, N. 2019. Precursor Concentration Effect on Physicochemical Properties of Zinc Oxide Nanoparticle Synthesized with Banana Peel Extract. *Key Engineering Materials.* 797:262–270.

Abdul Salam, H., Sivaraj, R. & Venckatesh, R. 2014. Green synthesis and characterization of zinc oxide nanoparticles from *Ocimum basilicum L. var. purpurascens* Benth.-Lamiaceae leaf extract. *Materials Letters*. 131:16–18.

Abdullah, F.H., Abu Bakar, N.H.H. & Abu Bakar, M. 2020. Low temperature biosynthesis of crystalline zinc oxide nanoparticles from *Musa acuminata* peel extract for visible-light degradation of methylene blue. *Optik*. 206:164279.

Abrahams, S.C. & Bernstein, J.L. 1969. Remeasurement of the structure of hexagonal ZnO. *Acta Crystallographica Section B Structural Crystallography and Crystal Chemistry*. 25(7):1233–1236.

Addy, M., Moran, J., Davies, R.M., Beak, A. & Lewis, A. 1982. The effect of single morning and evening rinses of chlorhexidine on the development of tooth staining and plaque accumulation: A blind cross-over trial. *Journal of Clinical Periodontology*. 9(2):134–140.

Afennich, F., Slot, D.E., Hossainian, N. & Van Der Weijden, G.A. 2011. The effect of hexetidine mouthwash on the prevention of plaque and gingival inflammation: A systematic review. *International Journal of Dental Hygiene*. 9 (3):182–190.

Agarwal, H., Venkat Kumar, S. & Rajeshkumar, S. 2017. A review on green synthesis of zinc oxide nanoparticles – An eco-friendly approach. *Resource-Efficient Technologies*. 3(4):406–413.

Agarwal, H., Menon, S., Venkat Kumar, S. & Rajeshkumar, S. 2018. Mechanistic study on antibacterial action of zinc oxide nanoparticles synthesized using green route. *Chemico-Biological Interactions*. 286:60–70.

Agarwal, H., Nakara, A. & Shanmugam, V.K. 2019. Anti-inflammatory mechanism of various metal and metal oxide nanoparticles synthesized using plant extracts: A review. *Biomedicine and Pharmacotherapy*. 109:2561–2572.

Aguilar-Méndez, M.A., Martín-Martínez, E.S., Ortega-Arroyo, L., Cobián-Portillo, G. & Sánchez-Espíndola, E. 2011. Synthesis and characterization of silver nanoparticles: Effect on phytopathogen *Colletotrichum gloesporioides*. *Journal of Nanoparticle Research*. 13(6):2525–2532.

Ahmad, N., Jafri, Z. & Khan, Z.H. 2020. Evaluation of nanomaterials to prevent oral Candidiasis in PMMA based denture wearing patients. A systematic analysis. *Journal of Oral Biology and Craniofacial Research*. 10:189–193.

Ahmed, S., Annu, Chaudhry, S.A. & Ikram, S. 2017. A review on biogenic synthesis of ZnO nanoparticles using plant extracts and microbes: A prospect towards green chemistry. *Journal of Photochemistry and Photobiology B: Biology*. 166:272-284.

Ajuwon, O.R., Marnewick, J.L. & Davids, L.M. 2015. Rooibos (*Aspalathus linearis*) and its Major Flavonoids — Potential Against Oxidative Stress-Induced Conditions. Joghi Thatha Gowder, S.J.T. (ed.), *Basic Principles and Clinical Significance of Oxidative Stress*. InTech: 171–218.

Akbar, S., Tauseef, I., Subhan, F., Sultana, N., Khan, I., Ahmed, U. & Haleem, K.S. 2020. An overview of the plant-mediated synthesis of zinc oxide nanoparticles and their antimicrobial potential. *Inorganic and Nano-Metal Chemistr*y. 50(4):257–271.

Alaghehmad, H., Mansouri, E., Esmaili, B., Bijani, A., Nejadkarimi, S. & Rahchamani, M. 2018. Effect of 0.12% chlorhexidine and zinc nanoparticles on the microshear bond strength of dentin with a fifth-generation adhesive. *European Journal of Dentistry*. 12(1):105–110.

Albanese, A., Tang, P.S. & Chan, W.C.W. 2012. The Effect of Nanoparticle Size, Shape, and Surface Chemistry on Biological Systems. *Annual Review of Biomedical Engineering*. 14(1):1–16.

Alexander, B.D., Procop, G.W., Dufresne, P., Fuller, J., Ghannoum, M.A., Hanson, K.E., Holliday, D., Holliday, N.M., *et al.* 2017. *CLSI. Performance Standards for Antifungal Susceptibility Testing of Filamentous Fungi. 1st ed. CLSI supplement M61*. 1st ed. Clinical and Laboratory Standards Institute.

Ali, A., Phull, A.R. & Zia, M. 2018. Elemental zinc to zinc nanoparticles: Is ZnO NPs crucial for life? Synthesis, toxicological, and environmental concerns. *Nanotechnology Reviews*. 7(5):413–441.

Ali, J., Irshad, R., Li, B., Tahir, K., Ahmad, A., Shakeel, M., Khan, N.U. & Khan, Z.U.H. 2018. Synthesis and characterization of phytochemical fabricated zinc oxide nanoparticles with enhanced antibacterial and catalytic applications. *Journal of Photochemistry and Photobiology B: Biology*. 183:349–356.

Ali, K., Dwivedi, S., Azam, A., Saquib, Q., Al-Said, M.S., Alkhedhairy, A.A. & Musarrat, J. 2016. Aloe vera extract functionalized zinc oxide nanoparticles as nanoantibiotics against multi-drug resistant clinical bacterial isolates. *Journal of Colloid and Interface Science*. 472:145–156.

AlKahtani, R.N. 2018. The implications and applications of nanotechnology in dentistry: A review. *The Saudi Dental Journal*. 30(2):107–116.

Allaker, R.P. 2010. The Use of Nanoparticles to Control Oral Biofilm Formation. *Journal of Dental Research*. 89 (11): 1175–1186.

Allaker, R.P. 2013. Chapter 10. Nanoparticles and the Control of Oral Biofilms. Subramani, K., Ahmed, W., Hartsfield, J.K. Jr (eds.), *Nanobiomaterials in Clinical Dentistry*. Elsevier Inc: 203–227.

Allaker, R.P. & Memarzadeh, K. 2014. Nanoparticles and the control of oral infections. *International Journal of Antimicrobial Agents*. 43(2):95–104.

Allaker, R.P. & Yuan, Z. 2019. Chapter 10 – Nanoparticles and the control of oral biofilms. Subramani, K., Ahmed, W. (eds.), *Nanobiomaterials in Clinical Dentistry*. Elsevier Inc: 243–275.

Allkja, J., Bjarnsholt, T., Coenye, T., Cos, P., Fallarero, A., Harrison, J.J., Lopes, S.P., Oliver, A., *et al.* 2020. Minimum information guideline for spectrophotometric and fluorometric methods to assess biofilm formation in microplates. *Biofilm*. 2:100010.

Almoudi, M.M., Hussein, A.S., Ibrahim, M., Hassan, A. & Zain, N.M. 2018. A systematic review on antibacterial activity of zinc against *Streptococcus mutans*. *The Saudi Dental Journal*. 30(4):283–291.

Altarawneh, S., Bencharit, S., Mendoza, L., Curran, A., Barrow, D., Barros, S., Preisser, J., Loewy, Z.G., *et al.* 2013. Clinical and Histological Findings of Denture Stomatitis as Related to Intraoral Colonization Patterns of *Candida albicans*, Salivary Flow, and Dry Mouth. *Journal of Prosthodontics*. 22(1):13–22.

de Alteriis, E., Maselli, V., Falanga, A., Galdiero, S., Di Lella, F.M., Gesuele, R., Guida, M. & Galdiero, E. 2018. Efficiency of gold nanoparticles coated with the antimicrobial peptide indolicidin against biofilm formation and development of Candida spp. clinical isolates. *Infection and Drug Resistance*. 11:915–925.

Alzahrani, E. & Ahmed, R.A. 2016. Synthesis of copper nanoparticles with various sizes and shapes: Application as a superior non-enzymatic sensor and antibacterial agent. *International Journal of Electrochemical Science*. 11(6):4712–4723.

Amona, F., Denning, D., Moukassa, D. & Hennequin, C. 2020. Current burden of serious fungal infections in the Republic of Congo. *Mycoses*. 63(6):543–552.

Anbuvannan, M., Ramesh, M., Viruthagiri, G., Shanmugam, N. & Kannadasan, N. 2015a. Anisochilus carnosus leaf extract mediated synthesis of zinc oxide nanoparticles for antibacterial and photocatalytic activities. *Materials Science in Semiconductor Processing*. 39:621–628.

Anbuvannan, M., Ramesh, M., Viruthagiri, G., Shanmugam, N. & Kannadasan, N. 2015b. Synthesis, characterization and photocatalytic activity of ZnO nanoparticles prepared by biological method. *Spectrochimica Acta - Part A: Molecular and Biomolecular Spectroscopy*. 143:304–308.

Andrade, V., Martínez, A., Rojas, N., Bello-Toledo, H., Flores, P., Sánchez-Sanhueza, G. & Catalán, A. Antibacterial activity against *Streptococcus mutans* and diametrical tensile strength of an interim cement modified with zinc oxide nanoparticles and terpenes: An in vitro study. *Journal of Prosthetic Dentistry*. 119(5):862.e1-862.e7.

Anil, S., Vellappally, S., Hashem, M., Preethanath, R.S., Patil, S. & Samaranayake, L.P. 2016. Xerostomia in geriatric patients: a burgeoning global concern. *Journal of investigative and clinical dentistry*. 7(1):5–12.

Ann, L.C., Mahmud, S., Bakhori, S.K.M., Sirelkhatim, A., Mohamad, D., Hasan, H., Seeni, A. & Rahman, R.A. 2014. Antibacterial responses of zinc oxide structures against *Staphylococcus aureus*, *Pseudomonas aeruginosa* and *Streptococcus pyogenes*. *Ceramics International*. 40(2):2993–3001.

Ansari, M.A. & Alzohairy, M.A. 2018. One-Pot Facile Green Synthesis of Silver Nanoparticles Using Seed Extract of Phoenix dactylifera and Their Bactericidal Potential against MRSA. *Evidence-based Complementary and Alternative Medicine, eCAM*. 2018. 1860280.

Applerot, G., Lipovsky, A., Dror, R., Perkas, N., Nitzan, Y., Lubart, R. & Gedanken, A. 2009. Enhanced Antibacterial Activity of Nanocrystalline ZnO Due to Increased ROS-Mediated Cell Injury. *Advanced Functional Materials*. 19(6):842–852.

Arciniegas-Grijalba, P.A., Patiño-Portela, M.C., Mosquera-Sánchez, L.P., Guerra Sierra, B.E., Muñoz-Florez, J.E., Erazo-Castillo, L.A. & Rodríguez-Páez, J.E. 2019. ZnO-based nanofungicides: Synthesis, characterization and their effect on the coffee fungi *Mycena citricolor* and *Colletotrichum sp*. *Materials Science and Engineering C*. 98:808–825.

Ardizzoni, A., Pericolini, E., Paulone, S., Orsi, C.F., Castagnoli, A., Oliva, I., Strozzi, E. & Blasi, E. 2018. In vitro effects of commercial mouthwashes on several virulence traits of

Candida albicans, viridans streptococci and *Enterococcus faecalis* colonizing the oral cavity. *PLOS ONE*. 13(11):e0207262.

Arendrup, M.C. 2013. *Candida* and Candidaemia: Susceptibility and Epidemiology. *Danish Medical Journal*. 60(11):1–32.

Ashraf, M.A., Peng, W., Zare, Y. & Rhee, K.Y. 2018. Effects of Size and Aggregation/Agglomeration of Nanoparticles on the Interfacial/Interphase Properties and Tensile Strength of Polymer Nanocomposites. *Nanoscale Research Letters*. 13:214.

Auld, D.S. 2001. Zinc coordination sphere in biochemical zinc sites. *BioMetals*. 14(3–4):271–313.

Axéll, T., Samaranayake, L.P., Reichart, P.A. & Olsen, I. 1997. A proposal for reclassification of oral candidosis. *Oral Surgery, Oral Medicine, Oral Pathology, Oral Radiology, and Endodontology*. 84(2):111–112.

Ayaz, M., Ullah, F., Sadiq, A., Ullah, F., Ovais, M., Ahmed, J. & Devkota, H.P. 2019. Synergistic interactions of phytochemicals with antimicrobial agents: Potential strategy to counteract drug resistance. *Chemico-Biological Interactions*. 308:294–303.

Azam, A., Ahmed, A.S., Oves, M., Khan, M.S., Habib, S.S. & Memic, A. 2012. Antimicrobial activity of metal oxide nanoparticles against Gram-positive and Gram-negative bacteria: A comparative study. *International Journal of Nanomedicine*. 7:6003–6009.

Azizi-lalabadi, M., Ehsani, A., Alizadeh-Sani, M., Khezerlou, A., Mirzanajafi-Zanjani, M., Divband, B., Zolfaghari, H. & Bagheri, V. 2019. Nanoparticles and Zeolites: Antibacterial Effects and their Mechanism against Pathogens. *Current Pharmaceutical Biotechnology*. 20(13):1074–1086.

Azizi, S., Ahmad, M.B., Namvar, F. & Mohamad, R. 2014. Green biosynthesis and characterization of zinc oxide nanoparticles using brown marine macroalga *Sargassum muticum* aqueous extract. *Materials Letters*. 116:275–277.

de Baat, C., Zweers, P.G.M.A., van Loveren, C. & Vissink, A. 2017. Medicaments and oral healthcare 5. Adverse effects of -medications and over-the-counter drugs on teeth. *Nederlands Tijdschrift voor Tandheelkunde*. 123(10):485–491.

Badiane, A.S., Ndiaye, D. & Denning, D.W. 2015. Burden of fungal infections in Senegal. *Mycoses*. 58:63–69.

Bakri, M.M., Hussaini, H.M., Holmes, A., Cannon, R.D. & Rich, A.M. 2010. Revisiting the association between candidal infection and carcinoma, particularly oral squamous cell carcinoma. *Journal of Oral Microbiology*. 2(2010):10.

Balouiri, M., Sadiki, M. & Ibnsouda, S.K. 2016. Methods for *in vitro* evaluating antimicrobial activity: A review. *Journal of Pharmaceutical Analysis*. 6(2):71–79.

Bandara, H.M.H.N., Matsubara, V.H. & Samaranayake, L.P. 2017. Future therapies targeted towards eliminating Candida biofilms and associated infections. *Expert Review of Anti-Infective Therapy*. 15(3):299–318.

Bandeira, M., Giovanela, M., Roesch-Ely, M., Devine, D.M. & da Silva Crespo, J. 2020. Green synthesis of zinc oxide nanoparticles: A review of the synthesis methodology and mechanism of formation. *Sustainable Chemistry and Pharmacy*. 15:100223.

Benelli, G. 2019. Green synthesis of nanomaterials. *Nanomaterials(Basel)*. 9(9):1275.

Bankar, A., Joshi, B., Kumar, A.R. & Zinjarde, S. 2010a. Banana peel extract mediated novel route for the synthesis of palladium nanoparticles. *Materials Letters*. 64(18):1951–1953.

Bankar, A., Joshi, B., Kumar, A.R. & Zinjarde, S. 2010b. Banana peel extract mediated novel route for the synthesis of silver nanoparticles. *Colloids and Surfaces A: Physicochemical and Engineering Aspects*. 368(1–3):58–63.

Bankar, A., Joshi, B., Ravi Kumar, A. & Zinjarde, S. 2010c. Banana peel extract mediated synthesis of gold nanoparticles. *Colloids and Surfaces B: Biointerfaces*. 80(1):45–50.

Baptista, P. V., McCusker, M.P., Carvalho, A., Ferreira, D.A., Mohan, N.M., Martins, M. & Fernandes, A.R. 2018. Nano-strategies to fight multidrug resistant bacteria-"A Battle of the Titans". *Frontiers in Microbiology*. 9:1441.

Baranwal, A., Mahato, K., Srivastava, A., Maurya, P.K. & Chandra, P. 2016. Phytofabricated metallic nanoparticles and their clinical applications. *RSC Advances*. 6 (107)105996–106010.

de Barros, P.P., Rossoni, R.D., de Souza, C.M., Scorzoni, L., Fenley, J.D.C. & Junqueira, J.C. 2020. Candida Biofilms: An Update on Developmental Mechanisms and Therapeutic Challenges. *Mycopathologia*. 185(3):415–424.

Basnet, P., Inakhunbi Chanu, T., Samanta, D. & Chatterjee, S. 2018. A review on bio-synthesized zinc oxide nanoparticles using plant extracts as reductants and stabilizing agents. *Journal of Photochemistry and Photobiology B: Biology*. 183:201–221.

Bates, C.H., White, W.B. & Roy, R. 1962. New High-Pressure Polymorph of Zinc Oxide. *Science*. 137(3534):993–993.

Benoit, D.S.W., Sims, K.R. & Fraser, D. 2019. Nanoparticles for Oral Biofilm Treatments. *ACS Nano*. 13(5):4869–4875.

Bescos, R., Ashworth, A., Cutler, C., Brookes, Z.L., Belfield, L., Rodiles, A., Casas-Agustench, P., Farnham, G., Liddle, L., Burleigh, M., White, D., Easton, C. & Hickson, M. 2020. Effects of Chlorhexidine mouthwash on the oral microbiome. *Scientific Reports*. 10(1):5254.

Berman, J. & Sudbery, P.E. 2002. *Candida albicans*: A molecular revolution built on lessons from budding yeast. *Nature Reviews Genetics*. 3:918–930.

Berkow, E.L., Lockhart, S.R. & Ostrosky-Zeichner, L. 2020. Antifungal Susceptibility Testing: Current Approaches. *Clinical Microbiology Reviews*. 33(3).

Bertoglio, F., Bloise, N., Oriano, M., Petrini, P., Sprio, S., Imbriani, M., Tampieri, A. & Visai, L. 2018. Treatment of biofilm communities: An update on new tools from the nanosized world. *Applied Sciences (Switzerland)*. 8(6):845.

Bertolini, M. & Dongari-Bagtzoglou, A. 2019. The Relationship of Candida albicans with the Oral Bacterial Microbiome in Health and Disease. *Advances in Experimental Medicine and Biology*. Springer. 1197:69–78.

Bertolini, M., Ranjan, A., Thompson, A., Diaz, P.I., Sobue, T., Maas, K. & Dongari-Bagtzoglou, A. 2019. *Candida albicans* induces mucosal bacterial dysbiosis that promotes invasive infection. *PLoS Pathogens*. 15(4).

Bhavikatti, S.K., Bhardwaj, S. & Prabhuji, M.L.V. 2014. Current applications of nanotechnology in dentistry: A review. *General Dentistry*. 62(4):72–77.

Bhuyan, T., Mishra, K., Khanuja, M., Prasad, R. & Varma, A. 2015. Biosynthesis of zinc oxide nanoparticles from *Azadirachta indica* for antibacterial and photocatalytic applications. *Materials Science in Semiconductor Processing*. 32:55–61.

Bianchi, C.M.P. de C., Bianchi, H.A., Tadano, T., Depaula, C.R., Hoffmann-Santos, H.D., Leite, D.P. & Hahn, R.C. 2016. Factors related to oral candidiasis in elderly users and non-users of removable dental prostheses. *Revista do Instituto de Medicina Tropical de Sao Paulo*. 58:17.

Biofilm Eradication Testing for Antimicrobial Efficacy. 2019. [Online], Available: https://emerypharma.com/biology/biofilm-eradication/ [Accessed: 2020, April 07].

Blignaut, E. 2017. Candidiasis - has anything changed in the way we manage these patients? *South African Dental Journal*. 72(8):355–359.

Bongomin, F., Gago, S., Oladele, R.O. & Denning, D.W. 2017. Global and multi-national prevalence of fungal diseases—estimate precision. *Journal of Fungi*. 3(4):57.

Borges, C.V., Belin, M.A.F., Amorim, E.P., Minatel, I.O., Monteiro, G.C., Gomez Gomez, H.A., Monar, G.R.S. & Lima, G.P.P. 2019. Bioactive amines changes during the ripening and thermal processes of bananas and plantains. *Food Chemistry*. 298:125020.

vanden Bossche, H., Dromer, F., Improvisi, I., Lozano-Chiu, M., Rex, J.H. & Sanglard, D. 1998. Antifungal drug resistance in pathogenic fungi. *Journal of Medical and Veterinary Mycology*. 3:119–128.

Bragg, W.L. & Darbyshire, J.A. 1932. The structure of thin films of certain metallic oxides. *Transactions of the Faraday Society*. 28(0):522–529.

Bramhanwade, K., Shende, S., Bonde, S., Gade, A. & Rai, M. 2016. Fungicidal activity of Cu nanoparticles against *Fusarium* causing crop diseases. *Environmental Chemistry Letters*. 14(2):229–235.

Brandão, N.L., Portela, M.B., Maia, L.C., Antônio, A., e Silva, V.L.M. & da Silva, E.M. 2018. Model resin composites incorporating ZnO-NPs: Activity against *S. mutans* and physicochemical properties characterization. *Journal of Applied Oral Science*. 26:1–10.

Budtz-Jørgensen, E. 1981. Oral mucosal lesions associated with the wearing of removable dentures. *Journal of Oral Pathology & Medicine*. 10(2):65–80.

Bueno, M., Urban, V., Barbério, G., da Silva, W., Porto, V., Pinto, L. & Neppelenbroek, K.H. 2015. Effect of antimicrobial agents incorporated into resilient denture relines on the *Candida albicans* biofilm. *Oral Diseases*. 21(1):57–65.

Bueno, M.G., Bonassa De Sousa, E.J., Hotta, J., Porto, V.C., Urban, V.M. & Neppelenbroek, K.H. 2017. Surface Properties of Temporary Soft Liners Modified by Minimum Inhibitory Concentrations of Antifungals. *Brazilian Dental Journal*. 28(2):158–164.

Bujdáková, H. 2016. Management of Candida biofilms: State of knowledge and new options for prevention and eradication. *Future Microbiology*. 11(2):235–251.

Busi, S. & Paramanantham, P. 2018. Metal and metal oxide mycogenic nanoparticles and their application as antimicrobial and antibiofilm agents. Prasad, R., Kumar, V., Kumar, M., Wang, S. (eds.), *Fungal Nanobionics: Principles and Applications*. Springer Singapore: 243–271.

Calderone, R.A. & Fonzi, W.A. 2001. Virulence factors of *Candida albicans*. *Trends in Microbiology*. 9(7):327–335.

Camarda, P., Messina, F., Vaccaro, L., Agnello, S., Buscarino, G., Schneider, R., Popescu, R., Gerthsen, D., Lorenzi, R., Gelardi, F. M. & Cannas, M. 2016. Luminescence mechanisms of defective ZnO nanoparticles. *Physical Chemistry Chemical Physics*. 18(24):16237–16244.

Cardona, A., Balouch, A., Abdul, M.M., Sedghizadeh, P.P. & Enciso, R. 2017. Efficacy of chlorhexidine for the prevention and treatment of oral mucositis in cancer patients: a systematic review with meta-analyses. *Journal of Oral Pathology & Medicine*. 46(9):680–688.

Carrouel, F., Viennot, S., Ottolenghi, L., Gaillard, C. & Bourgeois, D. 2020. Nanoparticles as anti-microbial, anti-inflammatory, and remineralizing agents in oral care cosmetics: A review of the current situation. *Nanomaterials*. 10 (1):140.

Castillo, H.A.P., Castellanos, L.N.M., Rigoberto, M.C., Martínez, R.R. & Borunda, E.O. 2019. Nanoparticles as New Therapeutic Agents against Candida albicans. Sandai, D. (ed.), *Candida Albicans*. InTechOpen:145–171.

Cavalheiro, M. & Teixeira, M.C. 2018. Candida Biofilms: Threats, challenges, and promising strategies. Frontiers in Medicine 5:28.

Černáková, L., Light, C., Salehi, B., Rogel-Castillo, C., Victoriano, M., Martorell, M., Sharifi-Rad, J., Martins, N., *et al.* 2019. Novel Therapies for Biofilm-Based Candida spp. Infections. *Advances in Experimental Medicine and Biology*. 1214:93–123.

Chandra, J., Mukherjee, P.K. & Ghannoum, M.A. 2008. *In vitro* growth and analysis of *Candida* biofilms. *Nature Protocols*. 3(12):1909–1924.

Chattopadhyay, I., Verma, M. & Panda, M. 2019. Role of Oral Microbiome Signatures in Diagnosis and Prognosis of Oral Cancer. *Technology in cancer research & treatment*. 18:1533033819867354.

Chaudhuri, S.K. & Malodia, L. 2017. Biosynthesis of zinc oxide nanoparticles using leaf extract of calotropis gigantea: Characterization and its evaluation on tree seedling growth in nursery stage. *Applied Nanoscience (Switzerland)*. 7(8):501–512.

Chavali, M.S. & Nikolova, M.P. 2019. Metal oxide nanoparticles and their applications in nanotechnology. *SN Applied Sciences*. 1:607.

Cheesman, M.J., Ilanko, A., Blonk, B. & Cock, I.E. 2017. Developing new antimicrobial therapies: Are synergistic combinations of plant extracts/compounds with conventional antibiotics the solution? *Pharmacognosy Reviews*. 11 (22):57–72.

Chen, L., Batjikh, I., Hurh, J., Han, Y., Huo, Y., Ali, H., Li, J.F., Rupa, E.J., *et al.* 2019. Green synthesis of zinc oxide nanoparticles from root extract of Scutellaria baicalensis and its photocatalytic degradation activity using methylene blue. *Optik*. 184:324–329.

Chiguvare, H. 2015. Phytochemical analyses, synthesis of silver nanoparticles from Filipendula ulmaria (L.) Maxin and Agathosma betulina (Berg.) Pillans and their bioassays. Available: http://libdspace.ufh.ac.za/handle/20.500.11837/443.

Chiguvare, H., Oyedeji, O.O., Matewu, R., Aremu, O., Oyemitan, I.A., Oyedeji, A.O., Nkeh-Chungag, B.N., Songca, S.P., *et al.* 2016. Synthesis of silver nanoparticles using buchu plant extracts and their analgesic properties. *Molecules*. 21(6):774.

Christensen, G.D., Simpson, W.A., Younger, J.J., Baddour, L.M., Barrett, F.F., Melton, D.M. & Beachey, E.H. 1985. Adherence of coagulase-negative staphylococci to plastic tissue

culture plates: A quantitative model for the adherence of staphylococci to medical devices. *Journal of Clinical Microbiology*. 22(6):996–1006.

Cierech, M., Wojnarowicz, J., Szmigiel, D., Bączkowski, B., Grudniak, A.M., Wolska, K.I., Łojkowski, W. & Mierzwińska-Nastalska, E. 2016b. Preparation and characterization of ZnO-PMMA resin nanocomposites for denture bases. *Acta of Bioengineering and Biomechanics*. 18(2):31-41.

Cierech, M., Kolenda, A., Grudniak, A.M., Wojnarowicz, J., Woźniak, B., Gołaś, M., Swoboda-Kopeć, E., Łojkowski, W., *et al.* 2016a. Significance of polymethylmethacrylate (PMMA) modification by zinc oxide nanoparticles for fungal biofilm formation. *International Journal of Pharmaceutics*. 510(1):323–335.

Cierech, M., Osica, I., Kolenda, A., Wojnarowicz, J., Szmigiel, D., Łojkowski, W., Kurzydłowski, K., Ariga, K., *et al.* 2018. Mechanical and physicochemical properties of newly formed ZnO-PMMA nanocomposites for denture bases. *Nanomaterials*. 8(5):1–13.

Cierech, M., Wojnarowicz, J., Kolenda, A., Krawczyk-Balska, A., Prochwicz, E., Woźniak, B., Łojkowski, W. & Mierzwińska-Nastalska, E. 2019. Zinc oxide nanoparticles cytotoxicity and release from newly formed PMMA–ZNO nanocomposites designed for denture bases. *Nanomaterials*. 9(9).

Contaldo, M., Romano, A., Mascitti, M., Fiori, F., Della Vella, F., Serpico, R. & Santarelli, A. 2019. Association between denture stomatitis, candida species and diabetic status. *Journal of biological regulators and homeostatic agents*. 33(3):35–41.

Coogan, M.M., Greenspan, J. & Challacombe, S.J. 2005. Oral lesions in infection with human immunodeficiency virus. *Bulletin of the World Health Organization*. 83:700–706.

Crozier, A., Jaganath, I.B. & Clifford, M.N. 2009. Dietary phenolics: Chemistry, bioavailability and effects on health. *Natural Product Reports*. 26(8):1001–1043.

Cuéllar-Cruz, M., Vega-González, A., Mendoza-Novelo, B., López-Romero, E., Ruiz-Baca, E., Quintanar-Escorza, M.A. & Villagómez-Castro, J.C. 2012. The effect of biomaterials and antifungals on biofilm formation by Candida species: A review. *European Journal of Clinical Microbiology and Infectious Diseases*. 31(10):2513–2527.

Cutler, J.E. 1991. *Putative Virulence Factors of Candida albicans*. [Online], Available: www.annualreviews.org [Accessed: 2020, April 23].

Dadar, M., Tiwari, R., Karthik, K., Chakraborty, S., Shahali, Y. & Dhama, K. 2018. *Candida albicans* - Biology, molecular characterization, pathogenicity, and advances in diagnosis and control – An update. *Microbial Pathogenesis*. 117:128–138.

Debanath, M.K. & Karmakar, S. 2013. Study of blueshift of optical band gap in zinc oxide (ZnO) nanoparticles prepared by low-temperature wet chemical method. *Materials Letters*. 111:116–119.

Deo, P.N. & Deshmukh, R. 2019. Oral microbiome: Unveiling the fundamentals. *Journal of Oral and Maxillofacial Pathology*. 23(1):122–128.

Dhanemozhi, A.C., Rajeswari, V. & Sathyajothi, S. 2017. Green Synthesis of Zinc Oxide Nanoparticle Using Green Tea Leaf Extract for Supercapacitor Application. *Materials Today: Proceedings*. 4(2):660–667.

Dhillon, G.S., Kaur, S. & Brar, S.K. 2014. Facile fabrication and characterization of chitosan-based zinc oxide nanoparticles and evaluation of their antimicrobial and antibiofilm activity. *International Nano Letters*. 4(2):1–11.

Diallo, A., Ngom, B.D., Park, E. & Maaza, M. 2015. Green synthesis of ZnO nanoparticles by Aspalathus linearis: Structural & optical properties. *Journal of Alloys and Compounds*. 646:425–430.

Dias, H.B., Bernardi, M.I.B., Marangoni, V.S., de Abreu Bernardi, A.C., de Souza Rastelli, A.N. & Hernandes, A.C. 2019. Synthesis, characterization and application of Ag doped ZnO nanoparticles in a composite resin. *Materials Science and Engineering C*. 96:391–401.

Dizaj, S.M., Lotfipour, F., Barzegar-Jalali, M., Zarrintan, M.H. & Adibkia, K. 2014. Antimicrobial activity of the metals and metal oxide nanoparticles. Materials Science and Engineering C 44 p.278–284.

Djurišić, A.B., Leung, Y.H., Tam, K.H., Ding, L., Ge, W.K., Chen, H.Y. & Gwo, S. 2006. Green, yellow, and orange defect emission from ZnO nanostructures: Influence of excitation wavelength. *Applied Physics Letter*. 88:103107.

Dube, P., Meyer, S. & Marnewick, J.L. 2017. Antimicrobial and antioxidant activities of different solvent extracts from fermented and green honeybush (Cyclopia intermedia) plant material. *South African Journal of Botany*. 110:184–193.

Dunaiski, C.M. & Denning, D.W. 2019. Estimated burden of fungal infections in Namibia. *Journal of Fungi*. 5(3):75.

Elhissi, A. & Subbiah, U. 2019. Chapter 1 – Introduction to nanotechnology. Karthikeyan Subramani, K., Ahmed, W. (eds.), *Nanobiomaterials in Clinical Dentistry (2nd edition)*. Elsevier Inc.:3–18.

Ellepola, A.N.B. & Samaranayake, L.P. 2007. The in vitro post-antifungal effect of nystatin on Candida species of oral origin. *Journal of Oral Pathology & Medicine*. 28(3):112–116.

Elumalai, K. & Velmurugan, S. 2015. Green synthesis, characterization and antimicrobial activities of zinc oxide nanoparticles from the leaf extract of *Azadirachta indica (L.)*. *Applied Surface Science*. 345:329–336.

Elumalai, K., Velmurugan, S., Ravi, S., Kathiravan, V. & Adaikala Raj, G. 2015. Bio-approach: Plant mediated synthesis of ZnO nanoparticles and their catalytic reduction of methylene blue and antimicrobial activity. *Advanced Powder Technology*. 26(6):1639–1651.

Emami, E., Kabawat, M., Rompre, P.H. & Feine, J.S. 2014. Linking evidence to treatment for denture stomatitis: A meta-analysis of randomized controlled trials. *Journal of Dentistry*. 42(2):99–106.

Emami, E., Taraf, H., de Grandmont, P., Gauthier, G., de Koninck, L., Lamarche, C. & de Souza, R.F. 2017. The association of denture stomatitis and partial removable dental prostheses: a systematic review. *The International journal of prosthodontics*. 25(2):113–9.

Eshed, M., Lellouche, J., Matalon, S., Gedanken, A. & Banin, E. 2012. Sonochemical coatings of ZnO and CuO nanoparticles inhibit S*treptococcus mutans* biofilm formation on teeth model. *Langmuir*. 28(33):12288–12295.

Espitia, P.J.P., Otoni, C.G. & Soares, N.F.F. 2016. Zinc Oxide Nanoparticles for Food Packaging Applications. in *Antimicrobial Food Packaging* Elsevier Inc. 425–431.

Faini, D., Maokola, W., Furrer, H., Hatz, C., Battegay, M., Tanner, M., Denning, D.W. & Letang, E. 2015. Burden of serious fungal infections in Tanzania. *Mycoses*. 58:70–79.

Fakhari, S., Jamzad, M. & Kabiri Fard, H. 2019. Green synthesis of zinc oxide nanoparticles: a comparison. *Green Chemistry Letters and Reviews*. 12(1):19–24.

Fang, J., Huang, B. & Ding, Z. 2020. Efficacy of antifungal drugs in the treatment of oral candidiasis: A Bayesian network meta-analysis. *Journal of Prosthetic Dentistry*. S0022-3913(20)30076–7.

Fang, K., Park, O.J. & Hong, S.H. 2020. Controlling biofilms using synthetic biology approaches. *Biotechnology Advances*. 40(2020):107518.

Felipe, L. de O., Júnior, W.F. da S., Araújo, K.C. de & Fabrino, D.L. 2018. *Lactoferrin, chitosan* and *Melaleuca alternifolia*—natural products that show promise in candidiasis treatment. *Brazilian Journal of Microbiology*. 49(2):212–219.

Ferrando-Magraner, E., Bellot-arcís, C., Paredes-gallardo, V., Almerich-silla, J.M., García-sanz, V., Fernández-alonso, M. & Montiel-company, J.M. 2020. Antibacterial properties of nanoparticles in dental restorative materials. A systematic review and meta-analysis. *Medicina (Lithuania)*. 56(2):1-22

Ficai, A., Ficai, D., Andronescu, E., Yetmez, M., Ozkalayci, N., Agrali, O.B., Sahin, Y.M., Gunduz, O., *et al*. 2016. Grumezescu, A. (ed.), Nanobiomaterials in Dentistry: Applications of Nanobiomaterials. *Nanotechnology in dentistry*. Elsevier Inc:11.187–210.

Fidel, P.L., Yano, J., Esher, S.K. & Noverr, M.C. 2020. Applying the host-microbe damage response framework to candida pathogenesis: Current and prospective strategies to reduce damage. *Journal of Fungi(Basel)*. 6(1):1-26.

Fierascu, I., Fierascu, I.C., Brazdis, R.I., Baroi, A.M., Fistos, T. & Fierascu, R.C. 2020. Phytosynthesized metallic nanoparticles-between nanomedicine and toxicology. A brief review of 2019's findings. *Materials*. 13(3):574.

Fierascu, R.C., Ortan, A., Avramescu, S.M. & Fierascu, I. 2019. Phyto-nanocatalysts: Green synthesis characterization, and applications. *Molecules*. 24(19):3418.

Fiorillo, L. 2019. Chlorhexidine Gel Use in the Oral District: A Systematic Review. *Gels (Basel, Switzerland)*. 5(2):31.

Fisher, M.C., Henk, D.A., Briggs, C.J., Brownstein, J.S., Madoff, L.C., McCraw, S.L. & Gurr, S.J. 2012. Emerging fungal threats to animal, plant and ecosystem health. *Nature*. 484(7393):186–194.

Fourie, J., Khammissa, R.A.G., Ballyram, R., Wood, N.H., Lemmer, J. & Feller, L. 2016. Oral candidosis: an update on diagnosis, aetiopathogenesis and management. *South African Dental Journal*. 71(7):314–318.

Frederickson, C.J., Koh, J.Y. & Bush, A.I. 2005. The neurobiology of zinc in health and disease. *Nature Reviews Neuroscience*. 6(6):449–462.

FTIR Spectrometer PerkinElmer Frontier | External Services | CIC nanoGUNE. Available from: https://externalservices.nanogune.eu/equipment/ftir-spectrometer-perkinelmer-frontier.

Fu, L. & Fu, Z. 2015. Plectranthus amboinicus leaf extract-assisted biosynthesis of ZnO nanoparticles and their photocatalytic activity. *Ceramics International*. 41(2):2492–2496.

Gad, M., Rahoma, A., Al-Thobity, A.M. & ArRejaie, A. 2016. Influence of incorporation of ZrO_2 nanoparticles on the repair strength of polymethyl methacrylate denture bases. *International Journal of Nanomedicine*. 11:5633–5643.

Ganesh, M., Lee, S.G., Jayaprakash, J., Mohankumar, M. & Jang, H.T. 2019. Hydnocarpus alpina Wt extract mediated green synthesis of ZnO nanoparticle and screening of its anti-microbial, free radical scavenging, and photocatalytic activity. *Biocatalysis and Agricultural Biotechnology*. 19:101129.

Garaicoa, J.L., Fischer, C.L., Bates, A.M., Holloway, J., Avila-Ortiz, G., Guthmiller, J.M., Johnson, G.K., Stanford, C., *et al.* 2018. Promise of Combining Antifungal Agents in Denture Adhesives to Fight Candida Species Infections. *Journal of Prosthodontics*. 27(8):755–762.

Garcia, P.P.N.S., Cardia, M.F.B., Francisconi, R.S., Dovigo, L.N., Spolidório, D.M.P., de Souza Rastelli, A.N. & Botta, A.C. 2017. Antibacterial activity of glass ionomer cement modified by zinc oxide nanoparticles. *Microscopy Research and Technique*. 80(5):456–461.

Garcia-Solache, M.A. & Casadevall, A. 2010. Global warming will bring new fungal diseases for mammals. *mBio*. 1(1) e00061–10.

Geetha, M.S., Nagabhushana, H. & Shivananjaiah, H.N. 2016. Green mediated synthesis and characterization of ZnO nanoparticles using Euphorbia Jatropa latex as reducing agent. *Journal of Science: Advanced Materials and Devices*. 1(3):301–310.

Gendreau, L. & Loewy, Z.G. 2011. Epidemiology and Etiology of Denture Stomatitis. *Journal of Prosthodontics*. 20(4):251–260.

Gharpure, S., Akash, A. & Ankamwar, B. 2019. A Review on Antimicrobial Properties of Metal Nanoparticles. *Journal of Nanoscience and Nanotechnology*. 20(6):3303–3339.

Gholizadeh, P., Eslami, H., Yousefi, M., Asgharzadeh, M., Aghazadeh, M. & Kafil, H.S. 2016. Role of oral microbiome on oral cancers, a review. *Biomedicine and Pharmacotherapy*. 84:552–558.

Girardot, M. & Imbert, C. 2016a. Novel strategies against Candida biofilms: Interest of synthetic compounds. *Future Microbiology*. 11(1):69–79.

Girardot, M. & Imbert, C. 2016b. Natural sources as innovative solutions against fungal biofilms. Donelli, G. (ed.), *Advances in Experimental Medicine and Biology*. Springer New York LLC: (931)105–125.

Goh, E.G., Xu, X. & McCormick, P.G. 2014. Effect of particle size on the UV absorbance of zinc oxide nanoparticles. *Scripta Materialia*. 78–79:49–52.

Griffiths, P.R. & De Haseth, J.A. 2006. *Fourier Transform Infrared Spectrometry: Second Edition*. Wiley:1–535.

Guinea, J. 2014. Global trends in the distribution of Candida species causing candidemia. *Clinical Microbiology and Infection*. 20:5–10.

Gulati, M., Lohse, M.B., Ennis, C.L., Gonzalez, R.E., Perry, A.M., Bapat, P., Arevalo, A.V., Rodriguez, D.L., *et al.* 2018. *In Vitro* Culturing and Screening of *Candida albicans* Biofilms. *Current Protocols in Microbiology*. 50(1):1–62.

Gunalan, S., Sivaraj, R. & Rajendran, V. 2012. Green synthesized ZnO nanoparticles against bacterial and fungal pathogens. *Progress in Natural Science: Materials International*. 22(6):693–700.

GuNPsuth, U.F., Le, H., Besinis, A., Tredwin, C. & Handy, R.D. 2019. Multilayered composite coatings of titanium dioxide nanotubes decorated with zinc oxide and hydroxyapatite

nanoparticles: Controlled release of Zn and antimicrobial properties against *Staphylococcus aureus. International Journal of Nanomedicine*. 14:3583–3600.

Gunsolley, J.C. 2010. Clinical efficacy of antimicrobial mouthrinses. *Journal of Dentistry*. 38(1):S6.

Gupta, M., Tomar, R.S., Kaushik, S., Mishra, R.K. & Sharma, D. 2018. Effective Antimicrobial Activity of Green ZnO Nano Particles of *Catharanthus roseus*. *Frontiers in Microbiology*. 9(SEP):2030.

Gutiérrez-Venegas, G., Gómez-Mora, J.A., Meraz-Rodríguez, M.A., Flores-Sánchez, M.A. & Ortiz-Miranda, L.F. 2019. Effect of flavonoids on antimicrobial activity of microorganisms present in dental plaque. *Heliyon*. 5(12):e03013.

Gutiérrez, M.F., Bermudez, J., Dávila-Sánchez, A., Alegría-Acevedo, L.F., Méndez-Bauer, L., Hernández, M., Astorga, J., Reis, A., *et al.* 2019. Zinc oxide and copper nanoparticles addition in universal adhesive systems improve interface stability on caries-affected dentin. *Journal of the Mechanical Behavior of Biomedical Materials*. 100(March):103366.

Guto, J.A., Bii, C.C. & Denning, D.W. 2016. Estimated burden of fungal infections in Kenya. *Journal of Infection in Developing Countries*. 10(8):777–784.

Halamoda-Kenzaoui, B., Ceridono, M., Urbán, P., Bogni, A., Ponti, J., Gioria, S. & Kinsner-Ovaskainen, A. 2017. The agglomeration state of nanoparticles can influence the mechanism of their cellular internalisation. *Journal of Nanobiotechnology*. 15(1):48.

Halbandge, S.D., Jadhav, A.K., Jangid, P.M., Shelar, A. V., Patil, R.H. & Karuppayil, S.M. 2019. Molecular targets of biofabricated silver nanoparticles in *Candida albicans*. *Journal of Antibiotics*. 72(8):640–644.

Halioua, B. & Ziskind, B. 2005. *Medicine in the days of the pharaohs*. Belknap Press of Harvard University Press.

Haney, E.F., Trimble, M.J., Cheng, J.T., Vallé, Q. & Hancock, R.E.W. 2018. Critical assessment of methods to quantify biofilm growth and evaluate antibiofilm activity of host defence peptides. *Biomolecules*. 8(2):29.

Happy, A., Soumya, M., Venkat Kumar, S., Rajeshkumar, S., Sheba Rani, N.D., Lakshmi, T. & Deepak Nallaswamy, V. 2019. Phyto-assisted synthesis of zinc oxide nanoparticles using *Cassia alata* and its antibacterial activity against *Escherichia coli*. *Biochemistry and Biophysics Reports*. 17:208–211.

He, L., Liu, Y., Mustapha, A. & Lin, M. 2011. Antifungal activity of zinc oxide nanoparticles against *Botrytis cinerea* and *Penicillium expansum*. *Microbiological Research*. 166(3):207–215.

Heinz, H., Pramanik, C., Heinz, O., Ding, Y., Mishra, R.K., Marchon, D., Flatt, R.J., Estrela-Lopis, I., *et al.* 2017. Nanoparticle decoration with surfactants: Molecular interactions, assembly, and applications. *Surface Science Reports*. 72(1):1–58.

Hellstein, J.W. & Marek, C.L. 2019. Candidiasis: Red and White Manifestations in the Oral Cavity. *Head and Neck Pathology*. 13(1):25–32.

Heng, B.C., Zhao, X., Tan, E.C., Khamis, N., Assodani, A., Xiong, S., Ruedl, C., Ng, K.W., *et al.* 2011. Evaluation of the cytotoxic and inflammatory potential of differentially shaped zinc oxide nanoparticles. *Archives of Toxicology*. 85(12):1517–1528.

Holgate, S.T. 2010. Exposure, uptake, distribution and toxicity of nanomaterials in humans. *Journal of Biomedical Nanotechnology*. 6(1):1–19.

Holt, J.E., Houston, A., Adams, C., Edwards, S. & Kjellerup, B. V. 2017. Role of extracellular polymeric substances in polymicrobial biofilm infections of *Staphylococcus epidermidis* and *Candida albicans* modelled in the nematode *Caenorhabditis elegans*. *Pathogens and Disease*. 75(5): ftx052.

Hong, N.H. 2018. Introduction to Nanomaterials: Basic Properties, Synthesis, and Characterization. *Nano-sized Multifunctional Materials: Synthesis, Properties and Applications.* Elsevier Inc:1–19.

Hornyak, G.L., Moore, J.J., Tibbals, H.F. & Dutta, J. 2018. *Fundamentals of Nanotechnology*. CRC Press.

Hoseinzadeh, E., Makhdoumi, P., Taha, P., Hossini, H., Stelling, J., Amjad Kamal, M. & Md. Ashraf, G. 2017. A Review on Nano-Antimicrobials: Metal Nanoparticles, Methods and Mechanisms. *Current Drug Metabolism*. 18(2):120–128.

Hoshyar, N., Gray, S., Han, H. & Bao, G. 2016. The effect of nanoparticle size on in vivo pharmacokinetics and cellular interaction. *Nanomedicine*. 11(6):673–692.

Hu, C., Wang, L.L., Lin, Y.Q., Liang, H.M., Zhou, S.Y., Zheng, F., Feng, X.L., Rui, Y.Y. & Shao, L. Q. 2019. Nanoparticles for the Treatment of Oral Biofilms: Current State, Mechanisms, Influencing Factors, and Prospects. *Advanced Healthcare Materials*. 8(24):1901301.

Hübsch, Z., Van Vuuren, S.F. & Van Zyl, R.L. 2014a. Can rooibos (*Aspalathus linearis*) tea have an effect on conventional antimicrobial therapies? *South African Journal of Botany*. 93:148–156.

Hübsch, Z., Van Zyl, R.L., Cock, I.E. & Van Vuuren, S.F. 2014b. Interactive antimicrobial and toxicity profiles of conventional antimicrobials with Southern African medicinal plants. *South African Journal of Botany*. 93:185–197.

Husen, A. 2019. Natural Product-Based Fabrication of Zinc-Oxide Nanoparticles and Their Applications. Husen, A., Iqbal, M. (eds.), *Nanomaterials and Plant Potential.* Springer International Publishing: 193–219.

Husen, A. & Iqbal, M. 2019. Nanomaterials and Plant Potential: An Overview. Husen, A., Iqbal, M. (eds.) *Nanomaterials and Plant Potential* Springer International Publishing: 3–29.

Husen, A. & Siddiqi, K.S. 2014. Phytosynthesis of nanoparticles: Concept, controversy and application. *Nanoscale Research Letters*. 9(1):1–24.

Hussein, J., El Naggar, M.E., Latif, Y.A., Medhat, D., El Bana, M., Refaat, E. & Morsy, S. 2018. Solvent-free and one pot synthesis of silver and zinc nanoparticles: Activity toward cell membrane component and insulin signalling pathway in experimental diabetes. *Colloids and Surfaces B: Biointerfaces*. 170:76–84.

Huttenhower, C., Gevers, D., Knight, R., Abubucker, S., Badger, J.H., Chinwalla, A.T., Creasy, H.H., Earl, A.M., *et al.* 2012. Structure, function and diversity of the healthy human microbiome. *Nature*. 486(7402):207–214

Ibrahim, H.M.M. 2015. Green synthesis and characterization of silver nanoparticles using banana peel extract and their antimicrobial activity against representative microorganisms. *Journal of Radiation Research and Applied Sciences*. 8(3):265–275.

Inkson, B.J. 2016. Scanning Electron Microscopy (SEM) and Transmission Electron Microscopy (TEM) for Materials Characterization. in *Materials Characterization Using Nondestructive Evaluation (NDE) Methods* Elsevier Inc. 17–43.

Institute of Medicine (US) Food Forum, Washington (DC). 2009. Safety and Efficacy of Nanomaterials in Food Products. in *Nanotechnology in Food Products: Workshop Summary*.

Iqbal, Z. & Zafar, M.S. 2016. Role of antifungal medicaments added to tissue conditioners: A systematic review. *Journal of Prosthodontic Research*. 60(4):231–239.

Iqbal, J., Abbasi, B.A., Mahmood, T., Kanwal, S., Ahmad, R. & Ashraf, M. 2019. Plant-extract mediated green approach for the synthesis of ZnONPs: Characterization and evaluation of cytotoxic, antimicrobial and antioxidant potentials. *Journal of Molecular Structure*. 1189:315–327.

Ishwarya, R., Vaseeharan, B., Kalyani, S., Banumathi, B., Govindarajan, M., Alharbi, N.S., Kadaikunnan, S., Al-anbr, M.N., et al. 2018. Facile green synthesis of zinc oxide nanoparticles using *Ulva lactuca* seaweed extract and evaluation of their photocatalytic, antibiofilm and insecticidal activity. *Journal of Photochemistry and Photobiology B: Biology*. 178:249–258.

Iwu, M.M. 2016. Food as medicine: Functional food plants of Africa. CRC Press.

Jabra-Rizk, M.A., Falkler, W.A. & Meiller, T.F. 2004. Fungal Biofilms and Drug Resistance. *Emerging Infectious Diseases*. 10(1):14–19.

Jacobsen, I.D., Wilson, D., Wächtler, B., Brunke, S., Naglik, J.R. & Hube, B. 2012. *Candida albicans* dimorphism as a therapeutic target. *Expert Review of Anti-infective Therapy*. 10(1):85–93.

Jalal, M., Ansari, M.A., Ali, S.G., Khan, H.M. & Rehman, S. 2018. Anticandidal activity of bioinspired ZnO NPs: effect on growth, cell morphology and key virulence attributes of Candida species. *Artificial Cells, Nanomedicine and Biotechnology*. 46(sup1):912–925.

Jamdagni, P., Khatri, P. & Rana, J.S. 2018. Green synthesis of zinc oxide nanoparticles using flower extract of Nyctanthes arbor-tristis and their antifungal activity. *Journal of King Saud University - Science*. 30(2):168–175.

James, P., Worthington, H. V, Parnell, C., Harding, M., Lamont, T., Cheung, A., Whelton, H. & Riley, P. 2017. Chlorhexidine mouthrinse as an adjunctive treatment for gingival health. *Cochrane Database of Systematic Reviews*. 3:CD008676.

Janaki, A.C., Sailatha, E. & Gunasekaran, S. 2015. Synthesis, characteristics and antimicrobial activity of ZnO nanoparticles. *Spectrochimica Acta - Part A: Molecular and Biomolecular Spectroscopy*. 144:17–22.

Janotti, A. & Van De Walle, C.G. 2009. Fundamentals of zinc oxide as a semiconductor. *Reports on Progress in Physics*. 72:126501.

Jansen, J., Karges, W. & Rink, L. 2009. Zinc and diabetes - clinical links and molecular mechanisms. *Journal of Nutritional Biochemistry*. 20(6):399–417.

Janus, M.M., Crielaard, W., Volgenant, C.M.C., der Veen, M.H. va., Brandt, B.W. & Krom, B.P. 2017. *Candida albicans* alters the bacterial microbiome of early *in vitro* oral biofilms. *Journal of Oral Microbiology*. 9(1):1270613.

Javed, F., Al-Kheraif, A.A., Kellesarian, S. V., Vohra, F. & Romanos, G.E. 2017. Oral candida carriage and species prevalence in denture stomatitis patients with and without diabetes. *Journal of Biological Regulators and Homeostatic Agents*. 31(2):343–346.

Jayabalan, J., Mani, G., Krishnan, N., Pernabas, J., Devadoss, J.M. & Jang, H.T. 2019. Green biogenic synthesis of zinc oxide nanoparticles using *Pseudomonas putida* culture and its *in vitro* antibacterial and anti-biofilm activity. *Biocatalysis and Agricultural Biotechnology*. 21:101327.

Jayaseelan, C., Rahuman, A.A., Kirthi, A.V., Marimuthu, S., Santhoshkumar, T., Bagavan, A., Gaurav, K., Karthik, L. & Rao, K. V. B. 2012. Novel microbial route to synthesize ZnO nanoparticles using Aeromonas hydrophila and their activity against pathogenic bacteria and fungi. *Spectrochimica Acta - Part A: Molecular and Biomolecular Spectroscopy*. 90:78–84.

Jeevanandam, J., Barhoum, A., Chan, Y.S., Dufresne, A. & Danquah, M.K. 2018. Review on nanoparticles and nanostructured materials: History, sources, toxicity and regulations. *Beilstein Journal of Nanotechnology*. 9(1):1050–1074.

Jensen, R.H. 2016. Resistance in human pathogenic yeasts and filamentous fungi: prevalence, underlying molecular mechanisms and link to the use of antifungals in humans and the environment. *Danish medical journal*. 63(10):B5288.

Jiang, J., Pi, J. & Cai, J. 2018. The Advancing of Zinc Oxide Nanoparticles for Biomedical Applications. *Bioinorganic Chemistry and Applications*. 2018:1062562.

Jindal, A.B. 2017. The effect of particle shape on cellular interaction and drug delivery applications of micro- and nanoparticles. *International Journal of Pharmaceutics*. 532(1):450–465.

Johnson, R., Beer, D. de, Dludla, P., Ferreira, D., Muller, C. & Joubert, E. 2018. Aspalathin from Rooibos (*Aspalathus linearis*): A Bioactive C-glucosyl Dihydrochalcone with Potential to Target the Metabolic Syndrome. *Planta Medica*. 84(09/10):568–583.

Jothiprakasam, V., Sambantham, M., Chinnathambi, S. & Vijayaboopathi, S. 2017. *Candida tropicalis* biofilm inhibition by ZnO nanoparticles and EDTA. *Archives of Oral Biology*. 73:21–24.

Jowkar, Z., Omidi, Y. & Shafiei, F. 2020. The effect of silver nanoparticles, zinc oxide nanoparticles, and titanium dioxide nanoparticles on the push-out bond strength of fiber posts. *Journal of Clinical and Experimental Dentistry*. 12(3):e249–e256.

Kadiyala, U., Kotov, N.A. & Scott Vanepps, J. 2018. Antibacterial Metal Oxide Nanoparticles: Challenges in Interpreting the Literature HHS Public Access. *Current Pharmaceutical Design*. 24(8):896–903.

Kadosh, D. 2019. Regulatory mechanisms controlling morphology and pathogenesis in Candida albicans. *Current Opinion in Microbiology*. 52:27–34.

Kalpana, V.N. & Devi Rajeswari, V. 2018. A Review on Green Synthesis, Biomedical Applications, and Toxicity Studies of ZnO NPs. *Bioinorganic Chemistry and Applications*. 2018:1–12.

Kalua, K., Zimba, B. & Denning, D.W. 2018. Estimated burden of serious fungal infections in Malawi. *Journal of Fungi*. 4(2):61.

Kamonkhantikul, K., Arksornnukit, M. & Takahashi, H. 2017. Antifungal, optical, and mechanical properties of polymethylmethacrylate material incorporated with silanized zinc oxide nanoparticles. *International Journal of Nanomedicine*. 12:2353–2360.

Kanwar, R., Rathee, J., Salunke, D.B. & Mehta, S.K. 2019. Green nanotechnology-driven drug delivery assemblies. *ACS Omega*. 4(5):8804–8815.

Kapadia, S.P., Pudakalkatti, P.S. & Shivanaikar, S. 2015. Detection of antimicrobial activity of banana peel (Musa paradisiaca L.) on *Porphyromonas gingivalis* and *Aggregatibacter actinomycetemcomitans*: An *in vitro* study. *Contemporary clinical dentistry*. 6(4):496–9.

Karmous, I., Pandey, A., Haj, K. Ben & Chaoui, A. 2019. Efficiency of the Green Synthesized Nanoparticles as New Tools in Cancer Therapy: Insights on Plant-Based Bioengineered Nanoparticles, Biophysical Properties, and Anticancer Roles. *Biological Trace Element Research.* 196:330–342.

Karnan, T. & Selvakumar, S.A.S. 2016. Biosynthesis of ZnO nanoparticles using rambutan (*Nephelium lappaceum L.*) peel extract and their photocatalytic activity on methyl orange dye. *Journal of Molecular Structure*. 1125:358–365.

Kasraei, S., Sami, L., Hendi, S., AliKhani, M.-Y., Rezaei-Soufi, L. & Khamverdi, Z. 2014. Antibacterial properties of composite resins incorporating silver and zinc oxide nanoparticles on *Streptococcus mutans* and *Lactobacillus*. *Restorative Dentistry & Endodontics*. 39(2):109.

Katas, H., Lim, C.S., Nor Azlan, A.Y.H., Buang, F. & Mh Busra, M.F. 2019. Antibacterial activity of biosynthesized gold nanoparticles using biomolecules from *Lignosus rhinocerotis* and chitosan. *Saudi Pharmaceutical Journal*. 27(2):283–292.

Kernien, J.F., Snarr, B.D., Sheppard, D.C. & Nett, J.E. 2018. The interface between fungal biofilms and innate immunity. *Frontiers in Immunology*. 8:1968.

Khan, A.U. & Gilani, A.H. 2006. Selective bronchodilatory effect of Rooibos tea (*Aspalathus linearis*) and its flavonoid, chrysoeriol. *European Journal of Nutrition*. 45(8):463–469.

Khan, S.T., Ahamed, M., Al-Khedhairy, A. & Musarrat, J. 2013. Biocidal effect of copper and zinc oxide nanoparticles on human oral microbiome and biofilm formation. *Materials Letters*. 97:67–70.

Khan, S.T., Ahamed, M., Musarrat, J. & Al-Khedhairy, A.A. 2014. Anti-biofilm and antibacterial activities of zinc oxide nanoparticles against the oral opportunistic pathogens *Rothia dentocariosa* and *Rothia mucilaginosa*. *European Journal of Oral Sciences*. 122(6):397–403.

Khan, M.F., Ansari, A.H., Hameedullah, M., Ahmad, E., Husain, F.M., Zia, Q., Baig, U., Zaheer, M.R., *et al.* 2016. Sol-gel synthesis of thorn-like ZnO nanoparticles endorsing mechanical stirring effect and their antimicrobial activities: Potential role as nano-Antibiotics. *Scientific Reports*. 6: 27689.

Khan, K. & Javed, S. 2018. Functionalization of Inorganic Nanoparticles to Augment Antimicrobial Efficiency: A Critical Analysis. *Current Pharmaceutical Biotechnology*. 19(7):523–536.

Khan, S.A., Noreen, F., Kanwal, S., Iqbal, A. & Hussain, G. 2018. Green synthesis of ZnO and Cu-doped ZnO nanoparticles from leaf extracts of *Abutilon indicum, Clerodendrum infortunatum, Clerodendrum inerme* and investigation of their biological and photocatalytic activities. *Materials Science and Engineering C*. 82:46–59.

Khatami, M., Alijani, H.Q., Heli, H. & Sharifi, I. 2018. Rectangular shaped zinc oxide nanoparticles: Green synthesis by Stevia and its biomedical efficiency. *Ceramics International*. 44(13):15596–15602.

Khezerlou, A., Alizadeh-Sani, M., Azizi-Lalabadi, M. & Ehsani, A. 2018. Nanoparticles and their antimicrobial properties against pathogens including bacteria, fungi, parasites and viruses. *Microbial Pathogenesis*. 123:505–526.

Khoshhesab, Z.M., Sarfaraz, M. & Asadabad, M.A. 2011. Preparation of ZnO nanostructures by chemical precipitation method. *Synthesis and Reactivity in Inorganic, Metal-Organic and Nano-Metal Chemistry*. 41(7):814–819.

Khurshid, Z., Zafar, M., Qasim, S., Shahab, S., Naseem, M. & AbuReqaiba, A. 2015. Advances in Nanotechnology for Restorative Dentistry. *Materials*. 8(2):717–731.

Kilian, M., Chapple, I.L.C., Hannig, M., Marsh, P.D., Meuric, V., Pedersen, A.M.L., Tonetti, M.S., Wade, W.G., *et al.* 2016. The oral microbiome - An update for oral healthcare professionals. *British Dental Journal*. 221(10):657–666.

Klein, R.S., Harris, C.A., Small, C.B., Moll, B., Lesser, M. & Friedland, G.H. 1984. Oral Candidiasis in High-Risk Patients as the Initial Manifestation of the Acquired Immunodeficiency Syndrome. *New England Journal of Medicine*. 311(6):354–358.

Klingshirn, C. 2007. ZnO: From basics towards applications. *Physica Status Solidi (B) Basic Research*. 244(9):3027–3073.

Kokoska, L., Kloucek, P., Leuner, O. & Novy, P. 2018. Plant-Derived Products as Antibacterial and Antifungal Agents in Human Health Care. *Current Medicinal Chemistry*. 26(29):5501–5541.

Kong, E. & Jabra-Rizk, M.A. 2015. The Great Escape: Pathogen Versus Host. *PLoS Pathogens*. 11(3):1–5.

Koo, H., Allan, R.N., Howlin, R.P., Stoodley, P. & Hall-Stoodley, L. 2017. Targeting microbial biofilms: Current and prospective therapeutic strategies. *Nature Reviews Microbiology*. 15(12):740–755.

Korgel, B.A., Lee, D.C., Hanrath, T., Yacaman, M.J., Thesen, A., Matijevic, M., Kilaas, R., Kisielowski, C., *et al.* 2006. Application of aberration-corrected TEM and image simulation to nanoelectronics and nanotechnology. *IEEE Transactions on Semiconductor Manufacturing*. 19:391–395.

Król, A., Pomastowski, P., Rafińska, K., Railean-Plugaru, V. & Buszewski, B. 2017. Zinc oxide nanoparticles: Synthesis, antiseptic activity and toxicity mechanism. *Advances in Colloid and Interface Science*. 249:37–52.

Kumar, C.S.S.R. 2013. UV-VIS and photoluminescence spectroscopy for nanomaterials characterization. Springer Berlin Heidelberg:1–64.

Kumar, I., Mondal, M., Meyappan, V. & Sakthivel, N. 2019. Green one-pot synthesis of gold nanoparticles using Sansevieria roxburghiana leaf extract for the catalytic degradation of toxic organic pollutants. *Materials Research Bulletin*. 117:18–27.

Lalla, R. V., Patton, L.L. & Dongari-Bagtzoglou, A. 2013. Oral candidiasis: pathogenesis, clinical presentation, diagnosis and treatment strategies. *Journal of the California Dental Association*. 41(4):263–268.

Langford, J.I. & Wilson, A.J.C. 1978. Scherrer after sixty years: A survey and some new results in the determination of crystallite size. *Journal of Applied Crystallography*. 11(2):102–113.

Leung, Y.H., Chen, X.Y., Ng, A.M.C., Guo, M.Y., Liu, F.Z., Djurišić, A.B., Chan, W.K., Shi, X.Q. & van Hove, M. A. 2013. Green emission in ZnO nanostructures - Examination of the roles of oxygen and zinc vacancies. *Applied Surface Science*. 271:202–209.

Lewis, M.A.O. & Williams, D.W. 2017. Diagnosis and management of oral candidosis. *British Dental Journal*. 223(9):675–681.

Liang, J., Peng, X., Zhou, X., Zou, J. & Cheng, L. 2020. Emerging applications of drug delivery systems in oral infectious diseases prevention and treatment. Molecules 25 (3):516.

Lipovsky, A., Nitzan, Y., Gedanken, A. & Lubart, R. 2011. Antifungal activity of ZnO nanoparticles—the role of ROS mediated cell injury. *Nanotechnology*. 22(10):1–5.

Liu, Y., Shi, L., Su, L., Van der Mei, H.C., Jutte, P.C., Ren, Y. & Busscher, H.J. 2019. Nanotechnology-based antimicrobials and delivery systems for biofilm-infection control. *Chemical Society Reviews*. 48(2):428–446.

Löe, H. & Rindom Schiøtt, C. 1970. The effect of mouthrinses and topical application of chlorhexidine on the development of dental plaque and gingivitis in man. *Journal of Periodontal Research*. 5(2):79–83.

Lohse, M.B., Gulati, M., Johnson, A.D. & Nobile, C.J. 2018. Development and regulation of single-and multi-species Candida albicans biofilms. *Nature Reviews Microbiology*. 16(1):19–31.

Lygre, H., Qasim, M., Singh, B.R., Naqvi, A.H., Paik, P., Das, D., Hamad, A., Kelkawi, A., *et al.* 2015. Prevention and treatment of Candida colonization on denture liners: A systematic review. *Journal of Prosthodontic Research*. 26(1):1–24.

Lyu, X., Zhao, C., Yan, Z.M. & Hua, H. 2016. Efficacy of nystatin for the treatment of oral candidiasis: A systematic review and meta-analysis. *Drug Design, Development and Therapy*. 10:1161–1171.

Madan, H.R., Sharma, S.C., Udayabhanu, Suresh, D., Vidya, Y.S., Nagabhushana, H., Rajanaik, H., Anantharaju, K.S., *et al.* 2016. Facile green fabrication of nanostructure ZnO plates, bullets, flower, prismatic tip, closed pine cone: Their antibacterial, antioxidant, photoluminescent and photocatalytic properties. *Spectrochimica Acta - Part A: Molecular and Biomolecular Spectroscopy*. 152:404–416.

Madhumitha, G., Elango, G. & Roopan, S.M. 2016. Biotechnological aspects of ZnO nanoparticles: overview on synthesis and its applications. *Applied Microbiology and Biotechnology*. 100(2):571–581.

Mahamuni-Badiger, P.P., Patil, P.M., Badiger, M. V., Patel, P.R., Thorat- Gadgil, B.S., Pandit, A. & Bohara, R.A. 2019. Biofilm formation to inhibition: Role of zinc oxide-based nanoparticles. *Materials Science and Engineering: C*:108110319.

Makhlouf, A.S.H. & Barhoum, A. 2018. Fundamentals of Nanoparticles: Classifications, Synthesis Methods, Properties and Characterization (Micro and Nano Technologies). Elsevier Inc:1–666.

Malaikozhundan, B., Vaseeharan, B., Vijayakumar, S., Pandiselvi, K., Kalanjiam, M.A.R., Murugan, K. & Benelli, G. 2017. Biological therapeutics of *Pongamia pinnata* coated zinc

oxide nanoparticles against clinically important pathogenic bacteria, fungi and MCF-7 breast cancer cells. *Microbial Pathogenesis*. 104:268–277.

Marquez, L. & Quave, C.L. 2020. Prevalence and therapeutic challenges of fungal drug resistance: role for plants in drug discovery. *Antibiotics*. 9(4):150.

Martins, N., Ferreira, I.C.F.R., Barros, L., Silva, S. & Henriques, M. 2014. Candidiasis: Predisposing Factors, Prevention, Diagnosis and Alternative Treatment. *Mycopathologia*. 177(5–6):223–240.

Maruthai, J., Muthukumarasamy, A. & Baskaran, B. 2018. Optical, biological and catalytic properties of ZnO/MgO nanocomposites derived via *Musa paradisiaca* bract extract. *Ceramics International*. 44(11):13152–13160.

Masondo, N.A. & Makunga, N.P. 2019. Advancement of analytical techniques in some South African commercialized medicinal plants: Current and future perspectives. *South African Journal of Botany*. 126:40–57.

Matinise, N., Fuku, X.G., Kaviyarasu, K., Mayedwa, N. & Maaza, M. 2017a. ZnO nanoparticles via Moringa oleifera green synthesis: Physical properties & mechanism of formation. *Applied Surface Science*. 406:339–347.

Matsubara, V.H., Bandara, H.M.H.N., Mayer, M.P.A. & Samaranayake, L.P. 2016. Probiotics as Antifungals in Mucosal Candidiasis. *Clinical infectious diseases : an official publication of the Infectious Diseases Society of America*. 62(9):1143–53.

McKay, D.L. & Blumberg, J.B. 2007. A review of the bioactivity of South African herbal teas: rooibos (*Aspalathus linearis*) and honeybush (Cyclopia intermedia). *Phytotherapy Research*. 21(1):1–16.

Melo, M.A.S., Guedes, S.F.F., Xu, H.H.K. & Rodrigues, L.K.A. 2013. Nanotechnology-based restorative materials for dental caries management. *Trends in Biotechnology*. 31(8):459–467.

Memarzadeh, K., Sharili, A.S., Huang, J., Rawlinson, S.C.F. & Allaker, R.P. 2015. Nanoparticulate zinc oxide as a coating material for orthopedic and dental implants. *Journal of Biomedical Materials Research - Part A*. 103(3):981–989.

Millsop, J.W. & Fazel, N. 2016. Oral candidiasis. *Clinics in Dermatology*. 34(4):487–494.

Mirhosseini, F., Amiri, M., Daneshkazemi, A., Zandi, H. & Javadi, Z.S. 2019. Antimicrobial Effect of Different Sizes of Nano Zinc Oxide on Oral Microorganisms. *Frontiers in Dentistry*. 16(2):105–112.

Mirzaei, H. & Darroudi, M. 2017. Zinc oxide nanoparticles: Biological synthesis and biomedical applications. *Ceramics International*. 43(1):907–914.

Mishra, R., Tandon, S., Rathore, M. & Banerjee, M. 2016. Antimicrobial Efficacy of Probiotic and Herbal Oral Rinses against Candida albicans in Children: A Randomized Clinical Trial. *International Journal of Clinical Pediatric Dentistry*. 9(1):25–30.

Mishra, P.K., Mishra, H., Ekielski, A., Talegaonkar, S. & Vaidya, B. 2017. Zinc oxide nanoparticles: A promising nanomaterial for biomedical applications. *Drug Discovery Today*. 22(12):1825–1834.

Moghaddam, A.B., Namvar, F., Moniri, M., Tahir, P.M., Azizi, S. & Mohamad, R. 2015. Nanoparticles biosynthesized by fungi and yeast: A review of their preparation, properties, and medical applications. *Molecules*. 20(9):16540–16565.

Mohamad Sukri, S.N.A., Shameli, K., Mei-Theng Wong, M., Teow, S.Y., Chew, J. & Ismail, N.A. 2019. Cytotoxicity and antibacterial activities of plant-mediated synthesized zinc oxide (ZnO) nanoparticles using *Punica granatum* (pomegranate) fruit peels extract. *Journal of Molecular Structure*. 1189:57–65.

Mohanan, P. V, Reshma, V.G., Syama, S., Sruthi, S., Reshma, S.C. & Remya, N.S. 2017. Engineered nanoparticles with Antimicrobial property. *Current Drug Metabolism*. 18(11):1040–1054.

Monteiro, D.R., Silva, S., Negri, M., Gorup, L.F., de Camargo, E.R., Oliveira, R., Barbosa, D.B. & Henriques, M. 2013. Antifungal activity of silver nanoparticles in combination with nystatin and chlorhexidine digluconate against *Candida albicans* and *Candida glabrata* biofilms. *Mycoses*. 56(6):672–680.

Monteiro, D.R., Takamiya, A.S., Feresin, L.P., Gorup, L.F., de Camargo, E.R., Delbem, A.C.B., Henriques, M. & Barbosa, D.B. 2015. Susceptibility of *Candida albicans* and *Candida glabrata* biofilms to silver nanoparticles in intermediate and mature development phases. *Journal of Prosthodontic Research*. 59(1):42–48.

Monteiro, D.R., Arias, L.S., Araujo, H.C., Caldeirão, A.C.M., Gulart, B.F., de Oliveira, J., dos Santos, M.B., Ramage, G., *et al.* 2020. Use of Nanoparticles to Manage Candida Biofilms. Shukla, A.K. (ed.), *Nanoparticles and their Biomedical Applications*. Springer Singapore: 191–216.

Moolla, A., Van Vuuren, S.F., Van Zyl, R.L. & Viljoen, A.M. 2007. Biological activity and toxicity profile of 17 *Agathosma* (*Rutaceae*) species. *South African Journal of Botany*. 73(4):588–592.

Moolla, A. & Viljoen, A.M. 2008. 'Buchu' - *Agathosma betulina* and *Agathosma crenulata* (*Rutaceae*): A review. *Journal of Ethnopharmacology*. 119(3):413–419.

Morse, D.J., Wilson, M.J., Wei, X., Bradshaw, D.J., Lewis, M.A.O. & Williams, D.W. 2019. Modulation of *Candida albicans* virulence in *in vitro* biofilms by oral bacteria. *Letters in Applied Microbiology*. 68(4):337–343.

Mothibe, J. V. & Patel, M. 2017. Pathogenic characteristics of *Candida albicans* isolated from oral cavities of denture wearers and cancer patients wearing oral prostheses. *Microbial Pathogenesis*. 110:128–134.

Mourdikoudis, S., Pallares, R.M. & Thanh, N.T.K. 2018. Characterization techniques for nanoparticles: Comparison and complementarity upon studying nanoparticle properties. *Nanoscale*. 10(27):12871–12934.

Mousavi, S.A., Ghotaslou, R., Kordi, S., Khoramdel, A., Aeenfar, A., Kahjough, S.T. & Akbarzadeh, A. 2018. Antibacterial and antifungal effects of chitosan nanoparticles on tissue conditioners of complete dentures. *International Journal of Biological Macromolecules*. 118(A):881–885.

Mousavi, S.A., Ghotaslou, R., Akbarzadeh, A., Azima, N., Aeinfar, A. & Khorramdel, A. 2019. Evaluation of antibacterial and antifungal properties of a tissue conditioner used in complete dentures after incorporation of ZnO–Ag nanoparticles. *Journal of Dental Research, Dental Clinics, Dental Prospects*. 13(1):11–18.

Munshi, T., Heckman, C.J. & Darlow, S. 2015. Association between tobacco waterpipe smoking and head and neck conditions: A systematic review. *Journal of the American Dental Association*. 146(10):760–766.

Nagajyothi, P.C., Minh An, T.N., Sreekanth, T.V.M., Lee, J. Il, Joo, D.L. & Lee, K.D. 2013. Green route biosynthesis: Characterization and catalytic activity of ZnO nanoparticles. *Materials Letters*. 108:160–163.

Naganathan, K. & Thirunavukkarasu, S. 2017. Green way genesis of silver nanoparticles using multiple fruit peels waste and its antimicrobial, anti-oxidant and anti-tumor cell line studies. *IOP Conference Series: Materials Science and Engineering*. 191(1):012009.

Naglik, J.R., König, A., Hube, B. & Gaffen, S.L. 2017. Candida albicans–epithelial interactions and induction of mucosal innate immunity. *Current Opinion in Microbiology*. 40:104–112.

Nam, K.Y. & Lee, C.J. 2019. Chapter 14 – Characterization of silver nanoparticles incorporated acrylic-based tissue conditioner with antimicrobial effect and cytocompatibility. Subramani, K., Ahmed, W. (eds.), *Nanobiomaterials in Clinical Dentistry*. Elsevier Inc: 335–348.

Narayanamma, A. 2016. Natural Synthesis of Silver Nanoparticles by Banana Peel Extract and as an Antibacterial Agent. *Journal of Polymer and Textile Engineering*. 3(1):17–25.

Nasrollahzadeh, M., Issaabadi, Z., Sajjadi, M., Sajadi, S.M. & Atarod, M. 2019. Types of Nanostructures. *Interface Science and Technology* Vol. 28. Elsevier Inc.: 29–80.

Nava, O.J., Soto-Robles, C.A., Gómez-Gutiérrez, C.M., Vilchis-Nestor, A.R., Castro-Beltrán, A., Olivas, A. & Luque, P.A. 2017a. Fruit peel extract mediated green synthesis of zinc oxide nanoparticles. *Journal of Molecular Structure*. 1147:1–6.

Nava, O.J., Luque, P.A., Gómez-Gutiérrez, C.M., Vilchis-Nestor, A.R., Castro-Beltrán, A., Mota-González, M.L. & Olivas, A. 2017b. Influence of Camellia sinensis extract on Zinc Oxide nanoparticle green synthesis. *Journal of Molecular Structure*. 1134:121–125.

Naveed Ul Haq, A., Nadhman, A., Ullah, I., Mustafa, G., Yasinzai, M. & Khan, I. 2017. Synthesis Approaches of Zinc Oxide Nanoparticles: The Dilemma of Ecotoxicity. *Journal of Nanomaterials*. 2017(12):1–14.

Neppelenbroek, K.H. 2016. Sustained drug-delivery system: a promising therapy for denture stomatitis? *Journal of Applied Oral Science*. 24(5):420–422.

Nett, J.E. 2016. The host's reply to Candida biofilm. *Pathogens*. 5(1):33.

Nett, J.E. & Andes, D.R. 2020. Contributions of the biofilm matrix to candida pathogenesis. *Journal of Fungi*. 3:6(1):21.

Ngom, I., Ngom, B.D., Sackey, J. & Khamlich, S. 2020. Biosynthesis of zinc oxide nanoparticles using extracts of *Moringa Oleifera*: Structural & optical properties. *Materials Today:* Proceedings, https://doi.org/10.1016/j.matpr.2020.05.323

Nikolova, M.P. & Chavali, M.S. 2020. Metal Oxide Nanoparticles as Biomedical Materials. *Biomimetics*. 5(2):27.

Nikou, S.A., Kichik, N., Brown, R., Ponde, N.O., Ho, J., Naglik, J.R. & Richardson, J.P. 2019. *Candida albicans* interactions with mucosal surfaces during health and disease. *Pathogens*. 8(2):53.

Nobile, C.J. & Johnson, A.D. 2015. *Candida albicans* Biofilms and Human Disease. *Annual review of microbiology*. 69:71–92.

Ocansey, B.K., Pesewu, G.A., Codjoe, F.S., Osei-Djarbeng, S., Feglo, P.K. & Denning, D.W. 2019. Estimated burden of serious fungal infections in Ghana. *Journal of Fungi*. 5(2):38.

Ohshima, T., Kojima, Y., Seneviratne, C.J. & Maeda, N. 2016. Therapeutic Application of Synbiotics, a Fusion of Probiotics and Prebiotics, and Biogenics as a New Concept for Oral Candida Infections: A Mini Review. *Frontiers in microbiology*. 7:10.

Oladele, R.O. & Denning, D.W. 2014. Burden of serious fungal infection in Nigeria. *West African journal of medicine* .33(2):107–114.

de Oliveira Santos, G.C., Vasconcelos, C.C., Lopes, A.J.O., Cartágenes, M. do S. d. S., Filho, A.K.D.B., do Nascimento, F.R.F., Ramos, R.M., Pires, E.R.R.B., *et al.* 2018. Candida infections and therapeutic strategies: Mechanisms of action for traditional and alternative agents. *Frontiers in Microbiology*. 9:1351.

Orsuwan, A., Shankar, S., Wang, L.F., Sothornvit, R. & Rhim, J.W. 2017. One-step preparation of banana powder/silver nanoparticles composite films. *Journal of Food Science and Technology*. 54(2):497–506.

Ozak, S.T. & Ozkan, P. 2013. Nanotechnology and dentistry. *European Journal of Dentistry*. 7(1):145–151.

Özgür, Ü., Alivov, Y.I., Liu, C., Teke, A., Reshchikov, M.A., Doğan, S., Avrutin, V., Cho, S.J., *et al.* 2005. A comprehensive review of ZnO materials and devices. *Journal of Applied Physics*. 98(4):1–103.

Padovani, G.C., Feitosa, V.P., Sauro, S., Tay, F.R., Durán, G., Paula, A.J., Durán, N., Prabu, L.S., *et al.* 2018. A Review on Green Synthesis, Biomedical Applications, and Toxicity Studies of ZnO NPs. *Bioinorganic Chemistry and Applications*. 2018(2):1–12.

Pasquet, J., Chevalier, Y., Couval, E., Bouvier, D., Noizet, G., Morlière, C. & Bolzinger, M.A. 2014. Antimicrobial activity of zinc oxide particles on five micro-organisms of the Challenge Tests related to their physicochemical properties. *International Journal of Pharmaceutics*. 460(1–2):92–100.

Patil, S., Rao, R.S., Majumdar, B. & Anil, S. 2015. Clinical Appearance of Oral Candida Infection and Therapeutic Strategies. *Frontiers in Microbiology*. 17(6):1391.

Patnaik, P. 2003. *Handbook of inorganic chemicals*. [Online], Available: ftp://pvictor.homeftp.net/public/Sci_Library/Chem Library/Handbooks/Patnaik P. Handbook of inorganic chemicals (MGH, 2003)(T)(1125s).pdf [Accessed:2020, April 21].

Patton, L.L. 2013. Oral lesions associated with human immunodeficiency virus disease. *Dental Clinics of North America*. 57(4):673–698.

Paulone, S., Malavasi, G., Ardizzoni, A., Orsi, C.F., Peppoloni, S., Neglia, R.G. & Blasi, E. 2017. *Candida albicans* survival, growth and biofilm formation are differently affected by mouthwashes: an in vitro study. *The new microbiologica*. 40(1):45–52.

Pellon, A., Sadeghi Nasab, S.D. & Moyes, D.L. 2020. New Insights in *Candida albicans* Innate Immunity at the Mucosa: Toxins, Epithelium, Metabolism, and Beyond. *Frontiers in Cellular and Infection Microbiology*. 10(81):1-14.

Pereira, D.M., Valentão, P., Pereira, J.A. & Andrade, P.B. 2009. Phenolics: From chemistry to biology. *Molecules*. 14(6):2202–2211.

Pereira, A. & Maraschin, M. 2015. Banana (Musa spp) from peel to pulp: Ethnopharmacology, source of bioactive compounds and its relevance for human health. *Journal of Ethnopharmacology*. 160:149–163.

Perelshtein, I., Lipovsky, A., Perkas, N., Gedanken, A., Moschini, E. & Mantecca, P. 2015. The influence of the crystalline nature of nano-metal oxides on their antibacterial and toxicity properties. *Nano Research*. 8(2):695–707.

Pillai, A.M., Sivasankarapillai, V.S., Rahdar, A., Joseph, J., Sadeghfar, F., Anuf A, R., Rajesh, K. & Kyzas, G.Z. 2020. Green synthesis and characterization of zinc oxide nanoparticles with antibacterial and antifungal activity. *Journal of Molecular Structure*. 1211:128107.

Prabu, L.S. 2018. Biosynthesis of zinc oxide nanoparticle: a review on greener approach. *MedCrave*. 5(3):151–154.

Qian, Y., Yao, J., Russel, M., Chen, K. & Wang, X. 2015. Characterization of green synthesized nano-formulation (ZnO-A. vera) and their antibacterial activity against pathogens. *Environmental Toxicology and Pharmacology*. 39(2):736–746.

Quindós, G., Gil-Alonso, S., Marcos-Arias, C., Sevillano, E., Mateo, E., Jauregizar, N. & Eraso, E. 2019. Therapeutic tools for oral candidiasis: Current and new antifungal drugs. *Medicina oral, patologia oral y cirugia bucal*. 24(2):e172–e180.

Rad, S.S., Sani, A.M. & Mohseni, S. 2019. Biosynthesis, characterization and antimicrobial activities of zinc oxide nanoparticles from leaf extract of *Mentha pulegium (L.)*. *Microbial Pathogenesis*. 131:239–245.

Raghunath, A. & Perumal, E. 2017. Metal oxide nanoparticles as antimicrobial agents: a promise for the future. *International Journal of Antimicrobial Agents*. 49(2):137–152.

Raghupathi, K.R., Koodali, R.T. & Manna, A.C. 2011. Size-Dependent Bacterial Growth Inhibition and Mechanism of Antibacterial Activity of Zinc Oxide Nanoparticles. *Langmuir*. 27(7):4020–4028.

Rai, M., Ingle, A.P., Gaikwad, S., Gupta, I., Gade, A. & Silvério da Silva, S. 2016. Nanotechnology based anti-infectives to fight microbial intrusions. *Journal of Applied Microbiology*. 120(3):527–542.

Raja, A., Ashokkumar, S., Pavithra Marthandam, R., Jayachandiran, J., Khatiwada, C.P., Kaviyarasu, K., Ganapathi Raman, R. & Swaminathan, M. 2018. Eco-friendly preparation of zinc oxide nanoparticles using Tabernaemontana divaricata and its photocatalytic and antimicrobial activity. *Journal of Photochemistry and Photobiology B: Biology*. 181:53–58.

Rajeshkumar, S., Lakshmi, T. & Naik, P. 2019. Recent advances and biomedical applications of zinc oxide nanoparticles. in *Green Synthesis, Characterization and Applications of Nanoparticles* Elsevier. 445–457.

Rajwade, J.M., Chikte, R.G. & Paknikar, K.M. 2020. Nanomaterials: new weapons in a crusade against phytopathogens. *Applied Microbiology and Biotechnology*. 104(4):1437–1461.

Rathour, R.K.S. & Bhattacharya, J. 2018. A green approach for single-pot synthesis of graphene oxide and its composite with Mn_3O_4. *Applied Surface Science*. 437:41–50.

Reddy, A., Kambalyal, P., Patil, S., Vankhre, M., Khan, M.A. & Kumar, T. 2016. Comparative evaluation and influence on shear bond strength of incorporating silver, zinc oxide, and titanium dioxide nanoparticles in orthodontic adhesive. *Journal of Orthodontic Science*. 5(4):127.

Reeve, C.M. & Van Roekel, N.B. 1987. Denture sore mouth. *Dermatologic clinics*. 5(4):681–686. .

Rigopoulos, N., Thomou, E., Kouloumpis, A., Lamprou, E.R., Petropoulea, V., Gournis, D., Poulios, E., Karantonis, H.C. & Giaouris, E. 2018. Optimization of Silver Nanoparticle Synthesis by Banana Peel Extract Using Statistical Experimental Design, and Testing of their Antibacterial and Antioxidant Properties. *Current Pharmaceutical Biotechnology*. 20(10):858–873.

Rodrigues, M.E., Henriques, M. & Silva, S. 2016. Disinfectants to fight oral Candida biofilms. *Advances in Experimental Medicine and Biology* Vol. 931. Springer New York: 83–93.

Rodrigues, C.F., Rodrigues, M.E. & Henriques, M.C.R. 2019. Promising Alternative Therapeutics for Oral Candidiasis. *Current Medicinal Chemistry*. 26(14):2515–2528.

Rosa-garcía, S.C. De, Martínez-torres, P., Gómez-cornelio, S., Corral-aguado, M.A., Quintana, P. & Gómez-ortíz, N.M. 2018. Antifungal Activity of ZnO and MgO Nanomaterials and Their Mixtures against *Colletotrichum gloeosporioides* Strains from Tropical Fruit. *Journal of Nanomaterials*. 2018(3):1–9.

Rozman, N.A.S., Yenn, T.W., Ring, L.C., Nee, T.W., Hasanolbasori, M.A. & Abdullah, S.Z. 2019. Potential antimicrobial applications of chitosan nanoparticles (ChNPS). *Journal of Microbiology and Biotechnology*. 29(7):1009–1013.

Ruddaraju, L.K., Pammi, S.V.N., Guntuku, G. Sankar, Padavala, V.S. & Kolapalli, V.R.M. 2020. A review on anti-bacterials to combat resistance: From ancient era of plants and metals to present and future perspectives of green nano technological combinations. *Asian Journal of Pharmaceutical Sciences*. 15(1):42–59.

Sacarlal, J. & Denning, D.W. 2018. Estimated burden of serious fungal infections in Mozambique. *Journal of Fungi*. 4(3):75.

Saffarpour, M., Rahmani, M., Tahriri, M. & Peymani, A. 2016. Antimicrobial and bond strength properties of a dental adhesive containing zinc oxide nanoparticles. *Brazilian Journal of Oral Sciences*. 15(1):66–69.

Samiei, M., Torab, A., Hosseini, O., Abbasi, T., Abdollahi, A.A. & Divband, B. 2018. Antibacterial effect of two nano zinc oxide gel preparations compared to calcium hydroxide and chlorhexidine mixture. *Iranian Endodontic Journal*. 13(3):305–311.

Sánchez-López, E., Gomes, D., Esteruelas, G., Bonilla, L., Laura Lopez-Machado, A., Galindo, R., Cano, A., Espina, M., Ettcheto, M., Camins, A., Silva, A.M., Durazzo, A., Santini, A., Garcia, M.L. & Souto, E.B. 2020. Metal-Based Nanoparticles as Antimicrobial Agents: An Overview. *Nanomaterials*. 10:292.

Sanders, W.C. 2018. *Basic principles of nanotechnology*. CRC Press: 1–78.

Sangeetha, G., Rajeshwari, S. & Venckatesh, R. 2011. Green synthesis of zinc oxide nanoparticles by aloe barbadensis miller leaf extract: Structure and optical properties. *Materials Research Bulletin*. 46(12):2560–2566.

Santhoshkumar, J., Kumar, S.V. & Rajeshkumar, S. 2017. Synthesis of zinc oxide nanoparticles using plant leaf extract against urinary tract infection pathogen. *Resource-Efficient Technologies*. 3(4):459–465.

Santos, J.S., Deolindo, C.T.P., Esmerino, L.A., Genovese, M.I., Fujita, A., Marques, M.B., Rosso, N.D., Daguer, H., Valese, A. C. and Granato, D. 2016. Effects of time and extraction temperature on phenolic composition and functional properties of red rooibos (*Aspalathus linearis*). *Food Research International*. 89:476–487.

Sasaki, M., Nishida, N. & Shimada, M. 2018. A Beneficial Role of Rooibos in Diabetes Mellitus: A Systematic Review and Meta-Analysis. *Molecules*. 23(4):839.

Saubolle, M.A. & Hoeprich, P.D. 1978. Disk agar diffusion susceptibility testing of yeasts. *Antimicrobial Agents and Chemotherapy*. 14(4):517–530.

Scheibler, E., da Silva, R.M., Leite, C.E., Campos, M.M., Figueiredo, M.A., Salum, F.G. & Cherubini, K. 2018. Stability and efficacy of combined nystatin and chlorhexidine against suspensions and biofilms of *Candida albicans*. *Archives of Oral Biology*. 89:70–76.

Schiefersteiner, M., Bichsel, D., Rücker, M. & Valdec, S. 2019. Antimycotics in dental routine – an update. *Swiss dental journal*. 129(5):403–405.

Schwartz, I.S., Boyles, T.H., Kenyon, C.R., Hoving, J.C., Brown, G.D. & Denning, D.W. 2019. The estimated burden of fungal disease in South Africa. *South African Medical Journal*. 109(11):885.

Selim, Y.A., Azb, M.A., Ragab, I. & H. M. Abd El-Azim, M. 2020. Green Synthesis of Zinc Oxide Nanoparticles Using Aqueous Extract of *Deverra tortuosa* and their Cytotoxic Activities. *Scientific Reports*. 10(1):1–9.

Seneviratne, C.J., Jin, L. & Samaranayake, L.P. 2008. Biofilm lifestyle of Candida: A mini review. Oral Diseases 14 (7) p.582–590.

Seong, M. & Lee, D.G. 2018. Reactive oxygen species-independent apoptotic pathway by gold nanoparticles in *Candida albicans*. *Microbiological Research*. 207:33–40.

Sevinç, B.A. & Hanley, L. 2010. Antibacterial activity of dental composites containing zinc oxide nanoparticles. *Journal of Biomedical Materials Research - Part B Applied Biomaterials*. 94(1):22–31.

Shaikh, S., Nazam, N., Rizvi, S.M.D., Ahmad, K., Baig, M.H., Lee, E.J. & Choi, I. 2019. Mechanistic Insights into the Antimicrobial Actions of Metallic Nanoparticles and Their Implications for Multidrug Resistance. *International journal of molecular sciences*. 20(10):2468.

Sharma, D., Sabela, M.I., Kanchi, S., Mdluli, P.S., Singh, G., Stenström, T.A. & Bisetty, K. 2016. Biosynthesis of ZnO nanoparticles using *Jacaranda mimosifolia* flowers extract: Synergistic antibacterial activity and molecular simulated facet specific adsorption studies. *Journal of Photochemistry and Photobiology B: Biology*. 162:199–207.

Sharma, A. 2018. Oral candidiasis: An opportunistic infection: A review Amrit Sharma. [Online], Available: www.oraljournal.com [Accessed: 2020, May 20].

Sharma, A. 2019. Oral Candidiasis: An Opportunistic infection-A Review. *International Journal of Applied Dental Sciences*. 5(1):23–27.

Sharmila, G., Thirumarimurugan, M. & Muthukumaran, C. 2019. Green synthesis of ZnO nanoparticles using *Tecoma castanifolia* leaf extract: Characterization and evaluation of its antioxidant, bactericidal and anticancer activities. *Microchemical Journal*. 145:578–587.

Shashirekha, G., Jena, A. & Mohapatra, S. 2017. Nanotechnology in Dentistry: Clinical Applications, Benefits, and Hazards. *Compendium of continuing education in dentistry*. 38(5):e1–e4.

Shayegan Mehr, E., Sorbiun, M., Ramazani, A. & Taghavi Fardood, S. 2018. Plant-mediated synthesis of zinc oxide and copper oxide nanoparticles by using *Ferulago angulata*

(schlecht) boiss extract and comparison of their photocatalytic degradation of Rhodamine B (RhB) under visible light irradiation. *Journal of Materials Science: Materials in Electronics*. 29(2):1333–1340.

Shekhawat, M.S. & Manokari, M. 2014. Biogenesis of Zinc oxide Nanoparticles using *Morinda pubescens*. International Journal of BioEngineering and Technology.5(1):1–6.

Sheppard, D.C. & Howell, P.L. 2016. Biofilm exopolysaccharides of pathogenic fungi: Lessons from bacteria. *Journal of Biological Chemistr*y. 291(24):12529–12537.

Shin, J., Prabhakaran, V.S. & Kim, K.-S. 2018. The multi-faceted potential of plant-derived metabolites as antimicrobial agents against multidrug-resistant pathogens. *Microbial Pathogenesis*. 116:209–214.

Shoeb, M., Singh, B.R., Khan, J.A., Khan, W., Singh, B.N., Singh, H.B. & Naqvi, A.H. 2013. ROS-dependent anticandidal activity of zinc oxide nanoparticles synthesized by using egg albumen as a biotemplate. *Advances in Natural Sciences: Nanoscience and Nanotechnology*. 4(3):035015.

Shukla, S.K. & Rao, T.S. 2017. An Improved Crystal Violet Assay for Biofilm Quantification in 96-Well Microtitre Plate. bioRxiv 100214

da Silva, B.L., Abuçafy, M.P., Manaia, E.B., Junior, J.A.O., Chiari-Andréo, B.G., Pietro, R.C.L.R. & Chiavacci, L.A. 2019a. Relationship between structure and antimicrobial activity of zinc oxide nanoparticles: An overview. *International Journal of Nanomedicine*. 14:9395–9410.

da Silva, B., Caetano, B.L., Chiari-Andréo, B.G., Pietro, R.C.L.R. & Chiavacci, L.A. 2019b. Increased antibacterial activity of ZnO nanoparticles: Influence of size and surface modification. *Colloids and Surfaces B: Biointerfaces*. 177:440–447.

Siddiqi, K.S. & Husen, A. 2016. Fabrication of Metal Nanoparticles from Fungi and Metal Salts: Scope and Application. *Nanoscale Research Letters*. 11(1):1–15.

Siddiqi, K.S., ur Rahman, A., Tajuddin & Husen, A. 2018. Properties of Zinc Oxide Nanoparticles and Their Activity Against Microbes. *Nanoscale Research Letters*. 13:141.

Simpson, D. 1998. Buchu - South Africa's amazing herbal remedy. *Scottish Medical Journal*. 43(6):189–191.

Singh, A., Verma, R., Murari, A. & Agrawal, A. 2014. Oral candidiasis: An overview. *Journal of Oral and Maxillofacial Pathology.* 18(5):81–85.

Singh, B., Singh, J.P., Kaur, A. & Singh, N. 2016. Bioactive compounds in banana and their associated health benefits - A review. *Food Chemistry*. 206:1–11.

Singh, J., Vishwakarma, K., Ramawat, N., Rai, P., Singh, V.K., Mishra, R.K., Kumar, V., Tripathi, D.K., *et al.* 2019. Nanomaterials and microbes' interactions: a contemporary overview. *3 Biotech*. 9(3):68.

Sirelkhatim, A., Mahmud, S., Seeni, A., Kaus, N.H.M., Ann, L.C., Bakhori, S.K.M., Hasan, H. & Mohamad, D. 2015. Review on zinc oxide nanoparticles: Antibacterial activity and toxicity mechanism. *Nano-Micro Letters.* 7(3):219–242.

Siriyong, T., Srimanote, P., Chusri, S., Yingyongnarongkul, B.E., Suaisom, C., Tipmanee, V. & Voravuthikunchai, S.P. 2017. Conessine as a novel inhibitor of multidrug efflux pump systems in *Pseudomonas aeruginosa*. *BMC Complementary and Alternative Medicine*. 17(1):1–7.

Skupien, J.A., Valentini, F., Boscato, N. & Pereira-Cenci, T. 2013. Prevention and treatment of Candida colonization on denture liners: A systematic review. *Journal of Prosthetic Dentistry*. 110(5):356–362.

Slot, D.E., Berchier, C.E., Addy, M., Van der Velden, U. & Van der Weijden, G.A. 2014. The efficacy of chlorhexidine dentifrice or gel on plaque, clinical parameters of gingival inflammation and tooth discoloration: A systematic review. *International Journal of Dental Hygiene*. 12(1):25–35.

Smith, C. & Swart, A. 2018. Aspalathus linearis (Rooibos) – a functional food targeting cardiovascular disease. *Food & Function*. 9(10):5041–5058.

Somu, P. & Paul, S. 2019. A biomolecule-assisted one-pot synthesis of zinc oxide nanoparticles and its bioconjugate with curcumin for potential multifaceted therapeutic applications. *New Journal of Chemistry*. 43(30):11934–11948.

Sorbiun, M., Shayegan Mehr, E., Ramazani, A. & Taghavi Fardood, S. 2018. Green Synthesis of Zinc Oxide and Copper Oxide Nanoparticles Using Aqueous Extract of Oak Fruit Hull (Jaft) and Comparing Their Photocatalytic Degradation of Basic Violet 3. *International Journal of Environmental Research*. 12(1):29–37.

Sportelli, M.C., Longano, D., Bonerba, E., Tantillo, G., Torsi, L., Sabbatini, L., Cioffi, N. & Ditaranto, N. 2020. Electrochemical preparation of synergistic nanoantimicrobials. *Molecules*. 25(1):49.

Stan, M., Popa, A., Toloman, D., Dehelean, A., Lung, I. & Katona, G. 2015. Enhanced photocatalytic degradation properties of zinc oxide nanoparticles synthesized by using plant extracts. *Materials Science in Semiconductor Processing*. 39:23–29.

Stan, M., Popa, A., Toloman, D., Silipas, T.D. & Vodnar, D.C. 2016. Antibacterial and antioxidant activities of ZnO nanoparticles synthesized using extracts of *Allium sativum*, *Rosmarinus officinalis* and *Ocimum basilicum*. *Acta Metallurgica Sinica (English Letters)*. 29(3):228–236.

Stepanović, S., Vuković, D., Dakić, I., Savić, B. & Švabić-Vlahović, M. 2000. A modified microtiter-plate test for quantification of staphylococcal biofilm formation. *Journal of Microbiological Methods*. 40(2):175–179.

Van Strydonck, D.A.C., Slot, D.E., Van Der Velden, U. & Van Der Weijden, F. 2012. Effect of a chlorhexidine mouthrinse on plaque, gingival inflammation and staining in gingivitis patients: A systematic review. *Journal of Clinical Periodontology*. 39(11):1042–1055.

Sun, Q., Li, J. & Le, T. 2018. Zinc Oxide Nanoparticle as a Novel Class of Antifungal Agents: Current Advances and Future Perspectives. *Journal of Agricultural and Food Chemistry*. 66(43):11209–11220.

Sundrarajan, M., Ambika, S. & Bharathi, K. 2015. Plant-extract mediated synthesis of ZnO nanoparticles using *Pongamia pinnata* and their activity against pathogenic bacteria. *Advanced Powder Technology*. 26(5):1294–1299.

Supranoto, S., Slot, D., Addy, M. & Van der Weijden, G. 2015. The effect of chlorhexidine dentifrice or gel versus chlorhexidine mouthwash on plaque, gingivitis, bleeding and tooth discoloration: *a systematic review*. *International Journal of Dental Hygiene*. 13(2):83–92.

Suresh, D., Nethravathi, P.C., Udayabhanu, Rajanaika, H., Nagabhushana, H. & Sharma, S.C. 2015. Green synthesis of multifunctional zinc oxide (ZnO) nanoparticles using *Cassia fistula* plant extract and their photodegradative, antioxidant and antibacterial activities.

Materials Science in Semiconductor Processing. 31:446–454.

Suresh, J., Pradheesh, G., Alexramani, V., Sundrarajan, M. & Hong, S.I. 2018. Green synthesis and characterization of zinc oxide nanoparticle using insulin plant (*Costus pictus D. Don*) and investigation of its antimicrobial as well as anticancer activities. *Advances in Natural Sciences: Nanoscience and Nanotechnology*. 9(1):015008.

Susewind, S., Lang, R. & Hahnel, S. 2015. Biofilm formation and *Candida albicans* morphology on the surface of denture base materials. *Mycoses*. 58(12):719–727.

Sydnes, M. 2014. One-Pot Reactions: A Step Towards Greener Chemistry. *Current Green Chemistry*. 1(3):216–226.

Taff, H.T., Nett, J.E. & Andes, D.R. 2012. Comparative analysis of Candida biofilm quantitation assays. *Medical Mycology*. 50(2):214–218.

Tariq, S., Wani, S., Rasool, W., Shafi, K., Bhat, M.A., Prabhakar, A., Shalla, A.H. & Rather, M.A. 2019. A comprehensive review of the antibacterial, antifungal and antiviral potential of essential oils and their chemical constituents against drug-resistant microbial pathogens. *Microbial Pathogenesis*. 134:103580.

Tavassoli Hojati, S., Alaghemand, H., Hamze, F., Ahmadian Babaki, F., Rajab-Nia, R., Rezvani, M.B., Kaviani, M. & Atai, M. 2013. Antibacterial, physical and mechanical properties of flowable resin composites containing zinc oxide nanoparticles. *Dental Materials*. 29(5):495–505.

Thema, F.T., Manikandan, E., Dhlamini, M.S. & Maaza, M. 2015a. Green synthesis of ZnO nanoparticles via *Agathosma betulina* natural extract. *Materials Letters*. 161:124–127.

Thema, F.T., Beukes, P., Gurib-Fakim, A. & Maaza, M. 2015b. Green synthesis of Monteponite CdO nanoparticles by *Agathosma betulina* natural extract. *Journal of Alloys and Compounds*. 646:1043–1048.

Thema, F.T., Manikandan, E., Gurib-Fakim, A. & Maaza, M. 2016. Single phase Bunsenite NiO nanoparticles green synthesis by *Agathosma betulina* natural extract. *Journal of Alloys and Compounds*. 657:655–661.

Tiew, P.Y., Mac Aogain, M., Ali, N.A.B.M., Thng, K.X., Goh, K., Lau, K.J.X. & Chotirmall, S.H. 2020. The Mycobiome in Health and Disease: Emerging Concepts, Methodologies and Challenges. *Mycopathologia*. 185(2):207–231.

Tobal, I.E., Roncero, A.M., Moro, R.F., Díez, D. & Marcos, I.S. 2020. Antibacterial natural halimanes: Potential source of novel antibiofilm agents. *Molecules*. 25(7):1707.

Tournu, H. & Van Dijck, P. 2012. Candida biofilms and the host: Models and new concepts for eradication. *International Journal of Microbiology*. 2012.

Treacy, M.M.J. & Higgins, J.B. 2007. Collection of Simulated XRD Powder Patterns for Zeolites Fifth (5th) Revised Edition. Elsevier:1-387.

Tsui, C., Kong, E.F. & Jabra-Rizk, M.A. 2016. Pathogenesis of *Candida albicans* biofilm. *Pathogens and disease*. 74(4):1-13.

Tufa, T.B. & Denning, D.W. 2019. The burden of fungal infections in Ethiopia. *Journal of Fungi*. 5(4):109.

Turner, M., Jahangiri, L. & Ship, J.A. 2008. Hyposalivation, xerostomia and the complete denture: A systematic review. *The Journal of the American Dental Association*. 139(2):146–150.

Umar, H., Kavaz, D. & Rizaner, N. 2019. Biosynthesis of zinc oxide nanoparticles using *Albizia lebbeck* stem bark, and evaluation of its antimicrobial, antioxidant, and cytotoxic activities on human breast cancer cell lines. *International Journal of Nanomedicine*. 14:87–100.

Uppuluri, P. & Chaffin, W.L. 2007. Defining *Candida albicans* stationary phase by cellular and DNA replication, gene expression and regulation. *Molecular Microbiology*. 64(6):1572–1586.

Vallet-Regí, M., González, B. & Izquierdo-Barba, I. 2019. Nanomaterials as promising alternative in the infection treatment. *International Journal of Molecular Sciences*. 20(15):3806.

Vanathi, P., Rajiv, P., Narendhran, S., Rajeshwari, S., Rahman, P.K.S.M. & Venckatesh, R. 2014. Biosynthesis and characterization of Phyto mediated zinc oxide nanoparticles: A green chemistry approach. *Materials Letters*. 134:13–15.

Vargas-Reus, M.A., Memarzadeh, K., Huang, J., Ren, G.G. & Allaker, R.P. 2012. Antimicrobial activity of nanoparticulate metal oxides against peri-implantitis pathogens. *International Journal of Antimicrobial Agents*. 40(2):135–139.

Verma, D., Garg, P.K. & Dubey, A.K. 2018. Insights into the human oral microbiome. *Archives of Microbiology*. 200(4):525–540.

Versiani, M.A., Abi Rached-Junior, F.J., Kishen, A., Pécora, J.D., Silva-Sousa, Y.T. & de Sousa-Neto, M.D. 2016. Zinc Oxide Nanoparticles Enhance Physicochemical Characteristics of Grossman Sealer. *Journal of Endodontics*. 42(12):1804–1810.

Vidhya, E., Vijayakumar, S., Prathipkumar, S. & Praseetha, P.K. 2020. Green way biosynthesis: Characterization, antimicrobial and anticancer activity of ZnO nanoparticles. *Gene Reports*. 20:100688.

Vijayakumar, S., Krishnakumar, C., Arulmozhi, P., Mahadevan, S. & Parameswari, N. 2018a. Biosynthesis, characterization and antimicrobial activities of zinc oxide nanoparticles from leaf extract of *Glycosmis pentaphylla* (Retz.) DC. *Microbial Pathogenesis*. 116:44–48.

Vijayakumar, S., Mahadevan, S., Arulmozhi, P., Sriram, S. & Praseetha, P.K. 2018b. Green synthesis of zinc oxide nanoparticles using *Atalantia monophylla* leaf extracts: Characterization and antimicrobial analysis. *Materials Science in Semiconductor Processing*. 82:39–45.

Vijayalakshmi, R. & Kumar, S. 2006. Nanotechnology in dentistry. *Indian Journal of Dental Research*. 17(2):62.

Vila, T., Sultan, A.S., Montelongo-Jauregui, D. & Jabra-Rizk, M.A. 2020. Oral candidiasis: A disease of opportunity. *Journal of Fungi*. 6(1):15.

Villanueva-Flores, F., Castro-Lugo, A., Ramírez, O.T. & Palomares, L.A. 2020. Understanding cellular interactions with nanomaterials: towards a rational design of medical nanodevices. *Nanotechnology*. 31(13):132002.

Vinotha, V., Iswarya, A., Thaya, R., Govindarajan, M., Alharbi, N.S., Kadaikunnan, S., Khaled, J.M., Al-Anbr, M.N., *et al.* 2019. Synthesis of ZnO nanoparticles using insulin-rich leaf extract: Anti-diabetic, antibiofilm and anti-oxidant properties. *Journal of Photochemistry and Photobiology B: Biology*. 197(June):111541.

Wahab, R., Kim, Y.S., Mishra, A., Yun, S. Il & Shin, H.S. 2010. Formation of ZnO Micro-Flowers Prepared via Solution Process and their Antibacterial Activity. *Nanoscale Research Letters*. 5(10):1675–1681.

Wang, D., Cui, L., Chang, X. & Guan, D. 2020. Biosynthesis and characterization of zinc oxide nanoparticles from *Artemisia annua* and investigate their effect on proliferation, osteogenic differentiation and mineralization in human osteoblast-like MG-63 Cells. *Journal of Photochemistry and Photobiology B: Biology*. 202:111652.

Wang, J., Du, L., Fu, Y., Jiang, P. & Wang, X. 2019. ZnO nanoparticles inhibit the activity of *Porphyromonas gingivalis* and *Actinomyces naeslundii* and promote the mineralization of the cementum. *BMC Oral Health*. 19(1):1–11.

Wang, J., Gao, S., Wang, S., Xu, Z. & Wei, L. 2018. Zinc oxide nanoparticles induce toxicity in CAL 27 oral cancer cell lines by activating PINK1/Parkin-mediated mitophagy. *International Journal of Nanomedicine*. 13:3441–3450.

Wang, L., Hu, C. & Shao, L. 2017. The antimicrobial activity of nanoparticles: Present situation and prospects for the future. *International Journal of Nanomedicine*. 12:1227–1249.

Wani, A.H. & Shah, M.A. 2012. A unique and profound effect of MgO and ZnO nanoparticles on some plant pathogenic fungi. *Journal of Applied Pharmaceutical Science*. 2012(03):40–44.

Webb, B.C., Thomas, C.J., Willcox, M.D., Harty, D.W. & Knox, K.W. 1998. Candida-associated denture stomatitis. Aetiology and management: a review. Part 1. Factors influencing distribution of Candida species in the oral cavity. *Australian dental journal*. 43(1):45–50.

Williams, D.B. & Carter, C.B. 1996. Scattering and Diffraction. in Transmission Electron Microscopy: A textbook for materials science. Springer US. 19–33.

Williams, D.B. & Carter, C.B. 2009. *Transmission electron microscopy: A textbook for materials science*. Second edition.Springer US:1–805

Witbooi, H., Okem, A., Makunga, N.P. & Kambizi, L. 2017. Micropropagation and secondary metabolites in *Agathosma betulina* (Berg.). *South African Journal of Botany*. 111:283–290.

Van Wyk, B.E. 2008. A broad review of commercially important southern African medicinal plants. *Journal of Ethnopharmacology*. 119(3):342–355.

Xie, Y., He, Y., Irwin, P.L., Jin, T. & Shi, X. 2011. Antibacterial activity and mechanism of action of zinc oxide nanoparticles against *Campylobacter jejuni*. *Applied and Environmental Microbiology*. 77(7):2325–2331.

Yamamoto, O. 2001. Influence of particle size on the antibacterial activity of zinc oxide. *International Journal of Inorganic Materials*. 3(7):643–646.

Yao, L.H., Jiang, Y.M., Shi, J., Tomás-Barberán, F.A., Datta, N., Singanusong, R. & Chen, S.S. 2004. Flavonoids in food and their health benefits. *Plant Foods for Human Nutrition*. 59(3):113–122.

Yusof, H.M., Mohamad, R., Zaidan, U.H. & Abdul Rahman, N.A. 2019. Microbial synthesis of zinc oxide nanoparticles and their potential application as an antimicrobial agent and a feed supplement in animal industry: A review. *Journal of Animal Science and Biotechnology*. 10(1):57.

Yuvakkumar, R., Suresh, J., Nathanael, A.J., Sundrarajan, M. & Hong, S.I. 2014a. Novel green synthetic strategy to prepare ZnO nanocrystals using rambutan (*Nephelium lappaceum L.*) peel extract and its antibacterial applications. *Materials Science and Engineering C*. 41:17–27.

Yuvakkumar, R., Suresh, J. & Hong, S.I. 2014b. Green Synthesis of Zinc Oxide Nanoparticles. *Advanced Materials Research*. 952(3):137–140.

Zacchino, S.A., Butassi, E., Liberto, M. Di, Raimondi, M., Postigo, A. & Sortino, M. 2017a. Plant phenolics and terpenoids as adjuvants of antibacterial and antifungal drugs. *Phytomedicine*. 37:27–48.

Zacchino, S.A., Butassi, E., Cordisco, E. & Svetaz, L.A. 2017b. Hybrid combinations containing natural products and antimicrobial drugs that interfere with bacterial and fungal biofilms. *Phytomedicine*. 37:14–26.

Zagorac, D., Schön, J., Pentin, V. & Jansen, M. 2011. Structure prediction and energy landscape exploration in the zinc oxide system. *Processing and Application of Ceramics*. 5(2):73–78.

Zanatta, F.B., Antoniazzi, R.P. & Rösing, C.K. 2010. Staining and calculus formation after 0.12% chlorhexidine rinses in plaque-free and plaque covered surfaces: A randomized trial. *Journal of Applied Oral Science*. 18(5):515–521.

Zare, E., Pourseyedi, S., Khatami, M. & Darezereshki, E. 2017. Simple biosynthesis of zinc oxide nanoparticles using nature's source, and it's *in vitro* bio-activity. *Journal of Molecular Structure*. 1146:96–103.

Zhang, H. & Chen, G. 2009. potent antibacterial activities of Ag/TiO2 nanocomposite powders synthesized by a one-pot sol-gel method. *Environmental Science and Technology*. 43(8):2905–2910.

Zhou, W. & Wang, Z.L. 2007. Scanning microscopy for nanotechnology: Techniques and applications. Springer New York:1–513.

APPENDIX

Supplemental tables

Supplemental Table 1: Actual measurements of inhibition zones diameters from the Kirby Bauer assay for the three intervention groups [CHX, GZnO NPs, and Zn $(NO_3)_2 \cdot 6H_2O$ solution]

Intervention	**Volume (µL)**	**Zones of inhibition (diameter in mm)**									**Average (mm)**
0.2% Chlorhexidine (CHX) gluconate	50	10	11	11	12	11	11	11	11.5	11.5	11.11
	100	22	22	22	22	22	22	22	22	21.5	21.94
	150	23.5	24	23.5	23	23.5	23	24	23.5	23.5	23.5
	200	28	27	28	26.5	27	26.5	28	26.5	26.5	27.11
Zinc oxide nanoparticles (GZnO NPs)	50	12	13	14	13	12.5	13	13	13	13	12.94
	100	21	21	22	20	20	19	21	20	21	20.55
	150	22	23	24	22.5	23	23	23	23	23.5	23
	200	30	30	32	31	32	30	29	30	30	30.44
Zinc nitrate hexahydrate [Zn $(NO_3)_2 \cdot 6H_2O$] solution	50	10.5	11	10	12	11	12	11	10.5	10.5	10.94
	100	13	13	12.5	13	13	13	14	13	13	13.05
	150	16	17	16	15.5	16	15	16	16	15.5	15.88
	200	18	17.5	17	17.5	18	17	18	17	17.5	17.5

Supplemental Table 2: The mean diameters of inhibition zone and their respective standard deviations using the Kirby Bauer assay for the three intervention groups

Intervention	**Volume (µL)**	**Zones of inhibition (mean) in mm**	**Standard deviation**	**n**
0.2% Chlorhexidine (CHX) gluconate	50	11.111	0.5465	9
	100	21.944	0.1667	9
	150	23.500	0.3536	9
	200	27.111	0.6972	9
Zinc oxide nanoparticles (GZnO NPs)	50	12.944	0.5270	9
	100	20.556	0.8819	9
	150	23.000	0.5590	9
	200	30.444	1.0138	9
Zinc nitrate hexahydrate [$Zn(NO_3)_2 \cdot 6H_2O$] solution	50	10.944	0.6821	9
	100	13.056	0.3909	9
	150	15.889	0.5465	9
	200	17.500	0.4330	9

Supplemental Table 3: The mean optical densities with their respective standard deviations using the CV staining assay for the three intervention groups

Intervention (100 µL)	Time (hours)	Mean for optical densities (560 nm)	Standard deviation	n
0.2% Chlorhexidine (CHX) gluconate	0	2.3442	0.143	28
	2	2.1187	0.256	28
	4	2.2440	0.017	28
	6	2.2677	0.041	28
	8	2.4592	0.058	28
	12	2.3781	0.168	28
	24	2.2864	0.101	28
	48	2.1821	0.068	28
	72	1.7611	0.188	28
Zinc Oxide Nanoparticles (GZnO NPs)	0	1.5578	0.259	28
	2	1.7072	0.467	28
	4	1.7431	0.043	28
	6	1.6815	0.019	28
	8	1.7851	0.201	28
	12	1.7638	0.100	28
	24	1.5206	0.437	28
	48	1.3513	0.313	28
	72	0.7912	0.107	28
Nystatin	0	2.1380	0.280	28
	2	1.8502	0.128	28
	4	1.8169	0.108	28
	6	1.5127	0.031	28
	8	1.4785	0.380	28
	12	2.1979	0.220	28
	24	1.8236	0.101	28
	48	1.5952	0.113	28
	72	1.3211	0.222	28

Supplemental Table 4: The confidence levels of the multiple comparisons (Tukey's HSD tests) using CV staining assay for the three intervention groups at different time points

Time (hours)	Intervention (I)	Intervention(J)	Mean difference (I-J) of optical density	Significance (P-value)	95% Confidence Interval	
					Lower Bound	Upper Bound
0	GZnO NPs	Chlorhexidine	0.08252	0.7300	-0.1291	0.2942
	GZnO NPs	Nystatin	-0.02783	0.9852	-0.2395	0.1838
	GZnO NPs	Negative control	0.2390	0.0211*	0.02730	0.4506
	CHX	Nystatin	-0.1104	0.5151	0.3220	0.1013
	CHX	Negative control	0.1564	0.2157	-0.05522	0.3681
	Nystatin	Negative control	0.2668	0.0081**	0.05513	0.4785
2	GZnO NPs	Chlorhexidine	0.3539	<.0001****	0.2225	0.4853
	GZnO NPs	Nystatin	0.3111	<.0100****	0.1797	0.4425
	ZnO NPs	Negative control	0.2070	0.0006***	0.07563	0.3384
	CHX	Nystatin	-0.04279	0.8230	-0.1742	0.08858
	CHX	Negative control	-0.1469	0.0228*	-0.2783	-0.01552
	Nystatin	Negative control	-0.1041	0.1656	-0.2355	0.02727
4	GZnO NPs	Chlorhexidine	0.3141	0.0076**	0.06656	0.5616
	GZnO NPs	Nystatin	0.3677	0.0013**	0.1202	0.6152
	GZnO NPs	Negative control	0.6684	<.0100****	0.4208	0.9159
	CHX	Nystatin	0.05361	0.9392	-0.1939	0.3011
	CHX	Negative control	0.3543	0.0021**	0.1067	0.6018
	Nystatin	Negative control	0.3007	0.0114*	0.05311	0.5482
6	GZnO NPs	Chlorhexidine	0.2427	0.0032**	0.06659	0.4188
	GZnO NPs	Nystatin	0.5210	<.0001****	0.3449	0.6971
	GZnO NPs	Negative control	0.5752	<.0001****	0.3991	0.7513
	CHX	Nystatin	0.2783	0.0006***	0.1022	0.4544
	CHX	Negative control	0.3325	<.0001****	0.1564	0.5086
	Nystatin	Negative control	0.05426	0.8458	-0.1218	0.2304
8	GZnO NPs	Chlorhexidine	0.2274	<.0001****	0.1201	0.3347
	GZnO NPs	Nystatin	0.64143066	<.0001****	0.5341	0.7488
	GZnO NPs	Negative control	0.6494	<.0001****	0.5421	0.7567

Time (hours)	Intervention (I)	Intervention(J)	Mean difference (I-J) of optical density	Significance (P-value)	95% Confidence Interval	
					Lower Bound	Upper Bound
	CHX	Nystatin	0.4140	<.0001****	0.3067	0.5214
	CHX	Negative control	0.4220	<.0001****	0.3147	0.5294
	Nystatin	Negative control	0.007989	0.9972	-0.09934	0.1153
12	GZnO NPs	Chlorhexidine	0.2549	<.0001****	0.1515	0.3584
	GZnO NPs	Nystatin	0.1229	<.0138*	0.01946	0.2264
	GZnO NPs	Negative control	0.1172	0.0205*	0.01374	0.2207
	CHX	Nystatin	-0.1320	0.0072**	-0.2355	-0.02857
	CHX	Negative control	-0.1377	0.0047**	-0.2412	-0.03429
	Nystatin	Negative control	-0.005719	0.9989	-0.1092	0.09774
24	GZnO NPs	Chlorhexidine	0.08156	0.0919	-0.009060	0.1722
	GZnO NPs	Nystatin	0.1553	0.0002****	0.06470	0.2459
	GZnO NPs	Negative control	0.1587	0.0001***	0.06808	0.2493
	CHX	Nystatin	0.07376	0.1481	-0.01686	0.1644
	CHX	Negative control	0.07714	0.1211	-0.01348	0.1678
	Nystatin	Negative control	0.003375	0.9996	-0.08725	0.09400
48	GZnO NPs	Chlorhexidine	-0.01543	0.9906	-0.1524	0.1216
	GZnO NPs	Nystatin	0.1556	0.0202*	0.01857	0.2926
	GZnO NPs	Negative control	0.1212	0.1003	-0.01579	0.2583
	CHX	Nystatin	0.1710	0.0089**	0.03400	0.3080
	CHX	Negative control	0.1367	0.0508	-0.0003604	0.2737
	Nystatin	Negative control	-0.03436	0.9096	-0.1714	0.1027
72	GZnO NPs	Chlorhexidine	-0.2918	<.0001****	-1.4367	-0.1470
	GZnO NPs	Nystatin	-0.1772	0.0107*	-0.3220	-0.03231
	GZnO NPs	Negative control	-0.08054	0.4593	-0.2254	0.06433
	CHX	Nystatin	0.1146	0.1665	-0.03021	0.2595
	CHX	Negative control	0.2113	0.0017**	-0.06642	0.3561
	Nystatin	Negative control	0.09663	0.2990	-0.04823	0.2415

Supplemental Table 5: Means optical density for biofilm reduction of *C. albicans* for the three inventions at consecutive time point across the 72 Hours using CV staining assay

Average gradients for each intervention	**2hr-0hr**	**12hr-2hr**	**24hr-12hr**	**48hr-24hr**	**72hr-48hr**	**MEANS**	**STDEV**
CHX	-0.113	0.026	-0.008	-0.004	-0.018	-0.023	0.047
Nystatin	-0.144	0.035	-0.031	-0.010	-0.011	-0.032	0.060
GZnO NPs	0.075	0.006	-0.020	-0.007	-0.023	0.006	0.036
Neg. Control	0.086	0.014	-0.022	-0.005	-0.013	0.012	0.039